The activation mechanisms of G protein-coupled receptors : the case of the adenosine A2B and HCA2/3 receptors

Liu, R.

The activation mechanisms of G protein-coupled receptors

The case of the adenosine A_{2B} and $HCA_{2/3}$ receptors

Rongfang Liu

The research described in this thesis was performed in the Division of Medicinal Chemistry at the Leiden Academic Centre for Drug Research, Leiden University (Leiden, The Netherlands).

Cover design: Eelke B. Lenselink
Thesis layout: Rongfang Liu
Printed by Ipskamp in the Netherlands

The activation mechanisms of G protein-coupled receptors

The case of the adenosine A_{2B} and $HCA_{2/3}$ receptors

Proefschrift

ter verkrijging van
de graad van Doctor aan de Universiteit Leiden,
op gezag van Rector Magnificus prof.mr. C.J.J.M. Stolker,
volgens besluit van het College voor Promoties
te verdedigen op donderdag 08 december 2016
klokke 10:00 uur

door

Rongfang Liu
geboren te Tacheng (Xinjiang), China
in 1986

Promotor: Prof. Dr. A.P. IJzerman

PROMOTIECOMMISSIE

Prof. Dr. J.A. Bouwstra, Leiden University, LACDR

Prof. Dr. M. Danhof, Leiden University, LACDR

Prof. Dr. M. Schmidt, RU Groningen

Prof. Dr. B. van de Water, Leiden University, LACDR

Dr. M. Siderius, VU Amsterdam

Contents

Chapter 1

General introduction

G protein-coupled receptors (GPCRs)

The G protein-coupled receptors (GPCRs) are a superfamily of seven transmembrane receptors (7TM) that communicate extracellular signals to the internal environment. Examples of extracellular signals that can be transmitted are: ions, photons, small organic molecules and proteins. Activation of GPCRs can induce signalling via multiple distinct pathways, such as β-arrestin or/and G protein pathways[1]. As the name implies receptors are coupled to so-called G proteins. These are heterotrimeric protein complexes comprised of three subunits, the α-, β- and γ-subunit, which together act like a switch and amplifier involved in cellular signal transduction (Fig. 1). GPCRs control many cellular and physiological responses in mammals, such as cell growth and differentiation, energy metabolism, cardiovascular function, neurotransmission and immune responses[2]. There are approximately 800 different GPCRs in the human genome. GPCRs are the target for around 30-40% of clinically prescribed drugs and for 25% of the top 100 in sales[3, 4]. GPCRs are divided into 6 different families according to their signature of conserved residues and ligand interaction: Class A, rhodopsin-like; Class B, secretin-like, Class C, glutamate; Class D, adhesion, Class E, frizzled-taste-2 receptors and Class F, other 7TM proteins[2, 5].

GPCR activation

GPCRs all have a similar structure: an extracellular N-terminus, seven transmembrane helices connected via three intracellular and three extracellular loops (TM1-7, IL1-3 and EL1-3), helix 8, and an intracellular C-terminus. Most structural studies have been performed on Class A (rhodopsin-like receptors), the largest and most known subfamily. Previous research identified important conserved residues and a shared common mechanism of receptor activation among different receptor families. The (D/E)RY motif is located at the interface between TM3 and IL2, which is involved in the well-studied mechanism of action that breaks the ionic lock/salt bridge between $R^{3.50}$ and $E^{6.30}$ after activation[7] (The superscript numbers of these residues are based on

Ballesteros-Weinstein numbering[8]). This mechanism is present in many Class A receptors, such as rhodopsin[9], β_2–adrenergic receptor[10], serotonin 2A receptor (5-hydroxytryptamine 2A, $5HT_{2A}$)[11, 12]. However, the ionic lock is not a key activation microswitch in many other GPCRs[7]. The NPxxY motif located in TM7 is another essential motif, which connects ligand binding with intracellular helix 8 and G protein activation[5]. Most Class A, rhodopsin-like, receptors have the NPxxY$(x)_{5,6}$F motif, which is located at the junction between TM7 and the connecting cytosolic helix 8, such as in rhodopsin itself[9, 13], mammalian melanin-concentrating hormone receptor 1[14], the type 1 angiotensin receptor[15], β_1–adrenergic receptor[16], α_{2B}-adrenergic receptor[17] and the A_1 adenosine receptor[18]. The important interaction between TM7, helix 8 can transfer the signal from outside ligand binding to inside G protein, such as in protease-activated receptor 1 has TM7-helix 8-IL1 activation mechanism[19], which may be conserved in other Class A. However, each receptor is unique and it binds its own outside ligands and triggers different downstream signalling pathways, some of which may be shared with other receptors. In a recent review Moreira et al. reported about the structural features of the G protein/GPCR interaction. Most key regions for GPCR/G protein coupling are located at the interface between transmembrane helices and intracellular loops, which are represented by a red rectangle (Fig. 2). It should be mentioned that even mutation of a single residue may lead to receptor silence and thus be critical for G protein coupling and receptor activation[20, 21].

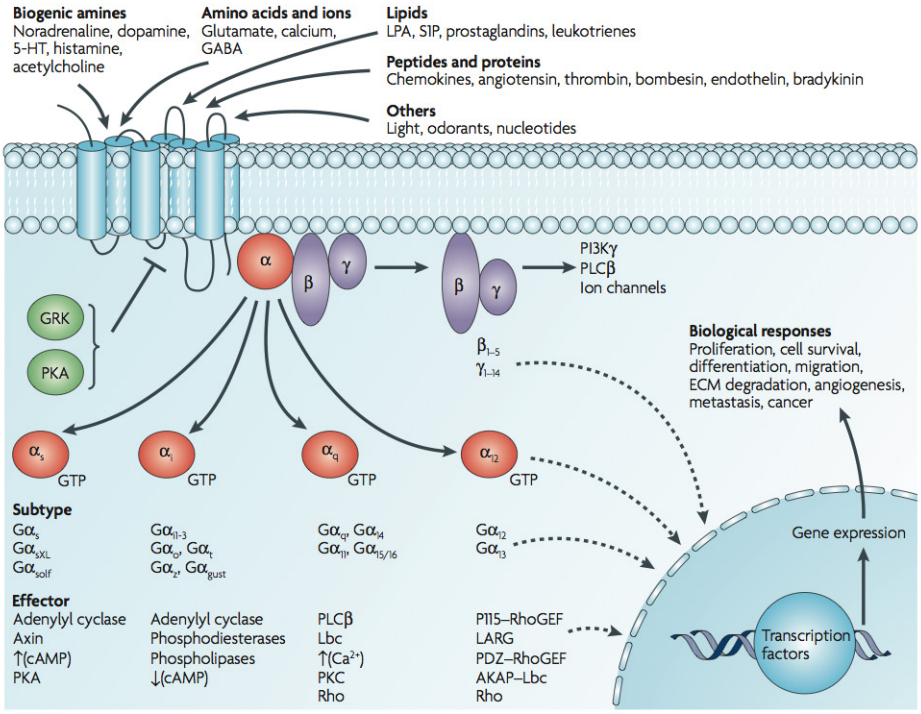

Fig. 1. Activation and signalling pathways of GPCRs and their respective G proteins[6]. Reproduced with permission.

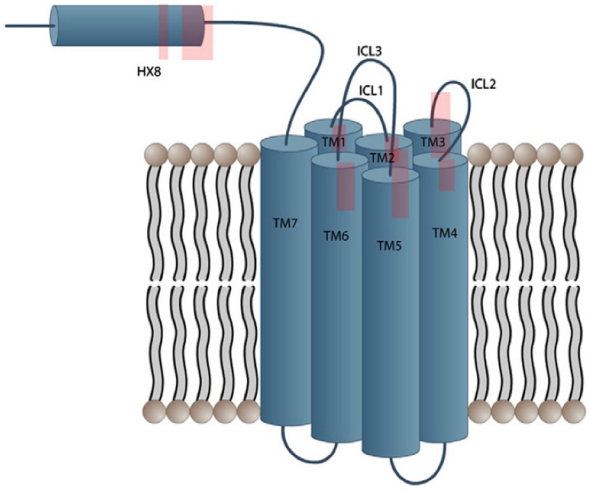

Fig. 2. Schematic representation of a G protein-coupled receptor. Key regions for GPCR/G protein coupling are represented by red rectangles (different sizes are related to the dimension of the interacting region)[22]. Please, note the influence of the 'rhodopsin community' in which it is common to draw the extracellular region upside down. Reproduced with permission.

G protein and G protein selectivity

With an agonist in the binding pocket of the GPCR the receptor is in the active state by stabilizing an agonist-preferring structural conformation. This change in conformation in turn changes the conformation of the G protein allowing it to be 'switched on' by exchanging guanosine-5'-diphosphate (GDP) for guanosine-5'-triphosphate (GTP) at the G_α subunit. This G_α subunit subsequently dissociates from the $\beta\gamma$-complex and interacts with an effector protein in the cell (Fig. 1). G proteins can be divided based on the G_α subunit and its sequence identity; there are 4 different families of G_α proteins: $G_{\alpha s}$, $G_{\alpha i}$, $G_{\alpha 12}$, and $G_{\alpha q}$[23] (Fig. 1). Effector proteins can be many, ranging from kinases to ion channels, which upon activation either increase or decrease the amount of secondary messengers associated with it (Fig. 1). Second messengers like cAMP or calcium ions (Ca^{2+}) induce physiological changes like proliferation, secretion or apoptosis. Hydrolysis of the GTP bound to the α-subunit to GDP deactivates the G_α subunit and leads to re-association with the $\beta\gamma$-complex, upon which the effector protein reverts back to its original state[6].

Even though the GPCRs are a very diverse family all of them bind to a much smaller number of G proteins. There are 21 G_α, 6 G_β, and 12 G_γ subunits in human cells[24]. Previous research has shown one GPCR can activate multiple G protein pathways, while at the same time different GPCRs can activate the same G protein pathways[25]. This dictates that the interface between G proteins and GPCRs has interactions that determine which G proteins can, and which G proteins cannot interact with a given receptor. Even though the mechanisms and dynamics of interaction between GPCRs and their G proteins are poorly understood, important regions of G_α subunits for GPCR-G_α protein binding and selectivity include the α4-helix and α4-β6 loop[26, 27], the N-terminus[28] and C-terminus of G_α subunits[29, 30]. Of those regions, the C-terminus of the G_α subunit is most intimately involved in binding to the receptor. This was already proved by available crystal structures[31, 32] and Kling et al. reported three residues at the C-terminus of $G_{\alpha s}$ are in close contact with at least 5 amino acids of the β_2–adrenergic receptor, based on molecular dynamics calculations[33]. Even though

the G_α subunit has most of the interactions with the receptor it is not the only G protein subunit that confers specificity. Both the G_β[34] and G_γ[35] subunits are also able to specify by which GPCRs they are activated. Many interactions have been identified both on the G protein side and on the receptor side, however, the exact nature of the connections is still unclear[17]. Hence it is very important to discover key residues or motifs within GPCRs or G proteins that can switch on/off G protein/GPCR activation, knowledge that eventually may be useful for drug discovery.

Adenosine A_{2B} receptor

All the adenosine receptors (P1 Purinergic receptors) are ubiquitously expressed in the human body[36]. They belong to the Class A subfamily of GPCRs and their endogenous ligand is adenosine. Adenosine is a purine nucleoside, which consists of an adenine ring bound to a ribose sugar group via a β-N_9-glycosidic bond. Normal levels of extracellular adenosine are well below 1 μM in unstressed cells. During inflammation and ischemia these levels can increase to upwards of 100 μM. For example, patients suffering from sepsis, which is associated with inflammation, have adenosine levels of about 8 μM[37]. Adenosine has been found to be involved in tissue protection and regeneration of injured tissue in a number of ways through the adenosine receptors[38]. The adenosine receptors include four subtypes: A_1, A_{2A}, A_{2B} and A_3 receptors, which have attracted much attention as therapeutic targets in recent years. They can target different intracellular signalling pathways by responding to the same endogenous ligand adenosine. The A_1 and A_3 adenosine receptors (which share 49% sequence identity) inhibit cAMP production while the A_{2A} and A_{2B} receptors (sharing 59% sequence identity) stimulate the production of cAMP.

The A_{2B} receptor has the lowest affinity for adenosine[39] and has been less investigated than other adenosine receptors. The A_{2B} receptor is coupled to the G_s and G_q proteins (Fig. 3A)[40], although the preference is more towards the G_s pathway[41]. The G_s subunit can open a calcium channel either directly by binding to it or indirectly through stimulating cAMP production by activating

protein kinase A (PKA), which is also capable of opening the calcium channel[42]. The G_q pathway can bind to phosphatidylinositol-specific phospholipase C (PI-PLC), leading to the production of inositol trisphosphate (IP_3) and diacylglycerol (DAG). IP_3 activates the mobilization of calcium from intracellular storage sites. DAG activates protein kinase C (PKC).

The A_{2B} receptor is widely expressed in many cell types and tissues[40] and plays many roles in different organs and pathologies[43] (Fig. 3B). Previous studies have described that inhibition of A_{2B} receptor signalling reduces experimental autoimmune encephalomyelitis, of relevance for the treatment of multiple sclerosis[44], and inhibits growth of prostate cancer cells[45], bladder tumors[46, 47] and breast tumors[48], and reduces obesity or insulin resistance[49]. On the other hand, activation of A_{2B} receptor signalling protects against trauma-hemorrhagic shock-induced lung injury[50], CHX-induced apoptosis[45], cardiac diseases[51], and also vascular injury[30, 52]. Likewise, it has been found that activation of the A_{2B} receptor plays a role in suppression of inflammation during tissue hypoxia[53], whereas antagonism might inhibit growth of lung tumors[54] and also hyperlipidemia[55]. Therefore, the A_{2B} receptor is a promising drug target for the treatment of kidney failure, inflammatory diseases, type 2 diabetes, asthma, ischemic injuries, diarrhea, and central nervous system disorders[56-60]. To understand the activation mechanism of the A_{2B} receptor is therefore very relevant for drug development at the A_{2B} receptor.

Human HCA_2 and HCA_3 receptors

The hydroxycarboxylic acid (HCA) receptors also belong to Class A subfamily of GPCRs and consist of three members HCA_1, HCA_2 and HCA_3, which function as metabolic sensors that are activated by intermediates of energy metabolism. Their endogenous ligands are hydroxycarboxylic acids: 2-hydroxy-propanoic acid (lactate), 3-hydroxybutyric acid and 3-hydroxy-octanoic acid for HCA_1, HCA_2 and HCA_3, respectively[61, 62] and they were deorphanized in 2008 (HCA_1, GPR81)[63, 64], 2005 (HCA_2, GPR109A/HM74A, high affinity nicotinic acid receptor)[65] and 2009 (HCA_3, GPR109B/HM74, low affinity nicotinic acid

receptor)[66], respectively. The HCA_1 receptor is the most divergent member with approximately 50% amino acid sequence identity with both HCA_2 and HCA_3. The HCA_2 and HCA_3 receptors are highly homologous with 95% sequence identity[62]. The main difference between the HCA_2 and HCA_3 receptors is that HCA_2 has a shorter C-terminus than HCA_3 that carries 24 amino acid residues more at its C-terminus. Although the two receptors have high overall sequence homology, there are also 17 different amino acid residues in other parts of the two receptors that mainly cluster around ECL1 and ECL2[62, 67].

The HCA_2 receptor has been found only in mammals, whereas the HCA_3 receptor is only expressed in higher primates, which indicate that this receptor is the result of a recent gene duplication[68]. They all are predominantly expressed in adipocytes, where they mediate antilipolytic effects through coupling to the $G_{\alpha i}$ protein pathway[69, 70]. An overview of cellular functions regulated by HCA receptors is shown in Figure 4[68]. Activation of the HCA_2 receptor can have therapeutic benefits, such as an anti-dyslipidemic effect[71], anti-inflammatory effect[72-74], neuroprotective effect[75, 76] and on energy metabolism[77]. For the past 50 years nicotinic acid has been used to treat patients who suffer from cardiovascular disease, dyslipidemia and progression of atherosclerosis[78,79]. However next to this beneficial anti-dyslipidemic effect, nicotinic acid also induces a HCA_2 receptor-mediated side effect of severe flushing, resulting in low patient compliance[80]. Earlier research was focused on deorphanizing and characterizing the HCA receptors, with a main emphasis of the pharmacological role of the HCA_2 receptor activated by nicotinic acid. That sparked the interest in the development of novel agonists with higher affinity and selectivity, and other therapeutic modalities such as partial agonists, allosteric agonists and positive allosteric modulators[70, 81]. Interestingly, so far no antagonists have been discovered for the HCA receptors. For the research presented in this thesis, we focused on two aspects, i) the screening of high affinity agonists with long residence time and ii) the G protein activation/G protein selectivity profile of the HCA_2 and HCA_3 receptors.

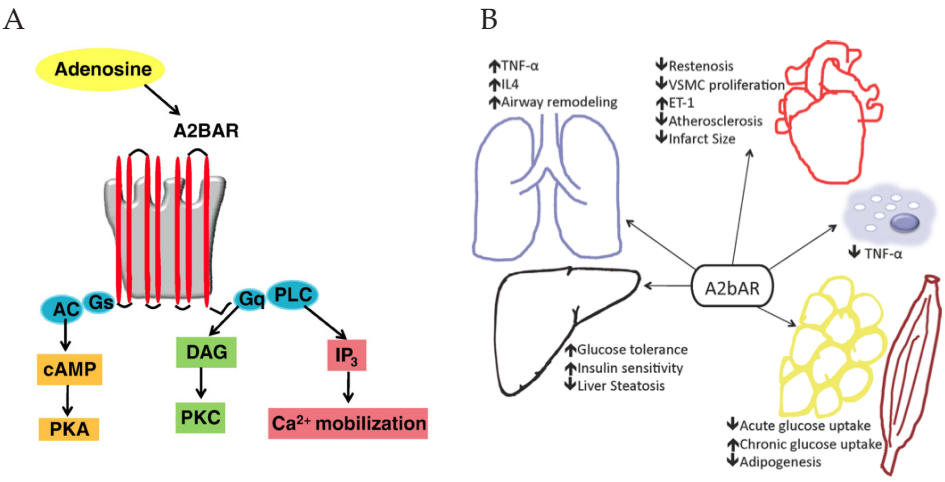

Fig. 3. (A) A schematic drawing of G protein activation and downstream signalling of the A_{2B} adenosine receptor[40]. (B) Important roles of the A_{2B} receptor in different organs and pathologies[43]. Reproduced with permission.

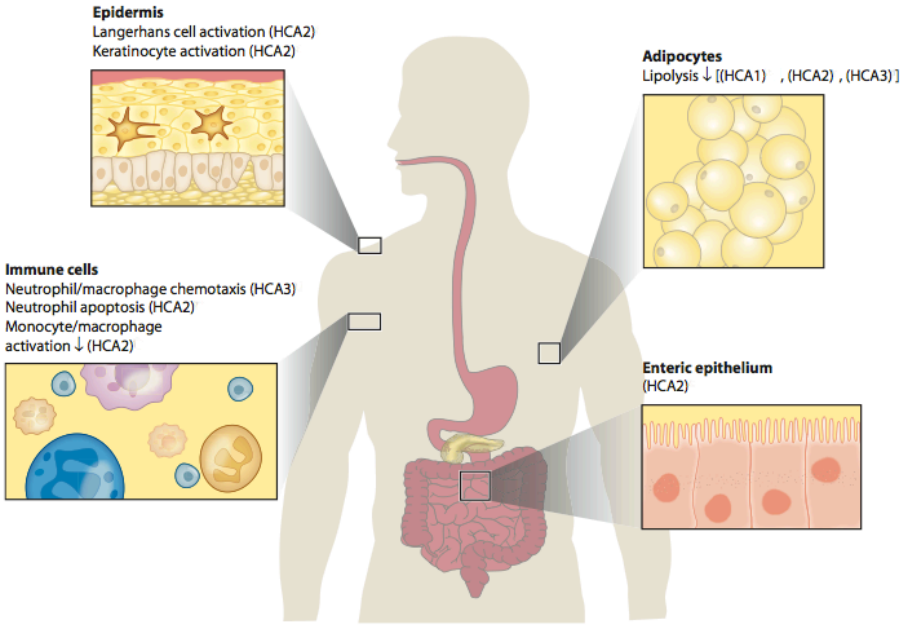

Fig. 4. Cellular functions regulated by the hydroxycarboxylic acid (HCA) receptors[68]. Reproduced with permission.

Saccharomyces cerevisiae system

Saccharomyces cerevisiae (*S. cerevisiae*) and *Pichia Pastoris* (*Pichia*) have been genetically well characterized as a model system among the many yeast species. For example, the two yeast strains are suitable 'production facilities' for membrane proteins as becomes evident from the crystal structures deposited in the PDB between 2010 and 2015[82]. The yeast system is as cheap and fast as E.coli, and which itself is 10 times cheaper and 4 times faster than insect cells and mammalian cells[83]. More than 50 GPCRs have been functionally expressed in various *S. cerevisiae* strains (more details of human GPCRs have been described in Chapter 2).

Many signal transduction pathways in *S. cerevisiae* have been discovered in the last three decades[84]. The yeast mating pheromone response pathway has been applied in GPCR research through the yeast MAP kinase pathway, which is not essential in the life of the yeast cell. In normal yeast cells the pheromone receptor (Ste2/Ste3) is bound to a heterotrimeric G protein consisting of a G_{α} (Gpa1p), G_{β} (Ste4p), and G_{γ} (Ste18p) subunit[85]. When $G_{\beta\gamma}$ is activated it signals to MAP kinase, which induces cell-cycle arrest (SST2) and mating gene transcription (Ste12p)[85]. *S. cerevisiae* has been engineered for GPCR ligand identification and for characterizing receptor pharmacology and signal transduction mechanisms[85,86]. It was found that the gene that induces cell-cycle arrest, FAR1, had to be disabled along with the negative regulator SST2 to improve the signalling characteristics of the assay[87]. Adding a reporter of Ste12p such as FUS1-HIS3 allows agonist-dependent growth on histidine-deficient medium[88] that will be used in the present thesis, while adding FUS1-LacZ would allow for quantitative readouts[89]. The biggest advantage of this system is that it provides a very clean and zero GPCR background. It has been coined 'a single-GPCR-one-G protein yeast system', because the original yeast GPCRs were knocked out. A schematic drawing of the wild-type and engineered pheromone pathway in *S. cerevisiae* is shown in Figure 5[90].

To investigate the activation mechanism of the receptor at the interface of the C terminus of the G_{α} subunit of the G protein, we expressed the yeast

plasmid with the receptor gene in eight different yeast *S. cerevisiae* strains with humanized G proteins (so called 'transplants'). The yeast strains used in this thesis are classified into five families: $G_{\alpha WT}$ (MMY12), $G_{\alpha s}$ (MMY28), $G_{\alpha i}$ (MMY23, MMY24 and MMY25), $G_{\alpha 12}$ (MMY19 and MMY20), and $G_{\alpha q}$ (MMY14, MMY16 and MMY21) corresponding to the last five C-terminal residues of the mammalian G_{α} subunit exchanged for the corresponding sequence stretch in the yeast G protein[91].

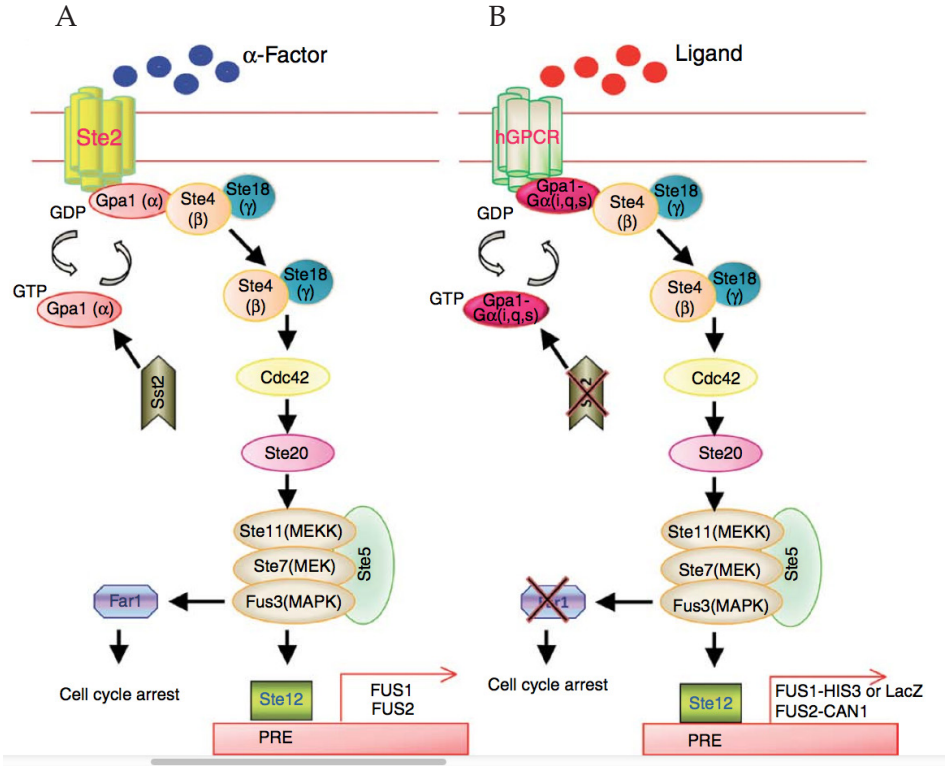

Fig.5. A schematic drawing of the wild-type and engineered pheromone pathway in *S. cerevisiae*[90]. (A) Pheromone signalling pathway mediated by yeast GPCR (Ste2) in wild-type yeast. (B) GPCR-mediated signalling pathway in an engineered yeast strain suitable for human GPCRs research. Reproduced with permission.

Aim and outline of this thesis

Identifying and elucidating the functions and activation of GPCRs will provide opportunities for novel drug discovery. In previous research it was shown that some sequence elements are important for GPCR activation, such as the DRY and NPxxY motifs. To obtain more information about receptor activation, we decided to study these and other sequence motifs to determine which parts of the receptor are key to its activation. We did so by mutating individual amino acids and meticulously checking the effect these mutations had on activation or G protein selectivity. We chose three receptors, the adenosine A_{2B} receptor and the HCA_2 and HCA_3 receptors, as paradigms. The functional assays in Chapters 3, 4 and 5 were based on the *S. cerevisiae* single-GPCR-one-G protein yeast system.

In **Chapter 2**, we summarized new developments regarding human G protein-coupled receptors in studies using *S. cerevisiae* ever since the year 2005 when we last reviewed this system. We described 11 families of GPCRs in detail including the principles and developments of each yeast system applied to these different GPCRs.

In **Chapter 3**, we predicted the residues that are important for A_{2B} receptor activation from homology modelling and we made site-directed single mutants and expressed these in yeast strains with a specific G protein pathway. This chapter focused on the above-mentioned DRY motif and on G protein selectivity.

In **Chapter 4** we studied the function of the NPxxY$(x)_{5,6}$F motif and each residue of helix 8 in receptor activation for which we used scanning mutagenesis of the two domains of the adenosine A_{2B} receptor.

In **Chapter 5**, we expressed the HCA_2 and HCA_3 wild-type receptors in yeast strains with specific G protein pathways. This chapter particularly focused on the different behaviors of these closely related receptors in G proteins coupling. The HCA_2 and HCA_3 receptors share high sequence identity but differ considerably in C-terminus length with HCA_3 having the longest tail. Hence we also made C-terminus 'swap' mutants of HCA_2 and HCA_3 to obtain insights in the function of the C terminus in G protein coupling.

Major pharmaceutical companies such as Merck, Arena and GlaxoSmithKline

have been working on the synthesis of agonists for the HCA_2 receptor in the past. Since nicotinic acid has long been the only drug on the market to raise HDL cholesterol levels, the focus of the pharmaceutical industry was on the synthesis of an HCA_2 agonist with the same desired effect, but without the flushing side effect. This resulted in a plethora of lead compounds and marketed drugs, for example Acifran and Acipimox.

In **Chapter 6** we focused on the design and synthesis of HCA_2 agonists with the additional quality of having a long residence time on the receptor, as the latter parameter may be linked to *in vivo* efficacy.

In **Chapter 7** we will summarize our findings in the present thesis and describe the advantages of the *S. cerevisiae* system and the importance of residues in conserved sequence motifs, such as DRY and NPxxY. Future perspectives for drug discovery based on our findings with respect to receptor activation and G protein coupling will conclude this thesis.

References

[1] Rominger, D.H., et al. *Biased ligands: pathway validation for novel GPCR therapeutics.* Curr. Opin. Pharmacol. (2014) 16: 108-115.

[2] Lagerström, M.C. and Schiöth, H.B. *Structural diversity of G protein-coupled receptors and significance for drug discovery.* Nat. Rev. Drug Disc. (2008) 7: 339-357.

[3] Schlyer, S. and Horuk, R. *I want a new drug: G-protein-coupled receptors in drug development.* Drug discovery today (2006) 11: 481-493.

[4] Thomsen, W., et al. *Functional assays for screening GPCR targets.* Curr. Opin. Biotechnol. (2005) 16: 655-665.

[5] O'Callaghan, K., et al. *Turning receptors on and off with intracellular pepducins: new insights into G-protein-coupled receptor drug development.* J. Biol. Chem.(2012) 287: 12787-12796.

[6] Dorsam, R.T. and Gutkind, J.S. *G-protein-coupled receptors and cancer.* Nat. Rev. Cancer (2007) 7: 79-94.

[7] Tehan, B.G., et al. *Unifying family A GPCR theories of activation.* Pharmacol. Ther. (2014) 143: 51-60.

[8] Ballesteros, J.A. and Weinstein, H. *Integrated methods for the construction of three-dimensional models and computational probing of structure-function relations in G protein-coupled receptors.* Methods Neurosci. (1995) 25: 366-428.

[9] Palczewski, K., et al. *Crystal structure of rhodopsin: A G protein-coupled receptor.* Science

(2000) 289: 739-745.

[10] Ballesteros, J.A., et al. *Activation of the β_2-adrenergic receptor involves disruption of an ionic lock between the cytoplasmic ends of transmembrane segments 3 and 6.* J. Biol. Chem. (2001) 276: 29171-29177.

[11] Shapiro, D.A. and Roth, B.L. *Insights into the structure and function of 5-HT2 familyserotonin receptors reveal novel strategies for therapeutic target development.* Exp. Op. Ther. Targets (2001) 5: 685-695.

[12] Shapiro, D.A., et al. *Evidence for a model of agonist-induced activation of 5-hydroxytryptamine 2A serotonin receptors that involves the disruption of a strong ionic interaction between helices 3 and 6.* J. Biol. Chem. (2002) 277: 11441-11449.

[13] Acharya, S. and Karnik, S.S. *Modulation of GDP release from transducin by the conserved Glu134-Arg135 sequence in rhodopsin.* J. Biol. Chem. (1996) 271: 25406-25411.

[14] Hamamoto, A., et al. *Mutation of Phe318 within the NPxxY(x)$_{5,6}$F motif in melanin-concentrating hormone receptor 1 results in an efficient signaling activity.* Front. Endocrinol. (2012) 3:

[15] Huynh, J., et al. *Role of helix 8 in G protein-coupled receptors based on structure–function studies on the type 1 angiotensin receptor.* Mol. Cell. Endocrinol. (2009) 302: 118-127.

[16] Santos, N.M.D., et al. *Characterization of the residues in helix 8 of the human β_1-adrenergic receptor that are involved in coupling the receptor to G proteins.* J. Biol. Chem. (2006) 281: 12896-12907.

[17] Duvernay, M.T., et al. *Anterograde trafficking of G protein-coupled receptors: function of the C-terminal F (X) 6LL motif in export from the endoplasmic reticulum.* Mol. Pharmacol. (2009) 75: 751-761.

[18] Málaga-Diéguez, L., et al. *Pharmacochaperoning of the A_1 adenosine receptor is contingent on the endoplasmic reticulum.* Mol. Pharmacol. (2010) 77: 940-952.

[19] Swift, S., et al. *Role of the PAR1 receptor 8th helix in signaling the 7-8-1 receptor activation mechanism.* J. Biol. Chem. (2006) 281: 4109-4116.

[20] Han, X., et al. *Leu128 (3.43)(l128) and Val247 (6.40)(V247) of CXCR1 are critical amino acid residues for G protein coupling and receptor activation.* PLOS ONE (2012) 7: e42765.

[21] Zhu, S., et al. *A single mutation in helix 8 enhances the angiotensin II type 1a receptor transport and signaling.* Cell. Signalling (2015) 27: 2371-2379.

[22] Moreira, I.S. *Structural features of the G-protein/GPCR interactions.* BBA-Gen. Subjects (2014) 1840: 16-33.

[23] Simon, M.I., Strathmann, M.P., and Gautam, N. *Diversity of G proteins in signal transduction.* Science (1991) 252: 802-808.

[24] Downes, G. and Gautam, N. *The G protein subunit gene families.* Genomics (1999) 62: 544-552.

[25] Brown, A.J., et al. *Functional coupling of mammalian receptors to the yeast mating pathway using novel yeast/mammalian G protein α-subunit chimeras.* Yeast (2000) 16: 11-22.

[26] Bae, H., et al. *Two Amino Acids within the α4 Helix of $G_{\alpha i1}$ Mediate Coupling with 5-Hydroxytryptamine1BReceptors.* J. Biol. Chem. (1999) 274: 14963-14971.

[27] Bae, H., et al. *Molecular determinants of selectivity in 5-hydroxytryptamine1B receptor-G protein interactions.* J. Biol. Chem. (1997) 272: 32071-32077.

[28] Taylor, J.M., et al. *Binding of an alpha 2 adrenergic receptor third intracellular loop peptide to G beta and the amino terminus of G alpha.* J. Biol. Chem. (1994) 269: 27618-27624.

[29] Blahos, J., et al. *Extreme C terminus of G protein α-subunits contains a site that discriminates between Gi-coupled metabotropic glutamate receptors.* J. Biol. Chem. (1998) 273: 25765-25769.

[30] Liu, R., et al. *A yeast screening method to decipher the interaction between the adenosine A2B receptor and the C-terminus of different G protein α-subunits.* Purinergic Signal. (2014) 10: 441-453.

[31] Scheerer, P., et al. *Crystal structure of opsin in its G-protein-interacting conformation.* Nature (2008) 455: 497-502.

[32] Rasmussen, S.G., et al. *Crystal structure of the β_2 adrenergic receptor-G_s protein complex.* Nature (2011) 477: 549-555.

[33] Kling, R.C., et al. *Active-State Models of Ternary GPCR Complexes: Determinants of Selective Receptor-G-Protein Coupling.* PLOS ONE (2013) 8: e67244.

[34] McIntire, W.E., MacCleery, G., and Garrison, J.C. *The G protein β subunit is a determinant in the coupling of Gs to the β1-adrenergic and A_{2a} adenosine receptors.* J. Biol. Chem. (2001) 276: 15801-15809.

[35] Hou, Y., et al. *Selective role of G protein γ subunits in receptor interaction.* J. Biol. Chem. (2000) 275: 38961-38964.

[36] Fredholm, B.B., et al. *Structure and function of adenosine receptors and their genes.* Naunyn-Schmiedeberg's Arch. Pharmacol. (2000) 362: 364-374.

[37] Martin, C., et al. *High adenosine plasma concentration as a prognostic index for outcome in patients with septic shock.* Crit. Care Med. (2000) 28: 3198-3202.

[38] Linden, J. *Adenosine in tissue protection and tissue regeneration.* Mol. Pharmacol. (2005) 67: 1385-1387.

[39] Fredholm, B.B., et al. *Comparison of the potency of adenosine as an agonist at human adenosine receptors expressed in Chinese hamster ovary cells.* Biochem. Pharmacol.(2001) 61: 443-448.

[40] Aherne, C.M., et al. *The resurgence of A_{2B} adenosine receptor signaling.* BBA-Biomembranes(2011) 1808: 1329-1339.

[41] Thimm, D., et al. *Ligand-specific binding and activation of the human adenosine A2B receptor.* Biochemistry (2013) 52: 726-740.

[42] Feoktistov, I. and Biaggioni, I. *Adenosine A_{2B} receptors.* Pharmacol. Rev. (1997) 49: 381-402.

[43] Eisenstein, A., et al. *The Many Faces of the A2b Adenosine Receptor in Cardiovascular and Metabolic Diseases.* J. Cell. Physiol. (2015)

[44] Wei, W., et al. *Blocking A_{2B} Adenosine Receptor Alleviates Pathogenesis of Experimental Autoimmune Encephalomyelitis via Inhibition of IL-6 Production and Th17 Differentiation.* J. Immunol. (2013) 190: 138-146.

[45] Wei, Q., et al. *A_{2B} adenosine receptor blockade inhibits growth of prostate cancer cells.* Purinergic Signal. (2013) 1-10.

[46] Owen, S.J., et al. *Loss of adenosine A_{2B} receptor mediated relaxant responses in the aged female rat bladder; effects of dietary phytoestrogens.* Naunyn-Schmiedeberg's Arch. Pharmacol.(2012) 385: 539-549.

[47] Cekic, C., et al. *Adenosine A_{2B} receptor blockade slows growth of bladder and breast tumors.* J. Immunol. (2012) 188: 198-205.

[48] Stagg, J., et al. *Anti-CD73 antibody therapy inhibits breast tumor growth and metastasis.* PNAS (2010) 107: 1547-1552.

[49] Figler, R.A., et al. *Links between insulin resistance, adenosine A_{2B} receptors, and inflammatory markers in mice and humans.* Diabetes (2011) 60: 669-679.

[50] Koscsó, B., et al. *Stimulation of A_{2B} adenosine receptors protects against trauma–hemorrhagic shock-induced lung injury.* Purinergic Signal. (2013) 1-6.

[51] Volpini, R., et al. *Medicinal chemistry and pharmacology of A_{2B} adenosine receptors.* Curr. Top. Med. Chem. (2003) 3: 427-443.

[52] Bot, I., et al. *Adenosine A_{2B} Receptor Agonism Inhibits Neointimal Lesion Development After Arterial Injury in Apolipoprotein E–Deficient Mice.* Artherioscl. Throm. Vas. (2012) 32: 2197-2205.

[53] Haskó, G., et al. *A_{2B} adenosine receptors in immunity and inflammation.* Trends Immunol. (2009) 30: 263-270.

[54] Ryzhov, S., et al. *Host A_{2B} Adenosine Receptors Promote Carcinoma Growth.* Neoplasia (2008) 10: 987-995.

[55] Koupenova, M., et al. *A_{2B} adenosine receptor regulates hyperlipidemia and atherosclerosis.* Circulation (2012) 125: 354-363.

[56] Sherbiny, F.F., et al. *Homology modelling of the human adenosine A_{2B} receptor based on X-ray structures of bovine rhodopsin, the β_2-adrenergic receptor and the human adenosine A_{2A} receptor.* J. Comput. Aided Mol. Des. (2009) 23: 807-828.

[57] Jacobson, K.A. and Gao, Z.-G. *Adenosine receptors as therapeutic targets.* Nat. Rev. Drug Disc. (2006) 5: 247-264.

[58] Muller, C. and Stein, B. *Adenosine receptor antagonists: structures and potential therapeutic applications.* Curr. Pharm. Des. (1996) 2: 501-530.

[59] Grenz, A., et al. *The reno-vascular A_{2B} adenosine receptor protects the kidney from ischemia.* PLoS Med (2008) 5: e137-e137.

[60] Holgate, S.T. *The Quintiles Prize Lecture 2004: the identification of the adenosine A_{2B} receptor as a novel therapeutic target in asthma.* Br. J. Pharmacol. (2005) 145: 1009-1015.

[61] Ahmed, K., et al. *Deorphanization of GPR109B as a receptor for the β-oxidation intermediate 3-OH-octanoic acid and its role in the regulation of lipolysis.* J. Biol. Chem.(2009) 284: 21928-21933.

[62] Offermanns, S., et al. *International Union of Basic and Clinical Pharmacology. LXXXII: nomenclature and classification of hydroxy-carboxylic acid receptors (GPR81, GPR109A, and GPR109B).* Pharmacol. Rev. (2011) 63: 269-290.

[63] Cai, T.Q., et al. *Role of GPR81 in lactate-mediated reduction of adipose lipolysis.* Biochem. Biophys. Res. Commun. (2008) 377: 987-991.

[64] Liu, C., et al. *Lactate inhibits lipolysis in fat cells through activation of an orphan G-protein-coupled receptor, GPR81.* J. Biol. Chem. (2009) 284: 2811-2822.

[65] Taggart, A.K., et al. *(D)-β-hydroxybutyrate inhibits adipocyte lipolysis via the nicotinic acid receptor PUMA-G.* J. Biol. Chem. (2005) 280: 26649-26652.

[66] Ahmed, K., et al. *Deorphanization of GPR109B as a receptor for the β-oxidation intermediate 3-OH-octanoic acid and its role in the regulation of lipolysis.* J. Biol. Chem. (2009) 284: 21928-21933.

[67] Blad, C.C., et al. *Biological and pharmacological roles of HCA receptors.* Adv. Pharmacol. (2011) 62: 219.

[68] Offermanns, S. *Free fatty acid (FFA) and hydroxy carboxylic acid (HCA) receptors.* Annu. Rev. Pharmacol. Toxicol. (2014) 54: 407-434.

[69] Bobileva, O., et al. *Synthesis and evaluation of (E)-2-(acrylamido) cyclohex-1-enecarboxylic acid derivatives as HCA1, HCA2, and HCA3 receptor agonists.* Bioorg. Med. Chem. (2014) 22: 3654-3669.

[70] Offermanns, S., et al. *International Union of Basic and Clinical Pharmacology. LXXXII: nomenclature and classification of hydroxy-carboxylic acid receptors (GPR81, GPR109A, and GPR109B).* Pharmacol. Rev. (2011) 63: 269-290.

[71] Raghavan, S., et al. *Tetrahydro anthranilic acid as a surrogate for anthranilic acid: Application to the discovery of potent niacin receptor agonists.* Bioorg. Med. Chem. Lett. (2008) 18: 3163-3167.

[72] Ahmed, K., Tunaru, S., and Offermanns, S. *GPR109A, GPR109B and GPR81, a family of hydroxy-carboxylic acid receptors.* Trends Pharmacol. Sci. (2009) 30: 557-562.

[73] Lukasova, M., et al. *Nicotinic acid inhibits progression of atherosclerosis in mice through its receptor GPR109A expressed by immune cells.* J. Clin. Invest. (2011) 121: 1163.

[74] Hanson, J., et al. *Role of HCA_2 (GPR109A) in nicotinic acid and fumaric acid ester-induced effects on the skin.* Pharmacol. Ther. (2012) 136: 1-7.

[75] Tai, Y.F., et al. *Imaging microglial activation in Huntington's disease.* Brain Res. Bull. (2007) 72: 148-151.

[76] Amor, S., et al. *Inflammation in neurodegenerative diseases.* Immunology (2010) 129: 154-169.

[77] Blad, C.C., et al. *G protein-coupled receptors for energy metabolites as new therapeutic targets.* Nat. Rev. Drug Disc. (2012) 11: 603-619.

[78] Gille, A., et al. *Nicotinic acid: pharmacological effects and mechanisms of action.* Annu. Rev. Pharmacol. Toxicol. (2008) 48: 79-106.

[79] Bodor, E. and Offermanns, S. *Nicotinic acid: an old drug with a promising future.* Br. J. Pharmacol. (2008) 153: S68-S75.

[80] Davidson, M.H. *Niacin use and cutaneous flushing: mechanisms and strategies for prevention.* Am. J. Cardiol. (2008) 101: S14-S19.

[81] Shen, H.C. and Colletti, S.L. *Novel patent publications on high-affinity nicotinic acid*

receptor agonists. Expert. Opin. Ther. Pat. (2009) 19: 957-967.

[82] Zorman, S., et al. *Advances and challenges of membrane–protein complex production.* Curr. Opin. Struct. Biol. (2015) 32: 123-130.

[83] He, Y., et al. *The recombinant expression systems for structure determination of eukaryotic membrane proteins.* Protein & cell (2014) 5: 658-672.

[84] Engelberg, D., et al. *Transmembrane signaling in Saccharomyces cerevisiae as a model for signaling in metazoans: State of the art after 25 years.* Cell. Signalling (2014) 26: 2865-2878.

[85] Minic, J., et al. *Yeast system as a screening tool for pharmacological assessment of g protein coupled receptors.* Curr. Med. Chem. (2005) 12: 961-969.

[86] Brown, A.J., et al. *Functional coupling of mammalian receptors to the yeast mating pathway using novel yeast/mammalian G protein α subunit chimeras.* Yeast (2000) 16: 11-22.

[87] Price, L.A., et al. *Functional coupling of a mammalian somatostatin receptor to the yeast pheromone response pathway.* Mol. Cell. Biol. (1995) 15: 6188-6195.

[88] Stevenson, B.J., et al. *Constitutive mutants of the protein kinase STE11 activate the yeast pheromone response pathway in the absence of the G protein.* Genes Dev.(1992) 6: 1293-1304.

[89] Nomoto, S., et al. *Regulation of the yeast pheromone response pathway by G protein subunits.* EMBO J. (1990) 9: 691.

[90] S. Dong, S.C.R., B.L. Roth. *Directed molecular evolution of DREADDs: a generic approach to creating next generation RASSLs.* Nat. Protoc. (2010) 5: 561-573.

[91] Dowell, S.J. and Brown, A.J. *Yeast assays for G protein-coupled receptors*, in *G Protein-Coupled Receptors in Drug Discovery*. (2009) Springer. 213-229.

Chapter 2

Human G protein-coupled receptor studies in *Saccharomyces cerevisiae*

This chapter is a slightly modified version of:

Liu, R., Wong, W., IJzerman, A. P.

Biochemical Pharmacology. ***2016*** *114: 103-115*

Abstract

G protein-coupled receptors (GPCRs) are one of the largest families of membrane proteins, with approximately 800 different GPCRs in the human genome. Signalling via GPCRs regulates many biological processes, such as cell proliferation, differentiation, and development. Moreover, many hormones and neurotransmitters are ligands for these receptors, and hence it is not surprising that many drugs, either mimicking or blocking the action of the bodily substances, have been developed. It is estimated that 30-40% of current drugs on the market target GPCRs. Further identifying and elucidating the functions of GPCRs will provide opportunities for novel drug discovery. The budding yeast *Saccharomyces cerevisiae (S. cerevisiae)* is a very important and useful platform in this respect. There are many advantages of using a yeast assay system, as it is a cheap, safe and stable; it is also convenient for rapid feasibility and optimization studies. Moreover, it offers "null" background when studying human GPCRs. New developments regarding human GPCRs expressed in a yeast platform are providing insight into GPCR activation and signalling, and facilitate agonist and antagonist identification. In this chapter we summarize the latest findings regarding human G protein-coupled receptors in studies using *S. cerevisiae*, ever since the year 2005 when we last published a review on this topic. We describe 11 families of GPCRs in detail, while including the principles and developments of each yeast system applied to these different GPCRs and highlight and generalize the experimental findings of GPCR function in these systems.

Introduction

G protein-coupled receptors (GPCRs) constitute one of the largest families of proteins in the mammalian genome[1, 2]. In the human genome, approximately 800 GPCR sequences have been identified, a relatively large number of which the cognate ligands are still unknown for[3, 4].

GPCRs are activated by a wide variety of extracellular stimuli, such as neurotransmitters, hormones, and growth factors. Upon stimulation, GPCRs exert their role as surface signalling protein by transferring extracellular signals to target molecules in the cytosol or nucleus. Signalling via GPCRs regulates many biological processes, such as cell proliferation, differentiation, and development. They also are central players in (patho)physiologic conditions, such as immunity, blood pressure and kidney function.

GPCR signalling is initiated through receptor activation by an agonist. The conformational change caused by agonist binding allows the GPCR to recruit an associated G protein by acting as a guanine nucleotide exchange factor on the α-subunit of the G protein[5]. Subsequent exchange of GDP for GTP in this subunit causes the other subunits of the G protein, G_{β} and G_{γ}, to dissociate as a $\beta\gamma$-dimer. Both G_{α}-GTP and $G_{\beta\gamma}$ can modulate various cellular signalling pathways, including regulation of adenylate cyclases, phospholipases and the mitogen-activated protein kinase (MAPK) pathway, ultimately leading to expression of target genes[6]. In mammals, several isoforms of each subunit are expressed, many of which have splice variants, resulting in a great amount of combinations of G proteins. Four main classes of these heterotrimeric G proteins are defined based on the sequence and function of their α-subunit: $G_{\alpha s}$, $G_{\alpha q}$, $G_{\alpha i}$, and $G_{\alpha 12}$[6].

The downstream effects of GPCR stimulation depend on the type of GPCR which is activated. Members of the GPCR superfamily share the same basic architecture of 7 transmembrane (7TM) α-helices, an extracellular N-terminal segment and an intracellular C-terminal tail. The 7TM α-helices are connected by three intracellular (IL1, IL2, and IL3) and three extracellular (EL1, EL2, and EL3) loops[7]. Based on their sequence homology, human GPCRs are

divided into five main families in the GRAFS classification system: glutamate, rhodopsin, adhesion, frizzled/taste2, and secretin[3].

Their key roles in diverse cellular signalling pathways have made GPCRs major targets of many drugs. Identifying and elucidating the functions of GPCRs will provide opportunities for further drug discovery.

However, the GPCR signalling system in mammalians is elaborate, and using mammalian host cells to study GPCR signalling is relatively time-consuming. Functional characterisation of GPCRs and their mutants in mammalian expression systems is problematic because of the abundance of endogenous receptors for their ligands, and can be expensive. On the other hand, yeast cells provide a useful and relatively cost-effective model system in which to analyse GPCRs.

Description of the research domain

The budding yeast *S. cerevisiae* is an attractive host cell system for the study of GPCR signalling, for which only two pathways have been identified in this organism. One of the GPCR signalling pathways affects glucose sensing, whereas the other is involved in mating[8]. Glucose sensing requires the yeast G protein-coupled receptor-1 (Gpr1) and the G_{α} protein Gpa2, which is coupled to Gpr1. Activation of the receptor leads to production of cyclic adenosine monophosphate (cAMP), which – via protein kinase A (PKA) – stimulates diverse cell responses, such as growth, stress resistance, and storage of carbohydrates.

Mating is activated by α-factor pheromone and a-factor pheromone binding to the α-factor receptor (Ste2p) and a-factor receptor (Ste3p), respectively. Yeast of the a-cell type expresses a-factor pheromone and Ste2p, while the α-cell type expresses α-factor and Ste3p. During mating, pheromone binding to either receptor activates the MAPK pathway through the G_{α} protein Gpa1, which results in cell cycle arrest. Thus, haploid yeast cells encode a single endogenous GPCR (Ste2p or Ste3p) capable of activating the transduction pathway. The use of yeast as a host system prevents signalling cross-talk and activation of intrinsic GPCRs, as this endogenous GPCR in yeast can be deleted and replaced with

a mammalian GPCR. Additional advantages of using yeast systems to analyse GPCRs include their rapid growth, simplicity, low cost of culturing, and ability to be manipulated robotically.

For these reasons, yeast has proven a useful system for the study of human GPCRs. The first heterologous GPCR to be coupled to this pheromone pathway in yeast was the human β_2-adrenergic receptor (hβ-AR)[9]. In 1990, King and colleagues achieved this by replacing the yeast Ste2 gene with a modified hβ-AR gene, and placing it under control of the galactose-inducible GAL1 promoter. Induction with galactose yielded functional hβ-AR expression. However, interaction of Gpa1 in yeast appears to be efficient with only several human GPCRs. The subsequent creation of chimeric Gpa1 subunits, in which the C-terminal 5 amino acid residues of yeast Gpa1 are replaced by the equivalent residues of the mammalian G_α protein, advanced coupling to different receptors[10, 11]. The creation of this chimeric Gpa1/G_α transplant enabled cell-based functional yeast assays to be performed in a eukaryotic host free from endogenous responses.

Mutagenesis studies have been used to identify functionally important residues, motifs, and domains within the GPCR structure. Techniques to introduce mutations into GPCRs range from site-directed to random mutagenesis. In site-directed mutagenesis, selective point mutations are introduced to reveal the importance of the respective amino acid. Random mutagenesis produces large numbers of mutants, for which additional selection assays are required to identify the mutations of interest.

Incorporation of a reporter gene, such as green fluorescent protein (GFP) or lacZ, and growth selection marker HIS3, facilitates the detection of downstream G protein signalling. LacZ encodes β-galactosidase, which is responsible for cleavage of X-gal to yield a colored product. HIS3 encodes an enzyme that is involved in the production of histidine, an essential amino acid for yeast growth. In cell culturing, this allows the selection of cells which survive in histidine-deficient medium. When these reporter genes are put under the control of a pheromone-responsive promoter, such as FUS1 or FUS3, production of the transcripts of these genes could be coupled to the endogenous yeast GPCR

signalling pathway.

The combination of mutagenesis studies and human GPCR expression in yeast is applied in high-throughput approaches to identify agonists, antagonists, and allosteric modulators of both known GPCRs and orphan receptors. In this context, Beukers and IJzerman reviewed and highlighted the use of random mutagenesis combined with a functional screening assay in yeast, in 2005[12]. Considering their major contribution in signal transduction from ligand to effector via G proteins, GPCRs remain interesting targets for research in the present and future. Better understanding of the fundamental processes underlying ligand binding and receptor activation of GPCRs is of major importance for identifying potential targets for the development of new therapeutic agents.

Developments since 2005

In the past decade, yeast cells have served as a robust platform for structural and functional studies of human GPCRs. In this chapter, discoveries since 2005 concerning different family members of human GPCRs will be described.

Adenosine receptors

Adenosine, a purine nucleoside, is a key endogenous molecule in regulation of immune and inflammatory systems[13]. The purine nucleoside is found in low levels in unstressed, healthy tissues. Under conditions of metabolic stress and cell damage, adenosine is accumulated in the extracellular space. Adenosine is capable of activating four different adenosine receptors: A_1, A_{2A}, A_{2B}, and A_3. All the adenosine receptors are ubiquitously expressed throughout the human body[14].

Adenosine A_1 receptor

Stewart and colleagues used yeast as a system to determine the relative efficacies of agonists and affinity values for both agonists and antagonists of the adenosine A_1 receptor[15]. For this purpose, *S. cerevisiae* strains expressing chimeric Gpa1/

G_{α} were transformed with a human adenosine A_1 receptor construct. Chimeras of Gpa1/$G_{\alpha q}$, Gpa/$G_{\alpha 12}$, Gpa1/$G_{\alpha o}$, Gpa1/$G_{\alpha i1/2}$, Gpa1/$G_{\alpha 3}$, and Gpa1/$G_{\alpha 5}$ were used in combination with the lacZ reporter gene, under the control of the FUS1 promoter. β-Galactosidase activity was measured using a fluorescent substrate to determine the ability of the agonists R-PIA and VCP-189 to elicit a response when coupled to an individual subtype of G protein. Results of these yeast signalling assays revealed that R-PIA was a high-efficacy agonist when coupled to $G_{\alpha o}$, $G_{\alpha i1/2}$, or $G_{\alpha i3}$ (Fig. 1, ●), whereas VCP-189 was a lower-efficacy partial agonist when coupled to $G_{\alpha i}$ proteins (Fig. 1, ▲). Validation of $G_{\alpha i/o}$ coupling preferences was further performed in Chinese hamster ovary cells expressing the human A_1 receptor.

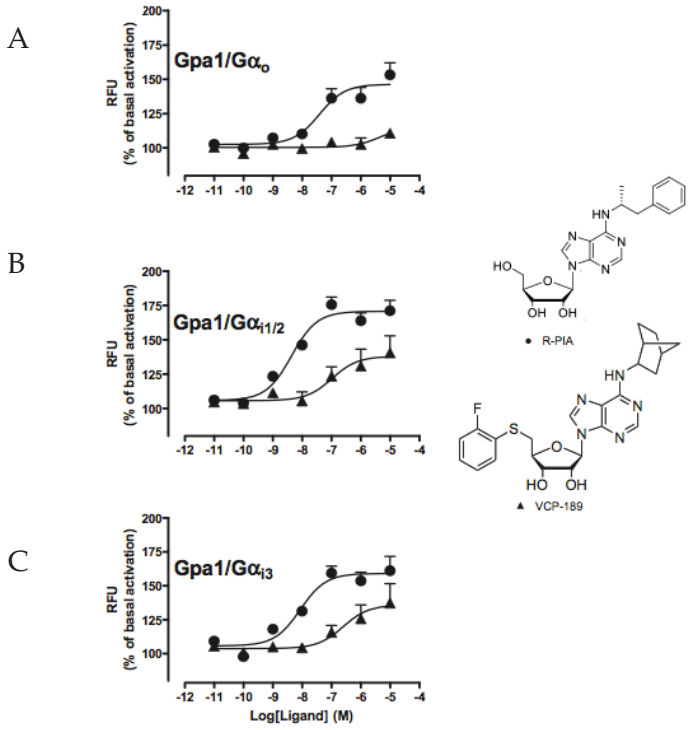

Fig. 1. Influence of G protein subtype on R-PIA and VCP-189 response. Yeast strains expressing the adenosine A_1 receptor with Gpa1/$G_{\alpha o}$ (A), Gpa1/$G_{\alpha i1/2}$ (B), or Gpa1/$G_{\alpha i3}$ (C) were incubated with a range of ligand concentrations for 18 to 24h. Ligand response is expressed in relative fluorescence unit (RFU) corrected for the fluorescence in the absence of ligand. Data points represent mean ± SEM obtained from three to five experiments performed in duplicate. *Reproducted with permission from* [15].

In addition to the G_α subunit, domains in the adenosine A_1 receptor itself also influence signalling activity. Within the GPCR structure, the intracellular and extracellular loop regions that connect the seven transmembrane domains are highly variable in length and sequence. In this context, the role of the second and third extracellular loops of the human adenosine A_1 receptor in activation and allosteric modulation was examined[16]. The *S. cerevisiae* expression vector containing the human adenosine A_1 receptor gene was used for mutagenesis. The second extracellular loop (EL2) was subjected to an $(Ala)_3$-scan, in which consecutive sets of three amino acids were replaced by alanine residues. On EL2 and the third extracellular loop (EL3), site-directed mutagenesis was performed too by introducing single alanine mutations to the loops. Plasmids containing the human adenosine A_1 receptor gene were transformed into a *S. cerevisiae strain*, which harbors chimeric Gpa1/$G_{\alpha i3}$ and is coupled to the FUS1-HIS3 reporter gene system. As an indicator of receptor activity, yeast growth in histidine-deficient medium was observed for the mutant receptors after agonist stimulation. In radioligand binding experiments, affinity of the mutant receptors for agonist CPA in the presence of radiolabeled antagonist DPCPX was explored. To investigate the sensitivity of the mutants to allosteric modulation, radioligand binding experiments were performed with agonist CPA in the presence of allosteric modulator PD81,723. Results of this study revealed the importance of many residues in the second and third extracellular loops in human adenosine A_1 receptor activation, since single point mutations affected the potency of CPA for the adenosine A_1 receptor. $W156^{EL2}$ and $E164^{EL2}$ were identified to be involved in allosteric modulation. After mutation to alanine in $W156^{EL2}$, PD81,723 lost its ability to enhance CPA potency, whereas mutation of $E164^{EL2}$ increased the effect of PD81,723 on CPA affinity. These data suggest that the binding site for PD81,723 is located in or close to the extracellular domains of the A_1 receptor.

Adenosine A_{2B} receptor

In chapter 3 of this thesis, we analysed the interaction between the low affinity adenosine A_{2B} receptor and the C-terminus of G_α subunits[17]. Plasmids containing the wild-type and mutant human adenosine A_{2B} receptor were transformed into

engineered *S. cerevisiae* yeast strains expressing different Gpa1/G_{α} chimeras. The FUS1-HIS3 reporter gene system enabled determination of G protein coupling and activation via observation of yeast growth after exposure to agonist 5'-*N*-ethylcarboxamido-adenosine (NECA). A tyrosine at the C-terminus of the G_{α} subunit was revealed to be essential in controlling A_{2B} receptor activation. In the receptor, R103$^{3.50}$ and I107$^{3.54}$ mutation to alanine eliminated receptor activation, whereas L213^{IL3} mutation to alanine improved coupling efficiency in all yeast strains. The S235$^{6.36}$A mutant receptor showed the most divergent humanized G protein coupling profile and substitution of L236$^{6.37}$ decreased receptor activation in all yeast strains representing the different G protein pathways. In chapter 4 of this thesis, we used the same 'a single-GPCR-one-G protein' yeast system to screen for key residues within the NPxxY(x)$_6$F motif and in helix 8 of the adenosine A_{2B} receptor[18]. Each residue was mutated to alanine through site-directed mutagenesis. Four mutants P287$^{7.50}$A, Y290$^{7.53}$A, R293$^{7.56}$A and I304$^{8.57}$A showed a complete loss of function.

Li et al. were the first to describe inverse agonists for the human adenosine A_{2B} receptor. Constitutively active mutants (CAMs) are mutant receptors that show basal activity independent of an agonist, and provide a useful tool to discriminate inverse agonists from neutral antagonists. The use of CAMs with varying levels of constitutive activity enabled determination of differences in relative intrinsic efficacy values of the three inverse agonists ZM241385, DPCPX, and MRS1706[19]. For this purpose, an engineered *S. cerevisiae* strain expressing chimeric Gpa1/$G_{\alpha i3}$ in combination with the FUS1-HIS3 reporter gene system was used. Nine CAMs were identified from a random mutation bank using yeast growth assays, which were used as screening tools to discover inverse agonists. The three compounds ZM241385, DPCPX, and MRS1706 were able to inactivate the constitutively active human adenosine A_{2B} receptor mutants, thus acting as inverse agonists on these CAMs. Consequently, these three compounds were defined as inverse agonists on the human adenosine A_{2B} receptor. The effects of the three inverse agonists on the A_{2B} receptor were dependent on the level of constitutive activity of the mutants. Two high-level CAMs appeared locked in an active state and were insensitive to the three inverse agonists. Three intermediate-

level CAMs were partially inhibited, whereas four low-level CAMs were almost completely inhibited.

The role of distinct domains within the adenosine A_{2B} receptor was examined in several studies. The first extracellular loop was selected to perform successive mutagenesis experiments to analyze changes in agonist potency, constitutive activity, and intrinsic activity[20]. Plasmids containing the human adenosine A_{2B} receptor gene were transformed into an *S. cerevisiae* strain, which was engineered to express chimeric Gpa1/$G_{\alpha i3}$. As mentioned before, the use of the FUS1-HIS3 reporter gene system enabled growth as a readout for receptor activity. First, random mutations were introduced in the fragment encoding for the first three transmembrane domains, the first extracellular loop, the first intracellular loop, and part of the second intracellular loop of the human A_{2B} receptor. The random mutagenesis screen revealed the involvement of $F71^{EL1}$ and $D74^{EL1}$ in receptor activation. Site-directed mutagenesis on these residues, and a subsequent yeast growth assay showed altered potency of agonist NECA. Additionally, the mutant receptors responded to the inverse agonist ZM241385 which suppressed constitutive activity. Then, site-saturation mutagenesis was performed on the respective positions in the first extracellular loop of the GPCR. Phenylalanine substitution at position 71 by serine, arginine, alanine, or glycine resulted in the largest decrease in potency and maximum intrinsic activity. Activation profiles of aspartic acid substitution at position 74 showed large variations. Remarkably, substitution at this position by glutamine, glutamic acid, asparagine or serine caused an increase in potency and constitutive activity. Radioligand binding assays revealed that almost all mutated receptors showed similar binding of the antagonist PSB603, indicating a similar expression level.

Using the same yeast strain, MMY24, random mutagenesis was performed on the fragment encoding the extracellular loop 2 (EL2) and its two adjacent transmembrane domains (TM4 and TM5) of the human adenosine A_{2B} receptor. By simply changing the concentration of the histidine synthesis inhibitor 3-AT and the introduction of a specific time frame, Peeters et al. mapped the residue locations of constitutively active mutants (CAMs)[20] and constitutively inactive mutants (CIMs) of the TM4-EL2-TM5 area[21]. For CAMs screening, 1 nM NECA

was used with 7 mM 3-AT and clones were picked up after three days. This yielded 12 different CAM mutant receptors with increased agonist potency containing mutations located at the top of TM4, in a cysteine-rich region of EL2, and at the bottom half of TM5. Among the mutant receptors, residues F141$^{4.61}$, C167^{EL2}, and Y202$^{5.58}$ were found to be mutated multiple times, indicating an essential role of these residues in A_{2B} receptor activation mechanisms. Substitution of Y202$^{5.58}$ by an asparagine residue resulted in a 38-fold increase as compared to the wild-type receptor. Substitution of F141$^{4.61}$ with leucine resulted in a 25-fold increase in potency for NECA compared with the wild-type receptor, as assessed by yeast growth assays. Moreover, radioligand binding assays revealed a 13-fold increase in NECA affinity compared with the wild-type receptor, suggesting an essential role of F141$^{4.61}$ in agonist binding. The CIM screening does not require the presence of an agonist or inverse agonist. At 1 mM 3-AT clones were picked up after 4 days and 6 days, identifying 22 CIMs containing a total of 25 different mutated amino acid positions that showed a decrease in constitutive activity as well as in agonist potency. Most CIMs were found in the top half of TM5 without a single CAM. However, a cluster of CAMs is found in EL2 without containing any CIMs. Interestingly, six residues, I136$^{4.56}$, F141$^{4.61}$, S146^{EL2}, T155^{EL2}, F173^{EL2} and Y202$^{5.58}$ were found in both CAM and CIM screening. These residues are most likely crucial players in activation or inactivation of the adenosine receptor. In this perspective CIMs and CAMs could correspond to the receptor in different conformational states.

Adenosine A_{2A} receptor

O'Malley et al. demonstrated a method for the production, purification, and characterisation of the human adenosine A_{2A} receptor[22]. For this purpose, human A_{2A} receptor, whether or not fused to GFP, was re-engineered with a C-terminal deca-histidine tag, and plasmids containing this vector were transformed into a *S. cerevisiae* strain. Facilitated by the presence of the attached GFP, yeast cells were screened for their ability to express the tagged A_{2A} receptor, and subsequently lysed to solubilise the A_{2A} receptor. Several purification steps, which included immobilized metal affinity chromatography, yielded purified and stabilised A_{2A}

receptor. Sufficient quantities of the receptor were obtained for spectroscopic studies, which confirmed that the A_{2A} receptor structure is largely α-helical.

For a better understanding of why many receptors improperly traffick or are inactive in heterologous expression systems, expression of 12 human GPCRs in *S. cerevisiae* was investigated[23]. Plasmids containing one of these 12 human GPCRs from the rhodopsin family, and an additional GFP-tag, were transformed into a yeast strain. Of these GPCRs, only the adenosine A_{2A} receptor was active in terms of ligand binding and was located primarily at the plasma membrane, as observed by radioligand binding assays and confocal imaging, respectively. The extent of leader sequence cleavage, which reflects processing and trafficking of the expressed GPCRs, was determined through a mobility shift experiment of GFP-tagged receptors. The A_{2A} and A_{2B} receptor were the only receptors to demonstrate both leader sequence processing and activity, indicating that translocation is a critical limiting step in the production of active human GPCRs in *S. cerevisiae*.

The yeast system is also used for screening thermostabilising mutations, which can improve the overall stability of receptor proteins to eventually obtain high-resolution crystal structures of GPCRs. Analysis of the mutations alone and in combination using the yeast assay, together with the known $A_{2A}R$ crystal structures provides information on the role of individual amino acids in receptor function. Bertheleme et al. found $R199^{5.60}$ and $L208^{IL3}$ play key roles in A_{2A} receptor function using the yeast cell growth assay in the MMY24 strain[24], as these mutations abolished constitutive activity of the A_{2A} receptor; In contrast, the $F79^{3.31}A$ mutation increased constitutive activity, potency and efficacy of the receptor, most likely at the expense of receptor stability.

Somatostatin receptor 5

The somatostatin receptor 5 (SSTR5) is a member of the γ-group of rhodopsin receptors in the GRAFS classification system of GPCRs[3]. Somatostatin is a cyclic neuropeptide known as a growth hormone release-inhibiting factor. Somatostatin regulates the human endocrine system by binding to somatostatin receptors (SSTRs), of which five subtypes have been identified: SSTR1-SSTR5[25,26]. Among

these subtypes, SSTR2 and SSTR5 predominantly regulate growth hormone secretion in acromegaly patients, and are expressed in the majority of growth hormone secreting tumors[27].

Several research groups used the human SSTR5 receptor as a model for a human GPCR. Iguchi et al. performed site-directed mutagenesis of asparagine residues on the two N-linked glycosylation motifs in the extracellular N-terminal domain of human SSTR5[28]. These Asn residues had been shown to be important for ligand affinity, and for plasma membrane localisation and signalling, as mutation of the Asn residues affected somatostatin ligand binding and adenylate cyclase activity in rat[29]. In the mutagenesis study, *S. cerevisiae* was used as a host to examine the effects of substitution of the $N13^{N\text{-term}}$ and $N26^{N\text{-term}}$ residues by alanine residues[28]. Enhanced green fluorescent protein (EGFP) was fused to the human SSTR5. Results showed the importance of these asparagine residues of the human SSTR5 receptor in signalling, since substitution significantly decreased signalling activity.

For agonist detection of human GPCRs, researchers continued to use SSTR5 as a model receptor[30]. The strategy of a feedback signal activation system was used to analyse agonist stimulation of GPCRs. It was aimed to express both the GFP reporter gene and G_β after G protein activation by agonist binding to a given GPCR. A *S. cerevisiae* strain with overexpression of the STE4 gene, which encodes for the yeast G_β, under the control of FIG1 promoter, was created. Overexpression of G_β was expected to result in the generation of free $G_{\beta\gamma}$ dimers, as a consequence of competing with endogenous γ-associated β subunits for binding to G_α. The free $G_{\beta\gamma}$ dimers were able to amplify the human yeast-coupled G protein signal. This feedback signal activation system resulted in MAPK cascade activation by $G_{\beta\gamma}$, and subsequent amplification of GFP expression. This high-sensitivity method for the detection of agonist activity of human GPCRs in yeast was applied to human SSTR5. Therefore, IMFD-70 and IMFD-70B yeast strains were transformed with plasmids expressing human SSTR5, exposed to different concentrations of somatostatin, and subjected to a transcription assay using the GFP fluorescent reporter gene. GFP fluorescence intensity induced by human SSTR5 in the feedback activation strain (IMFD-70B; Fig. 2, ●) was higher

than in the common activation strain (IMFD-70; Fig. 2, ▲) at all somatostatin concentrations tested. Interestingly, fluorescence intensity induced by human SSTR5 in the common activation strain (Fig. 2, ▲) was found to be lower compared with the fluorescence intensity induced by Ste2p (Fig. 2, Δ), whereas the intensities of the Ste2p (Fig. 2, ○) and SSTR5 (Fig. 2, ●) feedback activation strain were equivalent. These results suggest an improvement of agonist signal detection and SSTR5 response sensitivity by feedback signal activation.

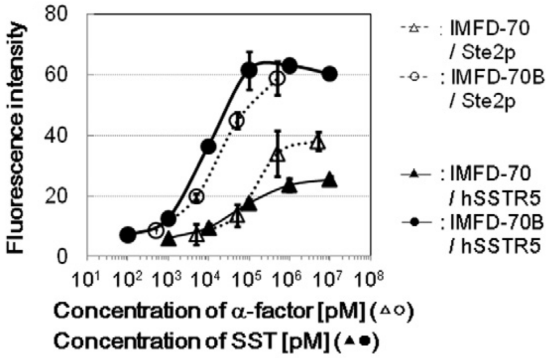

Fig. 2. Concentration-response curves of common and feedback activation strains of yeast expressing human SSTR5 in response to somatostatin. Yeast strains were transformed with plasmids containing human SSTR5, grown in SDM71 medium, and incubated with different concentrations of somatostatin for 18h. Fluorescence intensity of common activation strain (IMFD-70/hSSTR5) and the feedback signal activation strain (IMFD-70B/hSSTR5) in response to increasing somatostatin concentrations are displayed. The concentration-response curves of the corresponding yeast strains harboring Ste2p are presented by dashed lines. Data points represent fluorescence intensities of 10,000 cells defined as the geometric mean ± standard deviation (*n = 3*). *Reproduced with permission from* [30].

Researchers from the same department demonstrated somatostatin-specific signalling functions of human SSTR5 by addition of prepro- and pre-regions of α-factor, and a 20 amino acid N-terminal signalling sequence of yeast Ste2 (Ste2N) to the N-terminus of human SSTR5[31]. Additionally, the C-terminal 5 amino acid residues of Gpa1 were replaced by the equivalent residues of the human $G_{\alpha i3}$ to create a chimeric Gpa1/$G_{\alpha i3}$ transplant. Then, a yeast-based fluorescent signalling assay system that expresses the GFP reporter gene was used for evaluation of signalling activity of SSTR5 and response to somatostatin binding. Since the potency of somatostatin for native SSTR5 was lower than for

Ste2N-SSTR5, introduction of this yeast signal sequence apparently increased ligand sensitivity. Lastly, SSTR5 expression levels and localisation were examined using a cyan fluorescent protein tag, fused to the SSTR5 C-terminus. Ste2N-SSTR5 seemed to improve localisation to the plasma membrane as well, suggesting that SSTR5 was transported by different protein sorting pathways in the presence of the signalling sequence.

To improve identification of signal promotion by $G_{\alpha i}$-specific human GPCRs using flow cytometry, SSTR5 served as a model for heterologous GPCRs expressed in engineered *S. cerevisiae* yeast cells[32]. For this purpose, human SSTR5 was expressed from a multicopy episomal plasmid under the control of the PGK1 promoter, for substitution of yeast Ste2p. Chimeric Gpa1/$G_{\alpha i3}$ was used as replacement of yeast Gpa1. The GFP gene was again used as a reporter under the control of the FIG1 promoter, and somatostatin was added to the engineered yeast cells. To determine SSTR5 signalling via $G_{\alpha i}$, GFP fluorescence was measured using flow cytometry. In addition, several genes in yeast were deleted to improve flow cytometric separation. Sst2p, a Gpa1-specific GTPase-activating protein, was deleted to confer hypersensitivity to agonists. The FAR1 gene, which encodes a cyclin-dependent kinase inhibitor and mediates cell cycle arrest, was deleted to allow the recovery of episomal plasmids from signal-activated yeast cells, which is important for extensive screening. The constructed IMFD-72 strain, which contains the mentioned alterations, enabled improved flow cytometric separation to identify signal transduction mediated by the human SSTR5.

Recently, Nakamura and colleagues developed a method to simultaneously detect dimerisation and signalling of GPCRs in *S. cerevisiae* by a dual-color reporter system[33]. Two fluorescent proteins with distinct emission peaks, EGFP and DsRed-Express2 (E2-Crimson), were expressed under the control of the PGK1 promoter. Fluorescence signals were measured in yeast cells harboring these plasmids, and could be completely distinguished by flow cytometry. For the split-ubiquitin two-hybrid system, yeast strains were constructed to express E2-Crimson in response to the release of artificial transcription factor LexA-VP16 by ubiquitin-specific proteases. These proteases

recognize the NubG/Cub complex, which is formed by fusion of the proteins to which these two split tags (NubG and Cub) are attached. Based on this principle, this method permits detection of GPCR dimerisation. The yeast-based signalling assay, using EGFP, to study GPCR signalling was combined with the split-ubiquitin two-hybrid system to detect dimerisation and signalling simultaneously. The technique was validated by monitoring simultaneous homo- and hetero-dimerisation and somatostatin-induced signalling in human SSTR5. For this purpose, yeast strains co-expressing SSTR5-Cub-LexA-VP16 and various GPCR-NubG were exposed to somatostatin, and fluorescence was measured by flow cytometry (Fig. 3). Regarding GPCR dimerisation, cells co-expressing SSTR5-Cub-LexA-VP16 and SSTR2-NubG or ADRB2-NubG showed E2-Crimson fluorescence, while cells co-expressing SSTR5-Cub-LexA-VP16 and Ste2p-NubG and the mock control cells did not show E2-Crimson fluorescence (Fig. 3A). Regarding GPCR signalling, all cells displayed somatostatin-induced EGFP fluorescence, without significant difference between the groups (Fig. 3B). According to these results, SSTR5 could heterodimerise with SSTR2 and the β_2-adrenergic (ADRB2) receptor, which has no effect on signalling activity after somatostatin exposure.

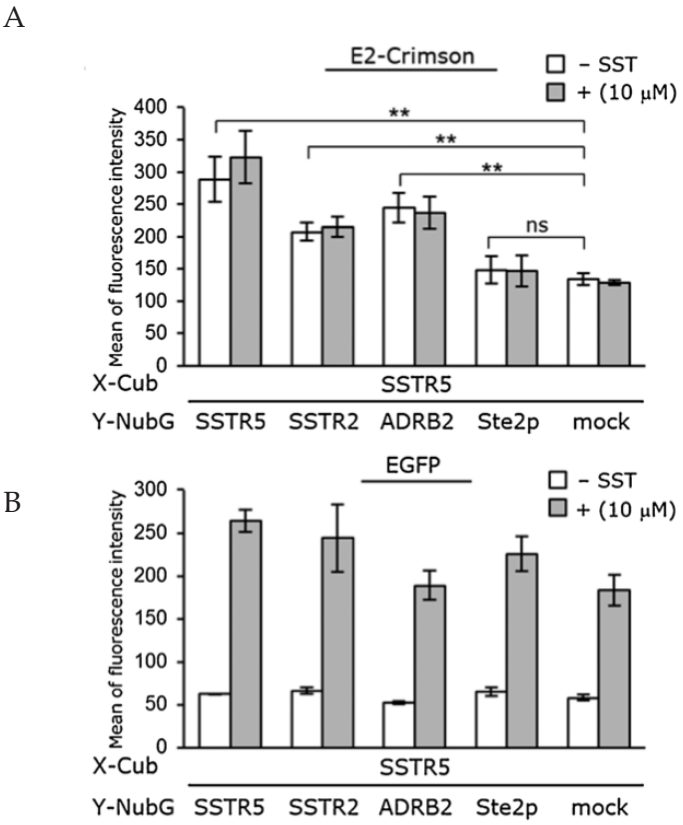

Fig. 3. Simultaneous detection of dimerisation and signalling by human SSTR5. Yeast strains were transformed with plasmids encoding various GPCR-NubG constructs ("Y-NubG") and SSTR5-Cub-LexA-VP16 ("X-Cub"), grown in SD selective medium for 18h, and incubated with or without 10μM somatostatin for 4h. Mock cells co-expressing SSTR5-Cub-LexA-VP16 and NubG served as negative control. E2-Crimson (A) and EGFP (B) fluorescence intensities of 10,000 cells were measured by flow cytometry. Values represent mean ± standard deviation. Statistical significance was assessed by the t-test (** $p < 0.01$; ns, not significant). SSTR5, somatostatin receptor 5; SSTR2, somatostatin receptor 2; ADRB2, β2-adrenergic receptor; Ste2p, yeast α-factor receptor. *Reproduced with permission from* [33].

Muscarinic acetylcholine receptor

The muscarinic acetylcholine receptors (mAChRs) are members of the biogenic amine receptor cluster of the α-group of rhodopsin receptors, according to the GRAFS classification system of GPCRs[3]. Acetylcholine, the first neurotransmitter identified, is released from vesicles in presynaptic nerve terminals and binds to either nicotinic (ion channels) or muscarinic receptors (GPCRs). Five subtypes of muscarinic acetylcholine receptors, M_1-M_5, have been

identified in human[34]. M_1, M_4, and M_5 mAChRs are predominantly expressed in the central nervous system, whereas M_2 and M_3 subtypes are expressed widely in the central nervous system and periphery[35, 36]. In the central nervous system, mAChRs regulate important central functions, including cognitive, behavioural, sensory, motor and autonomic processes. Peripheral mAChRs mediate acetylcholine-mediated decreases in heart rate, and increases in smooth-muscle contractility and glandular secretion. The muscarinic acetylcholine receptors are implicated in a variety of human diseases, including Alzheimer's disease, overactive bladder disorder, and chronic obstructive pulmonary disease[37].

Different *S. cerevisiae* strains expressing different Gpa1/G_{α} chimeras were coupled to the lacZ reporter gene for functional readout of M_3 mAChR ligands, previously established as orthosteric antagonists in mammalian cells[38]. The yeast strains were transformed with a vector containing the gene encoding a modified rat M_3 mAChR. Using this yeast platform, "antagonists" atropine and pirenzepine were found to be inverse agonists when the receptor was coupled to Gpa1/$G_{\alpha q}$, and low efficacy agonists when coupled to Gpa1/$G_{\alpha 12}$. This indicates functional selectivity at the M_3 mAChR. To validate these findings, studies with atropine were continued in mammalian 3T3 mouse embryonic fibroblasts expressing full-length human M_3 mAChR.

In an extended study, the applicability of this yeast platform to identify allosteric ligand-mediated functional G protein selectivity was tested[39]. For this purpose, the effect of brucine on carbachol affinity at the M_3 receptor was investigated. Results indicate that brucine is a partial allosteric agonist and positive modulator of carbachol when coupled to Gpa1/G_q, a positive modulator when coupled to Gpa1/G_{12}, and a neutral modulator when coupled to Gpa1/$G_{\alpha i1/2}$. For validation, human M_3 mAChR was further expressed in Chinese hamster ovary cells.

More recently, the X-ray crystal structure of active agonist-bound human M_2 mAChR was solved, and stabilised by a G protein mimetic nanobody for the M_2 receptors[40]. In this study, a *S. cerevisiae* strain was used for the conformational selection of these nanobodies for enhancement of the affinity of M_2 for its agonist iperoxo. Several selection rounds were performed with a post-

immune single variable domain nanobody complementary DNA library, which was constructed by PCR amplification and transformation into the yeast strain. Additionally, the X-ray crystal structure was solved for the M_2 receptor bound to both iperoxo and positive allosteric modulator LY2119620 in this research[40].

In another research group, Suharni et al. used *S. cerevisiae* as expression system to identify the epitope scFV 18A107 located in IL3 of the M_2 receptor[41]. A selected recombinant antibody fragment turned out to be highly specific for recognizing the M_2 receptor, because the amino acid sequence of scFV 18A107 does not exist in other mAChRs.

Neurotensin receptor type 1

The neurotensin receptor type 1 is a high-affinity neurotensin receptor, and belongs to the α-group of rhodopsin receptors in the GRAFS classification system for GPCRs[3]. Neurotensin is a tridecapeptide that acts as a neuromodulator of dopamine transmission in the nigrostriatal and mesocorticolimbic system of the central nervous system[42]. Peripherally, neurotensin plays a role in hormonal and neurocrine regulation in the gastrointestinal tract, including inhibition of small bowel motility and gastric acid secretions, and facilitation of fatty acid absorption[43]. Neurotensin exerts its effects by binding to neurotensin receptor type 1 (NTSR1), NTSR2, and NTSR3. Abnormal expression of NTSR1 during the early stages of cell transformation in relation with Wnt/β-catenin pathway deregulation is presumed to induce carcinogenesis[44, 45]. NTSR1 expression could serve as a prognosis marker in various types of cancer.

To monitor the activation of human NTSR1 signalling, a fluorescence-based microbial yeast biosensor was constructed[46]. Microbial *S. cerevisiae* strains IMFD-70, IMFD-72, and IMFD-74 were transformed with plasmids expressing human NTSR1. The constructed IMFD-74 strain expresses Gpa1/$G_{\alpha q}$ and harbors the same alterations as the IMFD-72 strain, in which the Gpa1/$G_{\alpha i3}$ transplant is expressed[32], whereas the IMFD-70 strain expresses intact Gpa1. GFP reporter gene under the control of FIG1 promoter was used to sense NTSR1 signalling in response to neurotensin peptide stimulation. The IMFD-74 (Fig. 4, □) strain induced higher fluorescence above 1 μM neurotensin peptide and relatively

lower fluorescence below 10 nM neurotensin peptide when compared to the IMFD-72 strain (Fig. 4, ∆). Moreover, the fluorescence levels induced by these two yeast strains, were higher than the fluorescence levels of IMFD-70 (Fig. 4, ○) at all concentrations of neurotensin peptide. According to these results, the use of the IMFD-74 yeast strain permitted convenient flow cytometric sensing of human NTSR1 signalling, induced by neurotensin, in yeast.

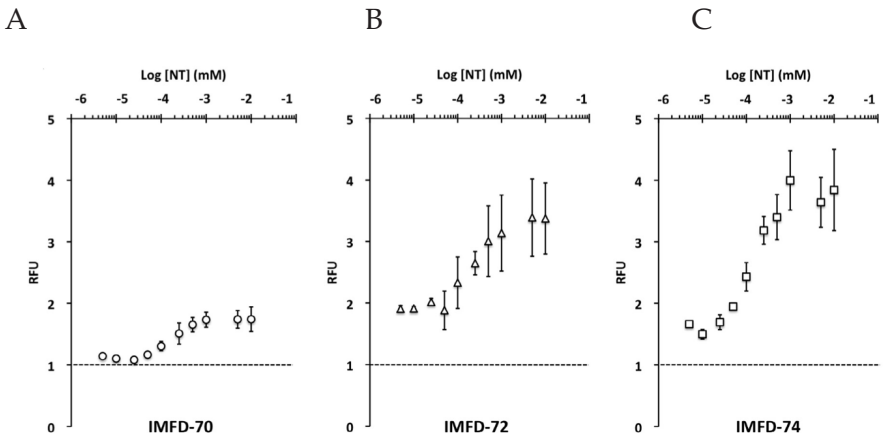

Fig. 4. Concentration-response curves for NTSR1 signalling after exposure to neurotensin peptide. Yeast strains IMFD-70 (A), IMFD-72 (B), and IMFD-74 (C) were incubated in SD selective medium containing various concentrations of neurotensin peptide for 10h. Data points represent relative fluorescence unit (RFU) ± standard deviation (*n = 3*). *Reproduced with permission from* [46].

Angiotensin II type 1 receptor

Angiotensin II (Ang II) type 1 receptor is a member of the rhodopsin receptors in the GRAFS classification system of GPCRs[3]. Ang II represents the primary effector molecule of the renin-angiotensin system, thus contributing to cardiovascular homeostasis[47, 48]. Ang II binds to two major subtypes of Ang II receptors, Ang II type 1 receptor (AGTR1) and Ang II type 2 receptor (AGTR2). However, most of the known physiological effects of Ang II are mediated by AGTR1, which is expressed in a variety of organ systems, including the heart, kidney, and brain[48].

Recently, Nakamura and colleagues investigated the functional activation of AGTR1-mediated signalling in yeast cells[49]. Interaction of $N295^{7.46}$ with $N111^{3.35}$

was suggested to play a role in determining the peptide binding selectivity of AGTR1 receptors[50, 51]. Therefore, a single alanine or serine mutation was introduced at $N295^{7.46}$ of human AGTR1, and the chimeric Gpa1/$G_{\alpha i3}$ transplant was used to enable functional activation of AGTR1 in *S. cerevisiae*. In this IMFD-72 strain, *Zoanthus* sp. green fluorescent protein (ZsGreen) reporter gene, under the control of the FIG1 promoter, was incorporated. The resulting IMFD-72ZsD yeast strain was exposed to Ang II and Ang II peptidic analogs which differ in affinity towards AGTR1. This resulted in successful signal transmission inside the yeast cell, as monitored using a fluorescence reporter assay. Subsequently, the IMFD-72ZsD yeast strains were transformed with the human $N295^{7.46}$-mutated ($N295^{7.46}$A and $N295^{7.46}$S) AGTR1 expression plasmids and peptide (Ang II and Ang III) expression plasmids. The yeast strain expressing AGTR1-$N295^{7.46}$A (Fig. 5, □) or AGTR1-$N295^{7.46}$S (Fig. 5, ■) and Ang II showed a 94-fold and 91-fold increase in ZsGreen fluorescence intensity, respectively, compared with the mock strain. Ang III induced a 36-fold and 45-fold increase in ZsGreen fluorescence intensity compared with the mock strain, for $N295^{7.46}$A (Fig. 5, □) or $N295^{7.46}$S (Fig. 5, ■), respectively. These results suggest that autocrine Ang II peptide and its analog, Ang III, produced and secreted by engineered yeast cells, can themselves promote AGTR1-mediated signalling.

C-X-C chemokine receptor type 4

CXCR4 is a member of the chemokine cluster of the γ-group of rhodopsin receptors, as classified by GRAFS[52]. Receptors for different types of chemokines (CC, CXC, C, and CX3C) are G protein-coupled receptors[53]. Whereas redundancy exists in the repertoire of chemokine- and receptor-binding activities, stromal cell-derived factor 1 (SDF-1/CXCL12) is the sole ligand for C-X-C chemokine receptor type 4 (CXCR4)[54]. CXCR4 is expressed on human hematopoietic stem cells, and plays a critical role in the development of B lymphocytes, the chemotaxis of lymphocytes, granulocytes and other inflammatory cells[52]. CXCR4 was the first coreceptor identified that was permissive for fusion and entry of human immunodeficiency virus type 1 (HIV-1) into $CD4^+$ human target

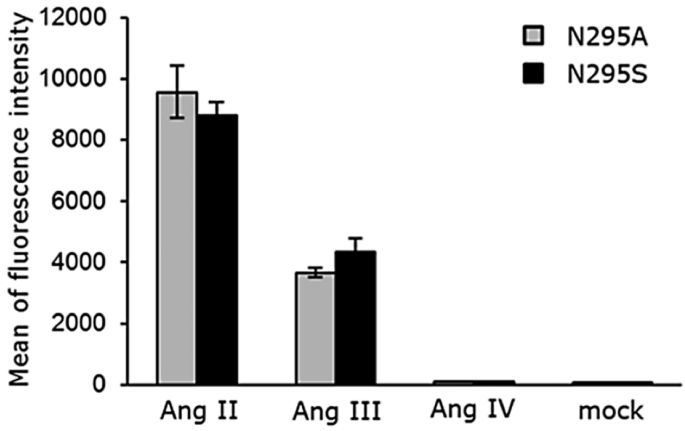

Fig. 5. Activation of human AGTR1 by agonistic peptides produced and secreted by the engineered IMFD-72ZsD yeast strain. Yeast strain IMFD-72ZsD was transformed with the human N295$^{7.46}$-mutated (N295$^{7.46}$A and N295$^{7.46}$S) AGTR1 expression plasmids and peptides (Ang II, Ang III and Ang IV) expression plasmids, incubated in SD selective medium for 9 h, and ZsGreen fluorescence was measured by flow cytometry. The mock strain was transformed with a plasmid lacking peptide expression, and served as negative control. Values represent fluorescence intensities of 10,000 cells defined as mean ± standard deviation ($n = 3$). *Reproduced with permission from* [49].

cells[55]. In addition, CXCR4 is expressed by tumor cells of many types of malignancies, and is implicated in cancer metastasis[56].

Yeast was used as host system in a series of experiments with the human CXCR4[57]. Wild-type and constitutively active mutant human CXCR4s were expressed in an *S. cerevisiae* strain coupled to reporter gene HIS3 or lacZ under the control of the FUS1 promoter. Using the FUS1-HIS3 reporter gene system, constitutively active CXCR4 mutants were selected after exposure to CXCL12 and subsequent evaluation of growth survival. Then, the FUS1-lacZ reporter gene system was introduced into the engineered yeast cells expressing human wild-type and mutant CXCR4 to perform screening assays. β-Galactosidase activity after exposure to compounds derived from T140, an inverse agonist for CXCR4, was measured using a fluorescent substrate. Alternatively, the FUS1-FUI permease reporter gene system was applied in a growth assay for characterization of inverse agonist FC131. Since FUI is a permease for 5-fluorouridine (5-FU), CXCR4-mediated activation of the pheromone response upregulates permease expression and sensitivity to 5-FU toxicity.

Complement factor 5a receptor

Complement factor 5a receptor (C5aR) is a rhodopsin-like GPCR, expressed on the surface of neutrophils and other myeloid cells. Complement factor 5a is a 74-amino acid peptide released during complement activation[58]. Binding to C5aR initiates neutrophil chemotaxis and release of proteolytic enzymes and superoxide.

The contribution of the first and third extracellular loops of C5aR in C5aR activation was investigated by subjecting these loops to random saturation mutagenesis[59]. Random amino acid substitutions were introduced into the first (EL1) and third (EL3) extracellular loops of C5aR. The resulting mutant receptors were subcloned into an ADE2 yeast expression vector. In the *S. cerevisiae* strain, yeast Gpa1 was replaced by chimeric Gpa1/$G_{\alpha i3}$, and coupled to reporter gene HIS3 under the control of the FUS1 promoter. The cells of this yeast strain were transformed with the EL1 and EL3 ADE2 libraries. Growth of yeast cells in histidine-deficient medium while coexpressing C5a ligand allowed the identification of functional receptors. To determine receptor signalling through activation of the MAPK pathway, yeast cells were incorporated with the lacZ reporter gene and transformed with the EL1 and EL3 libraries. After stimulation with agonist W5Cha, β-galactosidase activity was measured to determine the effect of a certain mutation in the EL1 or EL3 of C5aR on receptor function. Results provided proof for an essential WXFG motif in the first extracellular loop, as mutations in this motif disrupted receptor activation. However, C5a binding remained unaffected by mutations in the first extracellular loop of C5aR, indicating a role for the WXFG motif downstream of ligand binding.

Rana and Baranski performed a study to explore the role of EL3-N-terminus conserved cysteine pairs on receptor conformation and G protein activation[60]. The *S. cerevisiae* strain, harboring a chimeric Gpa1/$G_{\alpha(1/2)}$ as replacement of yeast Gpa1, was coupled to the FUS1-lacZ reporter gene. They first investigated wild-type and mutant CXCR4 plasmids, containing point mutations at cysteine residues, which were transformed to yeast and exposed to CXCL12. Mutations of $C28^{N\text{-}term}$ and $C274^{EL3}$ with a serine pair ($C28^{N\text{-}term}S$/ $C274^{EL3}S$) abrogated CXCR4 receptor activation. Introduction of either a salt

bridge pair ($C28^{N\text{-}term}R/C274^{EL3}E$) or an aromatic pair ($C28^{N\text{-}term}F/C274^{EL3}F$) restored CXCL12-mediated signalling.

For further investigation of the role of cysteine pairs, an artificial EL3-N-terminus cysteine pair ($C30^{N\text{-}term}$ and $C272^{EL3}$) was engineered into a novel constitutively active mutant ($N119^{3.35}S$ mutation) of C5aR, which originally had serine residues at these positions. This resulted in restrained constitutive signalling without affecting C5a-induced activation, as assessed by monitoring β-galactosidase activity. Single $S272^{EL3}C$ mutation resulted in impaired C5a-induced signalling, which could be rescued by introduction of another cysteine in the N-terminus ($S30^{N\text{-}term}C$ mutation). Additional mutational studies demonstrated that substitution of $S272^{EL3}$ with alanine or threonine impaired C5a-induced signalling too. The additional $S30^{N\text{-}term}C$ mutation did not affect constitutive signalling or C5a-induced signalling. However, the $S30^{N\text{-}term}C$ mutation rescued C5a-mediated signalling in wild-type C5aR, indicating that a covalent disulfide bond is not required for the rescue effect. These results indicate a possible noncovalent interaction between EL3 and the N-terminus in C5aR.

Hedgehog signalling receptor, Smoothened

The hedgehog signalling receptor, smoothened (SMOH), belongs to the frizzled/taste2 receptor family of the GPCRs[3]. The Hedgehog (Hh) signalling pathway regulates organ development during embryogenesis[61]. In adults, the pathway is reactivated by tissue damage and stimulates tissue repair, including peripheral nerve regeneration[62, 63]. Hh protein binding to Patched 1 protein (PTCH1) causes internalisation and destabilisation of this receptor. The smoothened receptor, which activity is inhibited by PTCH1, is then allowed to translocate to the plasma membrane to transduce the Hh signal[64]. Dysfunction of the Hh pathway in stem or precursor cells was found to contribute to tumorigenesis and neurodegenerative disorders[65, 66]. However, the mechanism by which SMOH activates Hh target genes in mammals remains unknown. Moreover, SMOH is present in very low concentrations in tissues, making overexpression in heterologous systems essential for biochemical and structural characterisation.

For this purpose, the human Hh signalling receptor SMOH was successfully overexpressed in its native conformational state in the yeast *S. cerevisiae*[67]. To achieve this, SMOH was subcloned in the expression vectors at the end of the N-terminus of the Multitag Affinity Purification (MAP) sequence, which was fused at the C-terminal end of SMOH. Yeast cells transformed with this vector were screened for expression of SMOH at the plasma membrane using antibodies directed against the hemagglutinin peptides present in the MAP sequence or C-terminal end of SMOH. Using a fluorescent derivative of a SMOH antagonist, the conformational state of SMOH expressed in yeast was visualized.

In a subsequent study, SMOH-MAP was solubilised with n-dodecyl-β-D-maltoside (DDM) detergent, and fully purified using a calmodulin and Ni-NTA affinity resin[68]. Additional replacement of a glycine by an arginine in the third intracellular loop of SMOH, and exchanging DDM with the fluorinated surfactant $C_8F_{17}TAC$ in the calmodulin resin increased the thermostability of SMOH.

Glucagon-like peptide-1 receptor

The glucagon-like peptide 1 (GLP-1) receptor belongs to the secretin receptor family of the GPCRs[3]. GLP-1 is the second incretin hormone discovered, after gastric inhibitory polypeptide (GIP)[69, 70]. GLP-1 is produced from posttranslational proteolytic cleavage of proglucagon, and is released from intestinal L-cells in response to nutrient ingestion. Binding of GLP-1 to the GLP-1 receptor on pancreatic β-cells leads to activation of adenylate cyclase activity, production of cyclic adenosine monophosphate (cAMP), and subsequent secretion of insulin from these cells. Diabetes type 2 patients display lowered GLP-1 concentrations and a reduced ability to promote insulin secretion[71]. Administration of GLP-1 peptide is able to induce glucose-dependent insulin secretion and regulate hyperglycaemia[72]. However, clinical effects appear to be dependent on the GLP-1 receptor response[73], which is not completely understood yet.

Yeast signalling assays were used to study individual ligand-receptor

G protein coupling preferences, and the quantification of the effect of GLP-1 receptor ligands on G protein selectivity[74]. Chimeric Gpa1/G_{α} transplants were created by replacing the five C-terminal amino acids of Gpa1 with the mammalian $G_{\alpha s}$, $G_{\alpha i}$, $G_{\alpha z}$, and $G_{\alpha q}$ homolog sequences. The GLP-1 receptor was then integrated in these strains derived from *S. cerevisiae*, under the control of the pheromone-responsive FUS3 promoter. Results of this study revealed successful coupling of the GLP-1 receptor to chimeric transplants representing the human $G_{\alpha s}$, $G_{\alpha i}$ and $G_{\alpha q}$ G protein subunits. Additionally, responses to ligands of the GLP-1 receptor appeared to be influenced by the G protein subunit type, as exenatide significantly preferred GPL-1 receptor interaction with $G_{\alpha i}$. Exenatide is a GLP-1 mimetic and clinically approved therapeutic agent in the treatment of type 2 diabetes. Lastly, signalling properties of two small-molecule allosteric compounds were studied using the chimeric transplants, demonstrating the comprehensive possibilities of this system. These two compounds, compound 2 and BETP, activated the GLP-1 receptor when coupled to Gpa1/$G_{\alpha s}$. When the GLP-1 receptor was coupled to the Gpa1/$G_{\alpha i}$ chimera, compound 2 reduced receptor activity after receptor stimulation.

Recently, Shigemori and colleagues established a novel functional screening system for yeast-secreted peptides acting on the GLP-1 receptor[75]. This system integrated the yeast *S. cerevisiae* as host for the production of a peptide library and a functional detection system using Chinese hamster ovary (CHO) cells. The GLP-1 receptor expressed on CHO cells was successfully activated by various yeast-secreted GLP-1 receptor agonistic peptides. Especially, the yeast-secreted exendin-4 showed the highest activation of the GLP-1 receptor (10 times higher than yeast-secreted GLP1). This novel functional screening system can be formatted to discover novel peptides activating (other) druggable GPCRs.

Olfactory receptors (ORs)

Olfactory receptors (ORs) belong to the class A rhodopsin-like family of GPCRs[76] and ORs bind to odorant ligands. Minic et al. optimized a *S. cerevisiae* yeast system for functional expression of rat I7 OR and subsequent characterization. The engineered yeasts were lacking the endogenous Gpa1 subunit (the yeast

G_{α} subunit) and a mammalian G_{α} subunit (G_{olf}) was co-expressed. When the receptor was activated by its ligands, MAK kinase signalling was switched on and luciferase (as a functional reporter) synthesis was induced[77]. Marrakchi et al. successfully expressed human olfactory receptor OR17-40 in *S. cerevisiae* based on Minic's biosensor system to detect the conductometric changes[78]. Fukutani et al. improved the bioluminescence-based signalling assay system by deleting some genes to further improve the sensitivity of the firefly luciferase reporter assay and by replacing Gpa1p (yeast G_{α} subunit) with $G_{\alpha olf}$ (the olfactory-specific G_{α} subunit). This improvement successfully caused signal activation through both OR and yeast Ste2p[79]. The same team improved the biomimetic odor-sensing system by replacing the N-terminal region of mOR226 with the corresponding domain of the rat I7 receptor[80]. Likewise the assay sensitivity of some but not all ORs could be improved by the coexpression of odorant accessory binding proteins or the receptor transporting protein 1 short (RTP1S)[81].

Human serotonin 1A receptor

The human serotonin 1A receptor is also known as 5-hydroxytryptamine (5-HT) receptor 1A (HTR1A), which is a member of the 5-HT receptor subfamily[82]. Recently, Nakamura et al. constructed a yeast strain (IMFD-72ZsD) that expressed the human HTR1A[83]. They generated a fluorescent biosensor able to detect signalling by HTR1A in response to the neurotransmitter serotonin (5-HT). The biosensor signalling pathway used yeast cells harboring ZsGreen reporter genes (the tetrameric Zoanthus sp. green fluorescent protein) and a G_{i3}TP gene by replacing the endogenous GPA1 locus with a chimeric gene coding for a yeast Gpa1-human $G_{\alpha i3}$ protein. The improved ZsGreen-containing HTR1A-expressing strains displayed higher levels of ligand-dependent fluorescence than the previous EGFP-containing versions of HTR1A-expressing yeast strains. The authors further validated that this yeast biosensor strain allowed the characterization of an antagonist and the analysis of site-directed mutants of human HTR1A.

Other developments in *S. cerevisiae*

Resolution of 3D structures of target GPCRs provides good initial models for drug design. However, difficulties in expression and purification have been a major obstacle, as large quantities of high-quality pure protein are required for X-ray crystallography. Overexpression of GPCRs in a heterologous host is necessary for structural studies. Suitable variants, which improve expression and stability of receptors, must be selected.

Recently, a platform has been developed for rapid construction and evaluation of functional GPCR variants for structural studies, using *S. cerevisiae*[84]. GPCR variants were designed and the genes were generated as PCR fragments. The genes were integrated into the pDDGFP-2 plasmid, which contains a GAL1 promoter, by homologous recombination in *S. cerevisiae* strain FGY217 via introduction of a mixture of linearised plasmid and PCR products. Using an agar plate without uracil, the GPCR variant was selected. Functional expression was evaluated by radioligand binding assays, and monodispersity – as indicator for receptor purity – by fluorescence size exclusion chromatography. This platform enables a screening cycle within 6-7 days, and may be capable of identifying a suitable GPCR variant for crystallography.

Interestingly, insertion of T4 lysozyme (T4L) into the third intracellular (IL3) loops of GPCRs was suggested to stabilise the protein in a single conformation that would be more likely to crystallise than the unmodified protein, which contains a flexible IL3 loop and is structurally dynamic. Insertion of a small, readily crystallised, soluble protein into GPCRs that lack aqueous-facing protein-interacting surfaces may provide new protein-protein contacts for crystallisation.

However, modification of the IL3 loops in GPCRs could impede G protein activation, as these loops have been implicated in G protein coupling. Mathew and colleagues developed a random screening approach for receptor constructs allowing insertion of T4L into diverse positions in the IL3 loop of the yeast Ste2p receptor[85]. This allowed the identification of Ste2p-T4L fusion constructs which retained ligand binding properties and signalling functions.

Conclusions and future perspectives

The budding yeast *S. cerevisiae* provides a useful system for the study of human G protein-coupled receptors. Chimeric Gpa1/G_{α} G protein 'transplants' to improve coupling efficiency to human GPCRs are often used in yeast cells.

Two *S. cerevisiae* strains, IMFD-72 and IMFD-74, were engineered to express Gpa1/$G_{\alpha i3}$ and Gpa1/$G_{\alpha q}$ respectively, and to harbor additional alterations for improved readout of GPCR signalling. The IMFD-72 strain enabled improved cytometric separation to identify signal transduction mediated by the $G_{\alpha i}$-selective human somatostatin receptor 5, whereas the IMFD-74 strain improved sensing of neurotensin receptor type 1 signalling. These two strains should be applicable for screening of human $G_{\alpha i}$-specific or $G_{\alpha q}$-specific receptors of the GPCR family, and might be beneficial for the screening and development of novel ligands.

Constitutively active mutant (CAM) receptors could be used to discriminate inverse agonists from neutral antagonists. In this respect, inverse agonist T140-derived compounds were detected for the CXCR4 receptor. Using CAMs with varying levels of constitutive activity, three compounds were characterised as inverse agonists on the adenosine A_{2B} receptor, and their relative intrinsic efficacy was determined. In high-throughput screening of libraries CAMs could be used to discover inverse agonists for other GPCRs.

Functional G protein selectivity of a certain GPCR can be investigated when chimeric transplants representing the human G_{α} subunit subtypes are coupled to the endogenous GPCR signalling pathway in yeast. In the first study using yeast as a system to determine the relative efficacies of agonists and affinity values for both agonists and antagonists of the adenosine A_1 receptor, two agonists showed different efficacy when coupled to different G_{α} subtypes. Several amino acid residues at the C-terminus of G_{α} subunits were found to be essential in controlling adenosine A_{2B} receptor activation. The M_3 muscarinic acetylcholine receptor displayed functional selectivity too, as orthosteric antagonists were found to be inverse agonists when coupled to $G_{\alpha q}$, and low efficacy partial agonists when coupled to $G_{\alpha 12}$. This system was capable of identifying G protein selective allosteric modulators as well. Additionally,

responses to ligands of the glucagon-like peptide-1 receptor appeared to be influenced by the G protein subunit type. Exenatide, a clinically approved therapeutic agent in the treatment of type 2 diabetes, showed significant bias for the $G_{\alpha i}$ pathway. Extended application of this system might serve to improve selectivity and efficacy of therapeutic compounds for members of the GPCR family. More interestingly, the system would allow introduction of patient-specific mutations, whose effects on ligand signalling could be quantified, leading to efficient screening of personalized drugs.

In combination with mutagenesis, chimeric Gpa/G_{α} expressing yeast cells could provide a useful system for studying the role of certain amino acid residues in the structure of GPCRs in receptor activation.

The MMY24 yeast strain, which expresses chimeric Gpa1/$G_{\alpha i3}$, served as a useful model for investigating the role of distinct amino acids within the adenosine A_{2B} receptor. In combination with a random mutagenesis screen, residues $F71^{EL1}$ and $D74^{EL1}$ in the first extracellular loop were found to be involved in A_{2B} receptor activation. Site-directed and site-saturation mutagenesis on these residues revealed that a unique structural feature is essential for normal receptor activation. Random mutagenesis yielded three residues in transmembrane domain 4, second extracellular loop, and transmembrane domain 5 of the A_{2B} receptor that seemed to be involved in agonist potency and affinity. In the adenosine A_1 receptor, residues in the second extracellular loop in particular were found to be important for receptor activation through site-directed mutagenesis. Regarding somatostatin receptor 5, $N13^{N\text{-term}}$ and $N26^{N\text{-term}}$ appeared to be important in signalling, as revealed by site-directed mutagenesis. Also, random saturation mutagenesis showed the importance of a WXFG motif in the first extracellular loop in activation, but not ligand binding of complement factor 5a receptor. Additionally, site-directed mutagenesis revealed a novel role of EL3-N terminus cysteine pairs in GPCR activation and signalling. As the EL3-N terminus cysteine pairs and the WXFG motif in EL1 are both found in many GPCRs in the rhodopsin family, additional studies are warranted for a better understanding of the activation and signalling mechanism in these GPCRs.

Interestingly, site-directed mutation of $N295^{7.46}$ in the angiotensin II type

1 receptor yielded the development of a secretory expression system in which autocrine Ang II and Ang III could promote AGTR1-mediated signalling. This secretory expression system, which was able to detect high-affinity or highly-active agonists, could be promising for screening agonistic peptides by using plasmid libraries to express autocrine peptides with random or site-directed mutations.

The usefulness of a reporter gene system was emphasized in a number of studies. A highly sensitive method, which acts via a feedback signal activation mechanism, was developed for the detection of agonists of the human somatostatin receptor 5. This novel approach could advance yeast-based screening of agonistic ligands for a variety of other human GPCRs. The dual-color reporter system enabled simultaneous detection of dimerisation and signalling of SSTR5, and is expected to serve as a powerful tool for defining the mechanisms and functions of GPCR dimerisation. This would advance the development of new therapeutic agents.

The production of active human GPCRs in *S. cerevisiae* is limited by improper translocation of the receptor to the plasma membrane. Retention in the endoplasmatic reticulum is suggested to be the reason for many GPCRs to be improperly trafficked in the yeast system. Introduction of the yeast signalling sequence Ste2N to the N-terminus of human SSTR5 significantly improved agonist potency and improved receptor localisation to the plasma membrane.

Resolution of 3D structures of human GPCRs provides good initial models for drug design. For such structural studies, large quantities of high-quality pure protein are required. The X-ray crystal structure was solved for agonist-bound human M_2 muscarinic receptor, with or without allosteric modulator bound. Mimetic nanobodies for stabilisation of the protein were selected in *S. cerevisiae*. Human hedgehog signalling receptor, smoothened, was overexpressed, purified, and stabilised in yeast. High levels of functional, purified human adenosine A_{2A} receptor were achieved in yeast as well. These yields may help in X-ray crystallography, and provide structural knowledge of GPCRs. Interestingly, a platform was developed for rapid construction and evaluation of functional GPCR variants with improved expression and stability.

This GFP-based *S. cerevisiae* system enables a screening cycle within 6-7 days, and might be powerful in identifying a suitable variant for crystallography. In addition, insertion of T4 lysozyme into the third intracellular loop of the yeast Ste2p receptor resulted in stability, while retaining ligand binding properties and signalling functions. Insertion of such soluble proteins into the flexible loop of transmembrane proteins aids crystallisation of the protein, and might be applied to human GPCRs.

The considerable amount of new developments regarding human G protein-coupled receptors in a yeast platform has provided insight into GPCR activation and signalling, and facilitated agonist and antagonist identification. The budding yeast *S. cerevisiae* is expected to advance understanding of underlying mechanisms of GPCR activation and signalling, by providing a robust platform to perform structural and functional studies on. This would be of major importance in both improvement of selectivity and efficacy of existing therapeutic compounds, and in identifying potential drug targets.

References

[1] Lander, E.S., et al. *International human genome sequencing consortium initial sequencing and analysis of the human genome.* Nature (2001) 409: 860-921.

[2] Venter, J.C. et al. *The sequence of the human genome.* Science (2001) 291: 1304-1351.

[3] Fredriksson, R., et al. *The G-protein-coupled receptors in the human genome form five main families. Phylogenetic analysis, paralogon groups, and fingerprints.* Mol. Pharmacol. (2003) 63: 1256-1272.

[4] Lundstrom, K. *An overview on GPCRs and drug discovery: structure-based drug design and structural biology on GPCRs*, in *G Protein-Coupled Receptors in Drug Discovery*. (2009) Springer. 51-66.

[5] Bourne, H.R. *How receptors talk to trimeric G proteins.* Curr. Opin. Cell Biol. (1997) 9: 134-142.

[6] Hamm, H.E. *The many faces of G protein signaling.* J. Biol. Chem. (1998) 273: 669-672.

[7] Probst, W.C., et al. *Sequence alignment of the G-protein coupled receptor superfamily.* DNA Cell Biol. (1992) 11: 1-20.

[8] Versele, M., et al. *Sex and sugar in yeast: two distinct GPCR systems.* EMBO Rep. (2001) 2: 574-579.

[9] King, K., et al. *Control of yeast mating signal transduction by a mammalian BZadrenergic receptor and Gs a subunit.* Science (1990) 250,121-123.

[10] Brown, A.J., et al. *Functional coupling of mammalian receptors to the yeast mating pathway using novel yeast/mammalian G protein α-subunit chimeras.* Yeast (2000) 16: 11-22.

[11] Dowell, S.J. and Brown, A.J. *Yeast assays for G protein-coupled receptors.* Methods Mol. Biol. (2009) 213-229.

[12] Beukers, M.W. and IJzerman, A.P. *Techniques: how to boost GPCR mutagenesis studies using yeast.* Trends Pharmacol. Sci. (2005) 26: 533-539.

[13] Haskó, G., et al. *Adenosine receptors: therapeutic aspects for inflammatory and immune diseases.* Nat. Rev. Drug Discov. (2008) 7: 759-770.

[14] Fredholm, B.B., et al. *Structure and function of adenosine receptors and their genes.* Naunyn Schmiedeberg Arch. Pharmacol. (2000) 362: 364-374.

[15] Stewart, G.D., et al. *Determination of adenosine A_1 receptor agonist and antagonist pharmacology using Saccharomyces cerevisiae: implications for ligand screening and functional selectivity.* J. Pharmacol. Exp. Ther. (2009) 331: 277-286.

[16] Peeters, M., et al. *The role of the second and third extracellular loops of the adenosine A_1 receptor in activation and allosteric modulation.* Biochem. Pharmacol. (2012) 84: 76-87.

[17] Liu, R., et al. *A yeast screening method to decipher the interaction between the adenosine A_{2B} receptor and the C-terminus of different G protein α-subunits.* Purinergic Signal. (2014) 10: 441-453.

[18] Liu, R., et al. *Scanning mutagenesis in a yeast system delineates the role of the $NPxxY(x)_{5,6}F$ motif and helix 8 of the adenosine A_{2B} receptor in G protein coupling.* Biochem. Pharmacol. (2015) 95: 290–300.

[19] Li, Q., et al. *ZM241385, DPCPX, MRS1706 are inverse agonists with different relative intrinsic efficacies on constitutively active mutants of the human adenosine A_{2B} receptor.* J. Pharmacol. Exp. Ther. (2007) 320: 637-645.

[20] Peeters, M.C., et al. *GPCR structure and activation: an essential role for the first extracellular loop in activating the adenosine A_{2B} receptor.* FASEB J. (2011) 25: 632-643.

[21] Peeters, M.C., et al. *Domains for activation and inactivation in G protein-coupled receptors–A mutational analysis of constitutive activity of the adenosine A_{2B} receptor.* Biochem. Pharmacol. (2014) 92: 348-357.

[22] O'Malley, M.A., et al. *High-level expression in Saccharomyces cerevisiae enables isolation and spectroscopic characterization of functional human adenosine A2a receptor.* J. Struct. Biol. (2007) 159: 166-178.

[23] O'Malley, M.A., et al. *Progress toward heterologous expression of active G-protein-coupled receptors in Saccharomyces cerevisiae: Linking cellular stress response with translocation and trafficking.* Protein Sci. (2009) 18: 2356-2370.

[24] Bertheleme, N., et al. *Arginine 199 and leucine 208 have key roles in the control of adenosine A_{2A} receptor signalling function.* PloS one (2014) 9: e89613.

[25] Raynor, K., et al. *Cloned somatostatin receptors: identification of subtype-selective peptides and demonstration of high affinity binding of linear peptides.* Mol. Pharmacol. (1993) 43: 838-844.

[26] Raynor, K., et al. *Characterization of cloned somatostatin receptors SSTR4 and SSTR5.*

Mol. Pharmacol. (1993) 44: 385-392.

[27] Jaquet, P., et al. *Human somatostatin receptor subtypes in acromegaly: distinct patterns of messenger ribonucleic acid expression and hormone suppression identify different tumoral phenotypes.* J. Clin. Endocrinol. Metab. (2000) 85: 781-792.

[28] Togawa, S., et al. *Importance of asparagine residues at positions 13 and 26 on the amino-terminal domain of human somatostatin receptor subtype-5 in signalling.* J. Biochem. (2010) 147: 867-873.

[29] Nehring, R.B., et al. *Glycosylation affects agonist binding and signal transduction of the rat somatostatin receptor subtype 3.* J. Physiol. Paris. (2000) 94: 185-192.

[30] Fukuda, N., et al. *Amplification of agonist stimulation of human G-protein-coupled receptor signaling in yeast.* Anal. Biochem. (2011) 417: 182-187.

[31] Iguchi, Y., et al. *Control of signalling properties of human somatostatin receptor subtype-5 by additional signal sequences on its amino-terminus in yeast.* J. Biochem. (2010) 147: 875-884.

[32] Ishii, J., et al. *Improved identification of agonist-mediated Gαi-specific human G-protein-coupled receptor signaling in yeast cells by flow cytometry.* Anal. Biochem. (2012) 426: 129-133.

[33] Nakamura, Y., et al. *Simultaneous method for analyzing dimerization and signaling of G-protein-coupled receptor in yeast by dual-color reporter system.* Biotechnol. Bioeng. (2014) 111: 586-596.

[34] Wess, J. *Molecular biology of muscarinic acetylcholine receptors.* Crit. Rev. Neurobiol. (1996) 10: 69-99.

[35] Volpicelli, L.A. and Levey, A.I. *Muscarinic acetylcholine receptor subtypes in cerebral cortex and hippocampus.* Prog. Brain Res. (2004) 24: 59.

[36] Abrams, P., et al. *Muscarinic receptors: their distribution and function in body systems, and the implications for treating overactive bladder.* Br. J. Pharmacol. (2006) 148: 565-578.

[37] Wess, J., et al. *Muscarinic acetylcholine receptors: mutant mice provide new insights for drug development.* Nat. Rev. Drug Discov. (2007) 6: 721-733.

[38] Stewart, G.D., et al. *Detection of novel functional selectivity at M3 muscarinic acetylcholine receptors using a Saccharomyces cerevisiae platform.* ACS Chem. Biol. (2010) 5: 365-375.

[39] Stewart, G.D., et al. *Prediction of functionally selective allosteric interactions at an M3 muscarinic acetylcholine receptor mutant using Saccharomyces cerevisiae.* Mol. Pharmacol. (2010) 78: 205-214.

[40] Kruse, A.C., et al. *Activation and allosteric modulation of a muscarinic acetylcholine receptor.* Nature (2013) 504: 101-106.

[41] Nomura, Y., et al. *Proteoliposome-based Selection of a Recombinant Antibody Fragment Against the Human M2 Muscarinic Acetylcholine Receptor.* Monoclon. Antib. Immunodiagn. Immunother. (2014) 33: 378-385.

[42] Gully, D., et al. *Biochemical and pharmacological profile of a potent and selective nonpeptide antagonist of the neurotensin receptor.* Proc. Natl. Acad. Sci. (1993) 90: 65-69.

[43] Hwang, J.I., et al. *Phylogenetic history, pharmacological features, and signal transduction*

of neurotensin receptors in vertebrates. Ann. N. Y. Acad. Sci. (2009) 1163: 169-178.

[44] Dupouy, S., et al. *The potential use of the neurotensin high affinity receptor 1 as a biomarker for cancer progression and as a component of personalized medicine in selective cancers.* Biochimie (2011) 93: 1369-1378.

[45] Souazé, F., et al. *Neurotensin receptor 1 gene activation by the Tcf/β-catenin pathway is an early event in human colonic adenomas.* Carcinogenesis (2006) 27: 708-716.

[46] Ishii, J., et al. *Microbial fluorescence sensing for human neurotensin receptor type 1 using Gα-engineered yeast cells.* Anal. Biochem. (2014) 446: 37-43.

[47] Greindling, K., et al. *Angiotensin receptors and their therapeutic implications.* Annu. Rev. Pharmacol. Toxicol. (1996) 36: 281-306.

[48] Mehta, P.K. and Griendling, K.K. *Angiotensin II cell signaling: physiological and pathological effects in the cardiovascular system.* Am. J. Physiol. Cell Physiol. (2007) 292: C82-C97.

[49] Nakamura, Y., et al. *Construction of a yeast-based signaling biosensor for human angiotensin II type 1 receptor via functional coupling between Asn295-mutated receptor and Gpa1/G_{i3} chimeric G_{α}.* Biotechnol. Bioeng. (2014) 111: 2220-2228.

[50] Groblewski, T., et al. *Mutation of Asn111 in the third transmembrane domain of the AT1A angiotensin II receptor induces its constitutive activation.* J. Biol. Chem. (1997) 272: 1822-1826.

[51] Balmforth, A.J., et al. *The conformational change responsible for AT1 receptor activation is dependent upon two juxtaposed asparagine residues on transmembrane helices III and VII.* J. Biol. Chem. (1997) 272: 4245-4251.

[52] Deichmann, M., Kronenwett, R., and Haas, R. *Expression of the human immunodeficiency virus type-1 coreceptors CXCR-4 (fusin, LESTR) and CKR-5 in CD34+ hematopoietic progenitor cells.* Blood (1997) 89: 3522-3528.

[53] Murphy, P.M., et al. *International union of pharmacology. XXII. Nomenclature for chemokine receptors.* Pharmacol. Rev. (2000) 52: 145-176.

[54] Bleul, C.C., et al. *The lymphocyte chemoattractant SDF-1 is a ligand for LESTR/fusin and blocks HIV-1 entry.* Nature (1996) 829-833.

[55] Feng, Y., et al. *HIV-1 entry cofactor: functional cDNA cloning of a seven-transmembrane, G protein-coupled receptor.* Science (1996) 272: 872-877.

[56] Müller, A., et al. *Involvement of chemokine receptors in breast cancer metastasis.* Nature (2001) 410: 50-56.

[57] Evans, B.J., et al. *Expression of CXCR4, a G-protein-coupled receptor for CXCL12 in yeast identification of new-generation inverse agonists.* Methods Enzymol. (2009) 460: 399-412.

[58] Gerard, C. and Gerard, N.P. *C5A anaphylatoxin and its seven transmembrane-segment receptor.* Ann. Rev. Immunol. (1994) 12: 775-808.

[59] Klco, J.M., et al. *Genetic analysis of the first and third extracellular loops of the C5a receptor reveals an essential WXFG motif in the first loop.* J. Biol. Chem. (2006) 281: 12010-12019.

[60] Rana, S. and Baranski, T.J. *Third extracellular loop (EC3)-N terminus interaction is important for seven-transmembrane domain receptor function.* J. Biol. Chem. (2010) 285:

31472-31483.

[61] Ingham, P.W. and McMahon, A.P. *Hedgehog signaling in animal development: paradigms and principles.* Genes Dev. (2001) 15: 3059-3087.

[62] Pola, R., et al. *The morphogen Sonic hedgehog is an indirect angiogenic agent upregulating two families of angiogenic growth factors.* Nat. Med. (2001) 7: 706-711.

[63] Calcutt, N.A., et al. *Therapeutic efficacy of sonic hedgehog protein in experimental diabetic neuropathy.* J. Clin. Invest. (2003) 111: 507.

[64] Rubin, L.L. and de Sauvage, F.J. *Targeting the Hedgehog pathway in cancer.* Nat. Rev. Drug Discov. (2006) 5: 1026-1033.

[65] Reya, T., et al. *Stem cells, cancer, and cancer stem cells.* Nature (2001) 414: 105-111.

[66] Lai, K., et al. *Sonic hedgehog regulates adult neural progenitor proliferation in vitro and in vivo.* Nat. Neurosci. (2003) 6: 21-27.

[67] De Rivoyre, M., et al. *Human receptor Smoothened, a mediator of Hedgehog signalling, expressed in its native conformation in yeast.* FEBS Lett. (2005) 579: 1529-1533.

[68] Nehmé, R., et al. *Stability study of the human G-protein coupled receptor, Smoothened.* Biochem. Biophys. Acta (BBA)-Biomembranes (2010) 1798: 1100-1110.

[69] Mojsov, S., et al. *Insulinotropin: glucagon-like peptide I (7-37) co-encoded in the glucagon gene is a potent stimulator of insulin release in the perfused rat pancreas.* J. Clin. Invest. (1987) 79: 616-619.

[70] Kreymann, B., et al. *Glucagon-like peptide-1 7-36: a physiological incretin in man.* Lancet (1987) 330: 1300-1304.

[71] Quddusi, S., et al. *Differential effects of acute and extended infusions of glucagon-like peptide-1 on first-and second-phase insulin secretion in diabetic and nondiabetic humans.* Diabetes Care (2003) 26: 791-798.

[72] Holst, J.J. and Seino, Y. *GLP-1 receptor agonists: targeting both hyperglycaemia and disease processes in diabetes.* Diabetes Res. Clin. Pract. (2009) 85: 1-3.

[73] Pabreja, K., et al. *Molecular mechanisms underlying physiological and receptor pleiotropic effects mediated by GLP-1R activation.* Br. J. Pharmacol. (2014) 171: 1114-1128.

[74] Weston, C., et al. *Investigating G protein signalling bias at the glucagon-like peptide-1 receptor in yeast.* Br. J. Pharmacol. (2014) 171: 3651-3665.

[75] Shigemori, T., Kuroda, K., and Ueda, M. *Functional screening system for yeast-secreted peptides acting on G-protein coupled receptors.* AMB Express (2015) 5: 26.

[76] Gaillard, I., et al. *Olfactory receptors.* Cell. Mol. Life Sci. (2004) 61: 456-469.

[77] Minic, J., et al. *Functional expression of olfactory receptors in yeast and development of a bioassay for odorant screening.* FEBS J. (2005) 272: 524-537.

[78] Marrakchi, M., et al. *A new concept of olfactory biosensor based on interdigitated microelectrodes and immobilized yeasts expressing the human receptor OR17-40.* Eur. Biophys. J. (2007) 36: 1015-1018.

[79] Fukutani, Y., et al. *An improved bioluminescence-based signaling assay for odor sensing with a yeast expressing a chimeric olfactory receptor.* Biotechnol. Bioeng. (2012) 109: 3143-3151.

[80] Fukutani, Y., et al. *The N-terminal replacement of an olfactory receptor for the development of a Yeast-based biomimetic odor sensor.* Biotechnol. Bioeng. (2012) 109: 205-212.

[81] Fukutani, Y., et al. *Improving the odorant sensitivity of olfactory receptor-expressing yeast with accessory proteins.* Anal. Biochem. (2015) 471: 1-8.

[82] Hoyer, D., et al. *International Union of Pharmacology classification of receptors for 5-hydroxytryptamine (Serotonin).* Pharmacol. Rev. (1994) 46: 157-203.

[83] Nakamura, Y., et al. *Applications of yeast-based signaling sensor for characterization of antagonist and analysis of site-directed mutants of the human serotonin 1A receptor.* Biotechnol. Bioeng. (2015) 112: 1906-1915.

[84] Shiroishi, M., et al. *Platform for the rapid construction and evaluation of GPCRs for crystallography in Saccharomyces cerevisiae.* Microb. Cell Fact. (2012) 11: 78-89.

[85] Mathew, E., et al. *Functional fusions of T4 lysozyme in the third intracellular loop of a G protein-coupled receptor identified by a random screening approach in yeast.* Protein Eng. Des. Sel. (2013) 26: 59-71.

Chapter 3

A yeast screening method to decipher the interaction between the adenosine A_{2B} receptor and the C-terminus of different G protein α-subunits

This chapter is based upon:

Rongfang Liu, Nick J. A. Groenewoud, Miriam C. Peeters, Eelke B. Lenselink, Ad P. IJzerman

Purinergic Signalling ***2014*** *10: 441-453*

Abstract

The expression of human G protein-coupled receptors (GPCRs) in *Saccharomyces cerevisiae* containing chimeric yeast/mammalian G_{α} subunits provides a useful tool for the study of GPCR activation. In this study, we used a one-GPCR-one-G protein yeast screening method in combination with molecular modeling and mutagenesis studies to decipher the interaction between GPCRs and the C-terminus of different α-subunits of G proteins. We chose the human adenosine A_{2B} receptor ($hA_{2B}R$) as a paradigm, a typical class A GPCR that shows promiscuous behavior in G protein coupling in this yeast system. The wild-type $hA_{2B}R$ and five mutant receptors were expressed in 8 yeast strains with different humanized G proteins, covering the four major classes: $G_{\alpha i}$, $G_{\alpha s}$, $G_{\alpha q}$ and $G_{\alpha 12}$. Our experiments showed that a tyrosine residue (Y) at the C-terminus of the G_{α} subunit plays an important role in controlling the activation of GPCRs. Receptor residues $R103^{3.50}$ and $I107^{3.54}$ are vital too in G protein-coupling and the activation of the $hA_{2B}R$, whereas $L213^{IL3}$ is more important in G protein inactivation. Substitution of $S235^{6.36}$ to alanine provided the most divergent G protein coupling profile. Finally, $L236^{6.37}$ substitution decreased receptor activation in all G protein pathways, although to a different extent. In conclusion, our findings shed light on the selectivity of receptor/G protein coupling, which may help in further understanding GPCR signaling.

Introduction

G protein-coupled receptors (GPCRs), also known as seven-transmembrane receptors (7TMRs), are a major class of targets for many of today's medicines, to combat ailments such as inflammation, cardiac malfunction, asthma and cancer. Ligands interact with these transmembrane proteins in many different ways, intervening with or mimicking their activation process, which is mediated mostly by a heterotrimeric G protein, composed of α, β and γ subunits[1, 2]. However, the exact mechanism of GPCR activation at the molecular level is still largely unknown. Here, we used the $hA_{2B}R$, a typical class A GPCR, as a paradigm to decipher the interaction between receptors and their G proteins.

The adenosine receptors include four subtypes: A_1R, $A_{2A}R$, $A_{2B}R$ and A_3R, which have attracted much attention as therapeutic targets in recent years. All the adenosine receptors are ubiquitously expressed in the human body[3] and can target different intracellular signaling pathways by responding to the same endogenous ligand adenosine. The $A_{2B}R$ has the lowest affinity for adenosine[4] and has been less investigated than other adenosine receptors. Several studies have shown that blocking $A_{2B}R$ signaling reduces experimental autoimmune encephalomyelitis[5] and inhibits growth of prostate cancer cells[6], breast tumors[7] and bladder tumors[8, 9]. On the other hand, stimulation of $A_{2B}R$ protects against trauma-hemorrhagic shock-induced lung injury[10] , CHX-induced apoptosis[6] and also vascular injury[11].

Yeast can provide a powerful platform for studying GPCRs and their G protein coupling and selectivity. *Saccharomyces cerevisiae* (*S. cerevisiae*) strains, each expressing a specific human G_α/yeast Gpa1 protein chimera, have been used to express heterologous GPCRs, for instance in high-throughput screening assays for drug discovery[12], to perform random mutagenesis screening[13, 14], and to assess the preference of G_α pathways[15] and functional selectivity of agonists and antagonists[16-18]. Several lines of evidence indicate that the C-terminal five amino acid residues of a G protein are sufficient for coupling with many human receptors, including the $hA_{2B}R$[19]. One of the advantages of the yeast system used is that while these five amino acids of many human G protein α-subunits were

'transplanted' to replace these residues on the yeast's endogenous G protein, Gpa1p (see also Table 1), all other aspects of the system remain the same and intact[20, 21].

In the present study, we used this one-GPCR-one-G protein yeast screening method in combination with molecular modeling and mutagenesis studies. Our goal was to provide more information about the mechanism of activation of the $hA_{2B}R$ and the role the binding pocket for the G_{α} protein's C-terminus plays in that process. Our findings provide further evidence for the A_{2B} receptor's G protein preferences, which in itself may be useful for designing and screening selective agonists and antagonists for this receptor. At the same time, our findings have a broader relevance as they reflect on the GPCR-G protein interface.

Table 1. The genotypes of the yeast strains used for transformations[20, 21, 49].

Strain	Genotype	The five C-terminal residues of G_{α}
MMY11	**MATa** *his3 ade2 leu2 trp1 ura3 can1 fus1:: FUS1-HIS3 FUS1-lacZ::LEU2 farΔ::ura3Δgpa1Δ ::ADE2Δsst2Δ ::ura3Δste2Δ::G418^R*	
MMY12 ($G_{\alpha WT}$)	MMY11*TRP1::GPA1*	KIGII^{COOH}
MMY23 ($G_{\alpha i1}$)	MMY11*TRP1::Gpa1/*$G_{\alpha i1(5)}$	DCGLF^{COOH}
MMY24 ($G_{\alpha i3}$)	MMY11*TRP1::Gpa1/*$G_{\alpha i3(5)}$	ECGLY^{COOH}
MMY28 ($G_{\alpha s}$)	MMY11*TRP1::Gpa1/*$G_{\alpha s(5)}$	QYELL^{COOH}
MMY14 ($G_{\alpha q}$)	MMY11*TRP1::Gpa1/*$G_{\alpha q(5)}$	EYNLV^{COOH}
MMY21 ($G_{\alpha 14}$)	MMY11*TRP1::Gpa1/*$G_{\alpha 14(5)}$	EFNLV^{COOH}
MMY19 ($G_{\alpha 12}$)	MMY11*TRP1::Gpa1/*$G_{\alpha 12(5)}$	DIMLQ^{COOH}
MMY20 ($G_{\alpha 13}$)	MMY11*TRP1::Gpa1/*$G_{\alpha 13(5)}$	QLMLQ^{COOH}

Materials and methods

hA_{2B} Receptor/G protein homology modeling

A homology model was created using Molsoft's ICM Homology tool (Version 3.7-2)[22]. The β_2 adrenergic receptor (β_2AR) in complex with the G_s protein[23] (PDB: 3SN6) was chosen as template since it was the closest (and currently only) homolog of the $hA_{2B}R$ containing the $G_{\alpha s}$ protein, with 30% sequence identity and 48% sequence similarity using a pair-wise sequence alignment method (EMBOSS_matcher; http://www.ebi.ac.uk/Tools/psa/emboss_matcher/). The $hA_{2B}R$ sequence (uniprot: P29275) was modeled onto 3SN6 and residues were selected to be individually mutated to alanine based on the following two criteria: 1) within *5 Å* distance from the last five amino acids of the $G_{\alpha s}$ protein (QYELL) and 2) oriented towards the $G_{\alpha s}$ protein. Final visualizations were created using PyMOL (The PyMOL Molecular Graphics System, Version 1.5.0.4 Schrödinger, LLC)[24].

Generation of point mutations

The S. *cerevisiae* expression vectors, the pDT-PGK and pDT-PGK_A_{2B} receptor plasmids, were kindly provided by Dr. Simon Dowell from GSK (Stevenage, UK). The DNA primers of the mutants of the A_{2B} receptor were designed by the QuikChange® Primer Design Program on the website of Agilent Technologies, and contained a single substitution resulting in a codon change for the desired amino acid substitution. The reverse primer sequence of each mutant was the reverse complement of the forward primer. These primers and their complements were synthesized (Eurogentec, the Netherlands) and then used to generate mutant plasmids according to the QuikChange method from Stratagene. The mutagenic reaction contained 40 ng of the pDT-PGK_A_{2B} construct plasmid as dsDNA template, 10 μM of each primer, 1 μl of dNTP mix, 2.5 μl of 10× reaction buffer and 2.5 U *PfuUltra* HF DNA polymerase. The following thermal cycling parameters were used in the PCR apparatus (T100™ Thermal Cycler, BIO-RAD): 95 °C for 30 s, 55 °C for 1 min, and 68 °C for 10 min. The number of mutagenic PCR cycles was set to 20. Methylated or hemimethylated non-mutated plasmid

DNA was removed by adding 5 U *Dpn* I restriction enzyme for 2 h at 37 °C. The mutated DNA products were transformed into XL-1 Blue supercompetent cells and other details were according to the manual of the QuikChange® II Site-Directed Mutagenesis Kit. Mutant plasmids were isolated from a single clone using a QIAprep midi plasmid purification kit (QIAGEN, the Netherlands). The mutants were confirmed by DNA sequencing (LGTC, Leiden, the Netherlands).

Transformation in *S. cerevisiae* strains

Each mutant plasmid was transformed according to the Lithium-Acetate procedure[25] into a panel of engineered *S. cerevisiae* yeast strains expressing different Gpa1p/G_α chimeras. The yeast strains were derived from the MMY11 strain and further adapted to communicate with mammalian GPCRs. The difference between these integrated Gpa1p/G_α chimeras is that the last five amino acids of the endogenous Gpa1p C-terminus have been replaced with the same sequence as that from mammalian G_α proteins[20, 21] (Table 1). To measure the signaling of GPCRs, the pheromone signaling pathway of these strains was coupled via the *FUS1* promoter to *HIS3* (imidazoleglycerol-phosphate dehydratase), an enzyme catalyzing the sixth step in histidine biosynthesis to produce histidine. 3-AT (3-amino-[1, 2, 4]- triazole), a competitive inhibitor of imidazoleglycerol-phosphate dehydratase, was added to the assay to reduce background activity caused by endogenous histidine[20]. The degree of receptor activation induced by an agonist of the GPCR was measured by the growth rate of the yeast on histidine-deficient medium.

Liquid growth assay

To measure the efficiency of GPCR-G protein coupling, concentration-growth curves were generated in a liquid growth assay[26]. This assay was carried out in 96-well plates and the growth was determined by measuring the absorption at a wavelength of approx. 600 nm (OD_{600}). To set up an assay, cells were grown to saturation selecting for the transformed plasmid, then seeded at low cell density (2×10^4 cells/ml) into assay medium (YNB + adenine + tryptophan + 10mM 3-AT) lacking histidine and dispensed into assay plates containing the adenosine

receptor agonist NECA (10^{-9} – 10^{-4} M). The 96-well plate was then incubated for 35 h at 30 °C in a Genios plate reader (Tecan, Durham, NC), keeping the cells in suspension by shaking every 10 min at 300 rpm for 1 min. Results were obtained from two independent experiments, performed in duplicate. EC_{50} values and E_{max} values of the liquid assay were analyzed using the nonlinear regression package available in Prism 5.0 software (GraphPad Software Inc., San Diego, CA, USA).

Whole cell radioligand binding experiments

Yeast cells from an overnight culture expressing the wild-type or mutated $hA_{2B}R$ were harvested from rich YAPD medium by centrifuging 2,000 *g* for 5 min. The pellet of cells was washed once with 0.9% NaCl. The cells were centrifuged again using the same speed and diluted in the assay buffer (50 mM Tris-HCl pH7.4 + 1 mM EDTA) to OD_{600} = 40 (OD_{600} = 1 ≈ 2.5×10^7 cells/ml). Binding experiments were performed with 1.5 nM of the A_{2B} receptor selective antagonist [^{3}H]PSB-603, and a final cell concentration of 25×10^7 cells/ml in a total volume of 100 µl. Nonspecific binding (NSB) was determined by additionally adding NECA at a final concentration of 1 mM. Samples were incubated for 1 h at 25 °C keeping the cells in suspension by shaking vigorously. 1 ml of ice-cold assay buffer was added to samples to terminate incubation and the samples were harvested on a Millipore manifold with GF/B filters pre-incubated in 0.1% polyethylenimine (PEI) at a pressure of 200 mbar, to separate free from receptor-bound radioligand by washing twice with 2 ml buffer (50 mM Tris-HCl pH7.4 + 1 mM EDTA + 0.1%BSA). The filters were transferred into mini-vials and 3.5 ml of PerkinElmer Emulsifier Safe was added, and subsequently incubated for at least 2 h. Filter-bound radioactivity was determined as counts per minute by scintillation spectrometry (Tri-Carb 2900TR; PerkinElmer Life and Analytical Sciences). Results were obtained from at least three independent experiments, performed in duplicate.

Preparation of yeast protein extractions and immunoblotting

Protein extractions were performed with trichloroacetic acid (TCA) according to

the Clontech Yeast Protocols Handbook 2001. Yeast transformants were grown in 2 ml YAPD medium and were harvested in mid-exponential phase (1.2×10^8 cells). The yeast cells were collected and washed with cold water. Subsequently the yeast cells were broken by vigorous vortexing with 20% TCA and glass beads. The broken yeast cells and the glass beads were washed twice with 200 µl 5% TCA and centrifuged at 3,000 rpm for 2 minutes. The supernatant was collected and centrifuged again at 6,000 rpm for 2 minutes. The pellets were resuspended with cold SDS/PAGE loading buffer (100 mM EDTA, 1 M Tris, 10% SDS, 0.5% Bromophenol blue) and 1 M Tris was added to neutralize all remaining TCA. The samples were incubated for 30 min at 37 °C and centrifuged again at 2,000 rpm for 10 min.

Each sample of 4 µl containing 24 µg protein was loaded on 12.5% SDS/PAGE gel and then blotted on Hybond-ECL membranes (GE Healthcare, the Netherlands) using a semi-automated electrophoresis technique (PhastSystem™, Amersham Pharmacia Biotech). The Hybond-ECL membranes were blocked with TBS containing 5% milk powder for 1 h and washed three times with TBST (0.05% Tween-20, TBS pH 7.6). The membranes were incubated with 1:1250 diluted rabbit anti-human A_{2B} receptor antibody for 1 h. This antibody was directed against the C-terminal region of the $A_{2B}R$ and was kindly provided by Dr. I. Feoktistov (Vanderbilt University, Nashville)[27]. After thorough removal of unbound antibody from the membranes by washing three times with TBST, the membranes were incubated with 1:2,500 diluted HRP-conjugated goat anti-rabbit IgG (Jackson ImmunoResearch Laboratories) for 1 h. The membranes were washed twice with TBST and once with TBS. The specific signal of the A_{2B} receptor was probed according to the ECL Western blotting analysis system (GE Heathcare, the Netherlands) using enhanced chemiluminescence (ChemiDox XRS, BIO-RAD). The nonspecific band at approx. 45 kDa was used as loading control and the specific $hA_{2B}R$ protein bands were at 29 kDa and 48 kDa. The ratio was determined between the density of the specific bands and density of the nonspecific band that was always present on the blots. MMY12 carrying wild-type or mutant receptor was set as 100% and MMY12 carrying the empty vector pDT-PGK without receptor was set as 0%.

Results

G protein selectivity of the wild-type hA_{2B} receptor

To investigate the activation mechanism of the hA_{2B} receptor at the interface of the C terminus of the G protein G_{α} subunit, we expressed the yeast plasmid pDT-PGK_hA_{2B}R in a panel of eight yeast *S. cerevisiae* strains with humanized G proteins. Corresponding to the replaced last five C-terminal residues of the mammalian G_{α} subunit, they were classified into five families: $G_{\alpha WT}$ (MMY12), $G_{\alpha s}$ (MMY28), $G_{\alpha i}$ (MMY23 and MMY24), $G_{\alpha 12}$ (MMY19 and MMY20), and $G_{\alpha q}$ (MMY14 and MMY21) (Table 1)[19]. When the expressed hA_{2B} receptor is activated by an agonist, the yeast pheromone signalling pathway is activated through a chimeric yeast/mammalian G protein leading to subsequent transcription of the HIS3 reporter gene and consequently histidine production[28]. Subsequent growth of the yeast cells on histidine-deficient medium was determined by measuring the absorption at a wavelength of 595 nm, which reflects the activation of the expressed receptor by the adenosine receptor agonist NECA. Concentration-response curves of NECA on the wild-type receptor in MMY28($G_{\alpha s}$), MMY24($G_{\alpha i3}$), MMY12($G_{\alpha WT}$), MMY19($G_{\alpha 12}$) and MMY14($G_{\alpha q}$) are shown in Figure 1 and the values of EC_{50}, and E_{max} of all strains are shown in Table 2.

We found the five humanized different G protein pathways MMY28($G_{\alpha s}$), MMY24($G_{\alpha i3}$), MMY21($G_{\alpha 14}$), MMY23($G_{\alpha i1}$) and MMY20($G_{\alpha 13}$) to show varying degrees of enhancement compared to the coupling efficiency of the wild-type hA_{2B}R in the wild-type yeast G_{α} strain MMY12($G_{\alpha WT}$). The most efficient yeast strain MMY28($G_{\alpha s}$) showed a significant 15-fold improvement in coupling efficiency and also MMY24($G_{\alpha i3}$) showed a significant 6.5-fold enhancement in coupling efficiency. Two strains, MMY14($G_{\alpha q}$) and MMY19($G_{\alpha 12}$), responded less to NECA, with significantly higher EC_{50} values for this agonist. In terms of intrinsic activity (E_{max} values) there was little difference between the strains, however. The one exception was in MMY28($G_{\alpha s}$) with a large degree of constitutive activity (approx. 30% of the maximal response of MMY12 in response to the agonist NECA (10^{-4} M). This may be a feature of the MMY28 strain itself since expression of plasmid pDT-PGK (without any receptor) yielded a similar degree

of constitutive activity (data not shown).

Bioinformatics and Molecular Modeling

To further decipher the interaction between the $hA_{2B}R$ and G proteins, we predicted a number of amino acid residues as important for activation of G proteins from $hA_{2B}R$ homology modeling. There are more than 75 crystal structures of 18 different class A GPCRs now[29], however, only two receptors, β_2AR and opsin (Ops), have been cocrystallised with the $G_{\alpha s}$ protein[23] and an 11 amino acid synthetic peptide of $G_{\alpha t}$[30], respectively. The β_2AR-G_s crystal structure (PDB: 3SN6) was chosen as template for mapping amino acid residues of $hA_{2B}R$ that are involved in G protein activation. The $h\beta_2$AR shares 30% sequence identity with the $hA_{2B}R$ (Fig. 2A), compared to 23% homology with bovine opsin. In many mammalian cells, the $hA_{2B}R$ prefers to couple to G_s next to G_q proteins[31], another indication of the validity of this particular homology modeling approach. The model predicted 16 amino acids to interact with $G_{\alpha s}$ (i.e. with QYELL, the last five amino acid residues of it): $D102^{3.49}$, $R103^{3.50}$, $A106^{3.53}$, $I107^{3.54}$, $Y113^{3.60}$, $I205^{5.61}$, $A209^{5.65}$, $Q212^{IL3}$, $L213^{IL3}$, $R215^{IL3}$, $H231^{6.32}$, $A232^{6.33}$, $S235^{6.36}$, $L236^{6.37}$, $R293^{8.46}$, $N294^{8.47}$.

Arginine (R) $103^{3.50}$, isoleucine (I) $107^{3.54}$, leucine (L) 213^{IL3}, serine (S) $235^{6.36}$ and leucine (L) $236^{6.37}$ were selected for mutation into alanine as they are both closest to the $G_{\alpha s}$ protein and with their side chains oriented towards the $G_{\alpha s}$ protein as well (Fig. 2B). These selected five residues are also shown in the snake plot of the $hA_{2B}R$ (Fig. 2C). $R103^{3.50}$ and $I107^{3.54}$ are located on the intracellular side of TM3 and are included in the consensus sequence (I/L)*XX*D$R^{3.50}$Y*XX*(I/V)$^{3.54}$[32]. $R^{3.50}$ is a part of the most conserved motif in the class A GPCRs: Asp-Arg-Tyr (DRY). The residues on positions 3.50, 3.54 and 6.36 according to Ballesteros-Weinstein numbering[33] are also conserved as part of the G protein-binding region in the bovine opsin-G_t peptide crystal structure[23, 29, 30].

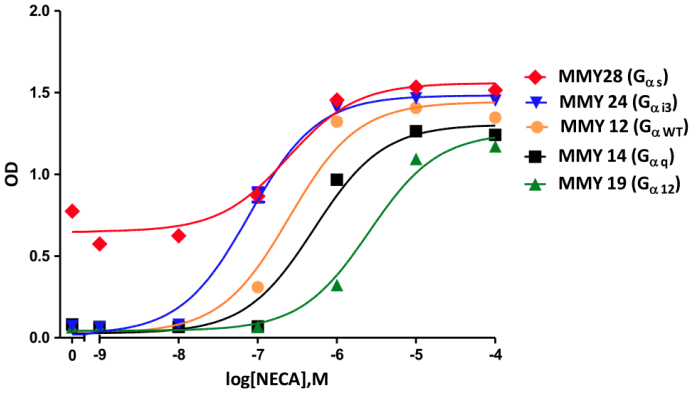

Fig. 1 Concentration-effect curves from liquid assay experiments are shown of the A_{2B} wild-type receptor in MMY28 ($G_{\alpha s}$), MMY24 ($G_{\alpha i3}$), MMY12 ($G_{\alpha WT}$), MMY14 ($G_{\alpha q}$) and MMY19 ($G_{\alpha 12}$) responding to the adenosine receptor agonist NECA. The assay was performed in YNB-ULH medium.

G protein coupling profiles of five mutant A_{2B} receptors

To assess the function of these five residues in G protein activation, we performed a functional yeast liquid assay to determine whether the G protein activation profiles of these mutants had changed or not. NECA concentration-response curves revealed that all five single amino acid changes in the receptor resulted in substantially different humanized G protein coupling profiles of the $hA_{2B}R$ (Table 2; Fig. 3).

The $R103^{3.50}A$ receptor failed to couple to all humanized G protein pathways except for MMY28($G_{\alpha s}$) with a comparable EC_{50} value, only 2-fold higher than wild-type receptor (Table 2). Mutant receptor $I107^{3.54}A$ only responded with higher than wild-type EC_{50} values for NECA of 7629 nM to MMY23($G_{\alpha i1}$) with a reduced E_{max} value of 37%, and 47 nM to MMY28($G_{\alpha s}$) with a maximal activation level. Other humanized G protein pathways did not respond to NECA anymore (Table 2).

A

```
A2B              11 VALELVIAALSVAGNVLVCAAVGTANTLQTPTNYFLVSLAAADVAVGLFA     60
                    :.:.|::.|: |.|||||..|:.....|||.||||:.|||.||:.:||..
beta2            38 IVMSLIVLAI-VFGNVLVITAIAKFERLQTVTNYFITSLACADLVMGLAV     86

A2B              61 IPFAITISLGFCTDF--YGCLFLACFVLVLTQSSIFSLLAVAVDRYLAIC     108
                    :||.....|.....|  :.|.|.....::...:||.:|..:|||||.|||.
beta2            87 VPFGAAHILMKMWTFGNFWCEFWTSIDVLCVTASIETLCVIAVDRYFAIT     136

A2B             109 VPLRYKSLVTGTRARGVIAVLWVLAFGIGLTPF-LGW-NSKDSATNNCTE     156
                    .|.:|:||:|..:||.:|.::|:::..|...|. :.| .:.......||..
beta2           137 SPFKYQSLLTKNKARVIILMVWIVSGLISFLPIQMHWYRATHQEAINCYA     186

A2B             157 P---WDGTTNESCCLVKCLFENVVPMSYMV--YFNFFGCVLPPLLIMLVI     201
                    .  .|..||::..:...:....||:..||  |...|......|..:....
beta2           187 NETCCDFFTNQAYAIASSIVSFYVPLVIMVFVYSRVFQEAKRQLQKIDKS     236

A2B             202 YIKIFLVACRQLQRTELMDH----SRTTLQREIHAAKSLAMIVGIFALCW     247
                    ..:..:....|:::.....|    |.....:|..|.|:|..:|:|.|.|||
beta2           237 EGRFHVQNLSQVEQDGRTGHGLRRSSKFCLKEHKALKTLGIIMGTFTLCW     286

A2B             248 LPVHAVNCVTLFQPAQGKNKPKWAMNMAILLSHANSVVNPIVYAYRNRDF     297
                    ||...||.|.:.|....:.:....:|.   :.:.||..||::|. |:.||
beta2           287 LPFFIVNIVHVIQDNLIRKEVYILLNW---IGYVNSGFNPLIYC-RSPDF     332

A2B             298 RYTFHKII    305
                    |..|.:::
beta2           333 RIAFQELL    340
```

B

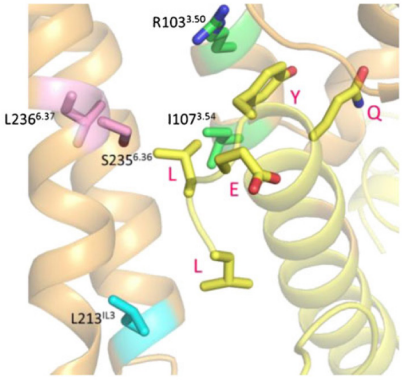

C

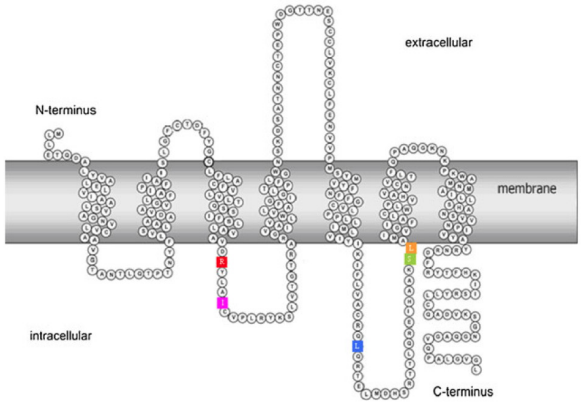

Fig. 2 (A) Sequence alignment (most similar regions only) between the $hA_{2B}R$ (A_{2B}; uniprot: P29275) and the $h\beta_2AR$ (beta2; uniprot:P07550). Conserved residues are shown as | between the two sequences. (B) A hA_{2B} Receptor/ G_s protein homology model was generated from the crystal structure of the β_2AR in contact with the $G_{\alpha s}$ protein[23] (PDB: 3SN6) to predict amino acids interacting with $G_{\alpha s}$. The last five C-terminal residues of mammalian $G_{\alpha s}$ subunit are $QYELL^{COOH}$, shown in red. (C) Snake plot of the $hA_{2B}R$. Five residues ($R103^{3.50}$, $I107^{3.54}$, $L213^{IL3}$, $S235^{6.36}$ and $L236^{6.37}$) were selected to be individually mutated to alanine based on the homology model in B).

The L213 ^{IL3}A mutant improved coupling efficiency in all yeast strains compared to the wild-type receptor, but to a different extent. The highest coupling efficiency was found in MMY28($G_{\alpha s}$) and MMY19($G_{\alpha 12}$) with a 10-fold decrease of NECA's EC_{50} values compared to the wild-type receptor in the same strain. This mutant receptor was also able to reach maximal activation levels in each yeast strain upon activation by NECA except in MMY14($G_{\alpha q}$) with a somewhat reduced E_{max} value of 76%.

The S235$^{6.36}$A mutant receptor showed the most divergent humanized G protein coupling profile. In MMY12 ($G_{\alpha WT}$) and MMY20($G_{\alpha 13}$), this mutant did not alter activation compared to the wild-type receptor in the same strain. However, it showed the largest increase of activation in MMY28($G_{\alpha s}$) with a one log-unit shift for the full agonist NECA's EC_{50}, and a 0.3-fold shift in MMY 23($G_{\alpha i1}$) (Table 2). In contrast, this mutant showed a decrease of activation in MMY24($G_{\alpha i3}$), MMY14($G_{\alpha q}$) and MMY21($G_{\alpha 14}$) (up to 3.1-fold in MMY21, Table 2) and a complete loss of activation was observed in MMY19($G_{\alpha 12}$). S235$^{6.36}$A was only able to reach near-maximal activation levels in MMY24($G_{\alpha i3}$) and MMY28($G_{\alpha s}$) strains. In other strains only a partial NECA response of approx. 80% was observed, except for MMY14($G_{\alpha q}$) (50%) and MMY19($G_{\alpha 12}$) (no activation) (Table 2).

L236$^{6.37}$A showed a decreased response to NECA in the magnitude of 1.3-fold to 21-fold in all yeast strains compared to the wild-type receptor in the same strain (Table 2). L236$^{6.37}$A reached near-maximal activation levels in most strains except for MMY19 (50%), MMY14 (83%) and MMY20 (85%). Interestingly, L236$^{6.37}$A also induced less constitutive activity in MMY28 than other receptors (wild-type and mutated) in this strain (data not shown).

Table 2. EC_{50}, fold of EC_{50} and E_{max} values of wild-type and mutant A_{2B} receptors in all examined MMY strains. The fold shift of EC_{50} was calculated by dividing the EC_{50} of the mutant receptor by the EC_{50} of the wild-type receptor of the same strain. $\%E_{max}$ represents the intrinsic activity of the receptor, where the mean maximal growth level of MMY12 carrying wild-type receptor in response to the agonist NECA (10^{-4}M) was set as 100%. Results were mostly obtained from two independent experiments, performed in duplicate (individual values in parentheses).

		EC_{50}	fold EC_{50}	% E_{max}
MMY 12	Wild-type	393 ± 92	1	100 ± 3
($G_{\alpha WT}$)	$R103^{3.50}A$	-	-	13 (17, 9)
	$I107^{3.54}A$	-	-	0 (0, 1)
	$L213^{IL3}A$	236 (152, 319)	0.6	100 (104, 96)
	$S235^{6.36}A$	384 (309, 459)	1	85 (83, 87)
	$L236^{6.37}A$	3099 (2503, 3694)	7.9	102 (109, 96)
MMY 14	Wild-type	1641 ± 552	1	99 ± 3
($G_{\alpha q}$)	$R103^{3.50}A$	-	-	1 (1, 1)
	$I107^{3.54}A$	-	-	(0, 0)
	$L213^{IL3}A$	483 (461, 504)	0.3	76 (75, 77)
	$S235^{6.36}A$	3109 (2102, 4115)	1.9	50 (48, 51)
	$L236^{6.37}A$	7069 (9827, 4310)	4.3	83 (83, 82)
MMY 19	Wild-type	2843 ± 1141	1	91 ± 8
($G_{\alpha 12}$)	$R103^{3.50}A$	-	-	2 (2, 1)
	$I107^{3.54}A$	-	-	1 (0, 1)
	$L213^{IL3}A$	272 (199, 345)	0.1	100 (100, 99)
	$S235^{6.36}A$	-	-	19 (8, 31)
	$L236^{6.37}A$	-	-	50 (60, 40)
MMY 20	Wild-type	384 ± 158	1	99 ± 7
($G_{\alpha 13}$)	$R103^{3.50}A$	-	-	6 (10, 2)
	$I107^{3.54}A$	-	-	3 (3, 3)
	$L213^{IL3}A$	90 (42, 137)	0.2	102 (107, 97)
	$S235^{6.36}A$	437 (501, 372)	1.1	77 (75, 80)
	$L236^{6.37}A$	5375 (4700, 6050)	14	85 (87, 84)
MMY 21	Wild-type	212 ± 91	1	108 ± 7
($G_{\alpha 14}$)	$R103^{3.50}A$	-	-	4 (5, 2)
	$I107^{3.54}A$	-	-	1 (0, 1)
	$L213^{IL3}A$	34 (17, 51)	0.2	107 (108, 106)
	$S235^{6.36}A$	664 (552, 776)	3.1	80 (78, 82)
	$L236^{6.37}A$	1335 (783, 1887)	6.3	99 (104, 94)
MMY 23	Wild-type	305 ± 137	1	91 ± 8
($G_{\alpha i1}$)	$R103^{3.50}A$	-	-	9 (15, 3)
	$I107^{3.54}A$	7629 (9162, 6095)	25	37 (38, 37)
	$L213^{IL3}A$	108 (72, 143)	0.4	95 (96, 94)
	$S235^{6.36}A$	84 (103, 65)	0.3	82 (76, 88)
	$L236^{6.37}A$	411 (398, 424)	1.3	98 (102, 95)
MMY 24	Wild-type	59 ± 10	1	113 ± 5
($G_{\alpha i3}$)	$R103^{3.50}A$	-	-	9 (7, 10)
	$I107^{3.54}A$	-	-	2 (2, 1)
	$L213^{IL3}A$	49 (25, 72)	0.8	104 (113, 96)
	$S235^{6.36}A$	175 (174, 176)	3	105 (109, 102)
	$L236^{6.37}A$	680 (504, 855)	11.6	112 (121, 103)
MMY 28	Wild-type	25 ± 6	1	112 ± 4
($G_{\alpha s}$)	$R103^{3.50}A$	57 (53, 61)	2.2	95 (98, 92)
	$I107^{3.54}A$	47 (25, 69)	1.9	103 (100, 106)
	$L213^{IL3}A$	23 (31, 15)	0.9	105 (104, 106)
	$S235^{6.36}A$	33 (42, 24)	1.3	105 (110, 100)
	$L236^{6.37}A$	538 (755, 321)	21	96 (95, 98)

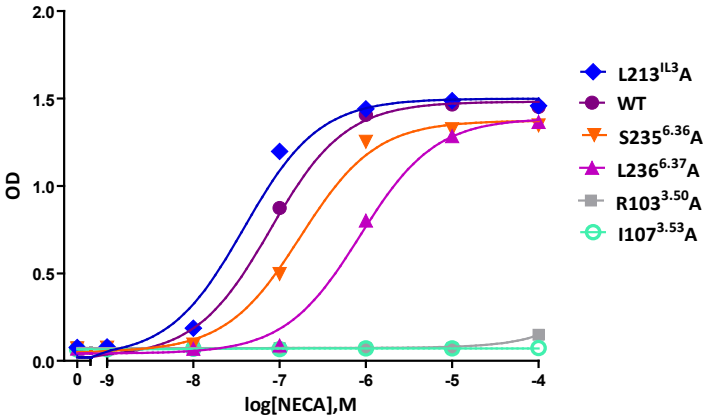

Fig. 3 Concentration-effect curves from liquid assay experiments. Curves are shown of the wild-type, and five mutant receptors L213 ^{IL3}A, S235$^{6.36}$A, L236$^{6.37}$A, R103$^{3.50}$A and I107$^{3.53}$A in the MMY24($G_{\alpha i3}$) strain responding to the adenosine receptor agonist NECA. The assay was performed in YNB-ULH medium.

Determination of expression level of the $hA_{2B}R$ in different yeast strains

In Figure 4A a Western blot analysis of the expression levels of the WT $hA_{2B}R$ and three mutants is shown. In each gel the antibody used recognized the top and bottom bands as specific bands of the $hA_{2B}R$ while the middle one was used as a reference band, since it is not specific for the receptor as evidenced by the MMY12 strain carrying the plasmid pDT-PGK without receptor. Quantitative bar graphs derived from the data in Figure 4A are shown in Figure 4B. Expression levels of the wild-type receptor in most strains were quite comparable (Fig. 4B). Even though mutants R103A and I107 did not respond to NECA in the liquid assay experiments, they did express in all yeast strains, except for MMY21_ I107A (Fig. 4B). These data confirm that the transformation protocols used led to robust receptor expression in (almost) all cases and, hence, provide further proof of the validity of the activation profiles established. Moreover, it seems a certain degree of receptor expression is sufficient for receptor activation. As an example, the density of the L213 ^{IL3}A mutant was lowest in MMY24 and highest in MMY28. Nevertheless, EC_{50} and E_{max} values for NECA were the virtually the same in both strains. To save costly (and commercially unavailable) antibody we did not screen S235A and L236A mutant receptors, since their transferred strains always showed NECA conentration-response curves with high E_{max} values.

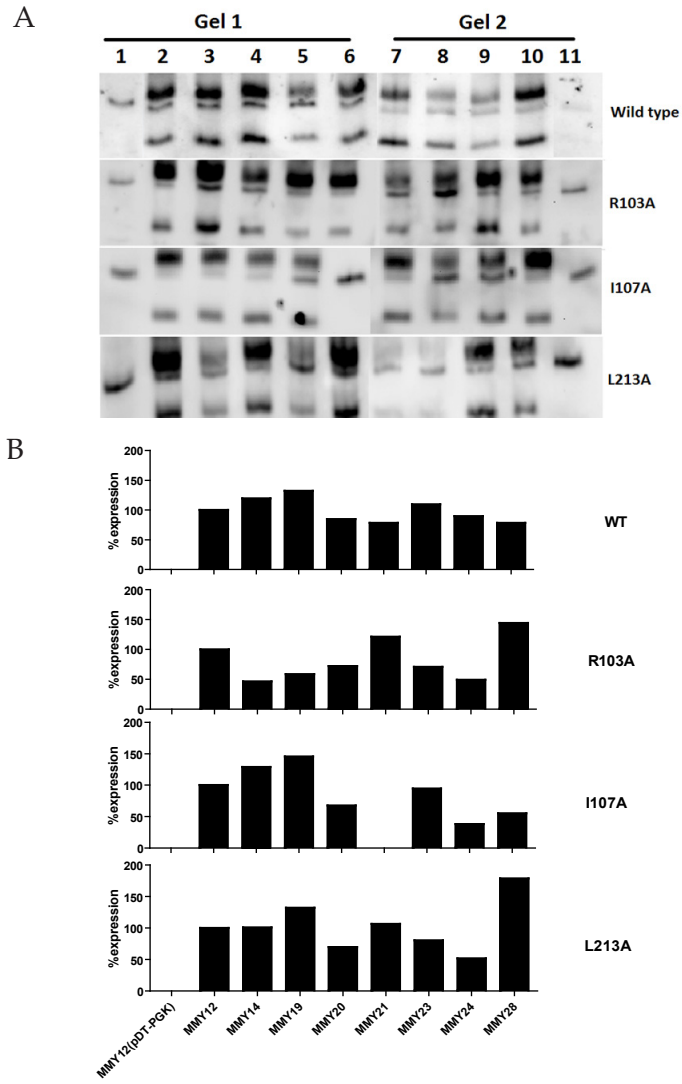

Fig. 4 Western blot analysis of the wild-type $hA_{2B}R$ and R103A, I107A and L213A mutations from top to bottom panel as expressed in different MMY strains. (A) Gel 1: Lane 1, MMY12 carrying pDT-PGK without receptor; Lane 2- 6, MMY12, MMY14, MMY19, MMY20 and MMY21 carrying pDT-PGK_A_{2B} wild-type or mutant receptor. Gel 2: Lane7-10, MMY23, MMY24, MMY28 and MMY12 carrying pDT-PGK_A_{2B} mutant receptor; Lane 11, MMY12 carrying pDT-PGK without receptor. The A_{2B} receptor specific bands are 29 kD and 50 kD, which are absent in MMY12 carrying pDT-PGK without receptor; Nonspecific band at approx. 45 kDa was used as loading control, which also appeared in MMY12 carrying pDT-PGK without receptor. (B) Bar graphs were calculated from a densitometric analysis of the blots. The ratio was determined between the density of the specific bands and that of the nonspecific band that is always present on the blots. MMY12 carrying wild-type or mutant receptor was set as 100% and MMY12 carrying the empty vector pDT-PGK without receptor was set as 0%.

Ligand binding assay of wild-type and mutant $hA_{2B}R$ expressed in MMY24($G_{\alpha i3}$)

To investigate whether the binding affinity of NECA was changed in the mutated receptors, we performed a number of radioligand binding experiments. Traditionally, this assay is cumbersome in yeast cells, but we managed to obtain sufficient levels of specific [^{3}H]PSB-603 binding to do displacement assays on wild-type, L213A and L236A receptors. The two mutant receptors had a similar IC_{50} value for NECA displacing [^{3}H]PSB-603 binding compared to the wild-type receptor (Table 3). However, the binding affinity of the radiolabeled antagonist for the other mutants, R103A, I107A and S235A, appeared to be decreased. As a consequence we did not obtain a high enough window of specific [^{3}H]PSB-603 binding to perform a radioligand displacement assay.

Table 3. Radioligand binding experiments of wild-type and mutant hA_{2B} receptors expressed in MMY24($G_{\alpha i3}$) using 1.5 nM [^{3}H]PSB-603. Specific binding of wild-type receptor was set at 100%. IC_{50} values were obtained from competition binding curves of five independent experiments, performed in duplicate.

Mutant	% specific binding	IC_{50}(μM)
Wild-type	100	1.85 ± 0.87
R103A	0	nd
I107A	12	nd
L213A	94	1.90 ± 1.64
S235A	20	nd
L236A	158	1.88 ± 0.6

nd: not determined

Discussion

Even though the mechanisms of interaction between GPCRs and their G proteins are largely unknown, the α4-helix and α4-β6 loop[34, 35], the N-terminus[36] and C-terminus of G_α subunits[37] have been described to be important for GPCR-G_α protein binding and selectivity. Of those the C-terminus of the G_α subunit appears most intimately involved in binding the receptor. This was already evident from available crystal structures[23, 30] and further confirmed in molecular dynamics

calculations by Kling et al., to show that three residues at the C-terminus of $G_{\alpha s}$ are in close contact with at least 5 amino acids of the β_2AR[38]. In the present study, we examined the mechanism of interaction between the A_{2B} receptor and the last five amino acid residues in the C-terminus of G_α subunits using a functional yeast system combined with homology modeling and mutagenesis experiments.

G protein-coupling profiles of the wild-type A_{2B} receptor

We found that the wild-type hA_{2B}R can activate many humanized G protein pathways, which is consistent with earlier findings by Brown et al. that the hA_{2B}R is quite promiscuous as it recognizes most strains with a similar rank order of activation[19]. These strains possess different humanized G proteins, in which the last five amino acid residues of the endogenous Gpa1p C-terminal have been replaced with the same sequence from mammalian G_α proteins, covering the four major classes: $G_{\alpha i}$, $G_{\alpha s}$, $G_{\alpha q}$ and $G_{\alpha 12}$. It is worth noting that the differences in activation profiles found in the present study can only be due to the variation in the five terminal amino acids of the humanized C-terminus of the G_α subunit. This has the advantage of providing a detailed snapshot of G protein activation without confounding factors such as further differences in the composition of the various G_α subunits.

The A_{2B} receptor is preferentially coupled to the G_s pathway and to a lesser degree to the G_q pathway in many cells[39], and these two G proteins also couple well in our yeast system (*S. cerevisiae* strains MMY28($G_{\alpha s}$), MMY14($G_{\alpha q}$) and MMY21($G_{\alpha 14/q}$), respectively). Interestingly, the receptor appears to couple well to two strains with a $G_{\alpha i}$ protein, MMY24($G_{\alpha i3}$) and MMY23($G_{\alpha i1}$), too, providing proof of the promiscuity mentioned above. However, this is not a "general" GPCR feature. For instance, Stewart et al used the same yeast system to study functional selectivity of agonists and antagonists of the adenosine A_1 receptor and learned that only the $G_{i/o}$ pathway was addressed[18]. Likewise, the hydroxy-carboxylic acid receptor HCA_3 can only activate the G_i pathway through its agonist acifran (preliminary data not shown).

G protein-coupling profiles of mutants of the $hA_{2B}R$

In the present study we sought to identify amino acid residues on the $hA_{2B}R$ that are vital in G protein coupling. The β_2AR-G_s crystal structure (PDB: 3SN6) was chosen as the template to predict such amino acids in the $hA_{2B}R$. $R103^{3.50}$, $I107^{3.54}$, L213 ^{IL3}, $S235^{6.36}$ and $L236^{6.37}$ were selected to be mutated into alanine because they are interacting with the last five amino acids of the $G_{\alpha s}$ protein in the β_2AR-G_s crystal structure. We will discuss these five amino acids in the light of our findings.

Residues $R103^{3.50}$ and $I107^{3.54}$

These two residues ($R103^{3.50}$ and $I107^{3.54}$) are located on the intracellular side of TM3 and are included in the consensus sequence (I/L)*XX*D$R^{3.50}$Y*XX*(I/V)$^{3.54}$[32]. $R^{3.50}$ is a part of the most conserved motif in the class A GPCRs: Asp-Arg-Tyr (DRY). This arginine is 100% conserved within the subfamily of adenosine receptors and nucleotide-like receptors, and 97% of all Class A rhodopsin-like receptors. This is less so for $I^{3.54}$ with 54% overall conservation (Table 4).

Not surprisingly $R^{3.50}$ has been the subject of many mutation studies, exemplified by their high occurrence in the GPCRDB mutation database[40]. The DRY-motif is part of a so-called "ionic lock"[41, 42], consisting of a number of interactions between the DRY-motif and amino acids in TM6; the interaction that is most prominent is the interaction between $R^{3.50}$ and a negatively charged residue in TM6, Asp (D) or Glu (E). These interactions are thought to stabilize the receptor in an inactive conformation and thereby decrease its basal activity[43]. When the receptor is activated the ionic lock is broken and TM6 is moving outward. Breaking the ionic look through mutation might thus lead to constitutive activity, which was shown to be the case on the adenosine A_3 receptor[44]. While this mechanism seems to hold true for some receptors it does not hold for every GPCR, as on the histamine H_4 receptor[45]. $R^{3.50}$ in this case turned out to be very important for G protein coupling. Our own results comply with data found for the α_{1b}-adrenergic receptor where mutations of $R^{3.50}$ resulted in a complete loss of receptor-mediated response in the majority of mutant receptors[46].

It has been proposed that there are many other conserved residues that help $R^{3.50}$ switch the receptor on or off, such as $D^{3.49}$ and $I/V^{3.54}$[32]. The latter position (3.54) is always conserved with a bulky β-branched, hydrophobic residue (Val or Ile). A mutagenesis study in the gonadotropin-releasing hormone (GnRH) receptor offered a hypothesis as to why there is a lack of receptor signaling in a receptor with a mutated $I^{3.54}$. According to Ballesteros et al. $I^{3.46}$, $A^{3.49}$, and $I^{3.54}$, all highly conserved amino acids, form a layer around $R^{3.50}$, the so-called arginine-cage motif. $I^{3.54}$A mutations caused significant reductions in receptor signaling efficacy and reduced the affinity for GnRH as well. In the WT receptor the bulky side chain of $I^{3.54}$ cannot move much as it readily clashes with the side chain of $R^{3.50}$. This does not occur in the $I^{3.54}$A mutant, which allows $R^{3.50}$ to take an unfavorable conformation with an orientation to the aqueous cytoplasm. This might prevent $R^{3.50}$ from taking part in receptor activation. Thus the purpose of $I^{3.54}$ appears to be a defined and strictly controlled positioning of $R^{3.50}$[32].

The results from our yeast screening assay add a layer of detail to these general findings, in that some G proteins seem more affected than others. We found that mutation to alanine of $R103^{3.50}$and $I107^{3.54}$ in the $hA_{2B}R$ abolished many humanized G protein pathways (Table 2) and, hence, we concluded they are very important for interaction with humanized G proteins. $R103^{3.50}$ is crucial for each pathway, except for $G_{\alpha s}$, whereas $I107^{3.54}$ is vital for most G protein pathways as well, although after mutation some interaction remained with both $G_{\alpha i1}$ and $G_{\alpha s}$.

Table 4. Sequence conservation of the four helical amino acids involved in G protein interaction, among adenosine receptors, nucleotide-like receptors*, and class A rhodopsin-like receptors as found on GMOS (GPCRs Motif Searcher, http://lmc.uab.cat/gmos/).

Amino acid in A_{2B}	Conservation in Adenosine receptors	Most occurring	Conservation in Nucleotide-like receptors	Most occurring	Conservation in Class A rhodopsin-like receptors	Most occurring
$R103^{3.50}$	100.0%	R - 100%	100.0%	R - 100%	96.98%	R - 96.98%
$I107^{3.54}$	35.29%	V - 64.70%	41.74%	V - 46.60%	53.68%	I - 53.68%
$S235^{6.36}$	85.29%	S - 85.29%	33.00%	S - 33.00%	2.81%	T - 32.25%
$L236^{6.37}$	85.29%	L - 85.29%	36.89%	L - 36.89%	38.59%	L - 38.59%

* Nucleotide-like receptors: adenosine A_1, A_{2A}, A_{2B}, A_3 receptors; P2RY1, 4, 5, 6, 8, 9, 10, 11; GPR23, 35, 91, 92, 174.

Other three residues $L213^{IL3}$, $S235^{6.36}$ and $L236^{6.37}$

Even though the investigated mutants only have one residue altered at the time, they show substantial differences in ligand activation of the receptor. A prominent enhancement was seen with the $L213^{IL3}A$ mutant; in all cases/strains NECA was more active than on the wild-type receptor, particularly in MMY19($G_{\alpha 12}$), with a 10-fold increase in potency. This result shows once more the dependency of agonist potency on amino acids other than those in the ligand binding site, and may even shed light on pharmacological principles such as receptor reserve. Apparently, the leucine on position 213 in the wild-type receptor acts as a deactivating switch.

The role of $S^{3.36}$ seems to be somewhat more ambiguous. This residue when mutated to alanine caused mostly a decrease of receptor signaling. $S^{6.36}$ is much conserved (Table 4) within the adenosine receptor subfamily (85%), but less so in the nucleotide-like receptors (33%) and hardly in all class A rhodopsin-like receptors (2.8%). Several mutations have been made in different receptors on the 6.36 position but none of the original amino acids was a serine. The closest mutation is a $T^{6.36}A$ in the human muscarinic acetylcholine M1 receptor where the mutant did not significantly differ from wild-type in PI turnover[47]. In the present study, the $S2^{6.36}A$ mutation showed a most divergent G protein profile: improved activation efficiency in MMY28($G_{\alpha s}$) and MMY23($G_{\alpha i1}$); no change in

MMY20($G_{\alpha i3}$) similar to MMY12($G_{\alpha WT}$); decreased activation in MMY14($G_{\alpha q}$), MMY24($G_{\alpha i3}$), MMY21($G_{\alpha 14}$) and a complete loss of activation in MMY19($G_{\alpha 12}$) (Table 2). Apparently the change from a hydrophilic (serine) to a hydrophobic (alanine) amino acid is dealt with differently by the G proteins studied.

$L^{6.37}$ is quite conserved: 85% in adenosine receptors, 37% in nucleotide-like receptors, and 39% in all class A rhodopsin-like receptors. In the A_{2A} receptor the $L^{6.37}A$ mutation along with several others was used to provide receptor thermostabilization for crystallographic purposes[48]. The mutant caused no effect on ligand pharmacology. In our hands, the $L236^{6.37}A$ mutation decreased activation in all humanized G protein pathways, most outspoken for MMY28. Apparently, the leucine residue is vital for G protein interaction and activation.

Function of hydroxyl-group at C-terminus of G_{α} subunits for wild-type $hA_{2B}R$

The slight differences in amino acid composition in some of the G_{α} subunits allow an almost atomic dissection of the observed effects. There is an 8-fold potency difference of NECA in the two G_q pathway strains MMY21($G_{\alpha 14}$) with an EC_{50} value of 212 nM and MMY14($G_{\alpha q}$) with an EC_{50} value of 1641 nM. Both have the same amino acid residues at the C-terminus of the G_{α} protein except for the fourth residue position counting from the end of the C-terminus with a tyrosine in MMY14 and a phenylalanine in MMY21 (Table 1). The only difference between tyrosine and phenylalanine is a hydroxyl-group, which leads to the large decrease in potency for NECA. However, there is an opposite phenomenon at the last amino acid of the C-terminus between two $G_{\alpha i}$ pathway strains, MMY24($G_{\alpha i3}$) and MMY23($G_{\alpha i1}$). A tyrosine as last amino acid of the end of the C-terminus position of MMY24 yielded an EC_{50} value of 59 nM for NECA, whereas the phenylalanine on the same position in MMY23 gave an EC_{50} value of 305 nM (Tables 1 and 2). This particular tyrosine hydroxyl-group is apparently enough to decrease the EC_{50} value by 6-fold, which is equivalent to an increase of activation and NECA potency. Taken together, subtle changes such as the presence or absence of a hydroxyl-group located in the C-terminus of the G_{α} protein control activation of GPCRs.

Concluding remarks

We reported on a yeast system that is very well suited for the study of a G protein-coupled receptor (the $hA_{2B}R$ in this case), its activation and its G protein preference. This highly efficient and inexpensive screening system was used to map residues at the cytoplasmic side of the receptor and in the C-terminus of different G_{α} subunits important for receptor activation. The results provided detailed information about receptor/G protein binding and G protein selectivity.

Acknowledgements

Rongfang Liu thanks the China Scholarship Council (CSC) for her PhD scholarship. NWO provided a TOP grant to A.P. IJ. (714.011.001). The authors are grateful to Prof C.E. Müeller of Bonn University for the generous gift of [^{3}H] PSB-603 and to Simon Dowell from GSK for providing the yeast strains and experimental protocols.

References

[1] Oldham, W.M., et al. *Mechanism of the receptor-catalyzed activation of heterotrimeric G proteins.* Nat. Struct. Mol. Biol. (2006) 13: 772-777.

[2] Baltoumas, F.A., et al. *Interactions of the alpha-subunits of heterotrimeric G-proteins with GPCRs, effectors and RGS proteins: A critical review and analysis of interacting surfaces, conformational shifts, structural diversity and electrostatic potentials.* J. Struct. Biol. (2013) 182: 209–218.

[3] Fredholm, B.B., et al. *Structure and function of adenosine receptors and their genes.* Naunyn-Schmiedeberg's Arch. Pharmacol. (2000) 362: 364-374.

[4] Fredholm, B.B., et al. *Comparison of the potency of adenosine as an agonist at human adenosine receptors expressed in Chinese hamster ovary cells.* Biochem. Pharmacol. (2001) 61: 443-448.

[5] Wei, W., et al. *Blocking A_{2B} adenosine receptor alleviates pathogenesis of experimental autoimmune encephalomyelitis via inhibition of IL-6 production and Th17 differentiation.* J. Immunol. (2013) 190: 138-146.

[6] Wei, Q., et al. *A_{2B} adenosine receptor blockade inhibits growth of prostate cancer cells.* Purinergic Signal. (2013) 1-10.

[7] Stagg, J., et al. *Anti-CD73 antibody therapy inhibits breast tumor growth and metastasis.*

Proc. Natl. Acad. Sci. (2010) 107: 1547-1552.

[8] Owen, S.J., et al. *Loss of adenosine A_{2B} receptor mediated relaxant responses in the aged female rat bladder; effects of dietary phytoestrogens.* Naunyn-Schmiedeberg's Arch. Pharmacol. (2012) 385: 539-549.

[9] Cekic, C., et al. *Adenosine A_{2B} receptor blockade slows growth of bladder and breast tumors.* J. Immunol. (2012) 188: 198-205.

[10] Koscsó, B., et al. *Stimulation of A_{2B} adenosine receptors protects against trauma–hemorrhagic shock-induced lung injury.* Purinergic Signal. (2013) 1-6.

[11] Bot, I., et al. *Adenosine A_{2B} receptor agonism inhibits neointimal lesion development after arterial injury in apolipoprotein E–deficient mice.* Arterioscler. Thromb. Vasc. Biol. (2012) 32: 2197-2205.

[12] Pausch, M.H. *G-protein-coupled receptors in Saccharomyces cerevisiae: high-throughput screening assays for drug discovery.* Trends Biotechnol. (1997) 15: 487-494.

[13] Peeters, M.C., et al. *Three "hotspots" important for adenosine A_{2B} receptor activation: a mutational analysis of transmembrane domains 4 and 5 and the second extracellular loop.* Purinergic Signal. (2011) 1-16.

[14] Mathew, E., et al. *Functional fusions of T4 lysozyme in the third intracellular loop of a G protein-coupled receptor identified by a random screening approach in yeast.* Protein Eng. Des. Sel. (2013) 26: 59-71.

[15] Jaeschke, H., et al. *Preferences of transmembrane helices for cooperative amplification of $G_{\alpha s}$ and $G_{\alpha q}$ signaling of the thyrotropin receptor.* Cell. Mol. Life Sci. (2008) 65: 4028-4038.

[16] Evans, B.J., et al. *Expression of CXCR4, a G-protein–coupled receptor for CXCL12 in Yeast: identification of new-generation inverse agonists.* Methods Enzymol. (2009) 460: 399-412.

[17] Minic, J., et al. *Yeast system as a screening tool for pharmacological assessment of G protein coupled receptors.* Curr. Med. Chem. (2005) 12: 961-969.

[18] Stewart, G.D., et al. *Determination of adenosine A_1 receptor agonist and antagonist pharmacology using Saccharomyces cerevisiae: implications for ligand screening and functional selectivity.* J. Pharm. Exp. Ther. (2009) 331: 277-286.

[19] Brown, A.J., et al. *Functional coupling of mammalian receptors to the yeast mating pathway using novel yeast/mammalian G protein α subunit chimeras.* Yeast (2000) 16: 11-22.

[20] Dowell, S.J. and Brown, A.J. *Yeast assays for G protein-coupled receptors.* Methods Mol. Biol. (2009) 552: 213-229.

[21] Dowell, S.J. *Yeast assays for G-protein–coupled receptors.* Receptors Channels (2002) 8: 343-352.

[22] Cardozo, T., et al. *Homology modeling by the ICM method.* Proteins: Struct., Funct., Bioinf. (2004) 23: 403-414.

[23] Rasmussen, S.G., et al. *Crystal structure of the β_2 adrenergic receptor-G_s protein complex.* Nature (2011) 477: 549-555.

[24] DeLano, D.W., *The PyMOL Molecular Graphics System, Version 1.5. 0.4 Schrödinger, LLC.*

[25] Gietz, D., et al. *Improved method for high efficiency transformation of intact yeast cells.*

Nucleic Acids Res. (1992) 20: 1425.

[26] Li, Q., et al. *ZM241385, DPCPX, MRS1706 are inverse agonists with different relative intrinsic efficacies on constitutively active mutants of the human adenosine A_{2B} receptor.* J. Pharmacol. Exp. Ther. (2007) 320: 637-645.

[27] Feoktistov, I., et al. *Immunological characterization of A_{2B} adenosine receptors in human mast cells.* Drug Dev. Res. (2003) 58: 461-471.

[28] Peeters, M., et al. *The role of the second and third extracellular loops of the adenosine A_1 receptor in activation and allosteric modulation.* Biochem. Pharmacol. (2012) 84: 76-87.

[29] Venkatakrishnan, A., et al. *Molecular signatures of G-protein-coupled receptors.* Nature (2013) 494: 185-194.

[30] Scheerer, P., et al. *Crystal structure of opsin in its G-protein-interacting conformation.* Nature (2008) 455: 497-502.

[31] Fredholm, B.B., et al. *International union of basic and clinical pharmacology. LXXXI. nomenclature and classification of adenosine receptors an update.* Pharmacol. Rev. (2011) 63: 1-34.

[32] Ballesteros, J., et al. *Functional microdomains in G-protein-coupled receptors the conserved arginine-cage motif in the gonadotropin-releasing hormone receptor.* J. Biol. Chem. (1998) 273: 10445-10453.

[33] Ballesteros, J.A. and Weinstein, H. *Integrated methods for the construction of three-dimensional models and computational probing of structure-function relations in G protein-coupled receptors.* Methods Neurosci. (1995) 25: 366-428.

[34] Bae, H., et al. *Two amino acids within the α4 helix of $G_{\alpha i1}$ mediate coupling with 5-hydroxytryptamine 1B receptors.* J. Biol. Chem. (1999) 274: 14963-14971.

[35] Bae, H., et al. *Molecular determinants of selectivity in 5-hydroxytryptamine1B receptor-G protein interactions.* J. Biol. Chem. (1997) 272: 32071-32077.

[36] Taylor, J.M., et al. *Binding of an alpha 2 adrenergic receptor third intracellular loop peptide to G beta and the amino terminus of G alpha.* J. Biol. Chem. (1994) 269: 27618-27624.

[37] Blahos, J., et al. *Extreme C terminus of G protein α-subunits contains a site that discriminates between G_i-coupled metabotropic glutamate receptors.* J. Biol. Chem. (1998) 273: 25765-25769.

[38] Kling, R.C., et al. *Active-state models of ternary GPCR complexes: determinants of selective receptor-G-protein coupling.* PLOS ONE (2013) 8: e67244.

[39] Thimm, D., et al. *Ligand-specific binding and activation of the human adenosine A_{2B} receptor.* Biochemistry (2013) 52: 726-740.

[40] Vroling, B., et al. *GPCRDB: information system for G protein-coupled receptors.* Nucleic Acids Res. (2011) 39: D309-D319.

[41] Vogel, R., et al. *Functional role of the "ionic lock"—an interhelical hydrogen-bond network in family A heptahelical receptors.* J. Mol. Biol. (2008) 380: 648-655.

[42] Scheer, A., et al. *Constitutively active mutants of the alpha 1B-adrenergic receptor: role of highly conserved polar amino acids in receptor activation.* EMBO J. (1996) 15: 3566.

[43] Flanagan, C.A. *A GPCR that is not "DRY".* Mol. Pharmacol. (2005) 68: 1-3.

[44] Chen, A., et al. *Constitutive activation of A_3 adenosine receptors by site-directed mutagenesis.* Biochem. Biophys. Res. Commun. (2001) 284: 596-601.

[45] Schneider, E.H., et al. *Impact of the DRY motif and the missing "ionic lock" on constitutive activity and G-protein coupling of the human histamine H4 receptor.* J. Pharmacol. Exp. Ther. (2010) 333: 382-392.

[46] Scheer, A., et al. *Mutational analysis of the highly conserved arginine within the Glu/Asp-Arg-Tyr motif of the α1b-adrenergic receptor: effects on receptor isomerization and activation.* Mol. Pharmacol. (2000) 57: 219-231.

[47] Högger, P., et al. *Activating and inactivating mutations in N-and C-terminal i3 loop junctions of muscarinic acetylcholine Hm1 receptors.* J. Biol. Chem. (1995) 270: 7405-7410.

[48] Doré, A.S., et al. *Structure of the adenosine A_{2A} aeceptor in complex with ZM241385 and the Xanthines XAC and Caffeine.* Structure (2011) 19: 1283-1293.

[49] Simon, M.I., et al. *Diversity of G proteins in signal transduction.* Science (1991) 252: 802-808.

Chapter 4

Scanning mutagenesis in a yeast system delineates the role of the NPxxY(x)$_{5,6}$F motif and helix 8 of the adenosine A_{2B} receptor in G protein coupling

This chapter is based upon:

Rongfang Liu, Dennis Nahon, Beau le Roy, Eelke B. Lenselink, Adriaan P. IJzerman

Biochemical Pharmacology ***2015*** *95: 290-300*

Abstract

The adenosine receptor subfamily includes four subtypes: the A_1, A_{2A}, A_{2B} and A_3 receptors, which all belong to the superfamily of G protein-coupled receptors (GPCRs). The adenosine A_{2B} receptor is the least investigated of the adenosine receptors, and the molecular mechanisms of its activation have hardly been explored. We used a single-GPCR-one-G protein yeast screening method in combination with mutagenesis studies, molecular modeling and bio-informatics to investigate the importance of the different amino acid residues of the NPxxY$(x)_6$F motif and helix 8 in the human adenosine A_{2B} receptor ($hA_{2B}R$) activation. A scanning mutagenesis protocol was employed, yielding 11 single mutations and one double mutation of the NPxxY$(x)_6$F motif and 16 single mutations of helix 8. The amino acid residues P287$^{7.50}$, Y290$^{7.53}$, R293$^{7.56}$ and I304$^{8.57}$ were found to be essential, since mutation of these amino acid residues to alanine led to a complete loss of function. Western blot analysis showed that mutant receptor R293$^{7.56}$A was not expressed, whereas the other proteins were. Amino acid residues that are also important in receptor activation are: N286$^{7.49}$, V289$^{7.52}$, Y292$^{7.55}$, N294$^{8.47}$, F297$^{8.50}$, R298$^{8.51}$, H302$^{8.55}$ and R307$^{8.60}$. The mutation Y290$^{7.53}$F lost 50% of efficacy, while F297$^{8.50}$A behaved similar to wild-type receptor. The double mutation, Y290$^{7.53}$F/F297$^{8.50}$Y, lost around 70% of efficacy and displayed a lower potency for the reference agonist 5′-(*N*-ethylcarboxamido)adenosine (NECA). This study provides new insight into the molecular interplay and impact of TM7 and helix 8 for hA_{2B} receptor activation, which may be extrapolated to other adenosine receptors and possibly to other GPCRs.

Introduction

The G protein-coupled receptors (GPCRs) form a membrane-bound protein superfamily of seven transmembrane (TM) receptors that transmit extracellular signaling to the intracellular environment[1]. All GPCRs have seven transmembrane spanning α-helices, an intracellular C-terminus with an additional α-helix ('helix 8'), an extracellular N-terminus, and 3 intra- and 3 extracellular loops. When a GPCR is activated by an extracellular stimulus (e.g., a hormone/neurotransmitter or a synthetic agonist), a change in receptor conformation is induced, leading to subsequent activation of a heterotrimeric G protein[2].

The NPxxY$(x)_{5,6}$F stretch of amino acids plays an important role in G protein activation[3], which includes the highly conserved NPxxY motif in TM7 across the class A (rhodopsin-like) GPCR family, that is linked to the intracellular helix 8, especially the residue phenylalanine (F) therein (5 or 6 residues after the NPxxY motif)[4]. Helix 8 located at the start of the carboxyl (C)-terminus of GPCRs is gaining recognition for its importance in GPCR function. Previous research has shown that key residues of helix 8 play a vital role in receptor activation, such as in the M1 muscarinic acetylcholine receptor[5], leukotriene B4 receptor[6], cannabinoid receptor 1[7], the type 1 angiotensin receptor[8] and the human β_1-adrenergic receptor[9]. However, there has been no study focusing on this helix 8 in the context of activation of adenosine receptors. All four adenosine receptors (A_1, A_{2A}, A_{2B} and A_3) are ubiquitously expressed in the human body[10] and can target different intracellular signaling pathways by responding to the same endogenous ligand adenosine. The A_{2B} receptor has the lowest affinity for adenosine[11] and has been less investigated than the other adenosine receptors. Several studies have shown that blocking A_{2B} receptor signaling reduces experimental autoimmune encephalomyelitis[12] and inhibits growth of prostate cancer cells[13], breast tumors[14] and bladder tumors[15, 16]. On the other hand, activation of the A_{2B} receptor protects against trauma-hemorrhagic shock-induced lung injury[17], CHX-induced apoptosis[13] and also vascular injury[18]. Thus, understanding the molecular mechanisms of hA_{2B} receptor activation is of

considerable relevance for drug design and disease prevention. In this context it would be of substantial interest to determine whether the same tyrosine ($Y^{7.53}$ of TM7)–phenylalanine ($F^{8.50}$) interaction exists in the hA_{2B} receptor, as e.g., apparent in the angiotensin II type 1 receptor[8], and also to find which key residues of helix 8 are involved in hA_{2B} receptor activation.

In this study, a single-GPCR-one-G protein system in *Saccharomyces cerevisiae*[19, 20] was examined. It has been used for studying GPCR activation, such as for the adenosine A_1 receptor[21] and the adenosine A_{2B} receptor by ourselves[22], and, recently, for the glucagon-like peptide-1 receptor[23] among many other GPCRs. To investigate the importance of the different amino acid residues of the $NPxxY(x)_6F$ motif and helix 8 in hA_{2B} receptor activation, an alanine-scanning mutagenesis approach was applied to each residue of the $NPxxY(x)_6F$ motif and of helix 8 (Fig. 1). We identified the function of each residue of the $NPxxY(x)_6F$ motif and whole helix 8 in G protein coupling and receptor activation, which may be extrapolated to other adenosine receptors and GPCRs.

Materials and methods

Materials

The *S. cerevisiae* expression vectors, the pDT-PGK and pDT-PGK_hA_{2B} receptor plasmids and the MMY24 strain were kindly provided by Dr. Simon Dowell (GSK, Stevenage, UK). Six mutations, $N286^{7.49}A$, $N286^{7.49}Q$, $N286^{7.49}R$, $Y290^{7.53}F$, $Y290^{7.53}N$ and $N294^{8.47}I$ had been generated before at Leiden University, The Netherlands. The QuikChange® II Site-Directed Mutagenesis Kit was purchased from Stratagene (Amsterdam, the Netherlands). The QIAprep midi plasmid purification kits were purchased from QIAGEN (Amsterdam, the Netherlands). NECA and 3-Amino-[1,2,4]-triazole (3-AT) were both purchased from Sigma–Aldrich (Zwijndrecht, the Netherlands). The Hybond-ECL membranes and the ECL Western blotting analysis system were purchased from GE Healthcare (Eindhoven, the Netherlands). The antibody used was directed against the C-terminal region of the hA_{2B} receptor and was kindly provided by Dr. I. Feoktistov (Vanderbilt University, Nashville, TN, USA) and goat anti-

rabbit IgG was purchased from Jackson ImmunoResearch Laboratories (West Grove, PA, USA). Rat anti-yeast α-tubulin monoclonal antibody was used as a reference protein (GTX76511, GeneTex, Irvine, CA, USA) with goat anti-rat IgG-HRP antibody (sc-2032, Santa Cruz Biotechnology, Heidelberg, Germany) as the second antibody. Adenosine deaminase was purchased from Roche (Almere, The Netherlands). Polyethylenimine (PEI) was purchased from Sigma (Zwijndrecht, the Netherlands).

Generation of point mutations

To investigate the importance of different amino acid residues of the NPxxY$(x)_6$F motif and of helix 8 (Fig. 1) in hA_{2B} receptor activation, a scanning mutagenesis was performed, yielding 11 single mutations and one double mutation of the NPxxY$(x)_6$F motif and 16 single mutations of helix 8. The DNA primers of the mutations of the hA_{2B} receptor (uniprot: P29275) were designed by the QuikChange Primer Design Program of Agilent Technologies (Santa Clara, CA, USA) and contained a single substitution resulting in a codon change for the desired amino acid substitution. The reverse primer sequence of each mutation was the reverse complement of the forward primer. These primers and their complements were synthesized (Eurogentec, Maastricht, the Netherlands) and then used to generate mutation plasmids according to the QuikChange method from Stratagene/Agilent Technologies. The mutagenic reaction contained 45 ng of the constructed pDT-PGK_hA_{2B} plasmid as dsDNA template, 10 μM of each primer, 1 μl of dNTP mix, 2.5 μl of 10 × reaction buffer and 2.5 U *PfuUltra* HF DNA polymerase. The following thermal cycling parameters were used in the PCR apparatus (T100™ Thermal Cycler, Bio-Rad, Hercules, CA, USA): 95 °C for 30 s, 55 °C for 1 min, and 68 °C for 10 min. The number of mutagenic PCR cycles was set to 22. Methylated or hemimethylated non-mutated plasmid DNA was removed by adding 5 U *Dpn* I restriction enzyme for 2 h at 37 °C. The mutated DNA products were transformed into XL-1 Blue supercompetent cells and other details were according to the manual of the QuikChange® II Site-Directed Mutagenesis Kit. The mutations were confirmed by DNA sequencing (LGTC, Leiden, the Netherlands).

Transformation in a *S. cerevisiae* strain (MMY24)

Each mutation plasmid was transformed according to the Lithium-Acetate procedure[24] into an engineered *S. cerevisiae* yeast strain, MMY24, expressing one specific Gpa1p/$G_{\alpha i3}$ chimeric G protein. The yeast strain was derived from the MMY11 strain and further adapted to communicate with mammalian GPCRs. Hereto the last five amino acid residues of C-terminus of Gpa1p/$G_{\alpha i3}$ chimera had been replaced with the same-length sequence from mammalian $G_{\alpha i3}$ protein[19]. The genotype of the MMY24 strain is: **MATa** *his3 leu2 trp1 ura3 can1 gpa1_::G_i3 far1 ::ura3 sst2_::ura3 Fus1::FUS1-HIS3 LEU2::FUS1-lacZ ste2_::G418R* and the sequence of these last 5 C-terminal amino acid residues of Gpa1p/$G_{\alpha i3}$ chimera is ECGLY^{COOH}.

Yeast solid growth assay

To characterize the activation of the mutated receptors, concentration–growth curves were generated with a solid growth assay. To measure the signaling of GPCRs, the pheromone signaling pathway of these strains was coupled via the *FUS1* promoter to *HIS3* (imidazoleglycerol-phosphate dehydratase), an enzyme catalyzing the sixth step in histidine biosynthesis to produce histidine. 3-AT, a competitive inhibitor of imidazoleglycerol-phosphate dehydratase, was added to the assay to reduce background activity caused by endogenous histidine and constitutive activity[20]. The degree of receptor activation induced by an agonist of the GPCR was measured by the growth rate of the yeast on a histidine-deficient medium. The solid assay was performed with yeast cells from an overnight culture in YNB-UL (YNB + adenine + tryptophan + histidine, lacking uracil and leucine). These yeast cells were diluted to around 600,000 cells/ml (OD_{600} ≈ 0.02), and droplets of 1.5 µl (≈ 900 cells) were spotted on selection agar plates, YNB-ULH (YNB + adenine + tryptophan lacking uracil, leucine and histidine), containing 7 mM 3-AT and the adenosine receptor agonist NECA (concentrations ranging from 10^{-9} to 10^{-4} M). After incubation at 30 °C for 50 h, the plates were scanned and receptor activation-mediated yeast growth was quantified with Quantity One imaging software of a GS-800 Calibrated Densitometer from Bio-Rad (Hercules, CA, USA).

Preparation of yeast protein extractions and immunoblotting

Protein extractions were performed with trichloroacetic acid (TCA) according to the Clontech Yeast Protocols Handbook 2001. Yeast transformants were grown in 3 ml YAPD medium and were harvested in mid-exponential phase (adjust OD_{600} = 6, in total 1.2×10^8 cells per sample). The yeast cells were collected and washed with cold water. Subsequently the yeast cells were broken by vigorous vortexing with 200 µl of 20% TCA and 200 µl glass beads. A small hole was burnt in the bottom of the 2 ml eppendorf tubes with a needle and these tubes were placed in 1.5 ml eppendorf tubes. This double layer of tubes was centrifuged at 3,000 rpm for 2 min allowing the TCA with the broken cells, but not the glass beads, to pass through the hole from the top eppendorf tube into the bottom one. The glass beads were washed twice with 200 µl 5% TCA and spun both times at 3,000 rpm for 2 min. The tubes containing the glass beads were discarded and the tubes containing the broken cells were spun at 6,000 rpm for 2 min. The supernatant was removed as much as possible. The pellets were resuspended with 55 µl 10% SDS loading buffer (100 mM EDTA, 1 M Tris, 10% SDS, 0.5% Bromophenol blue; pH = 8) and 35 µl 1 M Tris (pH = 8.0) was added to neutralize all remaining TCA. The samples were incubated for 30 min at 37 °C and centrifuged again at 2,000 rpm for 10 min.

Each sample of 4 µl (≈ 24 µg protein) was loaded on 12.5% SDS/PAGE gel and then blotted on Hybond-ECL membranes (GE Healthcare, Eindhoven, The Netherlands) using a semi-automated electrophoresis technique (PhastSystem™, Amersham Pharmacia Biotech, Piscataway, NJ, USA). The Hybond-ECL membranes were blocked with TBS containing 5% milk powder for 1 h and washed three times with TBST (0.05% Tween 20, TBS pH 7.6). The membranes were incubated with 1:1,250 diluted rabbit anti-human A_{2B} receptor antibody for 1 h. After thorough removal of unbound antibody from the membranes by washing three times with TBST, the membranes were incubated with 1:2,500 diluted HRP-conjugated goat anti-rabbit IgG (Jackson ImmunoResearch Laboratories, West Grove, PA, USA) for 1 h. The membranes were washed twice with TBST and once with TBS. The specific signal of the hA_{2B} receptor was probed according to the ECL Western blotting analysis system (GE Healthcare,

Eindhoven, The Netherlands) using enhanced chemiluminescence (ChemiDox XRS, Bio-Rad, Hercules, CA, USA). Tubulin as the reference household protein was analyzed simultaneously using rat anti-yeast α-tubulin monoclonal antibody at 1 µg/mL and then using goat anti-rat IgG-HRP antibody at 0.16 µg/mL as the second antibody.

Whole cell radioligand binding experiments

The whole cell radioligand binding experiments were performed as described by us before[25, 26]. Yeast cells from an overnight culture expressing the wild-type or mutated $hA_{2B}R$ were harvested from rich 3.5 ml YAPD medium by centrifuging at 2,000 × g for 5 min. The pellet of cells was washed once with 0.9% NaCl. The cells were centrifuged again using the same speed and diluted in the assay buffer (50 mM Tris–HCl pH 7.4 + 1 mM EDTA) to OD_{600} = 40 (OD_{600} = 1 ≈ 2.5 × 10^7 cells/ml) with 0.4 IU adenosine deaminase. Binding experiments were performed with 1.4 nM of the A_{2B} receptor selective antagonist [^{3}H]PSB-603, and a final cell concentration of 25 × 10^7 cells/ml in a total volume of 100 µl. Nonspecific binding (NSB) was determined by additionally adding NECA at a final concentration of 1 mM. Samples were incubated for 1 h at 25 °C keeping the cells in suspension by shaking vigorously. 1 ml of ice-cold assay buffer was added to samples to terminate incubation and the samples were harvested on a Millipore manifold with GF/B filters pre-incubated in 0.1% polyethylenimine (PEI) at a pressure of 200 mbar, to separate free from receptor-bound radioligand by washing twice with 2 ml buffer (50 mM Tris–HCl pH 7.4 + 1 mM EDTA + 0.1% BSA). The filters were transferred into mini-vials, 3.5 ml of PerkinElmer Emulsifier Safe was added, and were subsequently incubated for at least 2 h. Filter-bound radioactivity was determined as counts per minute (CPM) by scintillation spectrometry (Tri-Carb 2900TR; PerkinElmer Life and Analytical Sciences). Results were obtained from at least three independent experiments, performed in duplicate.

Data analysis

After incubation at 30 °C for 50 h, the plates of the solid growth assay were scanned and receptor mediated yeast growth was quantified with Quantity

One imaging software of the GS-800 Calibrated Densitometer from Bio-Rad (Hercules, CA, USA). After correction for the local background, the amount of yeast growth was calculated as the density (in OD/mm^2) of each spot. Results were obtained from four independent experiments, performed in triplicate. EC_{50} values and Emax values of the solid assay were calculated using the nonlinear regression package available in Prism 5.0 software (GraphPad Software Inc., San Diego, CA, USA). Differences in EC_{50} values were examined for significance by a two-tailed homoscedastic Student's *t*-test, yielding *p*-values. Fold EC_{50} is the EC_{50} value on the mutant receptor divided by the EC_{50} value on the wild-type (WT) hA_{2B} receptor.

Expression of the receptors was quantified using Quantity One imaging software from Bio-Rad after correction for the background; it was calculated as density (OD/mm^2). The α-tubulin, at approx. 130 kDa, was used as loading control and the specific hA_{2B} receptor protein bands were at 34 kDa and 55 kDa. The ratio was determined between the density of the specific bands and the density of loading control band. MMY24, carrying the wild-type hA_{2B} receptor, was set at 100% and MMY24, carrying the empty vector pDT-PGK without receptor, was set at 0%. Results were obtained from three independent experiments and all expression levels of mutant receptors were normalized by a wild-type receptor sample on the same blot.

Bio-informatics

Amino acid conservation was obtained for the $NPxxY(x)_{5,6}F$ motif and helix 8. Amino acid sequences of the adenosine receptors, nucleotide-like subfamily and class A (rhodopsin-like) family of GPCRs were collected from GPCRDB (http://www.gpcr.org/7tm/)[27]. Frequency plots displaying conservation were created using Weblogo (http://weblogo.berkeley.edu/logo.cgi)[28].

A chimera/homology model of the adenosine hA_{2B} receptor was constructed using the homology modeling tool within Maestro[29-32]. The model was based on both the β_2 adrenergic receptor/G_s complex crystal structure (PDB: 3SN6) and the crystal structure of the adenosine A_{2A} receptor co-crystallized with the agonist NECA (PDB: 2YDV). A chimera model was constructed to

ensure that the intracellular part of the homology model was in the G_s bound conformation. The model was primarily based on the adenosine A_{2A} crystal structure except for the following sequence regions which were based on the β_2 adrenergic receptor crystal structure: A31-N43, V99-I126, I203-L213, E229-G241 and V289-Y299. Moreover, residues 214–228 in ICL2 were deleted since they were (partly) missing in the crystal structures and not of interest in this study. The resulting homology model was merged with the G_s protein part of the β_2 adrenergic receptor–G_s complex crystal structure and energy-minimized. To further optimize the A_{2B}–G_s complex the side chains of the sequence regions that were based on the β_2 adrenergic receptor were re-predicted using Prime[30-32]; this was done using Monte Carlo sampling.

Results

We set out to investigate the importance of the different amino acid residues of the NPxxY$(x)_6$F motif and helix 8 in the activation of the human adenosine A_{2B} receptor. To that end we employed a scanning mutagenesis approach, yielding 11 single mutations and one double mutation of the NPxxY$(x)_6$F motif and 16 single mutations of helix 8. The amino acids in this scan have been color-coded in a so-called snake plot of the receptor (Fig. 1). We expressed the yeast plasmid pDT-PGK_hA_{2B}R and mutations in a yeast *S. cerevisiae* strain, MMY24. This particular strain was preferred over others (data not shown) as the receptor showed high affinity and efficacy of the reference agonist NECA, while it displayed low constitutive activity yielding a good window between control and agonist-stimulated receptor. When the expressed hA_{2B} receptor or mutations are activated by an agonist, the yeast pheromone signaling pathway is activated through the chimeric yeast-mammalian G protein, leading to transcription of the HIS3 reporter gene and consequently histidine production[33]. Subsequent growth of the yeast cells on a histidine-deficient agar plate was determined by measuring the absorption at a wavelength of 595 nm, which reflects the activation of the expressed receptor by the adenosine receptor agonist NECA. NECA concentration–response curves from the solid growth assay of the wild-

type and mutant receptors are shown in Fig. 2A–C and the values of Emax, EC_{50} and fold EC_{50} shift are listed in Table 1. All mutant receptors displayed negligible constitutive activity, similar to or lower than the WT receptor (data not shown).

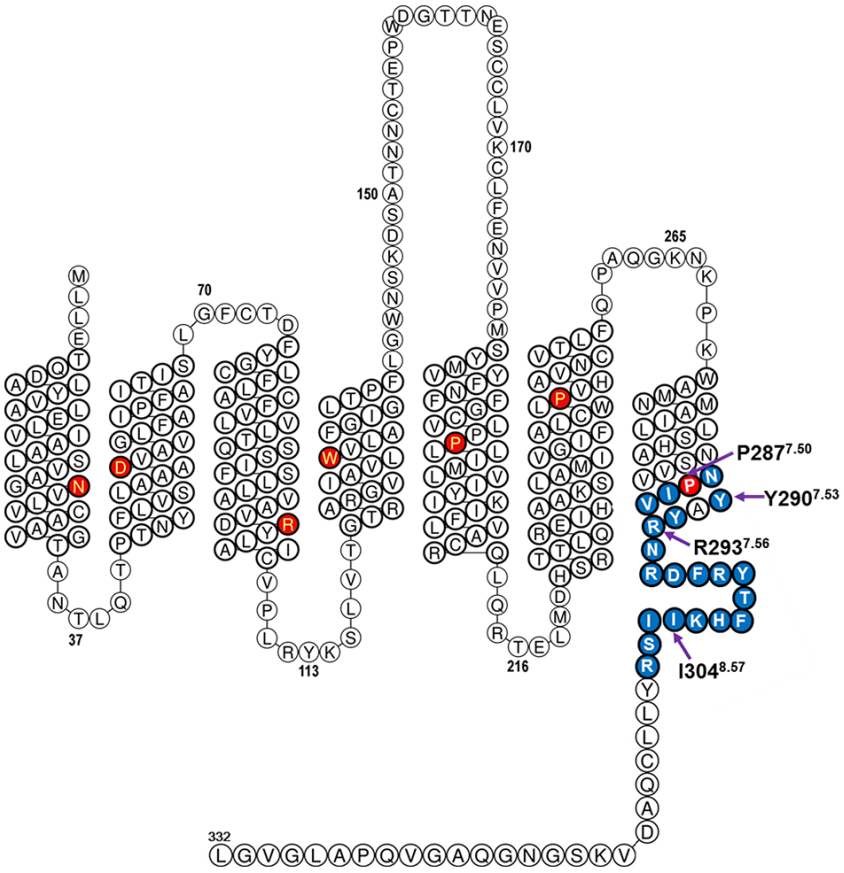

Fig. 1. Snake plot the human adenosine hA_{2B} receptor. The template was obtained from GPCRDB (http://www.gpcr.org/7tm/)[27]. Mutants were made in the $NPxxY(x)_{5,6}F$ motif and helix 8, shown as white bold letters. Four important amino acids have been labeled: $P287^{7.50}$, $Y290^{7.53}$, $R293^{7.56}$ and $I304^{8.57}$. Highly conserved residues are highlighted to indicate the Ballesteros–Weinstein numbering: $N^{1.50}$, $D^{2.50}$, $R^{3.50}$, $W^{4.50}$, $P^{5.50}$, $P^{6.50}$ and $P^{7.50}$[54].

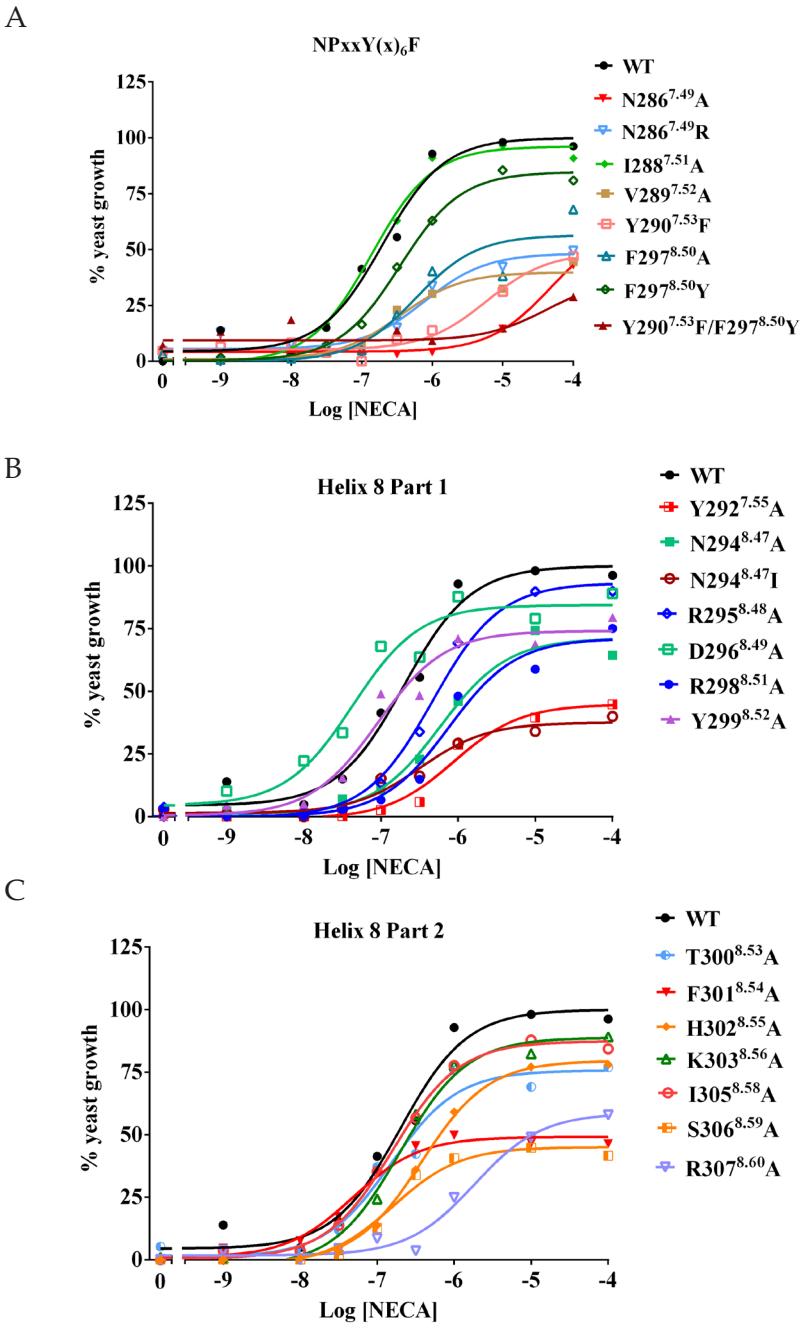

Fig. 2. Concentration–growth curves from solid assay experiments are shown for the hA_{2B} wild-type receptor and the $NPxxY(x)_6F$ mutations (A) and the hA_{2B} wild type receptor and the helix 8 mutations (B and C) responding to the adenosine receptor agonist NECA. The assay was performed on YNB-ULH agar plates. A representative experiment of a total of 4 for WT and each responsive mutation is shown.

Characterization of the function of the NPxxY(x)$_{5,6}$F motif in receptor activation

The NPxxY(x)$_{5,6}$F motif is a conserved stretch of amino acids among many subfamilies of GPCRs (Fig. 3A-C).

N286$^{7.49}$P287$^{7.50}$I288$^{7.51}$V289$^{7.52}$Y290$^{7.53}$(x)$_6$F297$^{8.50}$ is the motif present in the adenosine hA$_{2B}$ receptor.

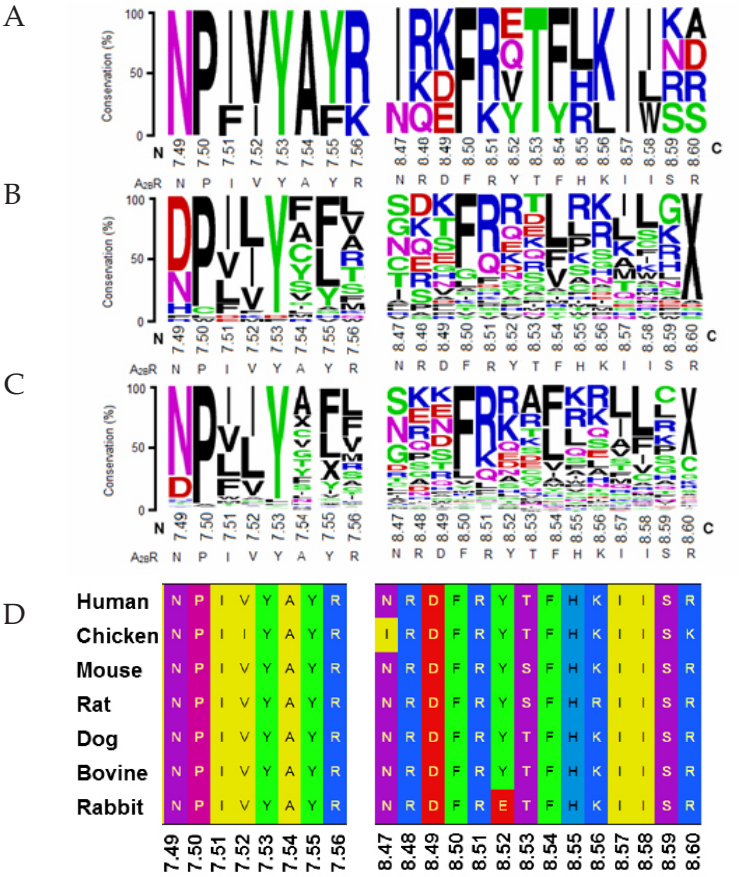

Fig. 3. Frequency plots of multiple sequence alignments for the NPxxY motif (7.49–7.56) and helix 8 (8.47–8.60) obtained from GPCRDB[27]. The size of the letters (one letter amino acid notation) corresponds to the degree of conservation across the alignment in question, with the largest letter (thus the highest degree of conservation) at the top. (A) Frequency plot of the conservation of the amino acids that were mutated in this research across the adenosine receptors; A_1, A_{2A}, A_{2B} and A_3. (B) Frequency plot of the conservation of the amino acids across the nucleotide-like subfamily (in total 32 receptors). (C) Frequency plot of the conservation of the amino acids across the class A (rhodopsin-like) family (in total 292 receptors). Gaps in the multiple sequence alignment are indicated with an X. (D) The alignment of these regions in the A_{2B} receptor between different species.

Residues of NPxxY(x)$_6$F mutated to alanine

In contrast with the wild-type hA_{2B} receptor (NECA: Emax = 100%; EC_{50} = 141 ± 79 nM), the two most conserved residues, P287$^{7.50}$ and Y290$^{7.53}$, showed a complete loss of function upon mutation to alanine; no curves could be generated in the solid growth assay, a feature similar to the empty plasmid pDT-PGK (Table 1). The efficacy values of the following three mutations, N286$^{7.49}$A, V289$^{7.52}$A and F297$^{8.50}$A were decreased to approx. 50% of the Emax value of the wild-type hA_{2B} receptor; the potency of NECA of these three mutations was significantly decreased ($p < 0.001$), although to a different extent: 160-fold, 2.7-fold and 5.7-fold, respectively (Table 1 and Fig. 2A). Only the mutation I288$^{7.51}$A did not show significant changes in both efficacy and potency of NECA, similar to the wild-type receptor (Table 1 and Fig. 2A).

Various other specific mutations

N286$^{7.49}$ was also mutated to glutamine (Q) and arginine (R) (Table 1). N286$^{7.49}$Q showed a complete loss of function and the efficacy of N286$^{7.49}$R was decreased with 42% and the potency of NECA by 5.6-fold (Fig. 2A). Y290$^{7.53}$ was also mutated to phenylalanine (F) and asparagine (N) (Table 1). The efficacy of Y290$^{7.53}$F was 63% and the potency of NECA on this mutant decreased by 30-fold (Fig. 2A). Y290$^{7.53}$N showed a complete loss of function. F297$^{8.50}$ was mutated to tyrosine (Y) and this mutation showed similar values of both efficacy and potency of NECA as the wild-type receptor. Besides these single mutations, one double mutation was made by swapping Y290$^{7.53}$ with F297$^{8.50}$, coined Y290$^{7.53}$F/F297$^{8.50}$Y (Table 1, Fig. 2A). This double mutation showed a 61% decreased efficacy and low potency of NECA, with a 129-fold reduction in EC_{50} value. The potency of NECA for the double mutation was decreased much more than expected from each single mutation.

Characterization of the function of helix 8 in receptor activation

The intracellular helix 8, close to the C-terminus of the GPCR, is increasingly recognized for its importance in G protein coupling and activation[5, 9]. To investigate the importance of the amino acid residues in this helix of the

adenosine hA_{2B} receptor, all residues were mutated one by one to alanine. Furthermore, N294$^{8.47}$ was also mutated to isoleucine (Fig. 3A), which is present in the other three adenosine receptors. F297$^{8.50}$ is part of helix 8 as well, but this residue was already discussed above, as it is often referred to in the context of the NPxxY motif.

Mutations showing a complete loss of function

R293$^{7.56}$A (Table 1), and I304$^{8.57}$A (Table 1) showed a complete loss of function; no curves were observed, similar to the empty plasmid pDT-PGK.

Mutations showing a slight increase in potency

The potency of D296$^{8.49}$A, Y299$^{8.52}$A and F301$^{8.54}$A was increased approx. 2-fold (EC_{50} from 51 nM to 87 nM), which was not significant. Y299$^{8.52}$A and F301$^{8.54}$A had partial decreases in efficacy of approx. 25% (Table 1, Fig. 2B and C), but D296$^{8.49}$A did not show a significant decrease, with 6% only, in efficacy (Table 1 and Fig. 2B).

Mutations showing a partial loss of function

There were 4 mutations of helix 8, Y292$^{7.55}$A, N294$^{8.47}$A, S306$^{8.59}$A and R307$^{8.60}$A that resulted in a partial loss of function when stimulated with NECA. Their efficacies were all decreased by more than 20%, up to 37% (R307$^{8.60}$A). These four mutations also showed a significant decrease of potency, although to a different extent: Y292$^{7.55}$A with 4.8-fold ($p < 0.001$), N294$^{8.47}$A with 3.2-fold ($p < 0.001$), S306$^{8.59}$A with 2-fold ($p = 0.015$) and R307$^{8.60}$A with 21-fold ($p < 0.001$). The specific mutation of N294$^{8.47}$I did not affect either efficacy or potency of NECA (Table 1, Fig. 2B and C).

Three other mutations of helix 8, R298$^{8.51}$A, H302$^{8.55}$A, and I305$^{8.58}$A, were slightly less affected, showing a partial loss of function when stimulated with NECA. The efficacies of these three mutations were slightly lower than wild-type, between 10% and 20% (R298$^{8.51}$A and H302$^{8.55}$A with a decrease of 19%, I305$^{8.58}$A with 13%). However, the potency of the agonist NECA was significantly reduced: R298$^{8.51}$A showed an 11-fold decrease of potency ($p < 0.001$), and

H302$^{8.55}$A had a 5.4-fold decrease of potency ($p < 0.001$); however, I305$^{8.58}$A only showed a 2.1-fold decrease of potency ($p = 0.015$) (Table 1, Fig. 2B and C).

The mutation K303$^{8.56}$A showed a significant decrease of potency of the agonist NECA (2.9-fold, $p = 0.002$), however, no significant decrease of efficacy (with 5% only) was observed (Table 1 and Fig. 2C).

Mutations with no or a slight decrease of receptor activation

Two mutations, R295$^{8.48}$A (Table 1 and Fig. 2B) and T300$^{8.53}$A (Table 1 and Fig. 2C) were more like the wild-type receptor. They showed only a 1.5-fold decrease of potency with concomitant slight decreases of efficacy around 15%.

Expression levels of wild-type receptor and all mutants

We performed a Western blot analysis to assess the expression levels of the wild-type hA_{2B} receptor, the NPxxY$(x)_6$F mutations (Fig. 4A) and the helix 8 mutations (Fig. 4B). A yeast reference protein, α-tubulin (top panel), was used as loading control, which is located at approx. 130 kDa and also appeared at the pDT-PGK MMY24 strain without receptor. The hA_{2B} receptor antibody recognized two bands (bottom panel) at 55 kDa and 34 kDa. The percentage expression level of all mutants was determined from the densities of the two specific bands and the loading control ($n = 3$, Table 1). MMY24 carrying wild-type receptor was set as 100% and MMY24 carrying the empty vector pDT-PGK without receptor was set as 0%. It should be mentioned here that these experiments reveal total receptor expression, and do not specify the location of the receptor, i.e. membrane-bound and/or intracellular.

The R293$^{7.56}$A mutant was not expressed at all, while N286$^{7.49}$A was only marginally expressed, to 15% of control. N286$^{7.49}$R,Y292$^{7.55}$A and Y299$^{8.52}$A also had significantly decreased expression levels, approx. 50% of wild-type receptor. Many mutants had expression levels not significantly different from wild-type receptor (N286$^{7.49}$Q, P287$^{7.50}$A, I288$^{7.51}$A, Y290$^{7.53}$A, Y290$^{7.53}$F, Y290$^{7.53}$N, N294$^{8.47}$A, N294$^{8.47}$I, R295$^{8.48}$A, D296$^{8.49}$A, F297$^{8.50}$A, F297$^{8.50}$Y, R298$^{8.51}$A, T300$^{8.53}$A, F301$^{8.54}$A, H302$^{8.55}$A, K303$^{8.56}$A, I304$^{8.57}$A, I305$^{8.58}$A, S306$^{8.59}$A and R307$^{8.60}$A). V289$^{7.52}$A and Y290$^{7.53}$F/F297$^{8.50}$Y showed significantly higher expression of the receptor.

[^{3}H]PSB-603 antagonist binding to wild-type receptor and all mutants

In Table 1 the percentage of specific [^{3}H]PSB-603 binding to every single mutant receptor is compared to the wild-type receptor (100%). Five mutants, N286$^{7.49}$Q, P287$^{7.50}$A, R293$^{7.56}$A, I304$^{8.57}$A and I305$^{8.58}$A lost antagonist binding completely. Four mutants, N286$^{7.49}$A, Y292$^{7.55}$A, T300$^{8.53}$A and F301$^{8.54}$A, showed slightly but not significantly higher antagonist binding than wild-type. Two mutants, R295$^{8.48}$A and Y299$^{8.52}$A, showed similar antagonist binding compared to wild-type. A majority of mutants showed significant decreases in antagonist binding, below 50% compared to wild-type receptor. They are I288$^{7.51}$A, V289$^{7.52}$A, Y290$^{7.53}$A, Y290$^{7.53}$F, Y290$^{7.53}$N, F297$^{8.50}$A, Y290$^{7.53}$F/F297$^{8.50}$Y, N294$^{8.47}$A, N294$^{8.47}$I, D296$^{8.49}$A, R298$^{8.51}$A, K303$^{8.56}$A, S306$^{8.59}$A and R307$^{8.60}$A. Three other mutants, N286$^{7.49}$R, F297$^{8.50}$Y and H302$^{8.55}$A, also showed lower antagonist binding compared to wild-type, but without significant differences.

Table 1 Characterization of the NPxxY(x)$_6$F motif and helix 8 mutations of the adenosine hA_{2B} receptor in the strain MMY24 ($G_{\alpha i3}$). Parameters of the NECA concentration-effect curves generated from four independent solid growth assays (n = 4), each performed in triplicate.

	Yeast solid assay			Radioligand binding assay	Western blot
	Emax (%)	EC_{50} (nM)	Fold EC_{50}	%[^{3}H]PSB-603 binding	% expression
WT_A_{2B}	100	141 ± 79		100 ± 11	100 ± 5
pDT-PGK	-	-	-	0	0
NPxxY(x)$_6$F					
N286$^{7.49}$A	58 ± 15	22557 ± 15293***	160	120 ± 14	15 ± 3***
N286$^{7.49}$Q	-	-	-	0	110 ± 23
N286$^{7.49}$R	58 ± 13	789 ± 671*	5.6	79 ± 16	68 ± 10*
P287$^{7.50}$A	-	-	-	0	143 ± 17
I288$^{7.51}$A	93 ± 6	193 ± 93	1.4	23 ± 9**	127 ± 10
V289$^{7.52}$A	44 ± 8	376 ± 239*	2.7	17 ± 7***	144 ± 15*
Y290$^{7.53}$A	-	-	-	17 ± 4**	93 ± 7
Y290$^{7.53}$F	63 ± 12	4197 ± 3760**	30	14 ± 9**	102 ± 9
Y290$^{7.53}$N	-	-	-	16 ± 10**	83 ± 14
F297$^{8.50}$A	46 ± 9	803 ± 188***	5.7	19 ± 8**	111 ± 5
F297$^{8.50}$Y	90 ± 10	392 ± 81***	2.8	88 ± 22	97 ± 1
Y290$^{7.53}$F/F297$^{8.50}$Y	39 ± 16	18170 ± 16357**	129	15 ± 10**	173 ± 12*
Helix 8					
Y292$^{7.55}$A	75 ± 13	679 ± 201***	4.8	122 ± 7	46 ± 14*
R293$^{7.56}$A	-	-	-	0	0
N294$^{8.47}$A	78 ± 4	449 ± 179***	3.2	24 ± 11**	122 ± 32
N294$^{8.47}$I	94 ± 11	251 ± 125	1.8	49 ± 15*	165 ± 30
R295$^{8.48}$A	86 ± 23	236 ± 151	1.7	100 ± 12	197 ± 54
D296$^{8.49}$A	94 ± 10	60 ± 31	0.4	44 ± 10**	116 ± 17
R298$^{8.51}$A	81 ± 17	1573 ± 765***	11	34 ± 12**	48 ± 18
Y299$^{8.52}$A	78 ± 11	87 ± 8	0.6	104 ± 19	54 ± 10*
T300$^{8.53}$A	83 ± 11	216 ± 63	1.5	122 ± 5	65 ± 26
F301$^{8.54}$A	73 ± 13	51 ± 8	0.4	144 ± 32	101 ± 15
H302$^{8.55}$A	81 ± 5	761 ± 321***	5.4	62 ± 13	77 ± 29
K303$^{8.56}$A	95 ± 7	403 ± 162**	2.9	45 ± 12*	99 ± 29
I304$^{8.57}$A	-	-	-	0	171 ± 36
I305$^{8.58}$A	87 ± 11	293 ± 106*	2.1	0	134 ± 31
S306$^{8.59}$A	74 ± 11	281 ± 82*	2	49 ± 14*	98 ± 27
R307$^{8.60}$A	63 ± 13	2932 ± 1776***	21	21 ± 7**	108 ± 46

Percentage maximal activity (% Emax) compared to the wild-type hA_{2B} receptor represents the intrinsic activity of the receptor. EC_{50} is the potency of the agonist NECA. The fold EC_{50} was calculated by dividing the EC_{50} of the mutant receptor by the EC_{50} of the wild-type receptor. " – " : Emax < 5%, EC_{50} and fold EC_{50} could not be determined. % [^{3}H]PSB-603 binding represents specific [^{3}H]PSB-603 binding to all mutants compared to the wild-type receptor (100%, n = 3 or 4). % expression level of all mutants was determined from the density of the two specific bands and that of the loading control (wild-type = 100%, n = 3). P-values were calculated by a two-tailed homoscedastic Student's t-test; significance is indicated as follows: *: $p < 0.05$, **: $p < 0.01$, ***: $p < 0.001$. The superscript numbers of residues are according to Ballesteros-Weinstein numbering[54].

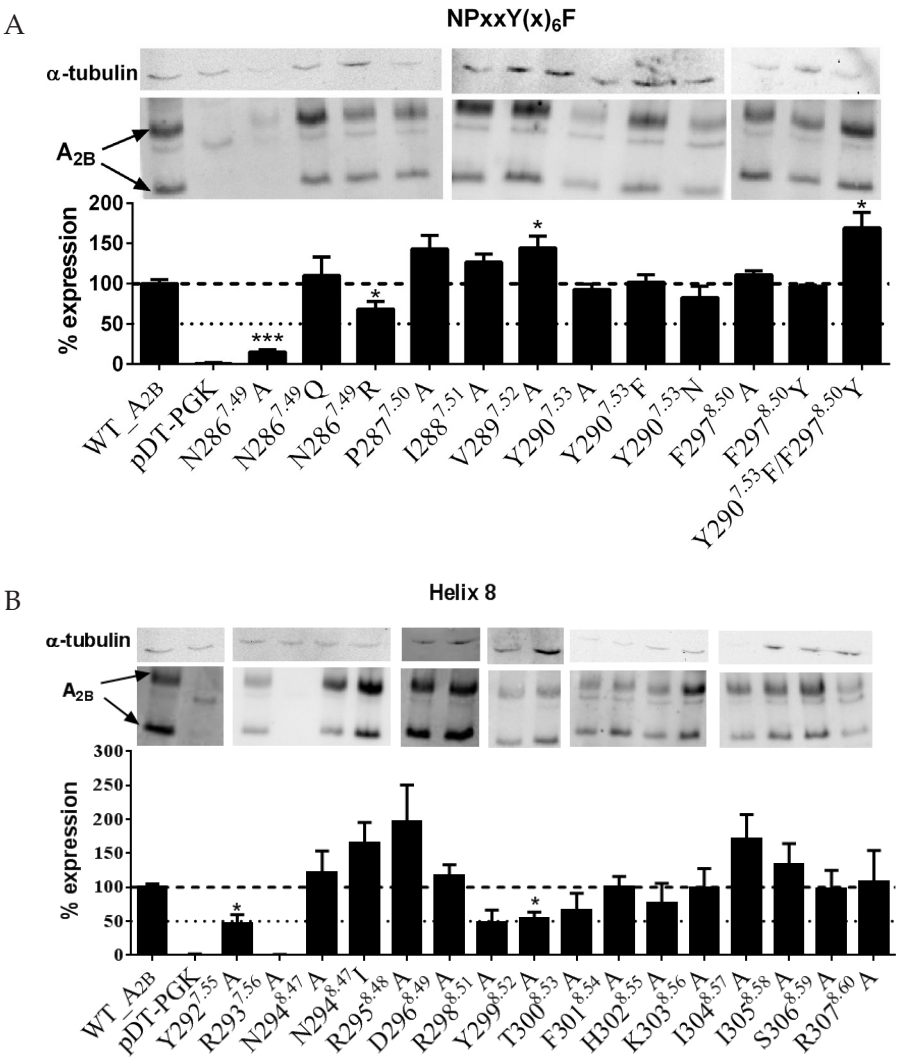

Fig. 4. Western blot analysis of the hA_{2B} wild-type receptor, pDT-PGK without any receptor, the $NPxxY(x)_6F$ mutations (A) and the helix 8 mutations (B). Yeast reference protein α-tubulin (top panel) was used as loading control, which is located at approx. 130 kDa and also appeared at pDT-PGK without receptor. The hA_{2B} receptor specific bands (bottom panel) are at 55 kDa and 34 kDa. All bands shown from a representative experiment. % expression level of all mutants in the bar graphs was determined between the density of the two specific bands and the loading control (n = 3). MMY24 carrying wild-type receptor was set as 100% and MMY24 carrying the empty vector pDT-PGK without receptor was set as 0%.

Discussion

Our previous research has shown that the single-GPCR-one-G protein yeast screening system is very well suited to study a G protein-coupled receptor and its G protein preference[26, 34]. The adenosine hA_{2B} receptor and its mutations were expressed and activated in a panel of eight yeast *S. cerevisiae* strains, covering the four major classes (corresponding to the replaced last five C-terminal residues of the mammalian G_{α} subunit): $G_{\alpha i}$, $G_{\alpha s}$, $G_{\alpha q}$ and $G_{\alpha 12}$[34]. In the current study we have identified the function of each residue of the NPxxY motif and the whole helix 8 in human A_{2B} receptor activation, as derived from the concentration–response curves of the reference agonist NECA on all mutations in a functional yeast growth assay. Firstly, our data confirmed this single-GPCR-one-G protein system is well suitable for studying GPCR activation with many advantageous features; it is cheap, fast, stable, robust and cell handling is easy. Most important, however, is that there is no (other) GPCR background and that the yeast strain has a specifically designed G protein pathway. Secondly, we found four key residues, $P287^{7.50}$, $Y290^{7.53}$, $R293^{7.56}$ and $I304^{8.57}$ that are essential in receptor activation. Thirdly, other amino acid residues were identified as quite crucial too: $N286^{7.49}$, $V289^{7.52}$, $Y292^{7.55}$, $N294^{8.47}$, $F297^{8.50}$, $R298^{8.51}$, $H302^{8.55}$ and $R307^{8.60}$. In the following paragraphs we will discuss the mechanisms of receptor activation in more detail using several sources with bio-informatics information and compare our findings with previous research. The conservation of each residue of the NPxxY motif and the whole helix 8 was compared across all adenosine receptors (Figure 3A), the nucleotide-like subfamily (Fig. 3B), and the entire class A (rhodopsin-like) family of GPCRs (Fig. 3C) and also compared within the A_{2B} receptor between different species (Fig. 3D).

NPxxY motif

The five amino acids NPxxY constitute a highly conserved motif across the rhodopsin-like GPCRs and are generally acknowledged as vital for G protein activation; the sequence motif N286$^{7.49}$P287$^{7.50}$I288$^{7.51}$V289$^{7.52}$Y290$^{7.53}$ is present in the human adenosine hA_{2B} receptor (Fig. 3C). N286$^{7.49}$, P287$^{7.50}$, and Y290$^{7.53}$ are all 100% conserved in the adenosine receptors. There are two key residues, P287$^{7.50}$ and Y290$^{7.53}$, since mutations at these positions showed a complete loss of function. N286$^{7.49}$ seems to be important too, but not as crucial as the two key residues P287$^{7.50}$ and Y290$^{7.53}$, as mutation N286$^{7.49}$A only showed a partial loss of function in both NECA efficacy and potency. However, I288$^{7.51}$A acted as the wild-type hA_{2B} receptor and V289$^{7.52}$A only showed a significant decrease in efficacy with a slight decrease in potency. These two mutants were well expressed, but showed lowered antagonist binding.

N286$^{7.49}$ and P287$^{7.50}$

When N286$^{7.49}$ was conservatively mutated to glutamine (Q), receptor activation was completely abolished. A recovery of function was observed when the asparagine was mutated to the positively charged arginine (R), which mutation showed 50% efficacy only and a 5.6-fold decrease in potency in comparison to the activity of the wild-type receptor (Table 1). The mutation to glutamine caused a complete loss of radiolabeled antagonist binding. It should be mentioned that a modest reduction in radioligand affinity may already lead to negligible binding in this assay. A receptor homology model based on the A_{2A} receptor crystal structure suggests that N$^{7.49}$ makes a stabilizing interaction with N$^{7.45}$[35]. The mutation N$^{7.49}$A in the human NK2 and CCR5 receptors showed a decrease of receptor activation as well[36, 37]. This might be explained by a possible interaction of N$^{7.49}$ with a conserved aspartate in helix 2, D52$^{2.50}$; Sealfon et al. found that swapping these two residues, D$^{2.50}$N/N$^{7.49}$D in the serotonin 5-HT_{2A} receptor restored receptor function while the D$^{2.50}$N mutation alone eliminated activation[38]. From our own results we hypothesize N286$^{7.49}$R would also be able to have this interaction with D$^{2.50}$, whereas N286$^{7.49}$Q would not keep this interaction anymore.

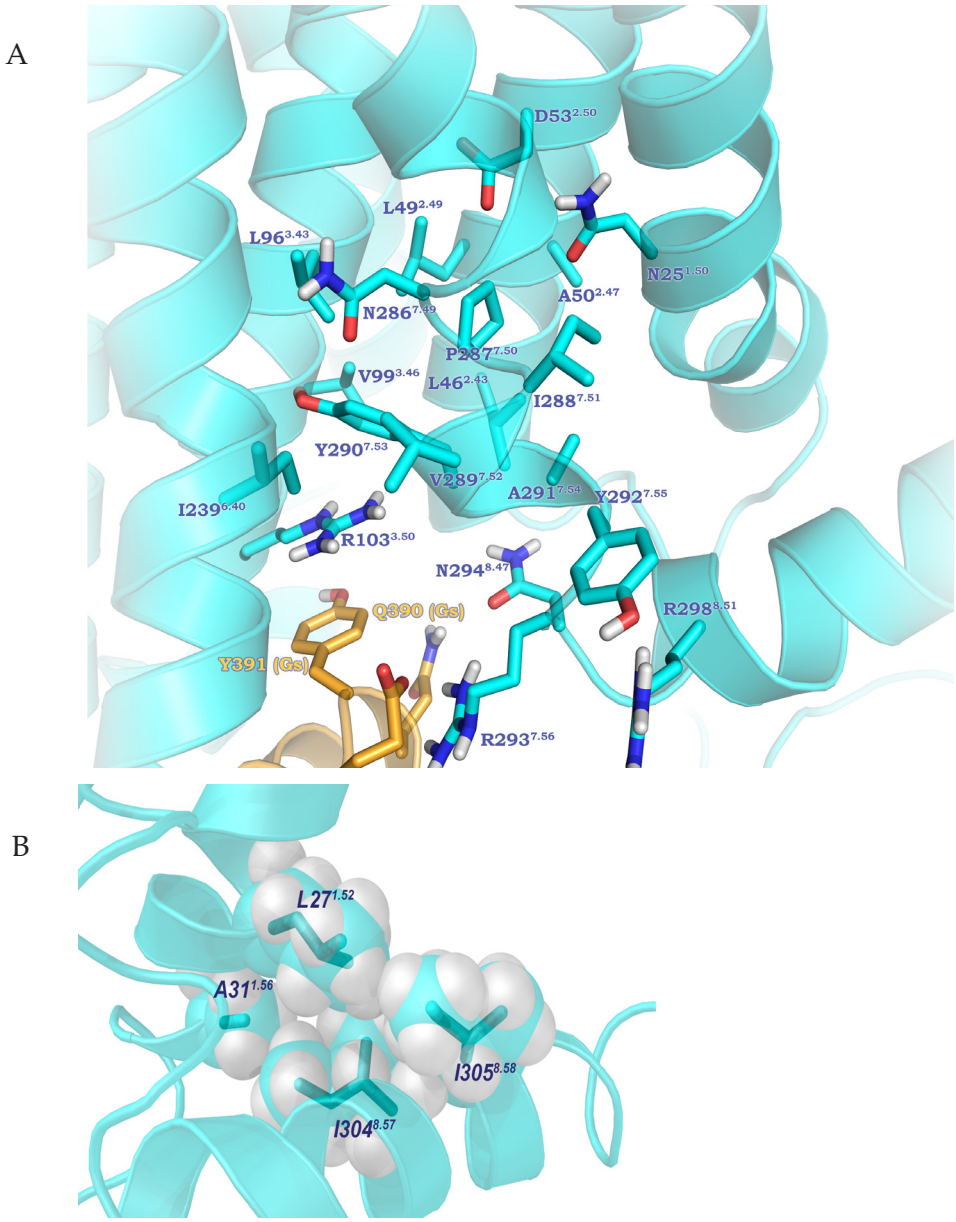

Fig. 5. The chimera/homology model of the adenosine A_{2B} receptor based on both the β_2 adrenergic receptor/G_s complex crystal structure (PDB: 3SN6) and the crystal structure of the adenosine A_{2A} receptor co-crystallized with the agonist NECA (PDB: 2YDV). (A) Residues within 4 Å of P287$^{7.50}$, Y290$^{7.53}$ and R293$^{7.56}$ are visualized. Possible interactions of residues are shown; R103$^{3.50}$ is interacting (π-cation interaction) withY391 (G_s)/Y290$^{7.53}$, R293$^{7.56}$ is interacting with E392 (G_s) and the backbone of Q390 (G_s), and N294$^{8.47}$ interacts with Q390 (G_s). (B) The interactions of loss-of-activation residue I304$^{8.57}$ and neighboring residue I305$^{8.58}$ are shown. I304$^{8.57}$ seems to be "hydrophobically locked" between residues L27$^{1.52}$ and A31$^{1.56}$, while I305$^{8.58}$ is more exposed.

The very high degree of conservation of amino acid P287$^{7.50}$ implies that it could be essential for GPCR activation, since the P287$^{7.50}$A mutation showed a complete loss of function, accompanied by a loss of antagonist binding, while receptor expression was unaffected (Table 1). Indeed, mutation of this amino acid to alanine not only abolished receptor activation in our research but also in the rat M3 muscarinic receptor[39]. However, Barak et al. found that mutation P$^{7.50}$A only reduced but not abolished agonist-mediated phosphorylation in the human β_2 adrenergic receptor; instead, they found that mutation of N$^{7.49}$A abrogated receptor phosphorylation[40]. In the rat type 1 angiotensin II receptor this was also the case: the mutation N$^{7.49}$A severely impaired receptor function, whereas P$^{7.50}$A only reduced receptor function[41]. These findings indicate that it is receptor specific whether N$^{7.49}$ or P$^{7.50}$ is essential for receptor activation; however, both seem to be important and working in close control of each other.

Y290$^{7.53}$ and F297$^{8.50}$

From Table 1 it follows that the mutations Y290$^{7.53}$A and Y290$^{7.53}$N both completely abolished activation of the receptor. The mutant Y290$^{7.53}$F showed a partial loss of function. All three mutants displayed normal receptor expression and reduced antagonist binding. This suggests that an aromatic side chain as in tyrosine and phenylalanine at this position is essential for activation. It also indicates that the hydroxyl group in tyrosine is very important in hA_{2B} receptor activation. The homology model suggests that Y290$^{7.53}$ is interacting with the conserved R103$^{3.50}$ of the DRY motif (Fig. 5A). Y$^{7.53}$ has been investigated and mutated in numerous GPCRs. The mutation Y$^{7.53}$A abolished agonist-mediated internalization, but did not influence its ability to maximally stimulate adenylyl cyclase in the human β_2 adrenergic receptor, Y$^{7.53}$F only slightly reduced this ability[42, 43]. In the human type 1 angiotensin II receptor mutation of this amino acid to either alanine or phenylalanine led to comparably and heavily impaired signaling[44]. Le Gouill et al. found that the Y$^{7.53}$A mutation in the human platelet-activating factor receptor abolished G protein coupling but not internalization, whereas the Y$^{7.53}$F mutation did not have a significant effect on either process[45]. In the murine GnRH receptor, the mutation Y$^{7.53}$A led to abrogation of inositol

phosphate production, substitution with phenylalanine resulted in normal G protein activation[46].

The mutation F297$^{8.50}$A showed a partial loss of function while the mutation F297$^{8.50}$Y behaved similarly to wild-type receptor. It has been postulated that an aromatic interaction, or pi/pi stacking, occurs between the Y290$^{7.53}$ and F297$^{8.50}$ residues, stabilizing the receptor in an inactive state[47]. However, this cannot be the only reason in view of our finding that the double mutation, Y290$^{7.53}$F/F297$^{8.50}$Y, showed a greater combined loss of function than both single mutations. Fritze et al. reported on the same double mutation in rhodopsin. The interaction between the two residues played an important role during the change from inactive to active state[47].

Key residues of helix 8: R293$^{7.56}$ and I304$^{8.57}$

Helix 8 is increasingly recognized as having a large role in assisting the receptor in G protein coupling[4]. In this study all amino acids of helix 8 in the adenosine A_{2B} receptor were mutated one by one to alanine to investigate their role in G protein activation. Two residues, R293$^{7.56}$ and I304$^{8.57}$, showed a complete loss of receptor activation. However, similar key residues had different locations in other receptors, such as in the M1 muscarinic acetylcholine receptor, where F425$^{8.50}$, R426$^{8.51}$, T428$^{8.53}$ and L432$^{8.57}$ were found important for G protein binding and signaling[5]; in the cannabinoid receptor 1 these were hydrophobic residues L404$^{8.50}$, F408$^{8.54}$, F412$^{8.58}$; in the β_1 adrenergic receptor these were D382$^{8.49}$ and R384$^{8.51}$ within a hydrophilic interface, possibly serving as a tethering site for the G protein[9]; in the type 1 angiotensin receptor Y312$^{8.53}$, F313$^{8.54}$ and L314$^{8.55}$ were identified as such[8].

R293$^{7.56}$

The mutation R293$^{7.56}$A showed a complete loss of function (Table 1), accompanied by a similar lack of receptor expression and antagonist binding. This makes it difficult to draw unambiguous conclusions. From the homology model provided (Fig. 5A) it is apparent that R293$^{7.56}$ has an interaction with the C terminal tail (QYELL^{COOH}) of the $G_{\alpha s}$ subunit, involved in activation of the adenosine hA_{2B}

receptor. However, the homology model is based on the β_2-adrenergic receptor–G_s complex crystal structure; the MMY24 cell line expresses the $G_{\alpha i3}$ subunit which has a different C terminal tail (ECGLY^{COOH}). The glutamic acid (E), with which R293$^{7.56}$ interacts, is present in both tails although at a different position, which might make this residue essential for G protein coupling. R$^{7.56}$ is highly conserved across the adenosine receptor family; the only other amino acid present is lysine, which is a large, basic, charged hydrophilic residue as well. The conservation of this amino acid across the nucleotide-like subfamily (Fig. 3B) and class A (rhodopsin-like) family (Fig. 3C) is rather low, however. This sequence element is the connection between TM7 and helix 8, which apparently is quite flexible, because it is missing in many receptors whereas some have an extra residue here (Fig. 3C). R$^{7.56}$ is also highly conserved in the A_{2B} receptor across different species (Fig. 3D). However, these results and explanations imply that the involvement of this amino acid residue R/K293$^{7.56}$ in G protein coupling may be quite specific for the adenosine receptors.

I304$^{8.57}$ and I305$^{8.58}$

The mutation I304$^{8.57}$A showed a complete loss of function, had no antagonist binding, but was very well expressed (Table 1). This I304$^{8.57}$ is present in all adenosine receptors. It has the highest rate of conservation across the nucleotide-like receptor subfamily and comes second in the entire class A (rhodopsin-like) family (Fig. 3). In contrast, mutation of L$^{8.57}$A in the human β_2 adrenergic receptor had no influence on expression, ligand binding, G protein coupling or adenylyl cyclase activity; only agonist-mediated receptor sequestration was markedly impaired[48]. Our homology model predicts that I304$^{8.57}$ is hydrophobically locked between residues L27$^{1.52}$ and A31$^{1.56}$ (Fig. 5B). This hydrophobic lock might stabilize the position of helix 8 resulting in a loss of function when this lock is broken. It is remarkable that mutation I305$^{8.58}$A, which is in close proximity of I304$^{8.57}$, showed no severe loss of function (Table 1). The reason for this might be that I305$^{8.58}$ is more exposed to the cytoplasm as opposed to I304$^{8.57}$. This isoleucine is less conserved (50%) in adenosine receptors than I304$^{8.57}$ (100%) and also less conserved in the nucleotide-like receptor subfamily and class A

(rhodopsin-like) family. The most conserved residue at both positions is leucine; however, there is a higher degree of conservation at position 8.58 (40%) than at position 8.57 (26%) (Fig. 3). This finding implies hydrophobic residues at position 8.57 and 8.58 are very common in many GPCRs, in which $I304^{8.57}$ is a key residue for hA_{2B} receptor activation.

Other residues

Five residues, $Y292^{7.55}$, $N294^{8.47}$, $R298^{8.51}$, $H302^{8.55}$ and $R307^{8.60}$ were also shown to be of high importance in receptor activation, while showing substantial receptor expression and antagonist binding. The substitution of these residues for alanine caused a significant decrease of NECA's potency ($p < 0.001$) and a reduction of its efficacy.

$R298^{8.51}$ and $R307^{8.60}$ significantly influenced the potency of NECA (EC_{50} fold > 10-fold upon mutation). $R^{8.51}$ is the second most conserved residue, next to the most conserved residue $F^{8.50}$ of helix 8 across the class A (rhodopsin-like) receptor family (Fig. 3C). However, $R307^{8.60}$ is not that conserved; this position shows different residues across the adenosine receptors, even more so across the nucleotide-like receptor subfamily and class A (rhodopsin-like) receptor family. This position is at the end of helix 8, and it appears to have very different functions in different receptors. In the adenosine A_{2A} receptor a serine is present at position 8.60; mutation $S^{8.60}A$ in the canine adenosine A_{2A} receptor showed a decrease of potency but not efficacy of adenylyl cyclase stimulation[49]. In the human dopamine D1 receptor mutation $C^{8.60}A$ had no effect on the stimulation of adenylyl cyclase[50]. Mutation $Y^{8.60}A$ in the rat type 1 angiotensin II receptor resulted in a reduction in internalization rate[51].

The neighboring residues of key amino acids $R293^{7.56}$ and $I304^{8.57}$ are very important as well, such as $Y292^{7.55}$ and $N294^{8.47}$ (neighbors of $R293^{7.56}$). Residue $Y292^{7.55}$ is highly conserved across the adenosine receptors, the other residue being the closely related phenylalanine (Fig. 3A). The tyrosine is not very conserved, but a phenylalanine is across the nucleotide-like receptor subfamily (Fig. 3B) and the class A rhodopsin-like receptor family (Fig. 3C). This may imply that an aromatic group at this position is important. Since this residue is

located in the linking sequence segment that connects TM7 and helix 8, it might be that an aromatic ring at this position is essential for a correct arrangement of these two helices with respect to each other. Secondly, it may team up with key residue R293$^{7.56}$ in receptor activation. The adenosine A_{2B} receptor carries an asparagine (N) at the 8.47 position and is unique with respect to the other adenosine receptors, which all have an isoleucine (I) at this position. Across the nucleotide-like receptor subfamily (Fig. 3B) and the class A rhodopsin-like receptor family (Fig. 3C) N$^{8.47}$ is more conserved than I$^{8.47}$ (Fig. 3B and C). However, the N$^{8.47}$I mutation did not cause significant decreases in both efficacy and potency of the agonist NECA compared to the wild-type receptor, less so than the N$^{8.47}$A mutation. These results imply that there is no apparent difference between N294$^{8.47}$ at the A_{2B} receptor or I294$^{8.47}$ in other receptors. Mutation of this amino acid in bovine rhodopsin had no effect on the GDP/GTP exchange within the G protein[52].

The conservation of H302$^{8.55}$ is low across the adenosine receptors (25%), the nucleotide-like receptor subfamily (3%) and the class A rhodopsin-like receptor family (2%). However, conservation of another basic amino acid, arginine, is the highest across the nucleotide-like receptor subfamily and the second highest across the entire Class A receptor family, in which lysine is the highest. So a charged, basic residue is common at this position. Leucine is often found as well; it is the third most conserved residue across all Class A GPCRs and accounts for half of the adenosine receptor family (Fig. 3). Sano et al. reported that L314$^{8.55}$A, together with Y312$^{8.53}$ and F313$^{8.54}$ in the cytosolic carboxyl-terminal region of the rat type 1 angiotensin II receptor is essential for coupling and activation, since mutations on these three positions resulted in a marked reduction in GTPγS effects on Ang II binding and inositol trisphosphate production[53].

In conclusion, the alanine scan of the NPxxY motif and the adjacent helix 8 of the adenosine A_{2B} receptor we performed in the present study identified a number of positions vital for receptor activation, some of which unknown at other receptors. In some instances we provided additional data by substituting alanine for other amino acids, mostly triggered by their presence in other

GPCRs. The latter approach could be brought further by, e.g., analyzing more conservative mutations in which the physicochemical nature of the substituted amino acid is taken into account. Homology modeling of the receptor and visualizing the likely interactions between amino acids in G protein and receptor provided insight into the putative molecular mechanisms for the deterioration of receptor activation.

Acknowledgements

Rongfang Liu thanks the China Scholarship Council (CSC) for her PhD scholarship. NWO provided a TOP grant to A.P. IJ. (714.011.001). Qilan Li made some of the receptor mutants. The authors are grateful to Prof C.E. Mueller of Bonn University (Germany) for the generous gift of [^{3}H]PSB-603 and to Dr. S. Dowell from GSK (Stevenage, UK) for providing the plasmids, the yeast strains and experimental protocols.

References

[1] Venkatakrishnan, A., et al. *Molecular signatures of G-protein-coupled receptors.* Nature (2013) 494: 185–194.

[2] Oldham, W.M., and Hamm, H.E. *Heterotrimeric G protein activation by G-protein-coupled receptors.* Nat. Rev. Mol. Cell Biol. (2008) 9: 60–71.

[3] O'Callaghan, K., et al. *Turning receptors on and off with intracellular pepducins: new insights into G-protein-coupled receptor drug development.* J. Biol. Chem. (2012) 287: 12787–12796.

[4] Oldham, W.M., et al. *Mechanism of the receptor-catalyzed activation of heterotrimeric G proteins.* Nat. Struct. Mol.Biol. (2006) 13: 772–777.

[5] Kaye, R.G., et al. *Helix 8 of the M1 muscarinic acetylcholine receptor: scanning mutagenesis delineates a G protein recognition site.* Mol. Pharmacol. (2011) 79: 701–709.

[6] Okuno, T., et al. *Leukotriene B4 receptor and the function of its helix 8.* J. Biol. Chem. (2005) 280: 32049–32052.

[7] Ahn, K.H., et al. *Hydrophobic residues in helix 8 of cannabinoid receptor 1 are critical for structural and functional properties.* Biochemistry (2009) 49: 502–511.

[8] Huynh, J., et al. *Role of helix 8 in G protein-coupled receptors based on structure–function studies on the type 1 angiotensin receptor.* Mol. Cell. Endocrinol. (2009) 302: 118–127.

[9] Santos, N.M.D., et al. *Characterization of the residues in helix 8 of the human β_1-adrenergic*

receptor that are involved in coupling the receptor to G proteins. J. Biol. Chem. (2006) 281: 12896–12907.

[10] Fredholm, B.B., et al. *Structure and function of adenosine receptors and their genes.* Naunyn-Schmiedeberg's Arch. Pharmacol. (2000) 362: 364–374.

[11] Fredholm, B.B., et al. *Comparison of the potency of adenosine as an agonist at human adenosine receptors expressed in Chinese hamster ovary cells. Biochem. Pharmacol.* (2001) 61: 443–448.

[12] Wei, W., et al. *Blocking A_{2B} adenosine receptor alleviates pathogenesis of experimental autoimmune encephalomyelitis via inhibition of IL-6 production and Th17 differentiation.* J. Immunol. (2013) 190: 138–146.

[13] Wei, Q., et al. A. *A_{2B} adenosine receptor blockade inhibits growth of prostate cancer cells.* Purinergic Signal. (2013) 9: 271–280.

[14] Stagg, J., et al. *Anti-CD73 antibody therapy inhibits breast tumor growth and metastasis.* Proc. Natl. Acad. Sci. U.S.A. (2010) 107: 1547–1552.

[15] Owen, S. J., Massa, H.H., and Rose'Meyer, R.B. *Loss of adenosine A_{2B} receptor mediated relaxant responses in the aged female rat bladder; effects of dietary phytoestrogens.* Naunyn-Schmiedeberg's Arch. Pharmacol. (2012) 385: 539–549.

[16] Cekic, C., et al. *Adenosine A_{2B} receptor blockade slows growth of bladder and breast tumors.* J. Immunol. (2012) 188: 198–205.

[17] Koscsó, B., et al. *Stimulation of A_{2B}adenosine receptors protects against trauma–hemorrhagic shock-induced lung injury.* Purinergic Signal. (2013) 9: 427–432.

[18] Bot, I., et al. *Adenosine A_{2B} receptor agonism inhibits neointimal lesion development after arterial injury in apolipoprotein E–deficient mice. Arterioscler.* Thromb. Vasc. Biol. (2012) 32: 2197–2205.

[19] Dowell, S.J., and Brown, A.J. *Yeast assays for G-protein-coupled receptors.* Receptors Channels (2002) 8: 343–352.

[20] Dowell, S.J., and Brown, A. J. *Yeast assays for G protein-coupled receptors.* Methods Mol. Biol. (2009) 552: 213–229.

[21] Stewart, G.D., et al. *Determination of adenosine A_1 receptor agonist and antagonist pharmacology using Saccharomyces cerevisiae: implications for ligand screening and functional selectivity.* J. Pharmacol. Exp. Ther. (2009) 331: 277–286.

[22] Peeters, M.C., et al. *Domains for activation and inactivation in G protein-coupled receptors–A mutational analysis of constitutive activity of the adenosine A_{2B} receptor.* Biochem. Pharmacol. (2014) 92: 348–357.

[23] Weston, C., et al. *Investigating G protein signaling bias at the glucagon-like peptide-1 receptor in yeast.* Br. J. Pharmacol. (2014) 171: 3651–3665.

[24] Gietz, D., et al. *Improved method for high efficiency transformation of intact yeast cells.* Nucleic Acids Res. (1992) 20: 1425.

[25] Peeters, M.C., et al. *GPCR structure and activation: an essential role for the first extracellular loop in activating the adenosine A_{2B} receptor.* FASEB J. (2011) 25: 632–643.

[26] Liu, R., et al. *A yeast screening method to decipher the interaction between the adenosine A_{2B}*

receptor and the C-terminus of different G protein α-subunits. Purinergic Signal. (2014) 10: 441–453.

[27] Isberg, V., et al. *GPCRDB: an information system for G protein-coupled receptors.* Nucleic Acids Res. (2014) 42: D422–D425.

[28] Crooks, G.E., et al. *WebLogo: a sequence logo generator. Genome Res.* (2004) 14: 1188–1190.

[29] **Schrödinger Release 2014-2**: Maestro v, (2014), Schrödinger, LLC, New York, NY.

[30] **Schrödinger Release 2014-2**: Prime v, (2014), Schrödinger, LLC, New York, NY.

[31] Jacobson, M.P., et al. *On the role of crystal packing forces in determining protein sidechain conformations.* J. Mol. Biol. (2002) 320: 597–608.

[32] Jacobson, M.P., et al. *A hierarchical approach to all-atom protein loop prediction.* Proteins: Struct. Funct. Bioinform. (2004) 55: 351–367.

[33] Peeters, M., et al. *The role of the second and third extracellular loops of the adenosine A_1 receptor in activation and allosteric modulation.* Biochem. Pharmacol. (2012) 84: 76–87.

[34] Peeters, M.C., et al. *Three "hotspots" important for adenosine A_{2B} receptor activation: a mutational analysis of transmembrane domains 4 and 5 and the second extracellular loop.* Purinergic Signal. (2012) 8: 23–38.

[35] Gutiérrez-de-Terán, H., et al. *The role of a sodium ion binding aite in the allosteric modulation of the A_{2A} adenosine G protein-coupled receptor.* Structure (2013) 21: 2175–2185.

[36] Donnelly, D., et al. *Conserved polar residues in the transmembrane domain of the human tachykinin NK2 receptor: functional roles and structural implications.* Biochem. J. (1999) 339: 55–61.

[37] Dragic, T., et al. *A binding pocket for a small molecule inhibitor of HIV-1 entry within the transmembrane helices of CCR5.* Proc. Natl. Acad. Sci. U.S.A. (2000) 97: 5639–5644.

[38] Sealfon, S.C., et al. *Related contribution of specific helix 2 and 7 residues to conformational activation of the serotonin 5-HT_{2A} receptor.* J. Biol. Chem. (1995) 270: 16683–16688.

[39] Wess, J., et al. *Functional role of proline and tryptophan residues highly conserved among G protein-coupled receptors studied by mutational analysis of the m3 muscarinic receptor.* EMBO J. (1993) 12: 331.

[40] Barak, L. S., et al. *The conserved seven-transmembrane sequence $NP(X)_{2,3}Y$ of the G-protein-coupled receptor superfamily regulates multiple properties of the β_2-adrenergic receptor.* Biochemistry (1995) 34: 15407–15414.

[41] Hunyady, L., et al. *A conserved NPLFY sequence contributes to agonist binding and signal transduction but is not an internalization signal for the type 1 angiotensin II receptor.* J. Biol. Chem. (1995) 270: 16602–16609.

[42] Gabilondo, A.M., et al. *Mutations of Tyr326 in the β_2-adrenoceptor disrupt multiple receptor functions.* Eur. J. Pharmacol. (1996) 307: 243–250.

[43] Barak, L.S., et al. *A highly conserved tyrosine residue in G protein-coupled receptors is required for agonist-mediated β_2-adrenergic receptor sequestration.* J. Biol. Chem. (1994) 269: 2790–2795.

[44] Laporte, S.A., et al. *The tyrosine within the NPX_nY motif of the human angiotensin II type 1 receptor is involved in mediating signal transduction but is not essential for internalization.* Mol. Pharmacol. (1996) 49: 89–95.

[45] Le Gouill, C., et al. *Structural and functional requirements for agonist-induced internalization of the human platelet-activating factor receptor.* J. Biol. Chem. (1997) 272: 21289–21295.

[46] Arora, K.K., Cheng, Z., and Catt, K.J. *Dependence of agonist activation on an aromatic moiety in the DPLIY motif of the gonadotropin-releasing hormone receptor.* Mol. Endocrinol. (1996) 10: 979–986.

[47] Fritze, O., et al. *Role of the conserved $NPxxY(x)_{5,6}F$ motif in the rhodopsin ground state and during activation.* Proc. Natl. Acad. Sci. U.S.A. (2003) 100: 2290–2295.

[48] Gabilondo, A.M., et al. *A dileucine motif in the C terminus of the β_2-adrenergic receptor is involved in receptor internalization.* Proc. Natl. Acad. Sci. U.S.A. (1997) 94: 12285–12290.

[49] Palmer, T.M., Stiles, G.L. *Identification of an A2a adenosine receptor domain specifically responsible for mediating short-term desensitization.* Biochemistry (1997) 36: 832–838.

[50] Jin, H., et al. *Elimination of palmitoylation sites in the human dopamine D_1 receptor does not affect receptor-G protein interaction.* Eur. J. Pharmacol. (1997) 324: 109–116.

[51] Thomas, W.G., et al. *Angiotensin II receptor endocytosis involves two distinct regions of the cytoplasmic tail. A role for residues on the hydrophobic face of a putative amphipathic helix.* J. Biol. Chem. (1995) 270: 22153–22159.

[52] Osawa, S., and Weiss, E.R. *The carboxyl terminus of bovine rhodopsin is not required for G protein activation.* Mol. Pharmacol. (1994) 46: 1036–1040.

[53] Sano, T., et al. *A domain for G protein coupling in carboxyl-terminal tail of rat angiotensin II receptor type 1A.* J. Biol. Chem. (1997) 272: 23631–23636.

[54] Ballesteros, J.A., and Weinstein, H. *Integrated methods for the construction of three-dimensional models and computational probing of structure–function relations in G protein-coupled receptors.* Methods Neurosci. (1995) 25: 366–428.

Chapter 5

The role of the C-terminus of the human hydroxycarboxylic acid receptors 2 and 3 in G protein activation using G_{α}-engineered yeast cells

This chapter is based upon:

Rongfang Liu, Jacobus P. D. van Veldhoven, Adriaan P. IJzerman

European Journal of Pharmacology ***2016*** *770: 70-77*

Abstract

In the present study we focused our attention on the family of hydroxycarboxylic acid (HCA) receptors, a GPCR family of three members, of which the HCA_2 and HCA_3 receptors share 95% high sequence identity but differ considerably in C-terminus length with HCA_3 having the longest tail. The two receptors were expressed and analysed for their activation profile in *Saccharomyces cerevisiae* MMY yeast strains that have different G protein G_α subunits. The $hHCA_2$ receptor was promiscuous in its G protein coupling preference. In the presence of nicotinic acid the $hHCA_2$ receptor activated almost all G protein pathways except $G_{\alpha q}$ (MMY14). However, the G_α protein coupling profile of the $hHCA_3$ receptor was less promiscuous, as the receptor only activated $G_{\alpha i1}$ (MMY23) and $G_{\alpha i3}$ (MMY24) pathways.

We then constructed two mutant receptors by 'swapping' the short (HCA_2) and long (HCA_3) C-terminus. The differences in HCA_2 and HCA_3 receptor activation and G protein selectivity were not controlled, however, by their C-terminal tails, as we observed only minor differences between mutant and corresponding wild-type receptor. This study provides new insights into the G protein coupling profiles of the HCA receptors and the function of the receptor's C terminus, which may be extended to other GPCRs.

Introduction

G protein-coupled receptors are important drug targets. The secondary structure of these cell membrane-bound proteins is composed of seven transmembrane domains, connected via three extra- and three intracellular loops, preceded by an extracellular N-terminus and followed by an intracellular C-terminus[1]. We have studied the role of various of these motifs in receptor and G protein activation. As an example, we learned and reviewed that the extracellular domains, while being quite distant from the G protein binding site at the receptor, contribute significantly to receptor activation[2]. In the current study we focused our attention to the C-terminus of the receptor, which considerably differs in length between receptors, suggesting its role can be very different from one receptor to the other[3].

Previous research has shown that the C-terminal domain is important in the regulation of intracellular trafficking[4], internalization[5, 6], transport[7], photoreceptor morphogenesis[8], blebbing phenotype[9], desensitization and sequestration[10], G protein coupling[11-14] and β-arrestin interaction[15]. However, C-terminus deletion does not affect the ability of rhodopsin to activate G proteins[16].

In the present study we focused our attention to the family of hydroxycarboxylic acid (HCA) receptors, a GPCR family of three members, of which the HCA_2 and HCA_3 receptors share high sequence identity but differ considerably in C-terminus length with HCA_3 having the longest tail. Both HCA_2 and HCA_3 receptors have been implicated in e.g., obesity and other dyslipidemic conditions[17].

We studied whether the C-terminus has an impact on receptor activation and G protein selectivity. We examined this research question in an engineered yeast strain[18, 19] that we have previously studied on a number of occasions, particular with respect to adenosine receptors[20-22]. This assay system has no endogenous GPCRs and expresses a panel of humanized G proteins, which makes it ideal for the study of receptor activation and to determine a receptor's G protein preferences.

Materials and methods

Materials

The *Saccharomyces cerevisiae* (*S. cerevisiae*) MMY strains and expression vectors, p426GPD, p426GPD_hHCA$_2$ and p426GPD_hHCA$_3$ were kindly provided by Dr. Simon Dowell (GSK, Stevenage, UK). The polymerase chain reaction (PCR) and construction of mutants were carried out with the *PfuUltra* HF DNA polymerase (Stratagene, Amsterdam, the Netherlands), dNTP mix/25mM (Bio-Connect, Huissen, the Netherlands), the restriction enzymes BstAPI (Bioke, Leiden, the Netherlands) and BlpI (Fisher Scientific, Amsterdam, the Netherlands), and T4 DNA ligase (Fisher Scientific, Amsterdam, the Netherlands). Ligands used in the liquid growth assay were nicotinic acid (Sigma-Aldrich, Zwijndrecht, the Netherlands), acifran (Tocris, Bristol, UK) and LUF7159 known as compound 6o[23] (synthesized in house), and 3-amino-[1,2,4]-triazole (Sigma-Aldrich, Zwijndrecht, the Netherlands). The Hybond-ECL membranes and the ECL Western blotting analysis system were purchased from GE Healthcare (Eindhoven, the Netherlands). Rabbit anti-human HCA$_2$/HCA$_3$ polyclonal antibody was purchased from Sigma-Aldrich (HPA028660, Zwijndrecht, the Netherlands) and goat anti-rabbit IgG as second antibody was purchased from Jackson ImmunoResearch Laboratories (West Grove, PA, USA). Rat anti-yeast α-tubulin monoclonal antibody was used as a reference protein (GTX76511, GeneTex, Irvine, CA, USA) with goat anti-rat IgG-HRP antibody (sc-2032, Santa Cruz Biotechnology, Heidelberg, Germany) as the second antibody. The medium YNB + Nitrogen - Nicotinic acid was purchased from Sunrise Science products (San Diego, CA, USA).

C-terminus modified hHCA$_2$ receptor and hHCA$_3$ receptor constructs

The following primers were synthesized (Eurogentec, the Netherlands) and used for cloning two receptor constructs in which we swapped the C-terminus of both receptors, which were named hHCA$_2$+C and hHCA$_3$-C.

5'-ATGAATCG***GCACCATCTGC***AGGATCACTTTCTG-3'

5'-TCCAGATAATTCTG***GCTGAGC***AGAACAGGATGATG-3'

Restriction sites in the primers, BstAPI and BlpI, are in italics and bold. The $hHCA_2$+C mutant was generated by switching part of the $hHCA_2$ receptor, which was cloned by PCR from p426GPD_$hHCA_2$, to the ligation vector p426GPD_$hHCA_3$ (for details see Fig. S1A). The $hHCA_3$-C mutant was generated by switching part of the $hHCA_3$ receptor, which was cloned by PCR from p426GPD_$hHCA_3$, to the ligation vector p426GPD_$hHCA_2$ (for details see Fig. S1B). Plasmids were amplified using DH5α *E. Coli* competent cells (Invitrogen, San Diego, CA, USA). This procedure yielded a total of four plasmids, which were all confirmed by DNA sequencing (LGTC, the Netherlands). Sequence alignment was performed using CLUSTALW[24].

Transformation in *S. cerevisiae* strains

The p426GPD, p426GPD_$hHCA_2$, p426GPD_$hHCA_3$, p426GPD_$hHCA_2$+C and p426GPD_$hHCA_3$-C plasmids were transformed according to the Lithium-Acetate procedure[25] into a panel of engineered *S. cerevisiae* yeast strains expressing different Gpa1p/G_α chimeras. The series of yeast strains are derived from the MMY11 strain and further adapted to communicate with mammalian GPCRs. The difference between these integrated Gpa1p/G_α chimeras is that the last five amino acids of the endogenous Gpa1p C-terminus have been replaced with the same five amino acids sequence motif of mammalian G_α proteins[18, 19, 26] (Table 1). The positive clones with an expression plasmid were selected in YNB-UL-NA medium (YNB + adenine + tryptophan + histidine, lacking uracil, leucine and also nicotinic acid).

Liquid growth assay

The degree of receptor activation was measured by the growth rate of the yeast on histidine-deficient medium via the *FUS1-HIS3* reporter gene induction, which has been described in our previous research except that nicotinic acid was omitted from the medium mix. The assays were performed in the absence or presence of the indicated concentrations of nicotinic acid, acifran or LUF7159, the structures of which are shown in Fig. 1A. Stock solutions of all compounds

Table 1. The genotypes of the humanized yeast strains used for transformations[18, 19, 26]. All these strains grow in YNB-L medium (YNB without leucine), while they do not grow in YNB-UL-NA medium (without uracil, leucine and nicotinic acid) unless the expressed receptors are present or activated.

Strain	Genotype	The five C-terminal residues of G_{α}
MMY11	**MATa** *his3 ade2 leu2 trp1 ura3 can1 fus1:FUS1-HIS3 FUS1-lacZ:LEU2 far1Δ:ura3Δgpa1Δ:ADE2Δsst2Δ:ura3 Δste2Δ:G418^R*	
MMY12 ($G_{\alpha WT}$)	MMY11*TRP1:GPA1*	KIGII^{COOH}
MMY14 ($G_{\alpha q}$)	MMY11*TRP1:Gpa1/*$G_{\alpha q}$*(5)*	EYNLV^{COOH}
MMY16 ($G_{\alpha 16}$)	MMY11*TRP1:Gpa1/*$G_{\alpha 16}$*(5)*	EINLL^{COOH}
MMY19 ($G_{\alpha 12}$)	MMY11*TRP1:Gpa1/*$G_{\alpha 12}$*(5)*	DIMLQ^{COOH}
MMY20 ($G_{\alpha 13}$)	MMY11*TRP1:Gpa1/*$G_{\alpha 13}$*(5)*	QLMLQ^{COOH}
MMY21 ($G_{\alpha 14}$)	MMY11*TRP1:Gpa1/*$G_{\alpha 14}$*(5)*	EFNLV^{COOH}
MMY23 ($G_{\alpha i1}$)	MMY11*TRP1:Gpa1/*$G_{\alpha i1}$*(5)*	DCGLF^{COOH}
MMY24 ($G_{\alpha i3}$)	MMY11*TRP1:Gpa1/*$G_{\alpha i3}$*(5)*	ECGLY^{COOH}
MMY25 ($G_{\alpha z}$)	MMY11*TRP1:Gpa1/*$G_{\alpha z}$*(5)*	YIGLC^{COOH}
MMY28 ($G_{\alpha s}$)	MMY11*TRP1:Gpa1/*$G_{\alpha s}$*(5)*	QYELL^{COOH}

were made in DMSO. Yeast cells with the $hHCA_2$ receptor or the $hHCA_2$+C receptor obtained from an overnight culture were diluted to around 2×10^4 cells/ml ($OD_{600} \approx 0.001$) and 50 µl was added into each well (approx. 1,000 cells/well). The yeast cells with the $hHCA_3$ receptor or the $hHCA_3$-C receptor were diluted to approx. 2×10^5 cells/ml ($OD_{600} \approx 0.01$) and 50 µl was added into each well (approx. 1×10^4 cells/well). Cell suspensions were aliquotted over a 96-well plate that was then incubated for 35 h at 30 °C in a Genios plate reader (Tecan, Durham, NC) measuring the absorption at a wavelength of 595 nm. The experiments presented in Table 2 (cells in suspension by shaking every 10 min at 300 rpm for 1 min) and Table 3 (without shaking), respectively, were done slightly different, such that EC_{50} values for both nicotinic acid and acifran are not fully comparable for

the MMY24 strain. Results were obtained from three independent experiments, performed in duplicate.

Yeast protein extraction and immunoblotting

Protein extractions were done according to the trichloroacetic acid (TCA) method from the Clontech Yeast Protocols Handbook 2001. More details were described in our previous research[21]. Target proteins were analyzed by immunoblotting using a rabbit anti-human HCA_2/HCA_3 polyclonal antibody at 0.3 μg/ml with Tris-buffered saline containing 0.05% tween 20 (TBST) (pH 7.6) containing 5% milk powder for all these four receptors. The immunogenic amino acid sequence of the receptors used was NRCLQRKMTGEPDNNRSTSVELTGDPNKTRGAPE ALMANSGEPWSPSYLGP. After thorough removal of unbound antibody from the membranes by washing them three times with TBST, the membranes were incubated with 1:2,500 diluted HRP-conjugated goat anti-rabbit IgG for 1 h. The membranes were washed twice with TBST and once with TBS. The specific signal of the $hHCA_2$/$hHCA_3$ receptor was probed with the ECL Western blotting analysis system (GE Healthcare, Eindhoven, the Netherlands) using enhanced chemiluminescence (ChemiDox XRS, Bio-Rad, Hercules, CA, USA). A reference protein (α-tubulin) was analyzed simultaneously using rat anti-yeast α tubulin monoclonal antibody at 1 μg/ml and then using goat anti-rat IgG-HRP antibody at 0.16 μg/ml as the second antibody.

Statistical analysis

EC_{50} values and E_{max} values of the liquid assay were analyzed using the nonlinear regression package available in Prism 5.0 software (GraphPad Software Inc., San Diego, CA). Differences were examined for significance by a two-tailed homoscedastic Student's *t*-test, yielding *p*-values.

Expression of the receptors was quantified using Quantity One imaging software from Bio-Rad after correction for the background; it was calculated as density (OD/mm^2). The α-tubulin, at approx. 130 kDa, was used as loading control and the specific $hHCA_2$ receptor protein bands were approx. at 29 kDa and 52 kDa. The ratio was determined between the density of the specific $hHCA_2$

bands and the density of loading control band. MMY12 carrying the wild-type $hHCA_2$ receptor, was set at 100%. Results were obtained from two independent experiments and all expression levels of the $hHCA_2$ receptor in different MMY strains were normalized to the $hHCA_2$ receptor in the MMY12 strain on the same blot.

Results

Characterization of the wild-type $hHCA_2$ and $hHCA_3$ receptors expressed in the MMY24 yeast strain with three agonist ligands

To characterize the activation of the $hHCA_2$ and $hHCA_3$ receptor in the yeast system, we first expressed the yeast expression plasmids: p426GPD, P426GPD_$hHCA_2$, p426GPD_$hHCA_3$ in a yeast *S. cerevisiae* strain, MMY24 (with $G_{\alpha i}$). The $hHCA_2$ receptor was activated by both nicotinic acid (EC_{50} = 35 nM) and acifran (EC_{50} = 56 nM), but not by LUF 7159, an agonist selective for the HCA_3 receptor[23]. Nicotinic acid's E_{max} value was slightly higher than for acifran, while the receptor itself displayed significant constitutive activity (CA) under these conditions (Fig. 1B and Table 2). The $hHCA_3$ receptor was activated by both LUF7159 (EC_{50} = 671 nM) and acifran (EC_{50} = 13,600 nM), but not by nicotinic acid. LUF7159 showed a 20-fold higher potency than acifran, while the E_{max} values for both ligands were the same. The HCA_3 receptor displayed lower constitutive activity than the HCA_2 receptor (Fig. 1C and Table 2).

A

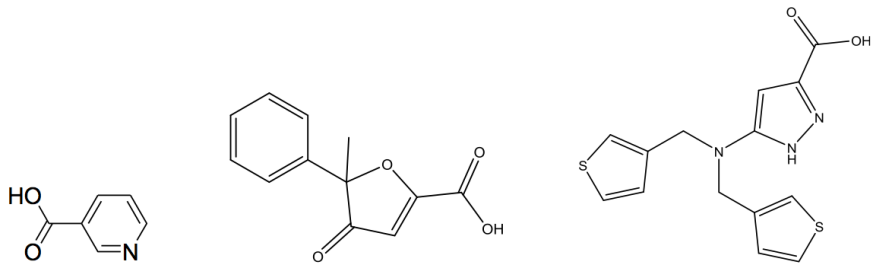

Nicotinic acid Acifran LUF7159

B

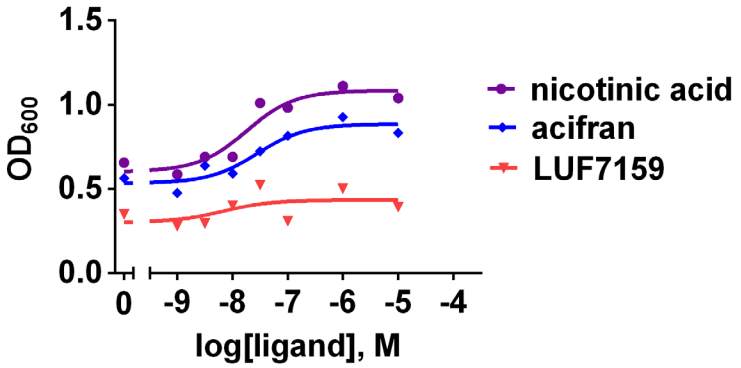

C

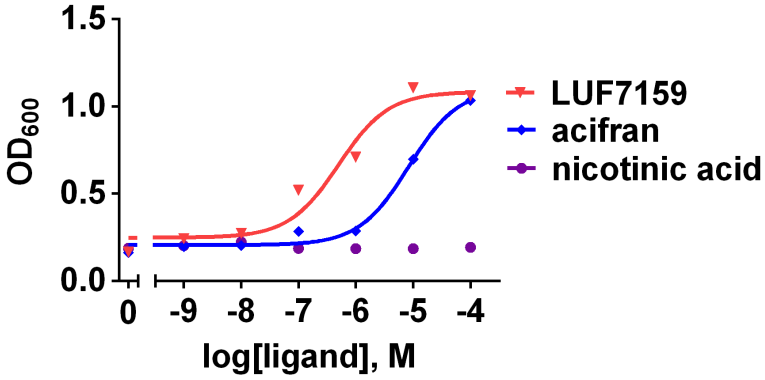

Fig. 1. (A) Chemical structures of ligands from left to right: nicotinic acid, acifran, and LUF7159. Concentration-effect curves of the wild-type receptor $hHCA_2$ (B) and $hHCA_3$ (C) in the MMY24($G_{\alpha i3}$) strain responding to nicotinic acid, acifran and LUF7159. The assay was performed in YNB-ULH-NA medium. A representative experiment is shown (of a total of n = 3).

Table 2. EC_{50}, constitutive activity (CA) and E_{max} values of the wild-type $hHCA_2$ receptor, the $hHCA_2$+C mutant receptor, the wild-type $hHCA_3$ receptor and the $hHCA_3$-C mutant receptor in MMY 24 ($G_{\alpha i3}$) strain in response to nicotinic acid, acifran and LUF7159. Results were obtained from 3 independent experiments, performed in duplicate.

	$hHCA_2$		
	EC_{50} (nM)	CA	Emax
nicotinic acid	35 ± 11	0.6 ± 0.03	1.0 ± 0.07
acifran	56 ± 37	0.4 ± 0.06	0.8 ± 0.07
LUF7159	-	-	-
	$hHCA_2$+C		
	EC_{50} (nM)	CA	Emax
nicotinic acid	46 ± 27	0.5 ± 0.07	1.3 ± 0.13
acifran	71 ± 37	0.5 ± 0.08	1.1 ± 0.16
LUF7159	-	-	-
	$hHCA_3$		
	EC_{50} (nM)	CA	Emax
nicotinic acid	-	-	-
acifran	13600 ± 5700	0.2 ± 0.04	1.2 ± 0.02
LUF7159	671 ± 91	0.2 ± 0.05	1.1 ± 0.04
	$hHCA_3$-C		
	EC_{50} (nM)	CA	Emax
nicotinic acid	-	-	-
acifran	4900 ± 1800	0.3 ± 0.07	1.2 ± 0.05
LUF7159	285 ± 136	0.3 ± 0.06	1.1 ± 0.05

Characterization of the different G protein coupling profiles of the $hHCA_2$ and $hHCA_3$ receptors

To investigate the activation mechanism of the $hHCA_2$ receptor and $hHCA_3$ receptor at the interface with the C terminus of the G protein G_α subunit, we expressed the yeast plasmid p426GPD, p426GPD_$hHCA_2$, and p426GPD_$hHCA_3$ in a panel of yeast *S. cerevisiae* strains with humanized G proteins. The difference between these ten integrated Gpa1p/G_α chimeras is that the last five amino acids of the endogenous Gpa1p C-terminus have been replaced with the same five amino acids sequence motif as that from mammalian G_α proteins[18, 19] (Table 1). Corresponding to the replaced last five C-terminal residues of the mammalian G_α subunit, they were classified into five families:

$G_{\alpha WT}$ (MMY12), $G_{\alpha s}$ (MMY28), $G_{\alpha i}$ (MMY23, MMY24 and MMY25), $G_{\alpha 12}$ (MMY19 and MMY20), and $G_{\alpha q}$ (MMY14, MMY16 and MMY21) (Table 1).

Concentration-effect curves of nicotinic acid (0, 10^{-9} - 10^{-4} M) on the wild-type $hHCA_2$ receptor in all strains except MMY20 and MMY28 are shown in Fig. 2A. The two latter strains, when only carrying the 'empty' plasmid p426GPD (without any receptor), already showed substantial growth of the yeast cells, and were excluded from further examination although they expressed the receptors well (see also Fig. 5). Please, note that the experiments in Table 2 were performed slightly differently (see M&M) from the ones in Table 3, yielding somewhat different EC_{50} values for nicotinic acid and acifran in case of the MMY24 strain.

We found the three different $G_{\alpha i}$ protein pathways MMY23 ($G_{\alpha i1}$), MMY24 ($G_{\alpha i3}$) and MMY25 ($G_{\alpha z}$) to show varying degrees of enhancement of both the efficacy and potency of nicotinic acid compared to the wild-type $hHCA_2$ in the wild-type yeast G_{α} strain MMY12 ($G_{\alpha WT}$). The most efficient yeast strains, MMY23 ($G_{\alpha i1}$) and MMY24 ($G_{\alpha i3}$) showed a significant increase in potency of the agonist nicotinic acid (71-fold or 42-fold, respectively) and a 2-fold increase in intrinsic activity, while the other $G_{\alpha i}$ strain, MMY25 ($G_{\alpha z}$), showed a significant 5-fold enhancement in potency, concurrent with the highest E_{max} value. The other strains showed less efficient G protein coupling. MMY14 ($G_{\alpha q}$) showed no activation at all; MMY16 ($G_{\alpha 16}$) showed a 2-fold decrease in potency of nicotinic acid. MMY21 ($G_{\alpha 14}$) showed a 3-fold increase in potency and a similar efficacy of nicotinic acid. The $G_{\alpha 12}$ protein pathway was less responsive, as MMY19 ($G_{\alpha 12}$) showed a 3-fold decrease of potency and similar efficacy of the agonist nicotinic acid (Table 3).

Concentration-effect curves of acifran (0, 10^{-7} - 10^{-3} M) on the wild-type $hHCA_3$ receptor in MMY23 ($G_{\alpha i1}$) and MMY24 ($G_{\alpha i3}$) are shown in Fig. 2B, and the resulting parameters in Table 3. The EC_{50} values for acifran were in the 10-100 micromolar range. However, no activation was observed in any of the other MMY strains.

Table 3 EC_{50}, constitutive activity (CA) and E_{max} values of wild-type $hHCA_2$ receptor in response to the ligand nicotinic acid (0, 10^{-9} M to 10^{-4} M) and $hHCA_3$ receptor in response to acifran (0, 10^{-7} M to 10^{-3} M) in all examined MMY strains. Results were obtained from three independent experiments, performed in duplicate. "-": no activation

	$hHCA_2$ receptor			$hHCA_3$ receptor		
	EC_{50} (μM)	CA	E_{max}	EC_{50} (μM)	CA	E_{max}
MMY12 ($G_{\alpha WT}$)	10 ± 4.7	0.07 ± 0.002	0.6 ± 0.03	-		
MMY14 ($G_{\alpha q}$)	-	0.07 ± 0.01	0.1 ± 0.03	-		
MMY16 ($G_{\alpha 16}$)	21.5 ± 6.9	0.09 ± 0.015	1.5 ± 0.03	-		
MMY19 ($G_{\alpha 12}$)	30 ± 6	0.1 ± 0.03	0.5 ± 0.18	-		
MMY21 ($G_{\alpha 14}$)	3 ± 0.58	0.08 ± 0.008	0.6 ± 0.06	-		
MMY23 ($G_{\alpha i1}$)	0.14 ± 0.04	0.5 ± 0.04	1.3 ± 0.02	68.7 ± 21.4	0.2 ± 0.01	1.2 ± 0.13
MMY24 ($G_{\alpha i3}$)	0.24 ± 0.15	0.3 ± 0.03	1.1 ± 0.08	88.2 ± 17.4	0.1 ± 0.03	1.2 ± 0.05
MMY25 ($G_{\alpha z}$)	2.25 ± 0.48	0.14 ± 0.014	1.8 ± 0.02	-		

Construction of the $hHCA_2$+C and $hHCA_3$-C mutant receptors

The main difference between the $hHCA_2$ and $hHCA_3$ receptors is that the $hHCA_2$ has a shorter C-terminus with the $hHCA_3$ carrying 24 more amino acid residues at its C-terminus. Although the two receptors have high overall sequence homology, there are also 17 different amino acid residues in other parts of the two receptors that mainly cluster around ECL1 and ECL2 (Fig. 3). To investigate the importance of the C-terminus of the $hHCA_2$ and $hHCA_3$ receptor in G protein coupling, we constructed two mutants by 'swapping' the C-terminus, which were named the $hHCA_2$+C receptor (the wild-type $hHCA_2$ receptor with the extra C terminus of the wild-type $hHCA_3$ receptor) and the $hHCA_3$-C receptor (the wild-type $hHCA_3$ receptor with the shorter C terminus of the wild-type $hHCA_2$ receptor) (Fig. 3 and S1).

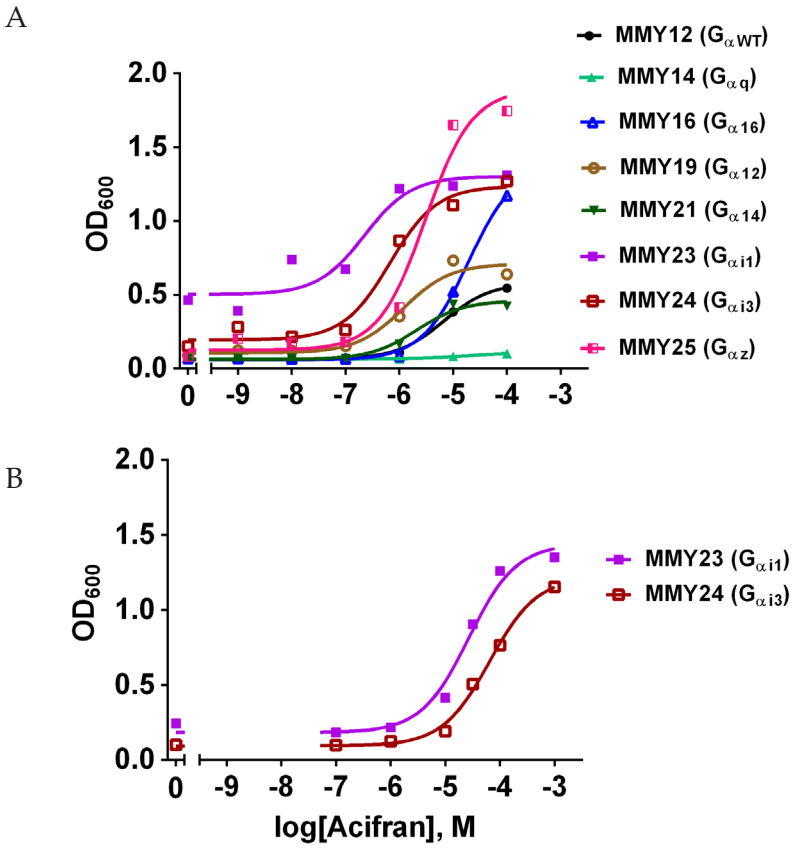

Fig. 2. Concentration-effect curves from liquid assay experiments. (A) Curves are shown of the wild-type receptor $hHCA_2$ in the different yeast strains: MMY25 ($G_{\alpha z}$), MMY23 ($G_{\alpha i1}$), MMY24 ($G_{\alpha i3}$), MMY16 ($G_{\alpha 16}$), MMY19 ($G_{\alpha 12}$), MMY12 ($G_{\alpha WT}$), MMY21 ($G_{\alpha 14}$), MMY14 ($G_{\alpha q}$) responding to the $hHCA_2$ agonist nicotinic acid. (B) The wild-type receptor $hHCA_3$ in the different strains: MMY23 ($G_{\alpha i1}$) and MMY24 ($G_{\alpha i3}$) responding to the $hHCA_2$/$hHCA_3$ agonist acifran. The $hHCA_3$ receptor was not activated in other strains, and, hence, no further curves are shown. The assays were performed in YNB-NA-ULH medium. A representative experiment is shown (of a total of n = 3).

Characterization of the $hHCA_2$+C and $hHCA_3$-C mutant receptors expressed in the MMY24 yeast strain with three agonist ligands

To characterize the activation of the $hHCA_2$+C and $hHCA_3$-C mutant receptors in the yeast MMY24 ($G_{\alpha i}$) strain we followed the same protocol as for the wild-type HCA_2 and HCA_3 receptors. The $hHCA_2$+C receptor was activated by nicotinic acid and acifran with similar potency and efficacy as WT $hHCA_2$, and could not be activated by the HCA_3-selective agonist LUF7159. The $hHCA_3$-C receptor

was only activated by acifran and LUF7159 with 3-fold and 2-fold increases in potency, respectively, with no changes in efficacy. The $hHCA_3$-C receptor could not be activated by nicotinic acid.

The role of the C terminus in G protein activation and selectivity

To investigate the role of the C terminus of both the $hHCA_2$ receptor and the $hHCA_3$ receptor at the interface of the C terminus of the G protein G_α subunit, we expressed the yeast plasmid p426GPD_$hHCA_2$+C and p426GPD_$hHCA_3$-C in a panel of 6 yeast *S. cerevisiae* strains with humanized G proteins. We did not include the MMY16 and MMY25 strains, as these two strains displayed a very low expression level of the HCA_2 receptor. The efficacy of these two mutants, $hHCA_2$+C and $hHCA_3$-C, compared to the two wild-type receptors, $hHCA_2$ and $hHCA_3$, are shown in Fig. 4, in the absence or presence of a saturating concentration of nicotinic acid (Fig. 4A and B) or acifran (Fig. 4C and D). The wild-type $hHCA_2$ significantly activated four of the six pathways examined, MMY12 ($G_{\alpha WT}$), MMY21 ($G_{\alpha 14}$), MMY23 ($G_{\alpha i1}$) and MMY24 ($G_{\alpha i3}$) (Fig. 4A). The $hHCA_2$+C receptor activated all six pathways (Fig. 4B), although the constitutive activity in MMY23 was so high that the response to nicotinic acid did not differ significantly from the basal value. The $hHCA_2$+C receptor tended to show higher activation levels, but otherwise behaved like the wild-type receptor in MMY12 ($G_{\alpha WT}$), MMY21 ($G_{\alpha 14}$), and MMY24 ($G_{\alpha i3}$), while it was additionally active in MMY14 ($G_{\alpha q}$). A comparison of the $hHCA_3$-C receptor (Fig. 4D) with the wild-type $hHCA_3$ receptor (Fig. 4C) revealed that the $hHCA_3$-C activates three rather than two pathways: MMY19 ($G_{\alpha 12}$) was activated with half the efficacy compared to activation in MMY23 ($G_{\alpha i1}$) or MMY24 ($G_{\alpha i3}$), while the basal activity of $hHCA_3$-C in MMY23 ($G_{\alpha i1}$) was increased.

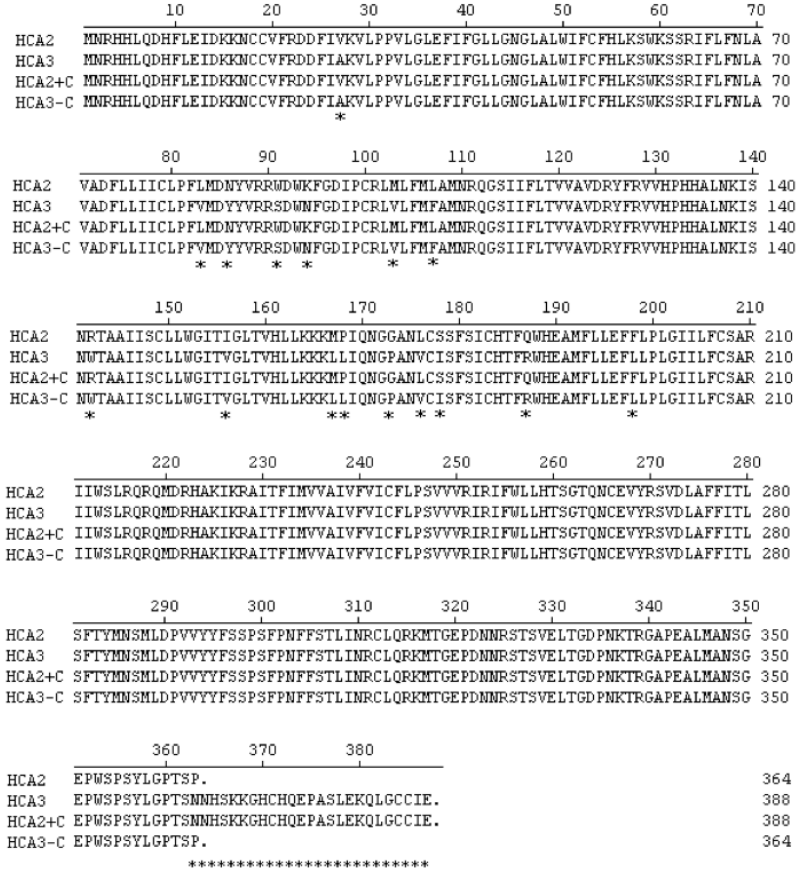

Fig. 3. Sequence alignment of the wild-type $hHCA_2$ receptor (GenBank: AAN71621.1), the wild-type $hHCA_3$ receptor (GenBank: BAA01721.1), the $hHCA_2$+C receptor and the $hHCA_3$-C receptor. The non-conserved residues are marked as *.

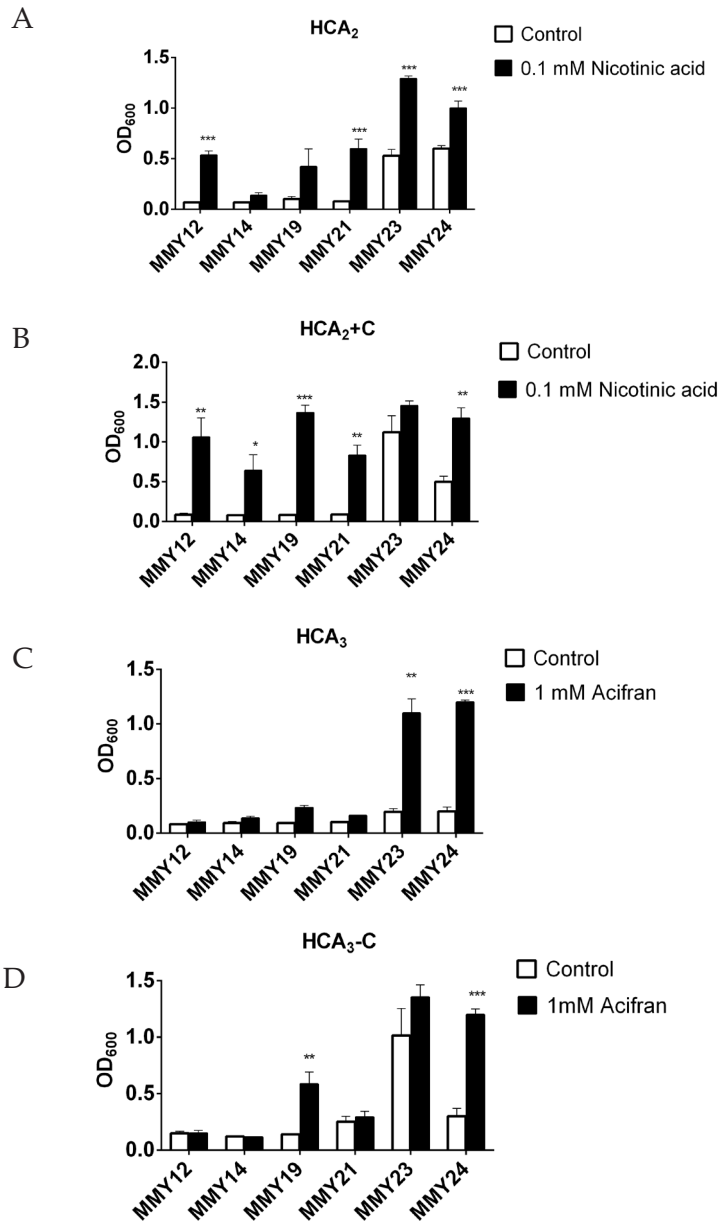

Fig. 4. Liquid assay experiments with the wild-type receptor $hHCA_2$ (A) and $hHCA_2$+C receptor (B) in the absence or presence of the agonist nicotinic acid (0.1 mM), and of the wild-type receptor $hHCA_3$ (C) and $hHCA_3$-C receptor (D) in the absence or presence of the agonist acifran (1 mM) in the different yeast strains. The assay was performed in YNB-ULH-NA medium. A representative experiment is shown (of a total of n = 2). Differences in receptor activation in the absence or presence of ligand in each strain were examined for significance by a two-tailed homoscedastic Student's *t*-test, yielding *p*-values, indicated as follows: *: $p < 0.05$, **: $p < 0.01$, ***: $p < 0.001$.

Determination of the expression levels of the $hHCA_2$ and $hHCA_3$ receptors in different yeast strains

In Fig. 5A a Western blot analysis is shown of the expression levels of the $hHCA_2$ receptor in all strains. A more quantitative bar graph analysis is depicted in Fig. 5B. Expression levels of the $hHCA_2$ receptor in most strains were quite comparable except for MMY16, MMY25 and MMY28.

Expression of the $hHCA_3$ receptor was detected in all other strains as well (Fig. 5D), but a more quantitative determination of $hHCA_3$ expression levels could not be performed due to the absence of its expression in the control MMY12 strain.

Unfortunately, the $hHCA_2$+C and $hHCA_3$-C mutant receptors failed to show in Western blot experiments, although these receptors showed concentration-effect curves with high E_{max} values in a number of strains (Fig. 4). Apparently the antibody developed for the two wild-type receptors did not react with the constructs.

Discussion

One-GPCR-one-G protein yeast system and MMY strains

Our previous research has shown that our one-GPCR-one-G protein yeast (*S. cerevisiae*) screening is very well suited to study a G protein-coupled receptor with respect to its G protein preference. The main principle is activation of the G protein pathway by a GPCR agonist making the yeast cells grow in medium lacking histidine through the *FUS1-HIS3* reporter gene[27, 28] in which the growth of the yeast cells quantitatively reflects the activation of the expressed receptor by the agonist. The advantage of this engineered yeast system over other (mammalian) systems is that it has zero background of G protein activation, which makes it suitable to detect the G protein profiles of individual receptor activation[19, 29, 30].

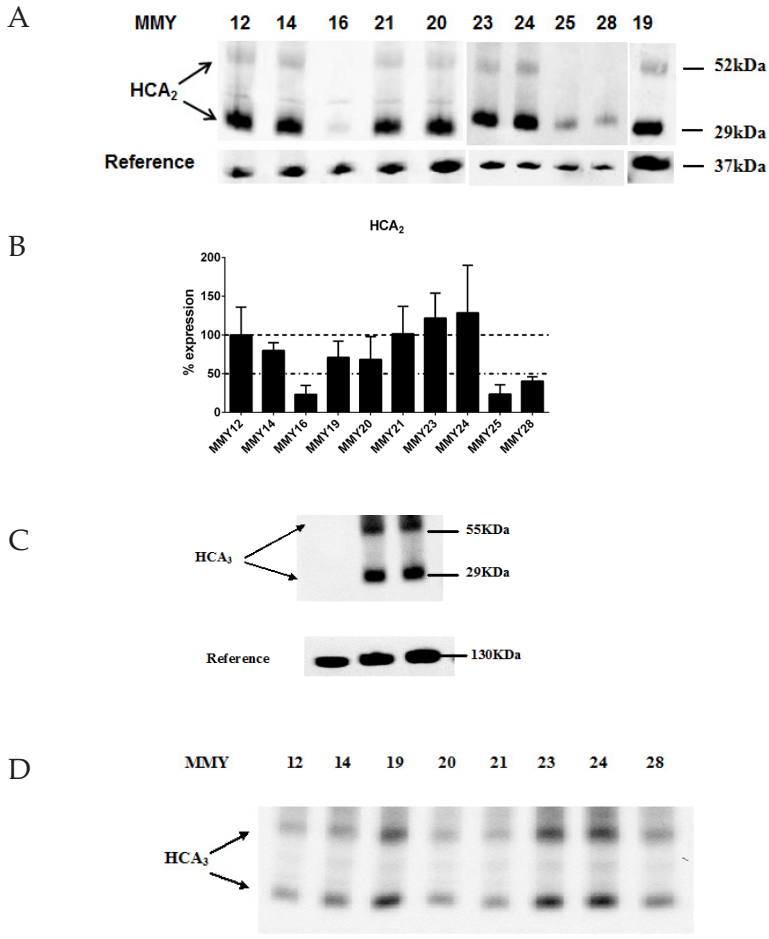

Fig. 5. Western blot analysis of the wild-type $hHCA_2$ and $hHCA_3$ receptor. (A) Representative blots of the $hHCA_2$ receptor in all strains in upper panel, i.e. MMY12, MMY14, MMY16, MMY21, MMY20, MMY23, MMY24, MMY25, MMY28, MMY12 andMMY19, all carrying the p426GPD-$hHCA_2$ transcript. The $hHCA_2$ receptor specific bands are located at 29 kD and 52 kD, which were absent in MMY12 carrying p426GPD without receptor (mock, not shown); α-tubulin (lower panel) is located at approx. 130kDa, which was used as loading control/ reference (it also appeared in MMY12 carrying p426GPD without receptor). (B) Bar graph analysis of $hHCA_2$ receptor expression in all strains, as calculated from a densitometric analysis of the blots. The ratio was determined between the density of the specific bands and that of the nonspecific band that was always present on the blots. MMY12 carrying wild-type $hHCA_2$ was set as 100%. All expression levels of the $hHCA_2$ receptor in different MMY strains were normalized against a $hHCA_2$ receptor in the MMY12 strain on the same blot. The experiment was performed two independent times. (C) Representative blot of the $hHCA_3$ receptor. Lane 1: MMY23($G_{\alpha i1}$)_p426GPD, Lane 2: MMY23($G_{\alpha i1}$)_p426GPD-$hHCA_3$, Lane 3: MMY24($G_{\alpha i3}$)_p426GPD-$hHCA_3$. The $hHCA_3$ receptor specific bands (upper panel) are located around 29kD and 55kD; α-tubulin (lower panel) is located at approx. 130kDa, which was used as loading control/reference (it also appeared in MMY23 carrying p426GPD without receptor). (D) Representative blot of the $hHCA_3$ receptor in all strains MMY12, MMY14, MMY19, MMY20, MMY21, MMY23, MMY24, and MMY28.

Brown et al (2000) reported that humanized yeast G_α proteins only containing a short (5 amino acids) C-terminal fragment of mammalian G_α fused to the remainder of the yeast's own Gpa1p G protein represent a significant improvement over other long (approx. 150 amino acids) Gpa1p/G_α chimeras. They chose 9 representative GPCRs to demonstrate this system is very suitable for the analysis of receptor and G protein function and their interplay, and showed some receptors to be more promiscuous than others, such as the adenosine A_{2B} receptor[30]. In the current study we applied 10 MMY strains, each with a specific humanized or WT yeast G_α protein. Corresponding to the replaced last five C-terminal amino acid residues of the mammalian G_α subunit, the strains can be classified into five families: $G_{\alpha WT}$ (MMY12), $G_{\alpha s}$ (MMY28), $G_{\alpha i}$ (MMY23, MMY24 and MMY25), $G_{\alpha 12}$ (MMY19 and MMY20), and $G_{\alpha q}$ (MMY14, MMY16 and MMY21)[18, 19, 26] (Table 1). It turned out that the combination of empty plasmid p426GPD with two different G proteins (MMY20 ($G_{\alpha 13}$) and MMY28 ($G_{\alpha s}$)) led to very high constitutive activity of the WT HCA_2 and HCA_3 receptor in the absence of agonist, and they were not examined further. Interestingly, standard commercial medium for yeast growth contains nicotinic acid, hence we used a special medium without nicotinic acid, as its presence would invariably activate all HCA_2 receptors. For comparison we applied the same medium for our studies on the HCA_3 receptor and its mutant, although nicotinic acid does not activate the HCA_3 receptor (see Fig. 1C).

Wise et al. (2003) reported EC_{50} values of nicotinic acid and acifran for the HCA_2 receptor of 904 nM and 3,000 nM, respectively, using a yeast growth assay through the *FUS1-LacZ* reporter gene in the MMY16 ($G_{\alpha 16}$) strain. They also studied the effect of acifran on the HCA_2 (EC_{50} value of 2,100 nM) and HCA_3 receptor (EC_{50} value of 20,000 nM) in a [^{35}S]GTPγS binding assay[31]. We came to comparable, although not similar, potencies for the agonists. For example, in the better-coupled MMY24 ($G_{\alpha i3}$) strain the EC_{50} value of nicotinic acid at the $hHCA_2$ varied between 35 nM (Table 2) and 240 nM (Table 3) in different experimental conditions. The EC_{50} value of acifran for the $hHCA_2$ receptor was 56 nM in the same MMY24 strain. Nicotinic acid is without effect at the $hHCA_3$ receptor, while the EC_{50} value of acifran for this receptor subtype varied from 14 μM

(Table 2) to 88 μM (Table 3). It is somewhat unfortunate that no antagonists have been identified yet for the two receptors, which would allow a more detailed pharmacological analysis.

The different G protein coupling profiles of the $hHCA_2$ receptor and $hHCA_3$ receptor

Although the $hHCA_2$ and $hHCA_3$ receptor share 95% sequence identity, their G protein coupling profiles are quite different. In the presence of nicotinic acid the $hHCA_2$ receptor activates almost all G protein pathways except $G_{\alpha q}$ (MMY14) (Fig. 2A and Table 3). In fact, the $hHCA_2$ receptor activated $G_{\alpha q}$ as well, when the agonist nicotinic acid was present for a longer time (48 h, data not shown). In contrast, the $hHCA_3$ receptor activated only two G protein pathways, MMY23 ($G_{\alpha i1}$) and MMY24 ($G_{\alpha i3}$), with no further activation of other G protein pathways after prolonged presence (48 h) of the agonist acifran (data not shown). In the model yeast system the $hHCA_2$ receptor thus activates G_{α} in the following order: $G_{\alpha i1} > G_{\alpha i3} > G_{\alpha z} > G_{\alpha 14} >$ Gpa1($G_{\alpha WT}$) $> G_{\alpha 16} > G_{\alpha q}$. However, the G_{α} protein coupling profile of the $hHCA_3$ receptor is less promiscuous: $G_{\alpha i1} > G_{\alpha i3} >>>$ all other pathways. Expression levels of the $hHCA_2$ receptor in most strains were quite comparable except for MMY16, MMY25 and MMY28 (Fig. 5A and B). Apparently, there was no clear connection between the activation profile and the expression of the receptor. For instance in the MMY14 strain there is good receptor expression, but receptor activation only happened after prolonged incubation of the agonist (see above). Expression of the $hHCA_3$ receptor was observed in all strains examined, with relatively high levels in MMY19, MMY23 and MMY24 strains (Fig. 5C and D).

The function of the C terminus in G protein activation and selectivity

Fusing the C-terminus of the HCA_3 receptor to the HCA_2 receptor did not change the ligand preference of the HCA_2 receptor, as in both cases nicotinic acid activated the receptor (Fig. 4A and B). This is not surprising, as the ligand binding site resides most likely in the upper part of the transmembrane domain, in the absence of a crystal structure[1]. The same finding was noticed for the

HCA_3 receptor when its C-terminus was deleted; both proteins were activated by acifran (Fig. 4C and D). Indeed, the typical selectivity profile for the two WT receptors remained intact when the three reference compounds were tested on the constructs (Table 2). Tunaru et al. systematically mutated each of the amino acid residues in the putative binding pocket of $hHCA_2$ into the corresponding residues of $hHCA_3$ and found that three amino acids, Asn86, Trp91 and Ser178 of $hHCA_2$ are required for high-affinity binding of nicotinic acid[32]. Ahmed et al. reported on $hHCA_3$-specific amino acid residues, again in the N-terminal half of the receptor, mediating the specific activation of $hHCA_3$ by 2-OH-octanoic acid[33]. As the C-terminus may be close to the intracellular G protein binding site we anticipated substantial effects on G protein coupling of either adding (HCA_2+C construct) or deleting (HCA_3-C construct) that part of the receptor. For instance, if the longer C terminus of the HCA_3 receptor would have been a determinant for the quite selective G protein preference of this receptor, addition of that part of the receptor to the HCA_2 receptor might have caused a similar narrow preference. However, this was by no means the case, as the HCA_2+C construct was even less fastidious than the WT receptor (Fig. 4A and B). Removing the C-terminus of the HCA_3 receptor (HCA3-C) made the receptor a bit more promiscuous but not very much (Fig. 4C and D).

Conclusions

The $hHCA_2$ receptor is more promiscuous in its G protein coupling preference than the $hHCA_3$ receptor, which may also be the case in physiology. However, these differences are not controlled by their C-terminal tails. This is an important finding as the C-terminus of GPCRs has been implicated in many other relevant physiological processes such as folding of the receptor, maturation and trafficking to the cell membrane, association with other intracellular proteins including scaffold and adapter proteins[34]. Apparently G protein coupling may not belong to this enumeration, if the findings for the HCA_2 and HCA_3 receptor can be extended to other GPCRs.

Acknowledgments

Rongfang Liu thanks the China Scholarship Council (CSC) for her PhD scholarship. The authors are grateful to Dr S. Dowell from GSK (Stevenage, UK) for providing the yeast strains and the plasmids.

References

[1] Venkatakrishnan, A., et al. *Molecular signatures of G-protein-coupled receptors.* Nature (2013) 494: 185-194.

[2] Peeters, M.C., et al. *Importance of the extracellular loops in G protein-coupled receptors for ligand recognition and receptor activation.* Trends Pharmacol. Sci. (2011) 32: 35-42.

[3] Unal, H. and Karnik, S.S. *Domain coupling in GPCRs: the engine for induced conformational changes.* Trends Pharmacol. Sci. (2012) 33: 79-88.

[4] Denlinger, L.C., et al. *Mutation of a dibasic amino acid motif within the C terminus of the $P2X_7$ nucleotide receptor results in trafficking defects and impaired function.* J. Immunol. (2003) 171: 1304-1311.

[5] Gabilondo, A.M., et al. *A dileucine motif in the C terminus of the β_2-adrenergic receptor is involved in receptor internalization.* Proc. Natl. Acad. Sci. (1997) 94: 12285-12290.

[6] Krasel, C., et al. *Dual role of the β_2-adrenergic receptor C terminus for the binding of β-arrestin and receptor internalization.* J. Biol. Chem. (2008) 283: 31840-31848.

[7] Bermak, J.C., et al. *Interaction of γ-COP with a transport motif in the D1 receptor C-terminus.* Eur. J. Cell Biol. (2002) 81: 77-85.

[8] Khattree, N., Ritter, L.M., and Goldberg, A.F. *Membrane curvature generation by a C-terminal amphipathic helix in peripherin-2/rds, a tetraspanin required for photoreceptor sensory cilium morphogenesis.* J. Cell Sci. (2013) 126: 4659-4670.

[9] Wilson, H.L., et al. *Epithelial membrane proteins induce membrane blebbing and interact with the $P2X_7$ receptor C terminus.* J. Biol. Chem. (2002) 277: 34017-34023.

[10] Garrad, R.C., et al. *Structural basis of agonist-induced desensitization and sequestration of the $P2Y_2$ nucleotide receptor: consequences of truncation of the C-terminus.* J. Biol. Chem. (1998) 273: 29437-29444.

[11] Georgoussi, Z., et al. *Selective interactions between G protein subunits and RGS4 with the C-terminal domains of the μ-and δ-opioid receptors regulate opioid receptor signaling.* Cell. Signalling (2006) 18: 771-782.

[12] Estall, J.L., et al. *The glucagon-like peptide-2 receptor C terminus modulates β-arrestin-2 association but is dispensable for ligand-induced desensitization, endocytosis, and G-protein-dependent effector activation.* J. Biol. Chem. (2005) 280: 22124-22134.

[13] Schröder, R., et al. *The C-terminal tail of CRTH2 is a key molecular determinant that constrains Gαi and downstream signaling cascade activation.* J. Biol. Chem. (2009) 284:

1324-1336.

[14] Kammermeier, P.J. *C-terminal deletion of metabotropic glutamate receptor 1 selectively abolishes coupling to Gαq.* Eur. J. Pharmacol. (2010) 627: 63-68.

[15] Kim, K.-M. and Caron, M.G. *Complementary roles of the DRY motif and C-terminus tail of GPCRS for G protein coupling and β-arrestin interaction.* Biochem. Biophys. Res. Commun. (2008) 366: 42-47.

[16] Osawa, S. and Weiss, E.R. *The carboxyl terminus of bovine rhodopsin is not required for G protein activation.* Mol. Pharmacol. (1994) 46: 1036-1040.

[17] Offermanns, S., et al. *International Union of Basic and Clinical Pharmacology. LXXXII: nomenclature and classification of hydroxy-carboxylic acid receptors (GPR81, GPR109A, and GPR109B).* Pharmacol. Rev. (2011) 63: 269-290.

[18] Dowell, S. and Brown, A. *Yeast assays for G-protein-coupled receptors.* Recept. Channels (2002) 8: 343-352.

[19] Dowell, S.J. and Brown, A.J. *Yeast assays for G protein-coupled receptors.* Methods Mol. Biol. (2009) 552: 213-229.

[20] Beukers, M.W. and IJzerman, A.P. *Techniques: how to boost GPCR mutagenesis studies using yeast.* Trends Pharmacol. Sci. (2005) 26: 533-539.

[21] Liu, R., et al. *A yeast screening method to decipher the interaction between the adenosine A_{2B} receptor and the C-terminus of different G protein α-subunits.* Purinergic Signal. (2014) 10: 441-453.

[22] Liu, R., et al. *Scanning mutagenesis in a yeast system delineates the role of the NPxxY $(x)_{5,6}$F motif and helix 8 of the adenosine A_{2B} receptor in G protein coupling.* Biochem. Pharmacol. (2015) 95: 290-300.

[23] Skinner, P.J., et al. *5-N, N-Disubstituted 5-aminopyrazole-3-carboxylic acids are highly potent agonists of GPR109b.* Bioorg. Med. Chem. Lett. (2009) 19: 4207-4209.

[24] Chenna, R., et al. *Multiple sequence alignment with the Clustal series of programs.* Nucleic Acids Res. (2003) 31: 3497-3500.

[25] Gietz, D., et al. *Improved method for high efficiency transformation of intact yeast cells.* Nucleic Acids Res. (1992) 20: 1425.

[26] Simon, M.I., et al. *Diversity of G proteins in signal transduction.* Science (1991) 252: 802-808.

[27] Bertheleme, N., et al. *Loss of constitutive activity is correlated with increased thermostability of the human adenosine A_{2A} receptor.* Br. J. Pharmacol. (2013) 169: 988-998.

[28] Peeters, M.C., et al. *Three "hotspots" important for adenosine A_{2B} receptor activation: a mutational analysis of transmembrane domains 4 and 5 and the second extracellular loop.* Purinergic Signal. (2012) 8: 23-38.

[29] Weston, C., et al. *Investigating G protein signalling bias at the glucagon-like peptide-1 receptor in yeast.* Br. J. Pharmacol. (2014) 171: 3651-3665.

[30] Brown, A.J., et al. *Functional coupling of mammalian receptors to the yeast mating pathway using novel yeast/mammalian G protein α-subunit chimeras.* Yeast (2000) 16: 11-22.

[31] Wise, A., et al. *Molecular identification of high and low affinity receptors for nicotinic acid.*

J. Biol. Chem. (2003) 278: 9869-9874.

[32] Tunaru, S., et al. *Characterization of determinants of ligand binding to the nicotinic acid receptor GPR109A (HM74A/PUMA-G).* Mol. Pharmacol. (2005) 68: 1271-1280.

[33] Ahmed, K., et al. *Deorphanization of GPR109B as a receptor for the β-oxidation intermediate 3-OH-octanoic acid and its role in the regulation of lipolysis.* J. Biol. Chem. (2009) 284: 21928-21933.

[34] Keuerleber, S., et al. *From cradle to twilight: The carboxyl terminus directs the fate of the A 2A-adenosine receptor.* Biochim. Biophys. Acta-Biomembranes (2011) 1808: 1350-1357.

Supplement data

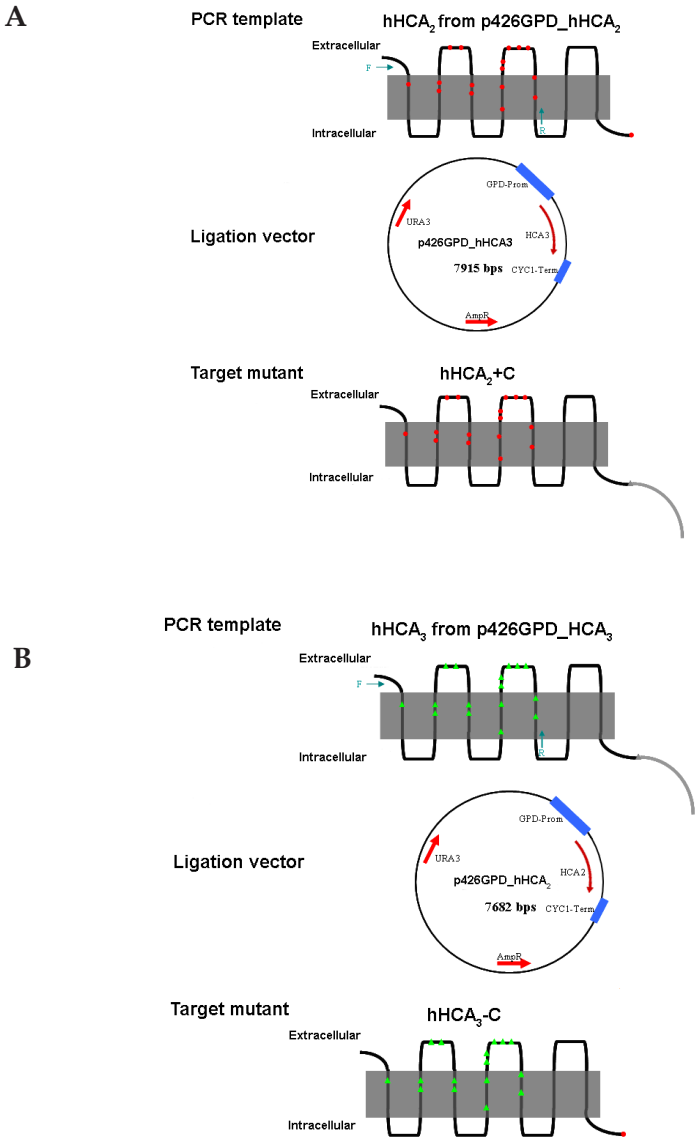

Fig. S1. Schematic drawing of the construction of the $hHCA_2$+C mutant (A) and the $hHCA_3$-C mutant (B). There are 16 different amino acids in both receptors preceding the C terminus; they are color-coded in both the $hHCA_2$/$hHCA_2$+C receptors (●) and the $hHCA_3$/$hHCA_3$-C receptors (▲). The one different amino acid at C-terminus is shown between the $hHCA_2$/$hHCA_3$-C receptors (●) and the $hHCA_3$/$hHCA_2$+C receptors (▲); the 24 –amino acid C-terminal extension is shown as gray lines in the $hHCA_3$/$hHCA_2$+C receptors. F: forward primer; R: reverse primer. The size of PCR products is 213 amino acids.

Chapter 6

Affinity and kinetics study of anthranilic acids as HCA_2 receptor agonists

This chapter is based upon:

Jacobus P. D. van Veldhoven[#], Rongfang Liu[#], Stephanie A. Thee, Yessica Wouters, Sanne J. M. Verhoork, Christiaan Mooiman, Julien Louvel, Adriaan P. IJzerman

[#] *These authors contributed equally*

Bioorganic Medicinal Chemistry ***2015*** *23: 4013-4025*

Abstract

Structure-affinity relationship (SAR) and structure-kinetics relationship (SKR) studies were combined to investigate a series of biphenyl anthranilic acid agonists for the HCA_2 receptor. In total, 27 compounds were synthesized and twelve of them showed higher affinity than nicotinic acid. Two compounds, **6g (**IC_{50} **=** 75 nM) and **6z** (IC_{50} = 108 nM) showed a longer residence time profile compared to nicotinic acid, exemplified by their kinetic rate index (KRI) values of 1.31 and 1.23, respectively. The SAR study resulted in the novel 2-F, 4-OH derivative (**6x**) with an IC_{50} value of 23 nM as the highest affinity HCA_2 agonist of the biphenyl series, although it showed a similar residence time as nicotinic acid. The SAR and SKR data suggest that an early compound selection based on binding kinetics is a promising addition to the lead optimization process.

Introduction

The hydroxycarboxylic acid (HCA) receptor family has three members: HCA_1, HCA_2 and HCA_3, which were deorphanized in 2008 (HCA_1, GPR81)[1, 2], 2005 (HCA_2, GPR109A, high affinity nicotinic acid receptor)[3] and 2009 (HCA_3, GPR109B, low affinity nicotinic acid receptor)[4], respectively. They all are G protein-coupled receptors and are predominantly expressed in adipocytes, where they mediate antilipolytic effects through coupling to the $G_{\alpha i}$ protein pathway[5, 6]. Activation of the HCA_2 receptor can have therapeutic benefits, such as an anti-dyslipidemic effect[7], neuroprotective effect[8, 9], and anti-inflammatory effect[10-12]. For the past 50 years nicotinic acid has been used to treat patients who suffer from dyslipidemia, cardiovascular disease and progression of atherosclerosis[13, 14]. However next to this beneficial anti-dyslipidemia effect, nicotinic acid also induces a HCA_2 receptor-mediated side effect of severe flushing, resulting in low patient compliance[15]. Since the cloning and the discovery of the pharmacological role of the HCA_2 receptor activated by nicotinic acid, the interest in the development of novel agonists increased, with many new classes developed in industry[6, 16]. In particular Arena Pharmaceuticals and Merck have been active in this field and their studies have resulted in aminopyrazole-based clinical candidates MK-0354[17, 18] and MK-1903[19], both of which failed in clinical studies due to a lack of efficacy (https://clinicaltrials.gov/ct2/show/NCT00847197). A more recently advanced compound with reportedly little flushing potential is the anthranilic acid derivative MK-6892[20]. Their structures are shown in Figure 1.

In general, the high attrition rates of clinical candidates are often due to a lack of efficacy[21], which led to the realization that equilibrium-derived *in vitro* parameters alone, such as measures of affinity (K_i) or potency (IC_{50}), are not necessarily correlated well with *in vivo* efficacy[22, 23]. A somewhat neglected parameter in early drug discovery, that is, the kinetics (association and dissociation rates, k_{on} and k_{off}) of the interaction between a drug and its target, may be relevant to predict *in vivo* efficacy, witnessed by some recently introduced drugs that favor certain kinetic aspects[23-26]. In particular, the

residence time ($1/k_{off}$) of a drug on its target may be more relevant for its *in vivo* efficacy than the typical *in vitro* equilibrium binding constants, for example, the compound's K_i value. In a survey of 50 drugs on 12 different drug targets, Swinney concluded that long residence time therapeutics often displayed higher efficacy than comparable faster dissociating drugs[27]. For instance, Casarosa et al. found the levels of bronchoprotection *in vivo* by high affinity antagonists of the human muscarinic M3 (hM3) receptor correlated well with their residence time (dissociation half-lives) from the hM3 receptor[28]. Glossop et al. found PF-3635659, a phase II clinical candidate for the treatment of chronic obstructive pulmonary disease (COPD), displayed a very long residence time (slow off-rate binding kinetics) at the M3 receptor mediating a long-lasting bronchodilation *in vivo* of more than one day[29]. However, no kinetics-directed studies on HCA_2 receptor agonists have been published. In this study we aimed to change that while examining the binding kinetics in the early stage of hit to lead optimization of the already extensively investigated class of anthranilic acid derivatives as HCA_2 receptor agonists. As shown in the initial publication by the Merck group, one of their first generation anthranilic acid agonists derived from their original high throughput screening hit is the biphenyl anthranilic acid compound **5a**[30]. Hence, **5a** will be the starting point in this study of both affinity and residence time.

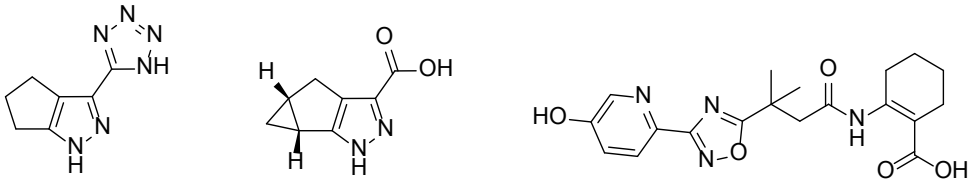

Fig. 1. Structures and potency data of MK-0354[17], MK-1903[19] and MK-6892[20].

Synthesis

The final compounds **5a–f, h–l, n–q** and **6g, m, r–aa** were obtained via two synthetic routes, which are shown in Scheme 1 and Scheme 2. The synthesis in Scheme 1 started from methyl 3-(4-bromophenyl)propanoate[31] (**1**) under Suzuki reaction conditions in dioxane/ethanol as the solvent mixture, the biphenyl compounds **2a–f, i–l, o–p, w** were obtained in good to high yields. Ester **1** was used since with the carboxylic acid analogue[30] as the starting material hard-to-purify mixtures were obtained. Next, saponification of the esters gave the pure carboxylic acids **3a–f, i–l, o–p, w** and under subsequent EDCI*HCl peptide coupling conditions, or via the acid chloride intermediate by the use of $SOCl_2$[30], anthranilic ester amides **4a–f, i–l, o–p, w** and the tetrahydroanthranilic derivative **4z** were isolated, respectively, in low yields. A second saponification of the anthranilic esters and the tetrahydroanthranilic ester, yielded **5a–f, i–l, o–p, w, z** and the successive demethylation of the methoxy compounds **5g, m, w** with BBr_3 in CH_2Cl_2[32] yielded the corresponding hydroxyl derivatives **6g, m, w**.

In Scheme 2 the synthetic approach[30] for compounds **5h, n, q** and **6r–v, x, y, aa** is shown. First, the reaction of 3-(4-iodophenyl)propanoic acid[33] (**7**) and $SOCl_2$ in toluene at 85 °C resulted in the corresponding acid chlorides, and the subsequent nucleophilic substitution with the commercially available methyl 2-aminobenzoate or methyl 2-aminothiophene-3-carboxylate gave both anthranilic ester **8a** in 96% yield and thiophene derivative **8b** in 38% yield. Similar Suzuki conditions as in Scheme 1, except for 6 equivalents instead of 2 equivalents of the base $NaHCO_3$ directly furnished the final Suzuki products as carboxylic acids (**5h, n, q–v, x, y**) after purification in 7–70% yield. The thiophene derivative **5aa** was obtained after the additional saponification of the related ester **4aa** by the use of NaOH (aq.). Finally, similar demethylation conditions as described in Scheme 1 gave the phenolic final compounds **6r–v, x, y, aa** in 2–96% yield as solids.

All final compounds had purities above 95% as determined by HPLC methods and the structures of the compounds were confirmed by ^{1}HNMR spectra.

Results

Both affinity and kinetics

In this study, the non-substituted biphenyl agonist **5a** was used as a starting point in the lead optimization showing an IC_{50} value of 290 ± 104 nM in our hands (Table 1), which is 2.5 times lower in affinity compared to the IC_{50} value of 94 nM reported by Raghavan et al[7]. Next to affinity, compounds with an IC_{50} value < 249 nM (IC_{50} value of nicotinic acid), together with nicotinic acid and **5a**, were tested in a binding kinetics assay using the one-concentration competition association assay with the radioligand [^{3}H]-nicotinic acid. This approach provided the so-called kinetic rate index (KRI) for the compounds, which is mainly driven by the dissociation rate constant (k_{off}) of the ligand–receptor complex[34].

Structure-Affinity Relationships (SAR)

As mentioned before, the non-substituted compound **5a** had an IC_{50} value of 290 ± 104 nM in our hands. Substituents at the 4 position (Table 1) decreased the affinity for the receptor in the cases of 4-Me (**5b**), 4-OMe (**5c**), 4-Cl (**5d**) and 4-CF_3(**5f**). The smaller 4-F (**5e**) was as well accepted (IC_{50} = 323 ± 104 nM) as the non-substituted **5a** by the receptor, but also this compound was still less active than nicotinic acid (Table 1). The hydrogen bond accepting and donating substituent 4-OH (**6g**) resulted in a 4 times improved IC_{50} value of 75 ± 5 nM (Table 1 and Fig. 2), similar to the approx. 6 times enhancement found by the Merck research team[35]. Introduction of a carbon between the aromatic system and the 4-hydroxy group yielding 4-CH_2OH (**5h**) was not allowed given the modest 51% displacement at a concentration of 10^{-5} M (Table 1). Substitutions at the 3-position (**5i–k**) were slightly better accommodated in the binding pocket of the HCA_2 receptor compared to the 4-substituted ones, except for the 3-OH group (**5m**) which showed a 12.5 times reduced affinity compared to the 4-OH substituent (**6g**). Again the smaller 3-F (**5l**) had an affinity (IC_{50} = 283 ± 25 nM) comparable to the non-substituted phenyl compound **5a** (Table 1). The 2-position seems to be preferred for a broader range of substituents (Table 1). Lipophilic groups such as 2-Me (**5n**) and 2-CF_3 (**5q**) were tolerated better at the 2-position

in contrast to the other positions, but both gave decreased affinities with respect to the non-substituted **5a**. Both halogens 2-Cl (**5o**) and 2-F (**5p**) increased the affinity to 94 ± 6 nM (19 nM in Ding et al.[36]) and 83 ± 18 nM, respectively. Also the polar 2-OH (**6r**) resulted in an improved IC_{50} value of 86 ± 13 nM.

Both of the abovementioned affinities of the mono-substituted analogues at the 2-position and, to a lesser extent, the 3-position indicate there is space in the binding pocket. Thus in combination with the highly preferred 4-OH substituent all of the di-substituted 3-R, 4-OH (**6s–u**) and 2-R, 4-OH (**6v–y**) compounds gained affinity when compared to their mono-substituted analogues (**5i, k, l** and **5n–p, 6r**) (Table 2). The novel 3,4-disubstituted compounds 3-Me, 4-OH (**6s**), 3-Cl, 4-OH (**6t**), and 3-F, 4-OH (**6u**) showed IC_{50} values of 201 ± 34, 365 ± 96 and 91 ± 20 nM, respectively, which resulted in a 3–4 times increased affinity with respect to **5i, k, l**. The 2,4-disubstituded **6v–y** were better tolerated in the receptor compared to the 3,4-disubstituted congeners (**6s–u**), as was also seen in the mono-substituted compounds. All of the 2-R, 4-OH compounds had higher affinities than the threshold value of IC_{50} = 249 nM (IC_{50} value of nicotinic acid) and were novel, except for **6w** with the often used substituent pattern 2-Cl, 4-OH[7, 35]. Again the 2-Me, 4-OH (**6v**); 2-Cl, 4-OH (**6w**) and 2-F, 4-OH (**6x**) displayed approx. 3–4 times improved IC_{50} values of 129 ± 19, 34 ± 2 and 23 ± 3 nM over the mono-substituted compounds (**5n–p**). The 2,4-diOH derivative (**6y**) resulted in an 1.4 times increase in affinity over **6r**. Novel tetrahydroanthranilic acid derivative (**6z**) (Fig. 2) and the thiophene bioisostere (**6aa**) of anthranilic acid compound **6g** (4-OH) resulted in slightly decreased affinities but well below the threshold (Table 3).

In summary, the novel 2-F, 4-OH (23 ± 3 nM) derivative showed the highest affinity in this series. In order to address the selectivity of the novel compounds a functional yeast growth assay was performed showing that the compounds are only active on the HCA_2, not HCA_3 receptor (Fig. S1).

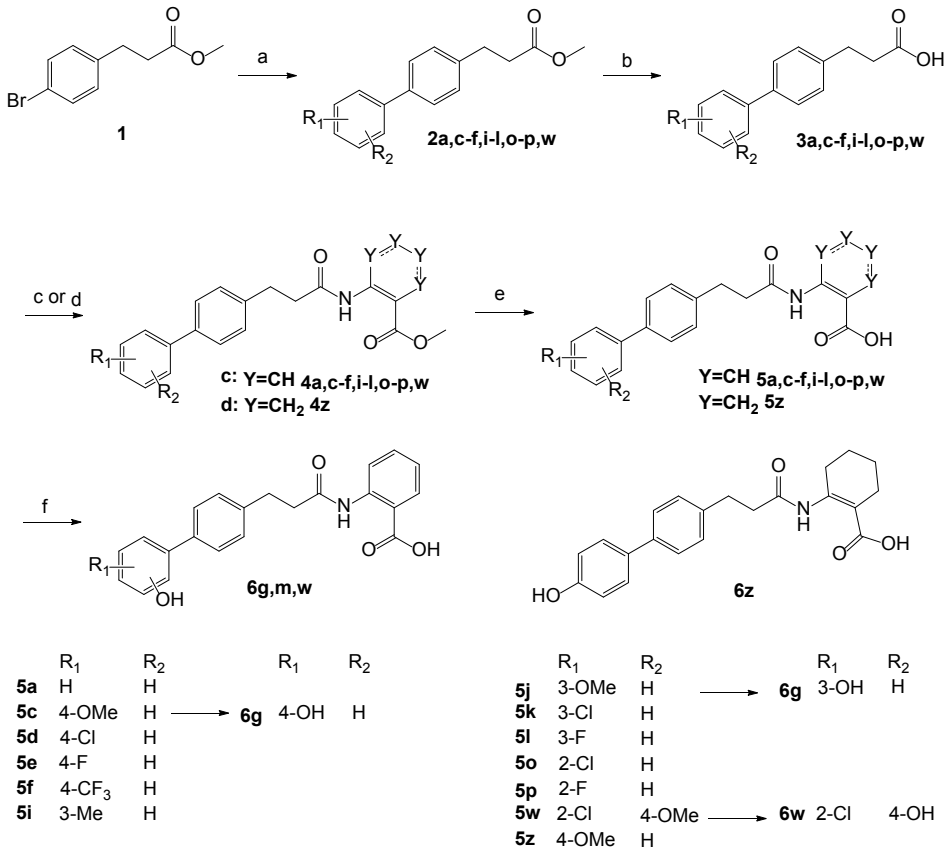

Scheme 1. Reagents and conditions: (a) appropriate phenylboronic acid, $Pd(PPh_3)_4$, 1 M $NaHCO_3$ (aq), dioxane, ethanol, 100 °C, 3 h, microwave; (b) 5 M NaOH (aq.), dioxane, room temperature, 3 h; (c) methyl-2-amino-benzoate, EDCI*HCl, DMAP, CH_2Cl_2, room temperature, 72 h; (d) i) **3c**, $SOCl_2$, reflux, 1.5 h ii) methyl 2-amino-1-cyclohexene-1-carboxylate, toluene at 70 °C overnight; (e) 5 M NaOH (aq.), dioxane, room temperature, 24 h; (f) 1M BBr_3, CH_2Cl_2, -78 °C to room temperature, 3 h.

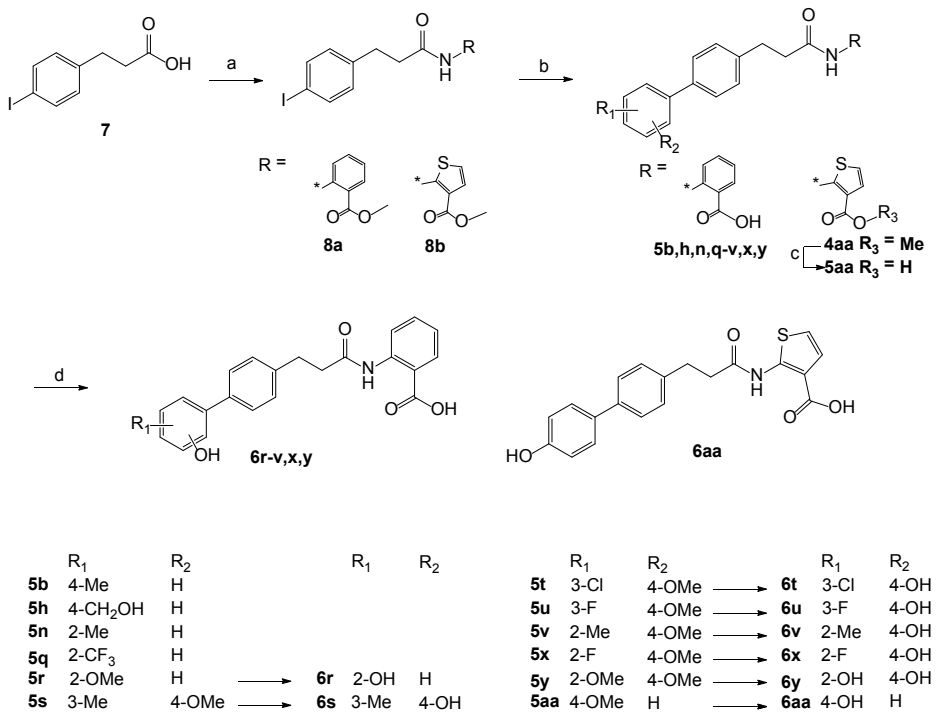

	R_1	R_2			R_1	R_2
5b	4-Me	H				
5h	4-CH_2OH	H				
5n	2-Me	H				
5q	2-CF_3	H				
5r	2-OMe	H	→	**6r**	2-OH	H
5s	3-Me	4-OMe	→	**6s**	3-Me	4-OH

	R_1	R_2			R_1	R_2
5t	3-Cl	4-OMe	→	**6t**	3-Cl	4-OH
5u	3-F	4-OMe	→	**6u**	3-F	4-OH
5v	2-Me	4-OMe	→	**6v**	2-Me	4-OH
5x	2-F	4-OMe	→	**6x**	2-F	4-OH
5y	2-OMe	4-OMe	→	**6y**	2-OH	4-OH
5aa	4-OMe	H	→	**6aa**	4-OH	H

Scheme 2. Reagents and conditions: (a) i) $SOCl_2$, reflux, 18 h under N2 atmosphere ii) methyl 2-aminobenzoate, toluene, room temperature, 18 h; (b) substituted phenyl boronic acid, PPh_3, $Pd(OAc)_2$, 1 M $NaHCO_3$ (aq.), dioxane, ethanol, 100 °C, 3 h, microwave; (c) 5 M NaOH (aq.), dioxane, room temperature, 24 h; (d) BBr_3, CH_2Cl_2, -78 °C to room temperature, 3 h.

Table 1 Structure-affinity relationships and Structure-kinetics relationships of 2-(monosubstituted biphenyl-3-propanamido)benzoic acids of **5a-f, h-l, n-q** and **6g, m, r.**

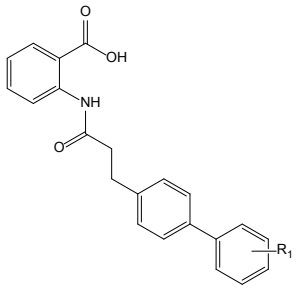

Compound	R_1	IC_{50} (nM) or % displacement[a]	KRI[b]
[^{3}H]nicotinic acid			0.70 ± 0.02
nicotinic acid		249 ± 48	0.80 ± 0.07
5a	H	290 ± 104	0.78 ± 0.04
5b	4-Me	68% (65, 72)	—
5c	4-OMe	46% (45, 48)	—
5d	4-Cl	60% (59, 61)	—
5e	4-F	323 ± 41	—
5f	4-CF_3	41% (43, 40)	—
6g	4-OH	75 ± 5	1.31 ± 0.06**
5h	4-CH_2OH	51% (58, 44)	—
5i	3-Me	800 ± 54	—
5j	3-OMe	769 ± 58	—
5k	3-Cl	1401 ± 245	—
5l	3-F	283 ± 25	—
6m	3-OH	940 ± 79	—
5n	2-Me	555 ± 164	—
5o	2-Cl	94 ± 6	0.79 ± 0.02
5p	2-F	83 ± 18	0.92 ± 0.10
5q	2-CF3	326 ± 78	—
6r	2-OH	86 ± 13	0.71 ± 0.03

[a] Percentage displacement of **5b-d**, **5f** and **5h** from single point [^{3}H]nicotinic acid displacement binding assay at 10^{-5} M of cold ligand (N = 2, individual values in parentheses). IC_{50} values in nM ± SEM (n = 3) from full curves of [^{3}H]nicotinic acid displacement binding assay.

[b] Averaged Kinetic Rate Index (KRI, individual values in parentheses), determined in the absence or presence (1 × IC_{50} value) of nicotinic acid, **5a**, **6g**, **5o**, **5p**, or **6r**, as the ratio of specific binding at time points t_1 = 7 minutes and t_2 = 90 minutes. Statistical evaluation (*p*-values) of KRI values was performed by a two-tailed homoscedastic Student's *t*-test using non-radioactive nicotinic acid as reference ligand; significance is indicated as follows: *: $p < 0.05$, **: $p < 0.01$, ***: $p < 0.001$.

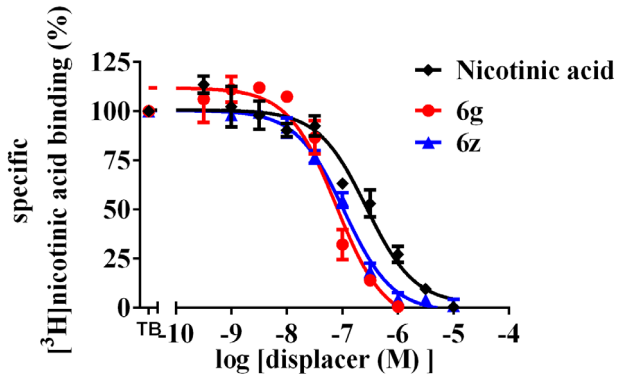

Fig. 2. Displacement of specific [^{3}H]nicotinic acid binding from the human HCA_2 receptor by nicotinic acid, **6g** and **6z** to reveal their affinity values. The assay was performed on HEK293T-$hHCA_2$ membranes. The mean curves of three independent experiments performed in duplicate are shown.

Table 2. Structure-affinity relationships and Structure-kinetics relationships of 2-(4-hydroxy-2 or 3 disubstituted biphenyl-3-propanamido)benzoic acids **6s-y.**

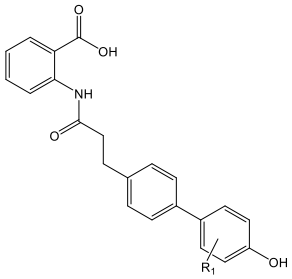

compound	R_1	IC_{50} (nM)[a]	KRI[b]
6s	3-Me	201 ± 34	0.83 ± 0.07
6t	3-Cl	365 ± 96	—
6u	3-F	91 ± 20	0.89 ± 0.06
6v	2-Me	129 ± 19	0.90 ± 0.04
6w	2-Cl	34 ± 2	0.98 ± 0.04
6x	2-F	23 ± 3	0.91 ± 0.12
6y	2-OH	58 ± 12	0.92 ± 0.09

[a] IC_{50} values in nM ± SEM (n = 3) from full curves of [^{3}H]nicotinic acid displacement binding assay.

[b] Averaged Kinetic Rate Index (KRI, individual values in parentheses), determined in the presence (1 × IC_{50} value) of **6s** or **6u-6y**, as the ratio of specific binding at time points t_1 = 7 minutes and t_2 = 90 minutes. Statistical evaluation (*p*-values) of KRI values was performed by a two-tailed homoscedastic Student's *t*-test using non-radioactive nicotinic acid as reference ligand; significance is indicated as follows: *: $p < 0.05$, **: $p < 0.01$, ***: $p < 0.001$.

Structure-Kinetics Relationships (SKR)

Kinetics of [^{3}H]-nicotinic acid

The association and dissociation experiments of [^{3}H]nicotinic acid (15 nM) were conducted at 25 °C on HEK293T-hHCA$_2$ membranes (35 μg of protein per well). The observed association rate constant, k_{obs} = 0.16 ± 0.03 min^{-1}, was calculated from the association binding experiment. The dissociation rate constant, k_{off}, was 0.27 ± 0.04 min^{-1}. Representative association and dissociation graphs are shown in Figure 3A and B, respectively.

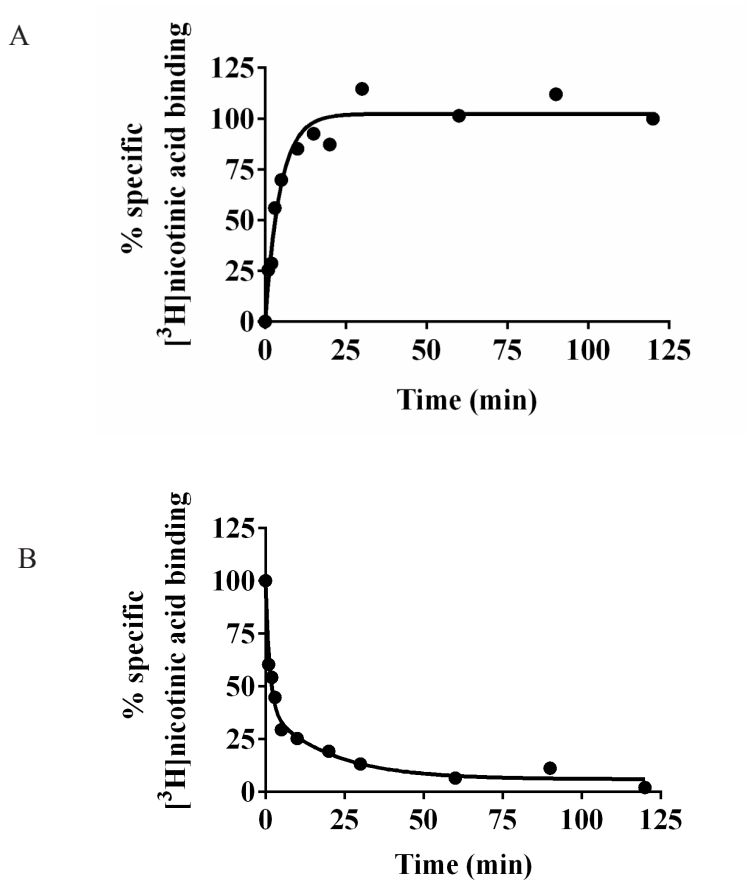

Fig. 3. The association (A) and dissociation (B) kinetics of [^{3}H]nicotinic acid binding at the hHCA$_2$ receptor at 25 °C. The assay was performed on HEK293T-hHCA$_2$ membranes. Representative graphs from one experiment performed in duplicate at same conditions.

Qualitative kinetics of anthranilic acid derivatives

Besides nicotinic acid, 12 compounds (**5a**, **5o**, **p** and **6g**, **r**, **s**, **u–y**, **z**, **aa**) had affinities < 249 nM (IC_{50} value of nicotinic acid) and these compounds were tested in a one-concentration competition association assay with the radioligand [^{3}H]nicotinic acid (Fig. S2). This provided the data for the determination of a kinetic rate index (KRI) value, which was obtained by dividing the specific radioligand binding measured at t_1 = 7 min (B_{t1}) by the binding at t_2 = 90 min (B_{t2}) in the presence of unlabeled competing ligands (KRI = B_{t1}/B_{t2}). With only the radioligand [^{3}H]nicotinic acid present a KRI value of 0.7 was obtained in the competition association assay (Fig. 4). In the competition association experiments with the reference agonist nicotinic acid or the non-substituted **5a**, the corresponding KRI values were both 0.8, very similar to the KRI value and kinetics of the radioligand. Similar patterns were seen with the 2-Cl (**5o**, KRI = 0.8), 2-F (**5p**, KRI = 0.9) and 2-OH (**6r**, KRI = 0.7) substituents. In contrast, the 4-OH derivative (**6g**) showed a significantly increased KRI value of 1.31 ± 0.06 ($p < 0.005$), which together with the typical profile of the curve in Figure 4 indicates a relatively long residence time on the receptor equivalent to a slow k_{off}. This made **6g** a logical starting point for a series of disubstituted compounds (Table 2). However, 3-substituted, 4-OH derivatives **6s** (3-Me, 4-OH) and **6u** (3-F, 4-OH) had decreased KRI values of 0.83 and 0.89, respectively. This trend was also observed for all the 2-R, 4-OH compounds **6v–y**, including the known 2-Cl, 4-OH derivative (**6w**, KRI = 0.98).

The influence of the anthranilic acid moiety itself was investigated by replacing it for a tetrahydroanthranilic moiety (**6z**) resulting in a similar higher KRI value of 1.23 ± 0.03 ($p < 0.005$) (Table 3) as the related anthranilic acid derivative with the 4-OH substituent (**6g**). However, replacement by the aromatic thiophene bioisostere (**6aa**) yielded a lower KRI value of 0.95 again (Table 3), which indicates that the binding kinetics can also be influenced by this part of the ligand.

Table 3. Structure-affinity relationships and Structure-kinetics relationships of tetrahydroanthranilic acid analogue and thiophene-anthranilic acid bioisostere **6z** and **6aa**.

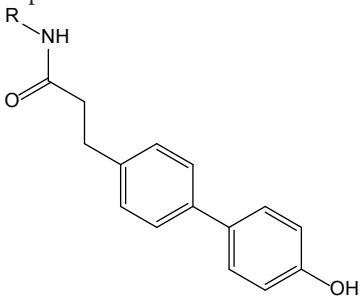

Compound	R	IC_{50} (nM)[a]	KRI[b]
6z	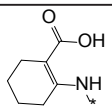	108 ± 4	1.23 ± 0.03 **
6aa	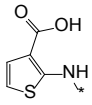	105 ± 12	0.95 ± 0.02

[a] IC_{50} values in nM ± SEM (n = 3) from full curves of [^{3}H]nicotinic acid displacement binding assay.
[b] Averaged Kinetic Rate Index (KRI, individual values in parentheses), determined in the presence (1 × IC_{50} value) of **6z** and **6aa**, as the ratio of specific binding at time points t_1 = 7 minutes and t_2 = 90 minutes. Statistical evaluation (*p*-values) of KRI values was performed by a two-tailed homoscedastic Student's *t*-test using non-radioactive nicotinic acid as reference ligand; significance is indicated as follows: *: $p < 0.05$, **: $p < 0.01$, ***: $p < 0.001$.

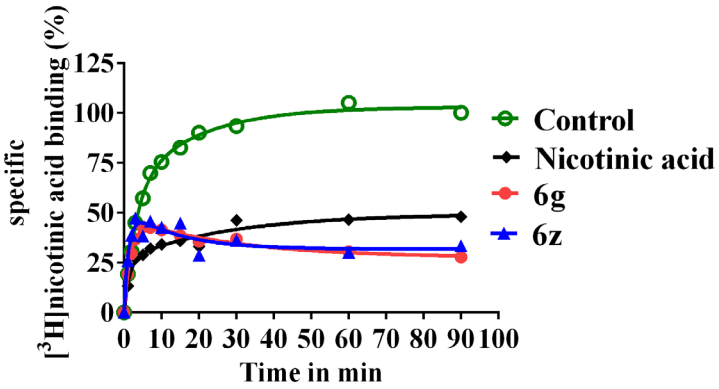

Fig. 4. [^{3}H]nicotinic acid competition association assay in the absence of ligand (control) and in the presence of 1 × IC_{50} of unlabeled **nicotinic acid**, **6g** and **6z** yield their kinetic profiles. Representative graphs from one experiment performed in duplicate.

Discussion

The affinities of compounds **5c, e, i–n, r** have been described previously in the broad range of 1 nM–15 μM[37]. In the present study we report new findings on the SAR and SKR of anthranilic acid-derived agonists for the HCA_2 receptor. The mono-substituted compounds with 4-OH (**6g**)[35, 38], 2-Cl **(5o**), 2-F (**5p**) and 2-OH (**6r**) were not significantly different with respect to affinity (75–94 nM) . This simple observation illustrates the difficulty in a typical drug discovery program to triage compounds for further development, suggesting the decision, which compound to select for further development cannot be made on the classical in vitro affinities alone. Hence, we added the additional parameter of drug-target kinetics. In this particular case we were faced with the problem that the association and dissociation characteristics of the radioligand precluded the determination of the kinetic rate constants. As the k_{obs} value (apparent association rate constant, 0.21 min^{-1}) was smaller than the dissociation rate constant (k_{off}, 0.33 min^{-1}) (Fig. 3A and B), the 'true' association rate constant (k_{on}) cannot be determined from the equation, $k_{on} = (k_{obs} - k_{off})/[radioligand]$. This problem could not be solved by changing temperature or time of incubation, the concentration of radioligand or membranes, or using cell lines with different expression levels of the $hHCA_2$ receptor (data not shown). Thus, the actual residence time values could not be determined from the competition association assay, as here both rate constants (k_{on} and k_{off}) for the radioligand are needed for the calculation. However, more indirect measures for the kinetics of unlabeled competing ligands, the so-called kinetic rate index (KRI)[34] can still be assessed in the competition association assay. Indeed, these KRI values of the different compounds were quite telling. In general, a KRI > 1.0 indicates a relatively slow dissociation from the target, while a KRI < 1.0, or in this case a KRI < 0.7 or 0.8, predicts a relatively fast dissociation rate compared to the dissociation rate of the radioligand [^{3}H]-nicotinic acid[34, 39]. The 4-OH derivative **6g** had the longest residence time, displaying a KRI value of 1.31 ± 0.06 ($p < 0.005$) compared to approx. 0.7–0.9 in the case of the similar-affinity compounds, 2-Cl **(5o**), 2-F (**5p**) and 2-OH (**6r**).

Di-substituted compounds bearing the 4-OH group lacked a longer

residence time, although yielding higher affinity compounds including the 2-Cl, 4-OH derivative (**6w**). This latter disubstitution pattern has often been employed by the Merck group, although clinical candidate MK6892 has a slightly different heterocyclic 4-hydroxy-2-pyridine moiety[20, 30, 35, 36]. The tetrahydroanthranilic acid (**6z**), whose moiety is also present in MK6892[7], did have a beneficial KRI profile in our hands.

Conclusions and outlook

We investigated the structure–affinity relationships (SAR) and the structure–kinetics relationships (SKR) of a series of biphenyl anthranilic acid agonists for the HCA_2 receptor. The SAR led us to the novel 2-F, 4-OH derivative (**6x**) with an IC_{50} value of 23 ± 3 nM as the highest affinity HCA_2 agonist of the biphenyl series. However because of its low KRI value of 0.9 as an indication of the residence time, we considered it less promising.

The selection approach by combining affinity and binding kinetics resulted in two interesting 4-OH substituted lead compounds. One was the known agonist **6g** with a 3 times compromised affinity of 75 ± 5 nM compared to **6x**, but with an interesting KRI value of 1.31 ± 0.06 ($p < 0.005$) indicating a longer residence time. Also the related novel tetrahydroanthranilic acid derivative **6z** had a similar KRI value of 1.23 ± 0.03 ($p < 0.005$) and an IC_{50} value of 108 ± 4 nM. On the other hand, the thiophene bioisostere of anthranilic acid **6aa** was also instructive to us, as it showed that not all 4-OH-biphenyl ligands possess a longer residence time for the HCA_2 receptor.

Chemistry

All solvents and reagents were purchased from commercial sources and were of analytical grade. Demineralized water is simply referred to as H_2O, because it was used in all cases, unless stated otherwise (i.e., brine). ^1H and ^{13}C NMR spectra were recorded on a Bruker AV 400 liquid spectrometer (^1H NMR, 400 MHz; ^{13}C NMR, 100 MHz) at ambient temperature. Chemical shifts are reported

in parts per million (ppm), are designated by δ, and are downfield to the internal standard tetramethylsilane (TMS). Coupling constants are reported in hertz and are designated as *J*. Analytical purity of the final compounds was determined by high-performance liquid chromatography (HPLC) with a Phenomenex Gemini 3 μm C18 110A column (50 × 4.6 mm, 3 μm), measuring UV absorbance at 254 nm. The sample preparation and HPLC method was as follows: 0.3–0.6 mg of compound was dissolved in 1 mL of a 1:1:1 mixture of $CH_3CN/H_2O/t$-BuOH and eluted from the column within 15 min at a flow rate of 1.3 mL/min. The elution method was set up as follows: 1–4 min isocratic system of H_2O/CH_3CN/1% TFA in H_2O, 80:10:10, from the 4th min, a gradient was applied from 80:10:10 to 0:90:10 within 9 min, followed by 1 min of equilibration at 0:90:10 and 1 min at 80:10:10. All compounds showed a single peak at the designated retention time and are at least 95% pure. Liquid chromatography–mass spectrometry (LC–MS) analyses were performed using Thermo Finnigan Surveyor–LCQ Advantage Max LC–MS system and a Gemini C18 Phenomenex column (50 × 4.6 mm, 3 μm). The elution method was set up as follows: 1–4 min isocratic system of H_2O/CH_3CN/1% TFA in H_2O, 80:10:10, from the 4th min, a gradient was applied from 80:10:10 to 0:90:10 within 9 min, followed by 1 min of equilibration at 0:90:10 and 1 min at 80:10:10. Thin-layer chromatography (TLC) was routinely consulted to monitor the progress of reactions, using aluminum-coated Merck silica gel F^{254} plates. Purification by column chromatography was achieved by use of Grace Davison Davisil silica column material (LC60A, 30–200 μm). Microwave reactions were carried out in a Biotage Emrys™ Optimizer using sealed tubes and at a set reaction temperature. The procedure for a series of similar compounds is given as a general procedure for all within that series, annotated by the numbers of the compounds.

Compounds **2a**[40], **2c**[41], **2e**[42], **2f**[43], **3a**[44], **3c**[32], **3e**[42], **3o**[45], **5a**[30], **5c**, **5e**, **5i**, **5j**, **5l**, **5o**, **5w**, **5n**, **5r**[37] are described in literature, but have been synthesized by another approach.

General procedure for the preparation of methyl 3-(4-(substitutedphenyl) phenyl) propionates (2a, c-f, i-l, o-p, w)[30]

Methyl 3-(4-bromophenyl)propanoate[31] **1** (1.0 equiv) and the appropriate commercially available (substituted-phenyl)boronic acid (1.5 equiv) were dissolved in a mixture of dioxane:EtOH (1:1) (concentration 1mL/mmol) and 1M aqueous $NaHCO_3$ (2.0 equiv). To the solution, $Pd(PPh_3)_4$ (2.5 mol%) was added and the mixture was heated in the microwave at 100 °C for 3 h, after which TLC showed full conversion. The reaction mixture was concentrated *in vacuo*, acidified to pH = 1 using 1 M HCl (aq), extracted with EtOAc, dried over $MgSO_4$ and concentrated under reduced pressure. Purification by column chromatography eluting with CH_2Cl_2:Pet ether (2:1) yielded the desired biphenyl esters as solids

Methyl 3-(4-(phenyl)phenyl]propanoate (2a)

Yield = 181 mg, 78%. ^{1}H NMR (400 MHz, $CDCl_3$): δ 7.57 (d, J = 7.6 Hz, 2H), 7.52 (d, J = 8.4 Hz, 2H), 7.42 (t, J = 8.0 Hz, 2H), 7.33 (t, J = 7.2 Hz, 1H), 7.27 (d, J = 8.4 Hz, 2H), 3.69 (s, 3H), 3.00 (t, J = 8.0 Hz, 2H), 2.67 (t, J = 7.6 Hz, 2H) ppm.

Methyl 3-(4-(4-methoxyphenyl)phenyl]propanoate (2c)

Yield = 212 mg, 76%. ^{1}H NMR (400 MHz, $CDCl_3$): δ 7.51-7.46 (m, 4H), 7.24 (d, J = 8.4 Hz, 2H), 6.97 (d, J = 8.8 Hz, 2H), 3.85 (s, 3H), 3.69 (s, 3H), 2.98 (t, J = 8.0 Hz, 2H), 2.67 (t, J = 8.0 Hz, 2H) ppm.

Methyl 3-(4-(4-chlorophenyl)phenyl)propanoate (2d)

Yield = 372 mg, 82%. ^{1}H NMR (400 MHz, $CDCl_3$): δ 7.51-7.47 (m, 4H), 7.40-7.37 (m, 2H), 7.28-7.25 (m, 2H), 3.68 (s, 3H), 2.99 (t, J = 7.6 Hz, 2H), 2.67 (t, J = 8.0 Hz, 2H) ppm.

Methyl 3-(4-(4-fluorophenyl)phenyl)propanoate (2e)

Yield = 337 mg, 77%. ^{1}H NMR (400 MHz, $CDCl_3$): δ 7.50-7.47 (m, 2H), 7.24 (d, J = 8.4 Hz, 2H), 7.25-7.21 (m, 2H), 7.10-7.05 (m, 2H), 3.65 (s, 3H), 2.97 (t, J = 7.6 Hz, 2H), 2.64 (t, J = 8.0 Hz, 2H) ppm.

Methyl 3-(4-(4-(trifluoromethyl)phenyl)phenyl)propanoate (2f)

Yield = 494 mg, 89%. ^{1}H NMR (400 MHz ,$CDCl_3$): δ 7.67 (t, J = 8.8 Hz, 4H), 7.53 (d, J = 8.0 Hz, 2H), 7.31 (d, J = 8.0 Hz, 2H), 3.69 (s, 3H), 3.01 (t, J = 7.6 Hz, 2H), 2.68 (t, J = 8.0 Hz, 2H) ppm.

Methyl 3-(4-(3-methylphenyl)phenyl)propanoate (2i)

Yield = 400 mg, 95%. ^{1}H NMR (400 MHz, $CDCl_3$): δ 7.47 (d, J = 8.0 Hz, 2H), 7.36-7.33 (m, 2H), 7.26 (t, J = 7.6 Hz, 1H), 7.21 (d, J = 8.0 Hz, 2H), 7.12-7.09 (m, 1H), 3.62 (s, 3H), 2.94 (t, J = 7.6 Hz, 2H), 2.61 (t, J = 8.0 Hz, 2H), 2.36 (s, 3H) ppm.

Methyl 3-(4-(3-methoxyphenyl)phenyl)propanoate (2j)

Yield = 557 mg, 71%. ^{1}H NMR (400MHz, $CDCl_3$): δ 7.51 (d, J = 8.4 Hz, 2H), 7.33 (t, J = 8.0 Hz, 1H), 7.26 (d, J = 8.0 Hz, 2H), 7.16 (d, J = 7.6 Hz, 1H), 7.10 (t, J = 2.0 Hz, 1H), 6.88 (dd, J = 8.0, 2.4 Hz, 1H), 3.85 (s, 3H), 3.68 (s, 3H), 2.99 (t, J = 8.0 Hz, 2H), 2.65 (t, J= 7.2 Hz, 2H) ppm.

Methyl 3-(4-(3-chlorophenyl)phenyl)propanoate (2k)

Yield = 393 mg, 69%. ^{1}H NMR (400 MHz, $CDCl_3$): δ 7.57-7.53 (m, 1H), 7.50-7.43 (m, 3H), 7.32 (t, J = 7.6 Hz, 1H), 7.30-7.23 (m, 3H), 3.68 (s, 3H), 3.00 (t, J = 8.0 Hz, 2H), 2.67 (t, J = 8.0, 2H) ppm.

Methyl 3-(4-(3-fluorophenyl)phenyl)propanoate) (2l)

Yield = 338 mg, 79%. ^{1}H NMR (400 MHz, $CDCl_3$): δ 7.47 (d, J = 8.4 Hz, 2H), 7.35-7.30 (m, 2H), 7.26-7.21 (m, 3H), 7.01-6.96 (m, 1H), 3.65 (s, 3H), 2.97 (t, J = 7.6 Hz, 2H), 2.64 (t, J = 8.0 Hz, 2H) ppm.

Methyl 3-(4-(2-chlorophenyl)phenyl)propanoate (2o)

Yield = 535 mg, 93%. ^{1}H NMR (400 MHz, $CDCl_3$): δ 7.46 (dd, J = 7.6, 1.2 Hz, 1H), 7.38 (d, J = 8.0 Hz, 2H), 7.34-7.30 (m, 2H), 7.29-7.24 (m, 3H), 3.70 (s, 3H), 3.01 (t, J = 8.0 Hz, 2H), 2.69 (t, J = 8.4 Hz, 2H) ppm.

Methyl 3-(4-(2-fluorophenyl)phenyl)propanoate (2p)

Yield = 386 mg, 91%. ^{1}H NMR (400 MHz, $CDCl_3$): δ 7.47 (dd, J= 8.0, 1.2 Hz, 2H), 7.40 (td, J = 7.8, 2.0 Hz, 1H), 7.30-7.25 (m, 3H), 7.19-7.10 (m, 2H), 3.67 (s, 3H), 2.99 (t, J = 8.0 Hz, 2H), 2.66 (t, J = 8.0 Hz, 2H) ppm.

Methyl 3-(4-(2-chloro-4-methoxyphenyl)phenyl)propanoate (2w)

Yield = 718 mg, 95%. ^{1}H NMR (400 MHz, $CDCl_3$): δ 7.35 (d, J = 8.0 Hz, 2H), 7.25-7.30 (m, 3H), 7.01 (d, J = 2.8 Hz, 1H), 6.86 (dd, J = 8.8, 2.8 Hz, 1H), 3.84 (s, 3H), 3.70 (s, 3H), 3.00 (t, J = 7.6 Hz, 2H), 2.69 (t, J = 8.0 Hz, 2H) ppm.

General procedure to obtain the phenyl propanoic acids (3a, c-f, i-l, o-p, w) by ester saponification

Ester **2a, c-f, i-l, o-p, w** (1.35 mmol, 1.0 eq.) was dissolved in dioxane (0.15mmol/mL) and a 5M aqueous NaOH (10.0 eq.) solution was added. After being stirred at room temperature for 3 h, the mixture was acidified, extracted with EtOAc, dried over $MgSO_4$ and concentrated *in vacuo* to obtain the carboxylic acids (**3a, c-f, i-l, o-p, w)** as solids.

3-(4-(Phenyl)phenyl)propanoic acid (3a)

Yield = 161 mg, 69%. ^{1}H NMR (400 MHz, $CDCl_3$): δ 7.57 (d, J = 8.0 Hz, 2H), 7.53 (d, J = 8.0 Hz, 2H), 7.43 (t, J = 7.6 Hz, 2H), 7.33 (t, J = 7.6 Hz, 1H), 7.29 (d, J = 8.0 Hz, 2H), 3.01 (t, J = 7.6 Hz, 2H), 2.63 (t, J = 7.6 Hz, 2H) ppm.

3-(4-(4-Methoxyphenyl)phenyl)propanoic acid (3c)

Yield = 172 mg, 86%. ^{1}H NMR (400 MHz, MeOD): δ 7.51 (d, J = 8.8 Hz, 2H), 7.47 (d, J = 8.0 Hz, 2H), 7.26 (d, J = 8.0 Hz, 2H), 6.97 (d, J = 8.4 Hz, 2H), 3.82 (s, 3H), 2.93 (t, J = 8.0 Hz, 2H), 2.62 (t, J = 7.6 Hz, 2H) ppm.

3-(4-(4-Chlorophenyl)phenyl)propanoic acid (3d)

Yield = 431 mg, quantitative. ^{1}H NMR (400 MHz, MeOD): δ 7.59-7.57 (m, 2H), 7.52 (d, J = 8.4 Hz, 2H), 7.43-7.40 (m, 2H), 7.31 (d, J = 8.0 Hz, 2H), 2.95 (t, J = 7.6 Hz, 2H), 2.63 (t, J = 8.0 Hz, 2H) ppm.

3-(4-(4-Fluorophenyl)phenyl)propanoic acid (3e)

Yield = 366 mg, quantitative. ^{1}H NMR (400 MHz, MeOD): δ 7.61-7.57 (m, 2H), 7.50 (d, J = 8.4 Hz, 2H), 7.29 (d, J = 8.0 Hz, 2H), 7.14 (t, J = 8.8 Hz, 2H), 2.95 (t, J = 7.6 Hz, 2H), 2.63 (t, J = 7.6 Hz, 2H) ppm.

3-[4-(4-(Trifluoromethyl)phenyl)phenyl]propanoic acid (3f)

Yield = 437 mg, 93%. ^{1}H NMR (400 MHz, MeOD): δ 7.79 (d, J = 8.0 Hz, 2H), 7.71 (d, J = 8.4 Hz, 2H), 7.60 (d, J = 8.0 Hz, 2H), 7.36 (d, J = 8.0 Hz, 2H), 2.97 (t, J = 7.6 Hz, 2H), 2.65 (t, J = 7.6 Hz, 2H) ppm.

3-(4-(3-Methylphenyl)phenyl)propanoic acid (3i)

Yield = 471 mg, quantitative. ^{1}H NMR (400 MHz, MeOD): δ 7.17 (d, J = 8.0 Hz, 2H), 7.07-7.03 (m, 2H), 6.97-6.92 (m, 3H), 6.79 (d, J = 7.2 Hz, 1H), 2.63 (t, J = 7.6 Hz, 2H), 2.32 (t, J = 8.0 Hz, 2H), 2.04 (s, 3H) ppm.

3-(4-(3-Methoxyphenyl)phenyl)propanoic acid (3j)

Yield = 473 mg, 90%. ^{1}H NMR (MeOD, 400 MHz): δ 7.52 (d, J = 8.0 Hz, 2H), 7.32-7.28 (m, 3H), 7.16 (dd, J = 7.6, 0.8 Hz, 1H), 7.11 (t, J = 2.4 Hz, 1H), 6.89-6.87 (m, 1H), 3.83 (s, 3H), 2.95 (t, J = 7.6 Hz, 2H), 2.63 (t, J = 7.6 Hz, 2H) ppm.

3-(4-(3-Chlorophenyl)phenyl)propanoic acid (3k)

Yield = 357 mg, 86%. ^{1}H NMR (400 MHz, MeOD): δ 7.59 (t, J = 2.0 Hz, 1H), 7.54-7.51 (m, 3H), 7.40 (t, J = 7.6 Hz, 1H), 7.34-7.31 (m, 5H), 2.96 (t, J = 7.6 Hz, 2H), 2.64 (t, J = 8.0 Hz, 2H) ppm.

3-(4-(3-Fluorophenyl)phenyl)propanoic acid (3l)

Yield = 319 mg, 99%. ^{1}H NMR (400 MHz, MeOD): δ 7.53 (d, J = 8.0 Hz, 2H), 7.45-7.38 (m, 2H), 7.31 (d, J = 8.4 Hz, 3H), 7.06-7.00 (m, 1H), 2.95 (t, J = 7.6 Hz, 2H), 2.63 (t, J = 7.6 Hz, 2H) ppm.

3-(4-(2-Chlorophenyl)phenyl)propanoic acid (3o)

Yield = 496 mg, quantitative. ^{1}H NMR (400 MHz, $CDCl_3$): δ 7.45 (d, J = 7.2 Hz, 1H), 7.37 (d, J =

8.0 Hz, 2H), 7.33-7.23 (m, 5H), 3.02 (t, J = 7.6 Hz, 2H), 2.74 (t, J = 8.0 Hz, 2H) ppm.

3-(4-(2-Fluorophenyl)phenyl)propanoic acid (3p)

Yield = 349 mg, 95%. ^{1}H NMR (400 MHz, MeOD): δ 7.47-7.42 (m, 3H), 7.36-7.30 (m, 3H), 7.22 (td, J = 7.6, 1.2 Hz, 1H), 7.18-7.13 (m, 1H), 2.96 (t, J = 7.6 Hz, 2H), 2.65 (t, J = 7.6 Hz, 2H) ppm.

3-(4-(2-Chloro-4-methoxyphenyl)phenyl)propanoic acid (3w)

Yield = 653 mg, 95%. 1H NMR (400 MHz, MeOD): δ 7.30-7.23 (m, 5H), 7.04 (d, J = 2.8 Hz, 1H), 6.92 (dd, J = 8.4, 2.4 Hz, 1H), 3.82 (s, 3H), 2.95 (t, J = 7.6 Hz, 2H), 2.64 (t, J = 8.0 Hz, 2H) ppm.

General procedure of the preparation of amides (4a, c-f, i-l, o-p, w) by the use EDCI*HCl

The respective biphenyl propionic acid (**3a, c-f, i-l, o-p, w**) (1.4 eq.), methyl-2-amino-benzoate (1.0 eq.), EDCI*HCl (2.0 eq.) and DMAP (0.1 eq.) were dissolved in dry CH_2Cl_2 and this solution was stirred at room temperature for 72 h under nitrogen. The reaction mixture was adsorbed on silica and purification by column chromatography (Pet. ether/EtOAc (9:1) or CH_2Cl_2/Pet. ether (1:1) to 100% CH_2Cl_2) was performed, which was followed by recrystallization from EtOAc.

Methyl 2-(3-(4-phenylphenyl)propanamido)benzoate (4a)

Pet. ether/EtOAc (9:1). Yield = 149 mg, 70%). 1H NMR (400 MHz, $CDCl_3$): δ 11.10 (s, 1H), 7.58-7.51 (m, 5H), 7.44-7.41 (m, 2H), 7.34-7.32 (m, 3H), 7.08 (t, J = 8.0 Hz, 1H), 3.89 (s, 3H), 3.13 (t, J = 7.6 Hz, 2H), 2.80 (t, J = 8.0 Hz, 2H) ppm.

Methyl 2-(3-(4-(4-methoxyphenyl)phenyl)propanamido)benzoate (4c)

Pet. ether/EtOAc (9:1). Yield = 72 mg, 27%. ^{1}H NMR (400 MHz, $CDCl_3$): δ 11.09 (s, 1H), 8.73 (d, J = 8.0 Hz, 1H), 8.03 (d, J = 1.6 Hz, 1H), 7.55-7.47 (m, 5H), 7.31 (d, J = 8.0 Hz, 2H), 7.08 (t, J = 7.2 Hz, 1H), 3.89 (s, 3H), 3.85 (s, 3H), 3.11 (t, J = 7.6 Hz, 2H), 2.79 (t, J = 8.0 Hz, 2H) ppm.

Methyl 2-(3-(4-(4-chlorophenyl)phenyl)propanamido)benzoate (4d)

Pet. ether/EtOAc (9:1). Yield = 98 mg, 15%). ^{1}H NMR (400 MHz, $CDCl_3$): δ 11.10 (s, 1H), 8.73 (d, J = 8.4 Hz, 1H), 8.00 (d, J = 8.0 Hz, 1H), 7.54 (t, J = 7.6 Hz, 1H), 7.49-7.58 (m, 4H), 7.37 (d, J = 8.4 Hz, 2H), 7.32 (d, J = 8.0 Hz, 2H), 7.07 (t, J = 7.6 Hz, 1H), 3.88 (s, 3H), 3.12 (t, J = 7.6 Hz, 2H), 2.79 (t, J = 8.0 Hz, 2H) ppm.

Methyl 2-(3-(4-(4-fluorophenyl)phenyl)propanamido)benzoate (4e)

Pet. ether/EtOAc (9:1). Yield = 95 mg, 19%. ^{1}H NMR (400 MHz, $CDCl_3$): δ 11.09 (s, 1H), 8.74 (dd, J = 8.4, 0.8 Hz, 1H), 8.00 (dd, J = 8.0, 1.6 Hz, 1H), 7.56-7.48 (m, 3H), 7.46 (d, J = 8.0 Hz, 2H), 7.12-7.05 (m, 3H), 3.88 (s, 3H), 3.12 (t, J = 7.6 Hz, 2H), 2.79 (t, J = 8.0 Hz, 2H) ppm.

Methyl 2-(3-(4-(4-trifluoromethylphenyl)phenyl)propanamido)benzoate (4f)

CH_2Cl_2/Pet. ether (1:1). Yield = 170 mg, 27%. ^{1}H NMR (400 MHz, $CDCl_3$): δ 11.11 (s, 1H), 8.74 (d, J = 8.4 Hz, 1H), 8.02 (d, J = 8.0 Hz, 1H), 7.69-7.65 (m, 4H), 7.57-7.52 (m, 3H), 7.37 (d, J = 8.0 Hz, 2H), 7.08 (t, J = 7.6 Hz, 1H), 3.90 (s, 3H), 3.14 (t, J = 7.2 Hz, 2H), 2.81 (t, J = 8.0 Hz, 2H) ppm.

Methyl 2-(3-(4-(3-methylphenyl)phenyl)propanamido)benzoate (4i)

Pet. ether/EtOAc (9:1). Yield = 127 mg, 22%. ^{1}H NMR (400 MHz, $CDCl_3$): δ 11.09 (s, 1H), 8.74 (d, J = 8.0 Hz, 1H), 7.99 (dd, J = 8.0, 1.6 Hz, 1H), 7.55-7.49 (m, 3H), 7.36 (d, J = 8.4 Hz, 2H), 7.12-7.28 (m, 3H), 7.13 (d, J = 7.2 Hz, 1H), 7.05 (t, J = 7.2 Hz, 1H), 3.87 (s, 3H), 3.11 (t, J = 7.6 Hz, 2H), 2.78 (t, J = 8.0 Hz, 2H), 2.40 (s, 3H) ppm.

Methyl 2-(3-(4-(3-methoxyphenyl)phenyl)propanamido)benzoate (4j)

CH_2Cl_2/Pet.ether (1:1). Yield = 249 mg, 35%. ^{1}H NMR (400 MHz, $CDCl_3$): δ 11.09 (s, 1H), 8.74 (d, J = 8.4 Hz, 1H), 8.01 (dd, J = 8.0, 1.6 Hz, 1H), 7.56-7.50 (m, 3H), 7.35-7.31 (m, 3H), 7.15 (d, J = 7.6 Hz, 1H), 7.10-7.05 (m, 2H), 6.87 (dd, J= 8.4, 2.4 Hz, 1H), 3.88 (s, 3H), 3.85 (s, 3H), 3.12 (t, J= 7.6 Hz, 2H), 2.79 (t, J= 8.0 Hz, 2H) ppm.

Methyl 2-(3-(4-(3-chlorophenyl)phenyl)propanamido)benzoate (4k)

Pet. ether/EtOAc (9:1) and a second column was performed with CH_2Cl_2/Pet.ether (2:1). Yield = 83 mg, 15%. ^{1}H NMR (400 MHz, $CDCl_3$): δ 11.10 (s, 1H), 8.73 (d, J = 8.4 Hz, 1H), 8.02 (d, J = 8.0 Hz, 1H), 7.57-7.43 (m, 5H), 7.35-7.26 (m, 4H), 7.08 (t, J = 7.6 Hz, 1H), 3.90 (s, 3H), 3.13 (t, J = 7.6 Hz, 2H), 2.80 (t, J = 8.0 Hz, 2H) ppm.

Methyl 2-(3-(4-(3-fluorophenyl)phenyl)propanamido)benzoate (4l)

CH_2Cl_2/Pet. ether (1:1) to 100% CH_2Cl_2. Yield = 15 mg, 6%. ^{1}H NMR (400 MHz, $CDCl_3$): δ 11.10 (s, 1H), 8.73 (d, J = 8.4 Hz, 1H), 8.01 (dd, J = 8.0, 1.6 Hz, 1H), 7.57-7.49 (m, 3H), 7.40-7.33 (m, 5H), 7.27-7.25 (m, 1H), 7.10-6.99 (m, 2H), 3.89 (s, 3H), 3.13 (t, J = 7.6 Hz, 2H), 2.80 (t, J = 8.0 Hz, 2H) ppm.

Methyl 2-(3-(4-(2-chlorophenyl)phenyl)propanamido)benzoate (4o)

DCM/Pet. ether (1:1) to 100% CH_2Cl_2. Yield = 245 mg, 33%. ^{1}H NMR (400 MHz, $CDCl_3$): δ 11.23 (s, 1H), 8.75 (d, J = 8.4, 1H), 7.98 (dd, J = 8.0, 1.2 Hz, 1H), 7.51 (t, J = 7.6 Hz, 1H), 7.42 (d, J = 8.4 Hz, 1H), 3.36 (d, J = 8.0 Hz, 2H), 7.32-7.19 (m, 5H), 7.03 (t, J = 8.0 Hz, 1H), 3.85 (s, 3H), 3.13 (t, J = 7.6 Hz, 2H), 2.80 (t, J = 8.4 Hz, 2H) ppm.

Methyl 2-(3-(4-(2-fluorophenyl)phenyl)propanamido)benzoate (4p)

CH_2Cl_2/Pet. ether (1:1) to 100% CH_2Cl_2. Yield = 176 mg, 33%. ^{1}H NMR (400 MHz, $CDCl_3$): δ 11.11 (s, 1H), 8.74 (d, J = 8.4 Hz, 1H), 7.98 (dd, J = 6.8, 1.6 Hz, 1H), 7.54-7.46 (m, 3H), 7.39 (td, J = 7.6, 1.6 Hz, 1H), 7.32 (d, J = 8.4 Hz, 2H), 7.29-7.22 (m, 1H), 7.18-7.02 (m, 3H), 3.86 (s, 3H), 3.12 (t, J = 7.6 Hz, 2H), 2.79 (t, J = 8.4 Hz, 2H) ppm.

Methyl 2-(3-(4-(2-chloro-4-methoxyphenyl)phenyl)propanamido)benzoate (4w)

CH_2Cl_2/Pet. ether (1:1) to 100% CH_2Cl_2. Yield = 298 mg, 31%. ^{1}H NMR (400 MHz, $CDCl_3$): δ 11.12 (s, 1H), 8.74 (dd, J =8.4, 0.8 Hz, 1H), 8.02 (dd, J =8.0, 1.6 Hz, 1H), 7.55 (td, J = 8.0, 0.8 Hz, 1H), 7.36-7.30 (m, 4H), 7.23 (d, J = 8.4 Hz, 1H), 7.08 (td, J = 6.8, 1.2 Hz, 1H), 7.01 (d, J = 2.8 Hz, 1H), 6.85 (dd, J = 8.8, 2.8 Hz, 1H), 3.91 (s, 3H), 3.83 (s, 3H), 3.13 (t, J = 7.2 Hz, 2H), 2.81 (t, J = 8.4 Hz, 2H) ppm.

Methyl 2-(3-(4-(4-methoxyphenyl)phenyl)propanamido)cyclohex-1-ene-1-carboxylate (4z)

Acid 3c (75 mg, 0.30 mmol, 1.0 eq.) was refluxed in $SOCl_2$ (10 mL) for 1.5 h under a N_2 atmosphere. The excess of $SOCl_2$ was evaporated (and co-evaporated with toluene twice) and the crude mixture was dissolved in toluene[30]. Methyl 2-amino-1-cyclohexene-1-carboxylate[20] (68 mg, 0.44 mmol, 1.5 eq.) was added and the mixture and was stirred overnight at 70 °C under a N_2 atmosphere. Upon completion of the reaction, the reaction mixture was filtered and the filtrate was concentrated. The filtrate was purified by column chromatography (Pet. ether/EtOAc 2:1) to yield 20 mg, 17% of the target compound 4z as a solid. ^{1}H NMR (400 MHz, $CDCl_3$): δ 11.60 (s, 1H), 7.59-7.44 (m, 5H), 7.28 (t, J = 7.6 Hz, 1H), 6.99-6.95 (m, 2H), 3.84 (s, 3H), 3.71 (s, 3H), 3.04-2.97 (m, 4H), 2.67 (t, J = 8.0 Hz, 2H), 2.29 (t, J = 8.0 Hz, 2H), 1.66-1.55 (m, 4H) ppm.

General procedure to yield the substituted anthranilic acids (5a, c-f, i-l, o-p, w, z, aa) by saponification

Anthranilic ester **4a, c-f, i-l, o-p, w, z, aa** (98 mg, 0.25 mmol) was dissolved in dioxane (0.1 mmol/mL) and NaOH (5M aq.) (10 eq.) was added. After being stirred at RT for 24 h, the reaction mixture was acidified to pH = 1 (1M HCl (aq.)), extracted with EtOAc, dried over $MgSO_4$ and the volatiles were evaporated in vacuo to yield the final anthranilic acids **5a, c-f, i-l ,o-p, w** and both the cyclohexene **5z** and thiophene analogues **5aa** as the pure solids.

2-(3-(4-Phenylphenyl)propanamido)benzoic acid (5a)

Yield = 16 mg, 67%. ^{1}H NMR (400 MHz, $CDCl_3$): δ 10.86 (s, 1H), 8.76 (d, J = 8.8 Hz, 1H), 8.09 (d, J = 8.0 Hz, 1H), 7.61 (t, J = 7.2 Hz, 1H), 7.56-7.51 (m, 4H), 7.40 (t, J = 7.6 Hz, 2H), 7.34-7.29 (m, 3H), 7.12 (t, J = 7.6 Hz, 1H), 3.13 (t, J = 7.6 Hz, 2H), 2.80 (t, J = 8.0 Hz, 2H) ppm. HPLC Rt = 10.16 min. purity 95%. ESI-MS: 345.93 $[M+H]^+$.

2-(3-(4-(4-Methoxyphenyl)phenyl)propanamido)benzoic acid (5c)

Yield = 52 mg, 75%. ^{1}H NMR (400 MHz, $CDCl_3$ + MeOD): **δ** 8.62 (d, J = 8.4 Hz, 1H), 8.09 (d, J = 7.6 Hz, 1H), 7.58-7.48 (m, 5H), 7.31 (d, J = 8.0 Hz, 2H), 7.12 (t, J = 7.6 Hz, 1H), 6.97 (d, J = 8.8 Hz, 2H), 3.85 (s, 3H), 3.10 (t, J = 7.6 Hz, 2H), 2.80 (t, J = 8.0 Hz, 2H) ppm. HPLC Rt = 10.09 min. purity 99%. ESI-MS: 376.00 $[M+H]^+$.

2-(3-(4-(4-Chlorophenyl)phenyl)propanamido)benzoic acid (5d)

Yield = 102 mg, 100%. Mp 196 °C. ^{1}H NMR (400 MHz, $CDCl_3$): δ 10.86 (s, 1H), 8.75 (d, J = 8.4 Hz, 1H), 8.09 (dd, J = 8.0, 1.2 Hz, 1H), 7.60 (t, J = 8.4 Hz, 1H), 7.49-7.47 (m, 4H), 7.38 (d, J = 8.4 Hz, 2H), 7.32 (d, J = 8.4 Hz, 2H), 7.11 (t, J = 7.2 Hz, 1H), 3.12 (t, J = 7.6 Hz, 2H), 2.78 (t, J = 8.0 Hz, 2H) ppm. HPLC Rt = 10.72 min. purity 98%. ESI-MS: 379.93 $[M+H]^+$.

2-(3-(4-(4-Fluorophenyl)phenyl)propanamido)benzoic acid (5e)

Yield = 88 mg, 97%. ^{1}H NMR (400 MHz, MeOD): δ 8.55 (d, J = 8.4 Hz, 1H), 8.06 (dd, J = 8.0, 1.6 Hz, 1H), 7.58-7.52 (m, 3H), 7.49 (d, J = 8.0 Hz, 2H), 7.32 (d, J = 8.0 Hz, 2H), 7.15-7.10 (m, 3H), 3.08 (t, J = 7.6 Hz, 2H), 2.77 (t, J = 7.6 Hz, 2H) ppm. HPLC Rt = 10.24 min. purity 100%. ESI-MS: 363.93 $[M+H]^+$.

2-(3-(4-(4-Trifluoromethylphenyl)phenyl)propanamido)benzoic acid (5f)

Yield = 150 mg, 91%. Mp 209 °C. ^{1}H NMR (400 MHz, MeOD): **δ** 8.56 (d, J = 8.4 Hz, 1H), 8.06 (d, J = 8.0 Hz, 1H), 7.77 (d, J = 8.0 Hz, 2H), 7.70 (d, J = 8.4 Hz, 2H), 7.59 (d, J = 8.0 Hz, 2H), 7.55 (t, J = 7.2 Hz, 1H), 7.38 (d, J = 8.4 Hz, 2H), 7.13 (t, J = 7.2 Hz, 1H), 3.10 (t, J = 7.6 Hz, 2H), 2.79 (t, J = 7.6 Hz, 2H) ppm. HPLC Rt = 10.85 min. purity 99%. ESI-MS: 413.93 $[M+H]^+$.

2-(3-(4-(3-Methylphenyl)phenyl)propanamido)benzoic acid (5i)

Yield = 122 mg, 100%. ^{1}H NMR (400 MHz, $CDCl_3$): **δ** 10.88 (s, 1H), 8.75 (d, J = 8.4 Hz, 1H), 8.09 (d, J = 8.0 Hz, 1H), 7.60 (t, J = 7.2 Hz, 1H), 7.50 (d, J = 8.0 Hz, 2H), 7.35 (d, J = 7.6 Hz, 2H), 7.30 (d, J = 8.4 Hz, 3H), 7.11 (t, J = 8.4 Hz, 2H), 3.12 (t, J = 7.2 Hz, 2H), 2.79 (t, J = 8.0, 2H), 2.39 (s, 3H) ppm. ^{13}C NMR (400 MHz, $CDCl_3$): **δ** 172.5, 171.7, 142.0, 140.9, 139.5, 138.4, 135.8, 131.9, 128.9, 128.7, 128.0, 127.9, 127.4, 124.2, 123.0, 120.8, 114.1, 40.5, 31.3, 21.6 ppm. HPLC Rt = 10.53 min. purity 100%. ESI-MS: 359.93 $[M+H]^+$.

2-(3-(4-(3-Methoxyphenyl)phenyl)propanamido)benzoic acid (5j)

After 3 days no conversion was shown by TLC. Added 10 eq. of LiOH (aq.) and refluxed for two hours, after which completion of the reaction was confirmed by TLC. Yield = 221 mg, 95%. ^{1}H NMR (400 MHz, MeOD): **δ** 8.55 (d, J = 8.4 Hz, 1H), 8.06 (d, J = 7.2 Hz, 1H), 7.54-7.50 (m, 3H), 7.33-7.28 (m, 3H), 7.14-7.09 (m, 3H), 6.86 (dd, J = 8.4, 2.0 Hz, 1H), 3.83 (s, 3H), 3.07 (t, J = 7.6 Hz, 2H), 2.76 (t, J = 7.6 Hz, 2H) ppm. HPLC Rt = 10.12 min. purity 98%. ESI-MS: 375.87 $[M+H]^+$.

2-(3-(4-(3-Chlorophenyl)phenyl)propanamido)benzoic acid (5k)

Yield = 55 mg, 69%. Mp 157 °C. ^{1}H NMR (400 MHz, MeOD): **δ** 8.55 (d, J = 8.4 Hz, 1H), 8.06 (d, J = 7.6 Hz, 1H), 7.58-7.50 (m, 5H), 7.41-7.30 (m, 4H), 7.13 (t, J = 7.6 Hz, 1H), 3.09 (t, J = 7.6 Hz, 2H), 2.78 (t, J = 7.6 Hz, 2H) ppm. HPLC Rt = 10.71 min. purity 97%. ESI-MS: 379.93 $[M+H]^+$.

2-(3-(4-(3-Fluorophenyl)phenyl)propanamido)benzoic acid (5l)

Yield = 7 mg, 48%. ^{1}H NMR (400 MHz, $CDCl_3$): **δ** 10.86 (s, 1H), 8.75 (d, J = 8.8 Hz, 1H), 8.10 (d,

J = 8.0 Hz, 1H), 7.61 (t, J = 8.0 Hz, 1H), 7.50 (d, J = 8.0 Hz, 2H), 7.37-7.31 (m, 4H), 7.26-7.23 (m, 1H), 7.13 (t, J = 8.0 Hz, 1H), 7.01-6.97 (m, 1H), 3.13 (t, J = 7.6 Hz, 2H), 2.80 (t, J = 7.6 Hz, 2H) ppm. HPLC Rt = 10.27 min. purity 100%. ESI-MS: 363.93 $[M+H]^+$.

2-(3-(4-(2-Chlorophenyl)phenyl)propanamido)benzoic acid (5o)

Yield = 217 mg, 92%. ^{1}H NMR (400 MHz, $CDCl_3$): δ 11.07 (s, 1H), 8.76 (d, J = 8.4 Hz, 1H), 8.11 (dd, J = 8.0, 1.2, 1H), 7.59 (td, J = 8.0, 1.6 Hz, 1H), 7.43 (dd, J = 7.2, 1.2 Hz, 1H), 7.36 (d, J = 8.0 Hz, 2H), 7.31 (d, J = 8.4 Hz, 2H), 7.30-7.20 (m, 3H), 7.11 (td, J = 8.0, 0.8 Hz, 1H), 3.15 (t, J = 7.2 Hz, 2H), 2.84 (t, J = 8.4 Hz, 2H) ppm. HPLC Rt = 10.42 min. purity 97%. ESI-MS: 379.93 $[M+H]^+$.

2-(3-(4-(2-Fluorophenyl)phenyl)propanamido)benzoic acid (5p)

Yield = 172 mg, 99%. Mp 162 °C. ^{1}H NMR (400 MHz, $CDCl_3$): **δ** 10.87 (s, 1H), 8.76 (d, J = 8.4 Hz, 1H), 8.11 (d, J = 8.0 Hz, 1H), 7.61 (t, J = 7.6 Hz, 1H), 7.48 (d, J = 8.0 Hz, 2H), 7.39 (t, J = 7.6 Hz, 1H), 7.34 (d, J = 8.0 Hz, 2H), 7.29-7.24 (m, 1H), 7.18-7.08 (m, 3H), 3.14 (t, J = 7.6 Hz, 2H), 2.82 (t, J = 8.0 Hz, 2H) ppm. HPLC Rt = 10.17 min. purity 98%. ESI-MS: 363.93 $[M+H]^+$.

2-(3-(4-(2-Chloro-4-methoxyphenyl)phenyl)propanamido)benzoic acid (5w)

Yield = 276 mg, 96%. ^{1}H NMR (400 MHz, DMSO): δ 13.58 (s, 1H), 11.16 (s, 1H), 8.49 (d, J = 8.4 Hz, 1H), 7.97 (d, J = 8.0 Hz, 1H), 7.60-7.56 (m, 5H), 7.16-7.12 (m, 2H), 6.99 (d, J = 8.4 Hz, 1H), 3.81 (s, 3H), 2.99 (t, J = 7.2 Hz, 2H), 2.77 (t, J = 7.6 Hz, 2H) ppm. HPLC Rt = 10.42 min. purity 97%

2-(3-(4-(4-Methoxyphenyl)phenyl)propanamido)cyclohex-1-ene-1-carboxylic acid (5z)

The product was crystallized from MeOH. Yield = 8 mg, 16%. ^{1}H NMR (400 MHz, MeOD): **δ** 7.58-7.46 (m, 4H), 7.28-7.25 (m, 2H), 6.97 (d, J = 8.8, 1.2 Hz, 2H), 3.84 (s, 3H), 3.03-2.99 (m, 4H), 2.66 (t, J = 8.0 Hz, 2H), 2.35 (t, J = 8.0 Hz, 2H), 1.65-1.59 (m, 4H) ppm. HPLC Rt = 10.09 min. purity 99%

2-(3-(4′-Methoxy-[1,1′-biphenyl]-4-yl)propanamido)thiophene-3-carboxylic acid (5aa)

Yield = 19 mg, 100%. ^{1}H NMR (400 MHz, $CDCl_3$) **δ** 10.67 (s, 1H), 7.49-7.45 (m, 4H), 7.29 (d, J = 8.0 Hz, 2H), 7.23 (d, J = 5.6 Hz, 1H), 6.98-6.91 (m, 2H), 6.76 (d, J = 6.0 Hz, 1H), 3.82 (s, 3H), 3.12 (t, J = 7.6 Hz, 2H), 2.86 (t, J = 8.0 Hz, 2H) ppm.

General Suzuki coupling procedure to yield products (5b, h, n, q-v, x, y and 4aa)

Slightly modified experimental procedure of general procedure **2a-f ,i, l, o-p, w**. Instead of $Pd(PPh_3)_4$ (2.5 mol%) as the catalyst $Pd(OAc)_2$ (0.1 eq.) and PPh_3 (0.3 eq.) were used. Next to this more $NaHCO_3$ (6 eq. 1M solution) was used. This gave better yields compared to the commercial available $Pd(PPh_3)_4$ and immediately the carboxylic acid instead of the ester was

obtained. Started from iodide **8a** or **8b** (1.0 eq.) and the respective commercially available phenyl boronic acids. Purified by column chromatography using Pet. ether: EtOAc (9:1) to EtOAc.

2-(3-(4-(4-Methylphenyl)phenyl)propanamido)benzoic acid (5b)

Yield = 73 mg, 70%. Mp 187 °C. ^{1}H NMR (400 MHz, MeOD): **δ** 10.85 (s, 1H), 8.76 (d, J = 8.4 Hz, 1H), 8.09 (d, J = 8.0, 1H), 7.61 (t, J = 8.4 Hz, 1H), 7.50 (d, J = 8.4 Hz, 2H), 7.45 (d, J = 8.0 Hz, 2H), 7.31 (d, J = 8.0 Hz, 2H), 7.20 (d, J = 7.6 Hz, 2H), 7.12 (t, J = 8.0 Hz, 1H), 3.12 (t, J = 7.2 Hz, 2H), 2.80 (t, J = 8.0, 2H), 2.37 (s, 3H) ppm. HPLC Rt = 10.00 min. purity 98%. ESI-MS: 360.00 $[M+H]^+$.

2-(3-(4-(4-Hydroxymethylphenyl)phenyl)propanamido)benzoic acid (5h)

Yield = 10 mg, 9%. Mp 182 °C. ^{1}H NMR (400 MHz, MeOD): **δ** 8.56 (d, J = 8.4 Hz, 1H), 8.06 (dd, J = 8.0, 1.2 Hz, 1H), 7.57-7.52 (m, 5H), 7.40 (d, J = 8.4 Hz, 2H), 7.33 (d, J = 8.4 Hz, 2H), 7.13 (td, J = 7.8, 1.2 Hz, 1H), 4.63 (s, 2H), 3.08 (t, J = 8.0 Hz, 2H), 2.77 (t, J = 7.6 Hz, 2H) ppm. HPLC Rt = 8.74 min. purity 99%. ESI-MS: 376.00 $[M+H]^+$.

2-(3-(4-(2-Methylphenyl)phenyl)propanamido)benzoic acid (5n)

Yield = 58 mg, 32%. ^{1}H NMR (400 MHz, MeOD): **δ** 8.49 (d, J = 8.4 Hz, 1H), 8.04 (dd, J = 8.0, 1.6 Hz, 1H), 7.38-7.32 (m, 3H), 7.21-7.12 (m, 6H), 7.04 (td, J = 8.0, 1.2 Hz, 1H), 3.10 (t, J = 7.8 Hz, 2H), 2.77 (t, J = 7.8, 2H), 2.19 (s, 3H) ppm. HPLC Rt = 5.73 min. purity 95%. ESI-MS: 359.93 $[M+H]^+$.

2-(3-(4-(2-Trifluoromethylphenyl)phenyl)propanamido)benzoic acid (5q)

Yield = 14 mg, 7%. Mp 168 °C. ^{1}H NMR (400 MHz, MeOD): **δ** 8.56 (d, J = 8.0 Hz, 1H), 8.07 (dd, J = 8.0, 1.2 Hz, 1H), 7.74 (d, J = 7.6 Hz, 1H), 7.60-7.51 (m, 3H), 7.33-7.29 (m, 3H), 7.21 (d, J = 8.0 Hz, 2H), 7.14 (t, J = 7.6 Hz, 1H), 3.10 (t, J = 8.0 Hz, 2H), 2.79 (t, J = 8.0 Hz, 2H) ppm. HPLC Rt = 5.58 min. purity 100%. ESI-MS: 413.93 $[M+H]^+$.

2-(3-(4-(2-Methoxyphenyl)phenyl)propanamido)benzoic acid (5r)

Yield = 40 mg, 21%. 1H NMR (400 MHz, $CDCl_3$): δ 10.80 (s, 1H), 8.74 (d, J = 8.4 Hz, 1H), 8.09 (dd, J = 8.0, 1.2 Hz, 1H), 7.60 (dt, J = 7.8, 1.2 Hz, 1H), 7.46 (d, J = 8.0 Hz, 2H), 7.30-7.27 (m, 4H), 7.11 (t, J = 8.0 Hz, 1H), 7.02-6.95 (m, 2H), 3.80 (s, 3H), 3.12 (t, J = 8.0 Hz, 2H), 2.81 (t, J = 8.0 Hz, 2H) ppm.

2-(3-(4-(4-Methoxy-3-methylphenyl)phenyl)propanamido)benzoic acid (5s)

Yield = 11 mg, 10%. ^{1}H NMR (400 MHz, MeOD): **δ** 8.56 (d, J = 8.0 Hz, 1H), 8.07 (dd, J = 8.0, 1.6 Hz, 1H), 7.54 (td, J = 7.2, 1.6 Hz, 1H), 7.46 (d, J = 8.0 Hz, 2H), 7.37 (dd, J = 10.8, 2.4 Hz, 2H), 7.29 (d, J = 8.4 Hz, 2H), 7.13 (td, J = 7.6, 1.2 Hz, 1H), 6.93 (d, J = 8.4 Hz, 1H), 3.85 (s, 3H), 3.06 (t, J = 8.0 Hz, 2H), 2.76 (t, J = 8.0 Hz, 2H), 2.23 (s, 3H) ppm.

2-(3-(4-(3-Chloro-4-methoxyphenyl)phenyl)propanamido)benzoic acid (5t)

Yield = 18 mg, yield 36%. ^{1}H NMR (400 MHz, $CDCl_3$): **δ** 11.25 (s, 1H), 8.73 (d, J = 8.4 Hz, 1H),

8.08 (dd, J = 8.0, 1.6 Hz, 1H), 7.50-7.40 (m, 5H), 7.30 (d, J = 8.4 Hz, 2H), 7.08 (t, J = 7.2, 1H), 6.96 (d, J = 8.4 Hz, 1H), 3.93 (s, 3H), 3.10 (t, J = 8.0 Hz, 2H), 2.77 (t, J = 8.4 Hz, 2H) ppm.

2-(3-(4-(3-Fluoro-4-methoxyphenyl)phenyl)propanamido)benzoic acid (5u)

Yield = 36 mg, 30%. ^{1}H NMR (400 MHz, $CDCl_3$ + MeOD): **δ** 8.68 (d, J = 8.0 Hz, 1H), 8.08 (dd, J = 8.0, 1.6 Hz, 1H), 7.55 (td, J = 8.6, 1.6 Hz, 1H), 7.46 (d, J = 8.0 Hz, 2H), 7.33-7.27 (m, 5H), 7.10 (td, J = 7.8, 1.2 Hz, 1H), 3.93 (s, 3H), 3.10 (t, J = 8.0 Hz, 2H), 2.78 (t, J = 8.0 Hz, 2H) ppm.

2-(3-(4-(4-Methoxy-2-methylphenyl)phenyl)propanamido)benzoic acid (5v)

Yield = 15 mg, 13%. ^{1}H NMR (400 MHz, MeOD): **δ** 8.56 (d, J = 8.4 Hz, 1H), 8.07 (d, J = 8.0 Hz, 1H), 7.67 (d, J = 7.6 Hz, 1H), 7.28 (d, J = 8.0 Hz, 2H), 7.19-7.10 (m, 3H), 7.05 (d, J = 8.4 Hz, 1H), 6.79-6.75 (m, 2H), 3.79 (s, 3H), 3.07 (t, J = 8.0 Hz, 2H), 2.77 (t, J = 8.0 Hz, 2H), 2.16 (s, 3H) ppm.

2-(3-(4-(2-Fluoro-4-methoxyphenyl)phenyl)propanamido)benzoic acid (5x)

Yield = 19 mg, 10%. ^{1}H NMR (400 MHz, $CDCl_3$): **δ** 10.99 (s, 1H), 8.75 (d, J = 8.4 Hz, 1H), 8.08 (d, J = 8.0, 1.2 Hz, 1H), 7.57-7.54 (m, 1H), 7.48-7.45 (m, 2H), 7.34-7.27 (m, 3H), 7.12 (t, J = 7.2 Hz, 1H), 6.76-6.67 (m, 2H), 3.35 (s, 3H), 3.13 (t, J = 7.2 Hz, 2H), 2.78 (t, J = 7.2 Hz, 2H) ppm.

2-(3-(4-(2,4-Dimethoxyphenyl)phenyl)propanamido)benzoic acid (5y)

Yield = 30 mg, 15%. ^{1}H NMR (400 MHz, $CDCl_3$ + MeOD): **δ** 11.53 (s, 1H), 8.62 (d, J = 8.4 Hz, 1H), 8.09 (dd, J = 8.0, 1.6 Hz, 1H), 7.55 (td, J = 8.0, 1.6 Hz, 1H), 7.41 (d, J = 8.0 Hz, 2H), 7.27 (d, J = 8.0 Hz, 2H), 7.19 (d, J = 9.2 Hz, 1H), 7.22 (t, J = 8.0 Hz, 1H), 6.58-6.56 (m, 2H), 3.85 (s, 3H), 7.77 (s, 3H), 3.08 (t, J = 8.0 Hz, 2H), 2.79 (t, J = 8.0 Hz, 2H) ppm.

Methyl 2-(3-(4'-methoxy-[1,1'-biphenyl]-4-yl)propanamido)thiophene-3-carboxylate (4aa)

Purified by column chromatography using Pet. ether/EtOAc (4:1) yielding 20 mg, 23% as a white solid. ^{1}H NMR (400 MHz, $CDCl_3$): **δ** 10.97 (s, 1H), 7.49 (t, J = 8.0 Hz, 4H), 7.27 (t, J = 8.0 Hz, 2H), 7.18 (d, J = 5.6 Hz, 1H), 6.96 (d, J = 8.8 Hz, 2H), 6.73 (d, J = 6.0 Hz, 1H), 3.86 (s, 3H), 3.84 (s, 3H), 3.12 (t, J = 8.0 Hz, 2H), 2.84 (t, J = 8.0 Hz, 2H) ppm.

General demethylation procedure by BBr_3 (6g, m, r-aa)

Demethylation of methoxyphenyl compounds (**5c, j, r-aa**) was performed following the protocol described in the patent of Daiichi Sankyo Company, Limited Chuo-ku[32]. The methoxyphenyl compounds **5c, j, r-aa** (1.0 eq.) were dissolved in dry CH_2Cl_2 (0.05 mmol/mL) and stirred at -78 °C under a nitrogen atmosphere. A 1M BBr_3 in CH_2Cl_2 (5.0 eq.) solution was slowly added drop wise and after the addition was completed the mixture was allowed to reach RT and stirring was continued for 4 h. The mixture was cooled to -78 °C and water was added. At RT the precipitated product was collected by filtration and washed with water and CH_2Cl_2 to obtain the pure hydroxyphenyl products **6g, m, r-aa** as solids.

2-(3-(4-(4-Hydroxyphenyl)phenyl)propanamido)benzoic acid (6g)[37]
Yield = 24 mg, 55%. ^{1}H NMR (400 MHz, MeOD): δ 8.56 (d, J = 8.4 Hz., 1H), 8.06 (d, J = 7.6 Hz, 1H), 7.55 (t, J = 7.6 Hz, 1H), 7.44 (d, J = 8.0 Hz, 2H), 7.40 (d, J = 8.4 Hz, 2H), 7.27 (d, J = 8.0 Hz, 2H), 7.13 (t, J = 7.6 Hz, 1H), 6.82 (d, J = 8.4 Hz, 2H), 3.05 (t, J = 7.6 Hz, 2H), 3.75 (t, J = 7.6 Hz, 2H) ppm. HPLC Rt = 9.00 min. purity 97%. ESI-MS: 361.93 $[M+H]^+$.

2-(3-(4-(3-Hydroxyphenyl)phenyl)propanamido)benzoic acid (6m)[37]
Yield = 61 mg, 39%. ^{1}H NMR (400 MHz, MeOD): δ 8.55 (d, J = 8.4 Hz, 1H), 8.05 (d, J = 7.6 Hz, 1H), 7.53-7.46 (m, 3H), 7.29 (d, J = 8.0 Hz, 2H), 7.20 (t, J = 7.6 Hz, 1H), 7.12 (t, J = 7.6 Hz, 1H), 7.04-6.99 (m, 2H), 6.73 (dd, J = 7.6, 1.6 Hz, 1H), 3.06 (t, J = 7.2 Hz, 2H), 2.75 (t, J = 8.0 Hz, 2H) ppm. HPLC Rt = 10.08 min. purity 97%. ESI-MS: 361.93 $[M+H]^+$.

2-(3-(4-(2-Hydroxyphenyl)phenyl)propanamido)benzoic acid (6r)[37]
Yield = 22 mg, 56%. ^{1}H NMR (400 MHz, Acetone-d6): **δ** 11.29 (s, 1H), 8.76 (d, J = 8.8 Hz, 1H), 8.35 (br s, 1H), 8.09 (d, J = 7.6 Hz, 1H), 7.60 (t, J = 7.8 Hz, 1H), 7.52 (d, J = 8.0 Hz, 2H), 7.34 (d, J = 8.0 Hz, 2H), 7.27 (d, J = 7.6 Hz, 1H), 7.19-7.11 (m, 2H), 6.97 (d, J = 8.0 Hz, 1H), 6.90 (t, J = 7.4 Hz, 1H), 3.07 (t, J = 7.6 Hz, 2H), 2.80 (t, J = 7.8 Hz, 2H) ppm. HPLC Rt = 9.28 min. purity 99%. ESI-MS: 361.93 $[M+H]^+$.

2-(3-(4-(4-Hydroxy-3-methylphenyl)phenyl)propanamido)benzoic acid (6s)
Yield = 7 mg, 62%. Mp 174 °C. ^{1}H NMR (400 MHz, MeOD): **δ** 8.55 (d, J = 8.4 Hz, 1H), 8.06 (d, J = 8.0 Hz, 1H), 7.55 (td, J = 7.8, 1.2 Hz, 1H), 7.44 (d, J = 8.0 Hz, 2H), 7.29-7.25 (m, 3H), 7.22 (dd, J = 8.4, 2.0 Hz, 1H), 7.13 (t, J = 7.6 Hz, 1H), 3.05 (t, J = 8.0 Hz, 2H), 2.75 (t, J = 8.0 Hz, 2H) ppm. HPLC Rt = 9.31 min. purity 98%. ESI-MS: 376.00 $[M+H]^+$.

2-(3-(4-(3-Chloro-4-hydroxyphenyl)phenyl)propanamido)benzoic acid (6t)
Yield = 1.0 mg, 2% . ^{1}H NMR (400 MHz, MeOD): **δ** 8.57 (d, J = 8.0 Hz, 1H), 8.07 (d, J = 7.2 Hz, 1H), 7.55-7.50 (m, 2H), 7.45 (d, J = 8.0 Hz, 2H), 7.35 (dd, J = 8.4, 2.4 Hz, 1H), 7.31 (d, J = 8.0 Hz, 2H), 7.13 (t, J = 7.2 Hz, 1H), 6.95 (d, J = 8.4 Hz, 1H), 3.07 (t, J = 7.6 Hz, 2H), 2.77 (t, J = 7.6 Hz, 2H) ppm. HPLC Rt = 9.49 min. purity 98%. ESI-MS: 395.93 $[M+H]^+$.

2-(3-(4-(3-Fluoro-4-hydroxyphenyl)phenyl)propanamido)benzoic acid (6u)
Yield = 21 mg, 59%. Mp 176 °C. ^{1}H NMR (400 MHz, MeOD): **δ** 8.55 (d, J = 8.4 Hz, 1H), 8.06 (dd, J = 8.0, 1.2 Hz, 1H), 7.55 (td, J = 8.2, 1.2 Hz, 1H), 7.46 (d, J = 8.0 Hz, 2H), 7.30-7.27 (m, 3H), 7.21 (dd, J = 8.4, 1.2 Hz, 1H), 7.13 (t, J = 8.0 Hz, 1H), 6.95 (t, J = 8.8 Hz, 1H), 3.06 (t, J = 8.0 Hz, 2H), 2.76 (t, J = 8.0 Hz, 2H) ppm. HPLC Rt = 9.13 min. purity 97%. ESI-MS: 380.00 $[M+H]^+$.

2-(3-(4-(4-Hydroxy-2-methylphenyl)phenyl)propanamido)benzoic acid (6v)
Yield = 14 mg, 96%. Mp 174 °C. ^{1}H NMR (400 MHz, MeOD): **δ** 8.56 (d, J = 8.4 Hz, 1H), 8.06 (dd, J = 8.0, 1.2 Hz, 1H), 7.54 (td, J = 8.0, 1.6 Hz, 1H), 7.26 (d, J = 8.0 Hz, 2H), 7.15-7.11 (m, 3H), 6.96

(d, J = 8.4 Hz, 1H), 6.67-6.61 (m, 2H), 3.07 (t, J = 7.6 Hz, 2H), 2.76 (t, J = 8.0 Hz, 2H), 2.12 (s, 3H) ppm. HPLC Rt = 9.16 min. purity 99%. ESI-MS: 375.93 $[M+H]^+$.

2-(3-(4-(2-Chloro-4-hydroxyphenyl)phenyl)propanamido)benzoic acid (6w)[37]

Yield = 119 mg, 59%. ^{1}H NMR (400 MHz, DMSO): **δ** 11.15 (s, 1H), 9.95 (s, 1H), 8.49 (d, J = 8.4 Hz, 1H), 7.97 (dd, J = 8.0, 1.2 Hz, 1H), 7.58 (t, J = 8.4 Hz, 1H), 7.33-7.27 (m, 4H), 7.19-7.12 (m, 2H), 6.90 (s, 1H), 6.80 (dd, J = 8.4, 2.4 Hz, 1H), 2.98 (t, J = 7.2 Hz, 2H), 2.76 (t, J = 6.6 Hz, 2H) ppm. HPLC Rt = 9.36 min. purity 99%. ESI-MS: 395.93 $[M+H]^+$.

2-(3-(4-(2-Fluoro-4-hydroxyphenyl)phenyl)propanamido)benzoic acid (6x)

Yield = 6 mg, 32%. Mp 205 °C. ^{1}H NMR (400 MHz, MeOD): **δ** 8.56 (d, J = 8.4 Hz, 1H), 8.07 (dd, J = 8.0, 1.2 Hz, 1H), 7.55 (t, J = 8.4 Hz, 1H), 7.38 (d, J = 6.8 Hz, 2H), 7.29 (d, J = 8.0 Hz, 2H), 7.24 (t, J = 8.8 Hz, 1H), 7.14 (t, J = 7.6 Hz, 1H), 6.65 (dd, J = 8.4, 2.4 Hz, 1H), 6.56 (dd, J = 12.8, 2.4 Hz, 1H), 3.07 (t, J = 8.0 Hz, 2H), 2.77 (t, J = 8.0 Hz, 2H) ppm. HPLC Rt = 9.16 min. purity 98%. ESI-MS: 380.00 $[M+H]^+$.

2-(3-(4-(2,4-Dihydroxyphenyl)phenyl)propanoylamino)benzoic acid (6y)

Yield = 12 mg, 45%. Mp 162 °C. ^{1}H NMR (400 MHz, MeOD): **δ** 8.56 (d, J = 8.0 Hz, 1H), 8.07 (dd, J = 8.0, 1.6 Hz, 1H), 7.55 (td, J = 7.2, 1.6 Hz, 1H), 7.41 (d, J = 8.0 Hz, 2H), 7.24 (d, J = 8.0 Hz, 2H), 7.13 (td, J = 7.6, 1.2 Hz, 1H), 7.03 (d, J = 8.0 Hz, 1H), 6.37-6.33 (m, 2H), 3.05 (t, J = 8.0 Hz, 2H), 2.76 (t, J = 8.0 Hz, 2H) ppm. HPLC Rt = 8.34 min. purity 97%. ESI-MS: 378.07 $[M+H]^+$.

2-(3-(4-(4-Hydroxyphenyl)phenyl)propanamido)cyclohex-1-ene-1-carboxylic acid (6z)

Yield = 2 mg, 27%. ^{1}H NMR (400 MHz, MeOD): **δ** 7.47-7.41 (m, 4H), 7.25 (d, J = 8.4 Hz, 2H) , 6.83 (d, J = 8.8 Hz, 2H), 2.99 (t, J = 7.6 Hz, 2H), 2.91-2.89 (m, 2H), 2.65 (t, J = 8.0 Hz, 2H), 2.36-2.30 (m, 2H), 1.67-1.61 (m, 4H) ppm. HPLC Rt = 9.21 min. purity 97%. ESI-MS: 366.93 $[M+H]^+$.

2-(3-(4-(4-Hydroxyphenyl)phenyl)propanamido)thiophene-3-carboxylic acid (6aa)

Yield = 2 mg, 7%. Mp 199 °C. ^{1}H NMR (400 MHz, MeOD): **δ** 7.46 (d, J = 8.0 Hz, 2H), 7.41 (dt, J = 8.4, 2.0 Hz, 2H), 7.28 (d, J = 8.0 Hz, 2H), 7.19 (d, J = 6.0 Hz, 1H), 6.85-6.81 (m, 3H), 3.06 (t, J = 7.6 Hz, 2H), 2.86 (t, J = 7.6 Hz, 2H) ppm. HPLC Rt = 8.78 min. purity 98% ESI-MS: 368.13 $[M+H]^+$.

General amidation procedure to yield compounds 8a-b

3-(4-iodophenyl)propanoic acid (7)[33] (1.0 eq.) was added to $SOCl_2$ (0.2 mmol/mL) under a nitrogen atmosphere. The mixture was refluxed for 1.5 h after which the $SOCl_2$ was evaporated in vacuo. The residue was co evaporated 2 times with toluene and subsequently dissolved in toluene (0.1 mmol/mL). Methyl-2-aminobenzoate or methyl 2-aminothiophene-3-carboxylate (1.4 eq.) was added and the mixture was stirred overnight at room temperature under a nitrogen atmosphere. Upon completion of the reaction, the precipitate was filtered off and the

filtrate was concentrated. The obtained residue was purified by column chromatography (Pet Et/EtOAc 4:1) to give the target compound.

Methyl 2-(3-(4-iodophenyl)propanamido)benzoate (8a)

Started from methyl-2-aminobenzoate, yielding 1.41 g (96%) of the product as a white solid. 1H NMR (400 MHz, $CDCl_3$) δ 11.07 (s, 1H), 8.70 (d, J = 8.4 Hz, 1H), 8.02 (dd, J = 8.0, 1.6 Hz, 1H), 7.61-7.59 (m, 2H), 7.54 (dt, J = 8.0, 1.6 Hz, 1H), 7.08 (dt, J = 8.0, 1.2 Hz, 1H), 7.01 (d, J = 8.0 Hz, 2H), 3.92 (s, 3H), 3.02 (t, J = 7.6 Hz, 2H), 2.73 (t, J = 7.6 Hz, 2H) ppm.

Methyl 2-(3-(4-iodophenyl)propanamido)thiophene-3-carboxylate (8b)

Started from methyl 2-aminothiophene-3-carboxylate, Yield = 15 mg, 38%, white solid. ^{1}H NMR (400 MHz, MeOD): δ 7.60 (d, J = 8.4 Hz, 2H), 7.18 (d, J = 6.0 Hz, 1H), 7.05 (d, J = 8.0 Hz, 2H), 6.85 (d, J = 5.6 Hz, 1H), 3.87 (s, 3H), 2.99 (t, J = 8.0 Hz, 2H), 2.84 (t, J = 8.0 Hz, 2H) ppm.

Biological assays

Cell culture and membrane preparation

Human embryonic kidney (HEK293T) cells were transfected with the N-Flag-tagged HCA_2 receptor in pcDNA3.1 using a standard calcium phosphate protocol[46]. The receptor expression levels of all positive stable clones were assessed with a radioligand binding assay[47]. In all assays the HEK293T cells with highest expression level of the human HCA_2 receptor (HEK293T-hHCA_2) were used. Cell culture and membrane preparation were performed as described by us before[48]. The membrane aliquots in all assays were 35 μg of protein per well.

[^{3}H]nicotinic acid equilibrium displacement assay

Membranes of the HEK293T-hHCA_2 cell line were incubated for 1 h at 25 °C with 15 nM [^{3}H]nicotinic acid (specific activity: 50 Ci/mmol), which was obtained from Biotrend (Cologne, Germany). At first, all compounds were tested at one concentration, such that a final concentration of 10^{-5} M of the test compound was added in assay buffer (50 mM Tris HCl, 1 mM $MgCl_2$, pH 7.4 at 25 °C). When radioligand displacement by the compounds was greater than 75%, full curves were recorded to obtain the compounds' IC_{50} values. Increasing concentrations of the test compounds in assay buffer were added by using a HP D300 digital

dispenser (Tecan Group Ltd, Männedorf, Switzerland). The total assay volume was 100 μL. To assess the total binding, a control without test compound was included. The nonspecific binding was determined in the presence of 10 μM unlabeled nicotinic acid. The final DMSO concentration in all samples was ≤ 0.25%. The incubation was terminated by rapid vacuum filtration to separate the bound and free radioligand through 96-well GF/B filter plates using a Perkin Elmer Filtermate-harvester (Perkin Elmer, Groningen, the Netherlands). Filters were subsequently washed three times with ice-cold buffer (50 mM Tris HCl, pH 7.4). The filter-bound radioactivity was determined by scintillation spectrometry using the P-E 1450 Microbeta Wallac Trilux scintillation counter (Perkin Elmer, Groningen, the Netherlands).

[^{3}H]nicotinic acid association and dissociation assays

The association binding assays were performed in a time-dependent manner by incubating membrane aliquots in a total volume of 100 μl assay buffer at 25 °C for a maximum of 120 min with 15 nM [^{3}H]-nicotinic acid. The nonspecific binding (as the 0 min time point) was determined in the presence of 10 μM unlabeled nicotinic acid. The dissociation binding assays were performed by pre-incubating membrane aliquots in a total volume of 100 μl assay buffer at 25 °C for 180 min with 15 nM [^{3}H]-nicotinic acid. After pre-incubation, dissociation was initiated by addition of 5 μl unlabeled nicotinic acid (final concentration 10 μM) for a total period of 120 min. The amounts of [^{3}H]nicotinic acid still bound to the receptor in both association and dissociation binding assays were measured at various time intervals during the incubation. Incubations were terminated and samples were harvested as described for the [^{3}H]nicotinic acid equilibrium displacement assay.

Competition association assay

The binding kinetics of unlabeled ligands were quantified using the competition association assay based on the theoretical framework by Motulsky and Mahan[49]. The competition association assay was performed in a total volume of 100 μL of assay buffer at 25 °C with 15 nM [^{3}H]nicotinic acid in the absence or presence of

$1 \times IC_{50}$ of an unlabeled competing ligand. The competition association assay was initiated by adding HEK293T-$hHCA_2$ receptor membrane aliquots at different time points with a maximum incubation time of 90 min. Incubations were terminated and samples were harvested as described for the [^{3}H]nicotinic acid equilibrium displacement assay.

Data analysis

All experimental data was analyzed by using GraphPad Prism 5.0 (GraphPad software Inc., San Diego, CA). Nonlinear regression was used to determine IC_{50} values from [^{3}H]nicotinic acid equilibrium displacement assays, and the mean IC_{50} values were obtained from three independent experiments performed in duplicate. Kinetic behavior of unlabeled competing ligands was assessed in the competition association assay, which was fitted using the *one phase exponential association* model. Kinetic rate index (KRI) values[34] were calculated by dividing the specific radioligand binding measured at t_1 = 7 min (B_{t1}) by the binding at t_2 = 90 min (B_{t2}) in the presence and absence of unlabeled competing ligands (KRI = B_{t1} / B_{t2}). Statistical evaluation (*p*-values) of KRI values was performed by a two-tailed homoscedastic Student's *t*-test using non-radioactive nicotinic acid as reference ligand; significance is indicated as follows: *: $p < 0.05$, **: $p < 0.01$, ***: $p < 0.001$.

Acknowledgments

Rongfang Liu thanks the China Scholarship Council (CSC) for funding her PhD scholarship. The Dutch Research Council (NWO) provided a TOP grant (714.011.001) to A.P. IJ. We thank Prof. S. Offermanns and Dr. S. Tunaru (MPI, Bad Nauheim, Germany) for providing the HCA_2 plasmid. Our former coworkers Dr C.C. Blad and Dr J.R. Lane are acknowledged for the generation and validation of the cell line used.

References

[1] Cai, T.Q., et al. *Role of GPR81 in lactate-mediated reduction of adipose lipolysis.* Biochem. Biophys. Res. Commun. (2008) 377: 987-991.

[2] Liu, C., et al. *Lactate inhibits lipolysis in fat cells through activation of an orphan G-protein-coupled receptor, GPR81.* J. Biol. Chem. (2009) 284: 2811-2822.

[3] Taggart, A.K., et al. *(D)-β-hydroxybutyrate inhibits adipocyte lipolysis via the nicotinic acid receptor PUMA-G.* J. Biol. Chem. (2005) 280: 26649-26652.

[4] Ahmed, K., et al. *Deorphanization of GPR109B as a receptor for the β-oxidation intermediate 3-OH-octanoic acid and its role in the regulation of lipolysis.* J. Biol. Chem. (2009) 284: 21928-21933.

[5] Bobileva, O., et al. *Synthesis and evaluation of (E)-2-(acrylamido) cyclohex-1-enecarboxylic acid derivatives as HCA1, HCA2, and HCA3 receptor agonists.* Bioorg. Med. Chem. (2014) 22: 3654-3669.

[6] Offermanns, S., et al. *International union of basic and clinical pharmacology. LXXXII: nomenclature and classification of hydroxy-carboxylic acid receptors (GPR81, GPR109A, and GPR109B).* Pharmacol. Rev. (2011) 63: 269-290.

[7] Raghavan, S., et al. *Tetrahydro anthranilic acid as a surrogate for anthranilic acid: Application to the discovery of potent niacin receptor agonists.* Bioorg. Med. Chem. Lett. (2008) 18: 3163-3167.

[8] Tai, Y.F., et al. *Imaging microglial activation in Huntington's disease.* Brain Res. Bull. (2007) 72: 148-151.

[9] Amor, S., et al. *Inflammation in neurodegenerative diseases.* Immunology. (2010) 129: 154-169.

[10] Ahmed, K., Tunaru, S., and Offermanns, S. *GPR109A, GPR109B and GPR81, a family of hydroxy-carboxylic acid receptors.* Trends Pharmacol. Sci. (2009) 30: 557-562.

[11] Lukasova, M., et al. *Nicotinic acid inhibits progression of atherosclerosis in mice through its receptor GPR109A expressed by immune cells.* J. Clin. Invest. (2011) 121: 1163.

[12] Hanson, J., Gille, A., and Offermanns, S. *Role of HCA_2 (GPR109A) in nicotinic acid and fumaric acid ester-induced effects on the skin.* Pharmacol. Ther. (2012)

[13] Gille, A., et al. *Nicotinic acid: pharmacological effects and mechanisms of action.* Annu. Rev. Pharmacol. Toxicol. (2008) 48: 79-106.

[14] Bodor, E. and Offermanns, S. *Nicotinic acid: an old drug with a promising future.* Br. J. Pharmacol. (2008) 153: S68-S75.

[15] Davidson, M.H. *Niacin use and cutaneous flushing: mechanisms and strategies for prevention.* Am. J. Cardiol. (2008) 101: S14-S19.

[16] Shen, H.C. and Colletti, S.L. *Novel patent publications on high-affinity nicotinic acid receptor agonists.* Expert Opin. Ther. Pat. (2009) 19: 957-967.

[17] Semple, G., et al. *3-(1 H-tetrazol-5-yl)-1, 4, 5, 6-tetrahydro-cyclopentapyrazole (MK-0354): a partial agonist of the nicotinic acid receptor, G-protein coupled receptor 109a, with antilipolytic but no vasodilatory activity in mice.* J. Med. Chem. (2008) 51: 5101-5108.

[18] Lai, E., et al. *Effects of a niacin receptor partial agonist, MK-0354, on plasma free fatty acids, lipids, and cutaneous flushing in humans.* J. Clin. Lipidol. (2008) 2: 375-383.

[19] Boatman, P.D., et al. *(1a R, 5a R) 1a, 3, 5, 5a-Tetrahydro-1 H-2, 3-diaza-cyclopropa [a] pentalene-4-carboxylic Acid (MK-1903): A potent GPR109a agonist that lowers free fatty acids in humans.* J. Med. Chem. (2012) 55: 3644-3666.

[20] Shen, H.C., et al. *Discovery of a biaryl cyclohexene carboxylic acid (MK-6892): a potent and selective high affinity niacin receptor full agonist with reduced flushing profiles in animals as a preclinical candidate.* J. Med. Chem. (2010) 53: 2666-70.

[21] Arrowsmith, J. and Miller, P. *Trial watch: phase II and phase III attrition rates 2011-2012.* Nat. Rev. Drug. Disc. (2013) 12: 569-569.

[22] Dahl, G. and Akerud, T. *Pharmacokinetics and the drug–target residence time concept.* Drug Discovery Today. (2013) 18: 697-707.

[23] Guo, D., et al. *Drug-target residence time—A case for G protein-coupled receptors.* Med. Res. Rev. (2014) 34: 856-892.

[24] Copeland, R.A., Pompliano, D.L., and Meek, T.D. *Drug–target residence time and its implications for lead optimization.* Nat. Rev. Drug. Disc. (2006) 5: 730-739.

[25] Swinney, D.C. *Biochemical mechanisms of new molecular entities (NMEs) approved by United States FDA during 2001-2004: mechanisms leading to optimal efficacy and safety.* Curr. top. Med. Chem. (2006) 6: 461-478.

[26] Zhang, R. and Monsma, F. *The importance of drug-target residence time.* Curr. Opin. Drug Discovery Dev. (2009) 12: 488-496.

[27] Swinney, D.C. *Biochemical mechanisms of drug action: what does it take for success?* Nat. Rev. Drug. Disc. (2004) 3: 801-808.

[28] Casarosa, P., et al. *Preclinical evaluation of long-acting muscarinic antagonists: comparison of tiotropium and investigational drugs.* J. Pharmacol. Exp. Ther. (2009) 330: 660-668.

[29] Glossop, P.A., et al. *Inhalation by design: novel tertiary amine muscarinic m3 receptor antagonists with slow off-rate binding kinetics for inhaled once-daily treatment of chronic obstructive pulmonary disease.* J. Med. Chem. (2011) 54: 6888-6904.

[30] Shen, H.C., et al. *Discovery of biaryl anthranilides as full agonists for the high affinity niacin receptor.* J. Med. Chem. (2007) 50: 6303-6306.

[31] Christiansen, E., Due-Hansen, M.E., and Ulven, T. *A rapid and efficient Sonogashira protocol and improved synthesis of free fatty acid 1 (FFA1) receptor agonists.* J. Org. Chem. (2010) 75: 1301-1304.

[32] Suzuki, K. *Patent application EP2308838A1* . (2011)

[33] Cheung, S.Y., et al. *Synthesis of organometallic poly (dendrimer) s by macromonomer polymerization: effect of dendrimer size and structural rigidity on the polymerization efficiency.* Chem. Eur. J. (2009) 15: 2278-2288.

[34] Guo, D., et al. *Dual-point competition association assay A fast and high-throughput kinetic screening method for assessing ligand-receptor binding kinetics.* J. Biomol. Screen. (2013) 18: 309-320.

[35] Imbriglio, J.E., et al. *The discovery of high affinity agonists of GPR109a with reduced serum*

shift and improved ADME properties. Bioorg. Med. Chem. Lett. (2011) 21: 2721-2724.

[36] Ding, F.X., et al. *Discovery of pyrazolyl propionyl cyclohexenamide derivatives as full agonists for the high affinity niacin receptor GPR109A.* Bioorg. Med. Chem. Lett. (2010) 20: 3372-3375.

[37] Chen, W., et al., *Niacin receptor agonists, compositions containing such compounds and methods of treatment*, in *Patent application WO2006057922A2*. 2006.

[38] Schmidt, D., et al. *Anthranilic acid replacements in a niacin receptor agonist.* Bioorg. Med. Chem. Lett. (2010) 20: 3426-3430.

[39] Louvel, J., et al. *Agonists for the adenosine A1 receptor with tunable residence time. A case for nonribose 4-amino-6-aryl-5-cyano-2-thiopyrimidines.* J. Med. Chem. (2014) 57: 3213-3222.

[40] Grovenstein, E. and Cheng, Y.M. *Carbanions. XII. p-Biphenylyl migration in reactions of 1-chloro-2-p-biphenylylethane-1, 1-d2 with alkali metals.* J. Am. Chem. Soc. (1972) 94: 4971-4977.

[41] Rosen, B.M., et al. *Predicting the structure of supramolecular dendrimers via the analysis of libraries of AB3 and constitutional isomeric AB2 biphenylpropyl ether self-assembling dendrons.* J. Am. Chem. Soc. (2009) 131: 17500-17521.

[42] Viswajanani, J.S. *Patent application WO200823336A2* . (2008)

[43] Chiriano, G., et al. *A small chemical library of 2-aminoimidazole derivatives as BACE-1 inhibitors: Structure-based design, synthesis, and biological evaluation.* Eur. J. Med. Chem. (2012) 48: 206-213.

[44] Hardouin, C., et al. *Structure–activity relationships of α-ketooxazole inhibitors of fatty acid amide hydrolase.* J. Med. Chem. (2007) 50: 3359-3368.

[45] Diamond, J. *Patent application US3966801A1* . (1976)

[46] Kingston, R.E., Chen, C.A., and Rose, J.K. *Calcium phosphate transfection.* Curr. Protoc. Mol. Biol. (2003) 9.1. 1-9.1. 11.

[47] Wise, A., et al. *Molecular identification of high and low affinity receptors for nicotinic acid.* J. Biol. Chem. (2003) 278: 9869-9874.

[48] Li, Z., et al. *Effects of pyrazole partial agonists on HCA2-mediated flushing and VLDL-triglyceride levels in mice.* Br. J. Pharmacol. (2012) 167: 818-825.

[49] Motulsky, H.J. and Mahan, L. *The kinetics of competitive radioligand binding predicted by the law of mass action.* Mol. Pharmacol. (1984) 25: 1-9.

Supporting information

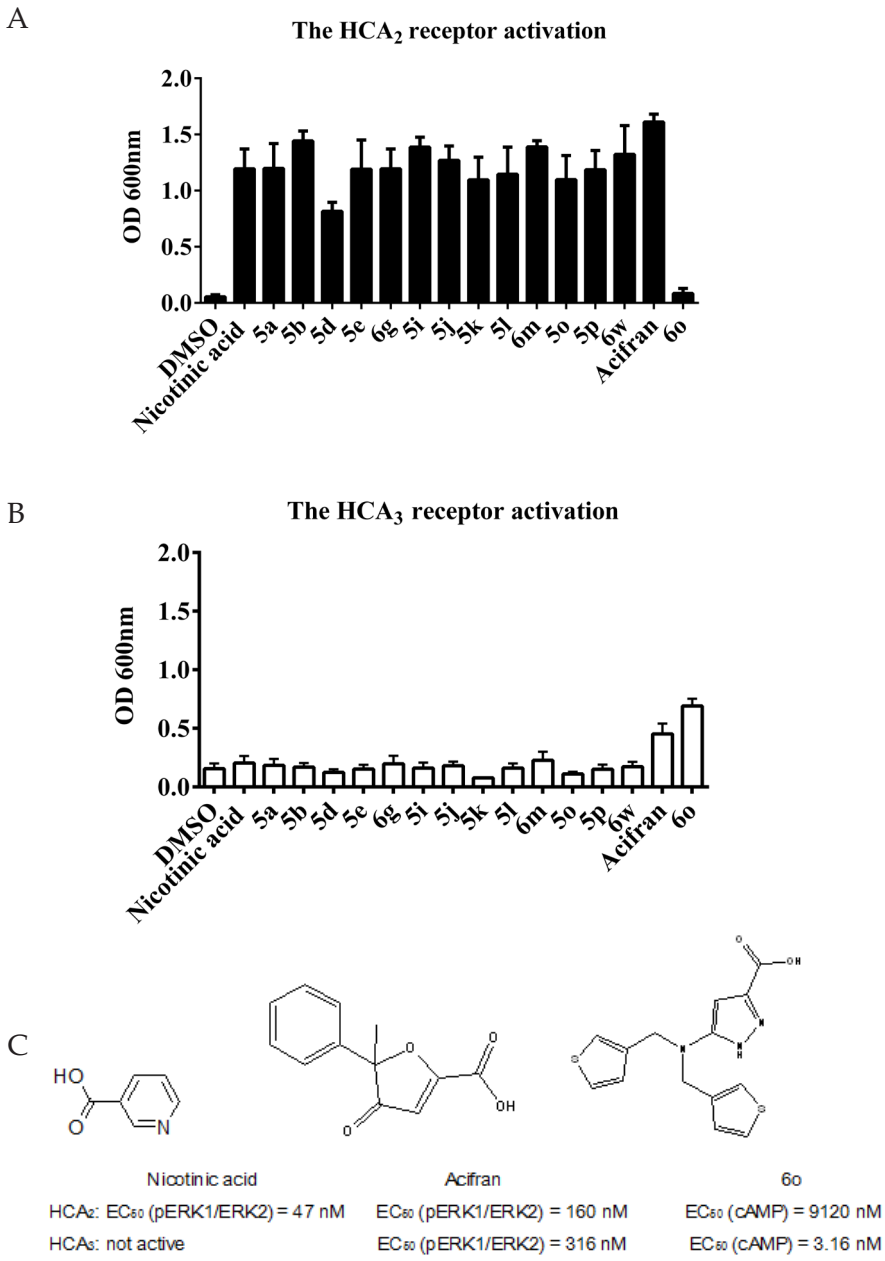

Fig. S1. HCA_2 receptor activation (A) and HCA_3 receptor activation (B) were tested in yeast liquid growth assays in the absence of ligand (DMSO) or in the presence of 100 μM of selected derivatives, or nicotinic acid, or acifran or reference ligand **6o**[1]; (C) Chemical structures of reference ligands: nicotinic acid[2], acifran[2], and **6o**[1].

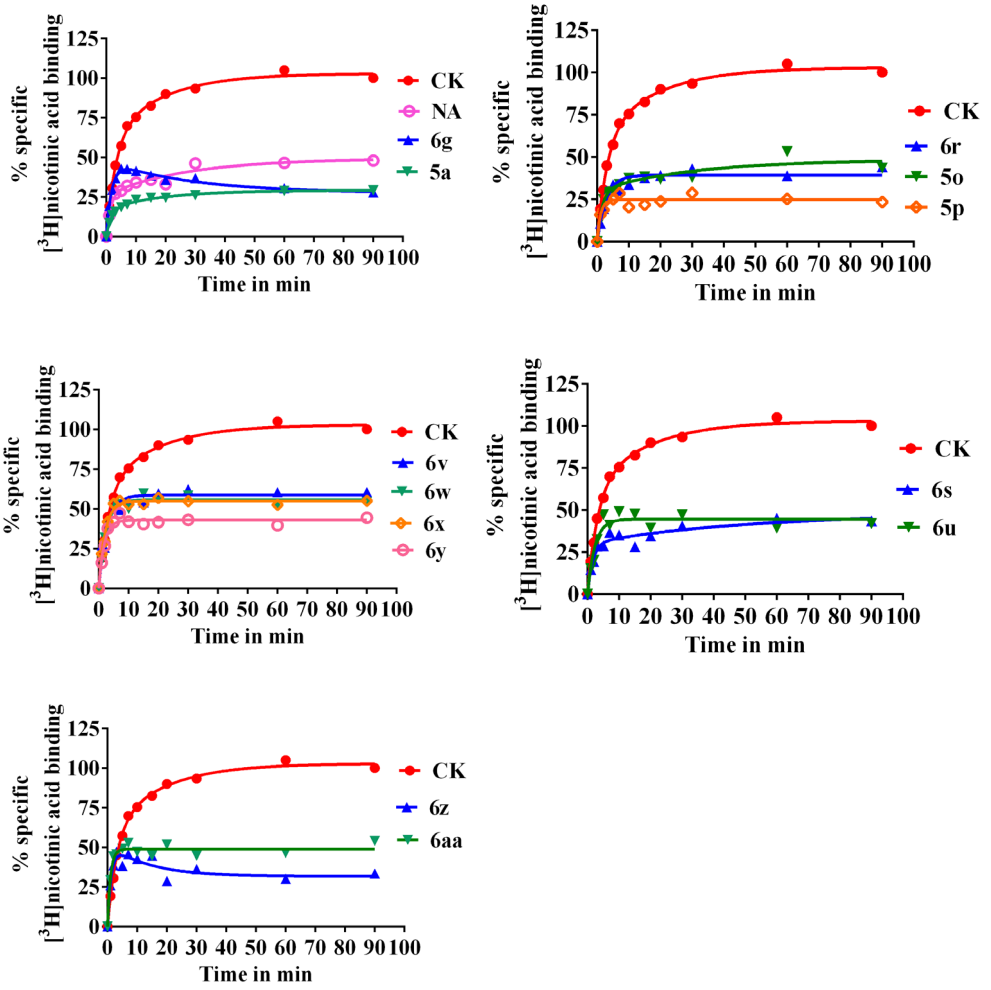

Fig. S2. [^{3}H]nicotinic acid competition association assay in the absence of ligand (control CK) and in the presence of 1 × IC_{50} of unlabeled ligands. Representative graphs from one experiment performed in duplicate. (A) **Nicotinic acid** (NA), **5a** (non-substituted) and **6g** (4-OH) yield their kinetic profiles in Table 1; (B) Mono-substituted analogues at 2-position: **6r** (2-OH), **5o** (2-Cl) and **5p** (2-F) yield their kinetic profiles in Table 1; (C) Di-substituted 2-R, 4-OH analogues: **6v** (2-Me), **6w** (2-Cl), **6x** (2-F) and **6y** (2-OH) yield their kinetic profiles in Table 2; (D) Di-substituted 3-R, 4-OH analogues: **6s** (3-Me), **6u** (3-F) yield their kinetic profiles in Table 2; (E) Tetrahydroanthranilic acid derivative **6z** and the thiophene bioisostere **6aa** yield their kinetic profiles in Table 3.

Selectivity assay

Transformation in a S. cerevisiae strain (MMY24)

The p426GPD_HCA_2 or p426GPD_HCA_3 plasmid was transformed according to the Lithium-Acetate procedure[3] into an engineered Saccharomyces Cerevisiae (S. cerevisiae) yeast strain, MMY24, expressing one specific Gpa1p/$G_{\alpha i3}$ chimeric G protein. The yeast strain was derived from the MMY11 strain and further adapted to communicate with mammalian GPCRs. Hereto the last five amino acid residues of the C-terminus of Gpa1p/$G_{\alpha i3}$ chimera had been replaced with the same-length sequence from mammalian $G_{\alpha i3}$ protein.[4, 5] The genotype of the MMY24 strain is: MATahis3 leu2 trp1ura3can1 gpa1_::G_i3 far1::ura3 sst2_::ura3 Fus1::FUS1-HIS3 LEU2::FUS1-lacZste2_::G418R and the sequence of these last 5 C-terminal amino acid residues of Gpa1p/$G_{\alpha i3}$ chimera is $ECGLY^{COOH}$[4, 5].

Liquid growth assay

The degree of receptor activation was measured by the growth rate of the yeast on histidine-deficient medium via the *FUS1-HIS3* reporter gene induction, which was described in our previous research[6] except that nicotinic acid was omitted from the YNB-UL mix (YNB + adenine + tryptophan + histidine, lacking uracil and leucine). Both the HCA_2 receptor and HCA_3 receptor were tested in liquid growth assays in the absence of any ligand (DMSO) or in the presence of 100 μM of selected derivatives, or nicotinic acid (Sigma, The Netherlands), or acifran (Tocris, USA) or reference ligand **6o**[1] (synthesized by Jacobus P. D. van Veldhoven again in our lab). Yeast cells with the HCA_2 receptor from an overnight culture were diluted to around 2×10^4 cells/mL ($OD_{600}\approx 0.001$) and 50 μL was added into each well (approx. 1,000 cells/well). Results were obtained from three independent experiments, performed in duplicate. Yeast cells with the HCA_3 receptor were diluted to approx. 2×10^5 cells/mL ($OD_{600} \approx 0.01$) and 50 μL was added into each well (approx. 1×10^4 cells/well). Results were obtained from two independent experiments, performed in duplicate.

Emax values of the liquid assay were assessed from the nonlinear regression package Prism 5.0 (GraphPad Software Inc., San Diego, CA).

References

[1] Skinner, P.J., et al. *5-N, N-Disubstituted 5-aminopyrazole-3-carboxylic acids are highly potent agonists of GPR109b.* Bioorg. Med. Chem. Lett. (2009) 19: 4207-4209.

[2] Mahboubi, K., et al. *Triglyceride modulation by acifran analogs: activity towards the niacin high and low affinity G protein-coupled receptors HM74A and HM74.* Biochem. Biophys. Res. Commun. (2006) 340: 482-490.

[3] Gietz, D., et al. *Improved method for high efficiency transformation of intact yeast cells.* Nucleic Acids Res. (1992) 20: 1425.

[4] Dowell, S.J. and Brown, A.J. *Yeast assays for G protein-coupled receptors.* G Protein-Coupled Receptors in Drug Discovery (2009) 552: 213-229.

[5] Dowell, S.J. *Yeast assays for G-protein–coupled receptors.* Receptors and Channels (2002) 8: 343-352.

[6] Liu, R., et al. *A yeast screening method to decipher the interaction between the adenosine A_{2B} receptor and the C-terminus of different G protein α-subunits.* Purinergic Signal. (2014) 10: 441-453.

Chapter 7

Conclusions and perspectives

Conclusions

Saccharomyces cerevisiae system

In **Chapter 2** we summarized the principles and developments in yeast research applied to 11 different G protein-coupled receptors (GPCRs), and highlighted and generalized the experimental findings of GPCR function in the *Saccharomyces cerevisiae (S. cerevisiae)* system since the year 2005. These yeast systems are very useful platforms in GPCR research providing insight into GPCR activation and signaling, and facilitate agonist and antagonist identification. There are many advantages of using a yeast assay system, as it is a cheap, safe and stable; it is also convenient for rapid feasibility and optimization studies. Moreover, it offers "null" background when studying human GPCRs.

Here, we summarize the principles of how we developed 'a single-GPCR-one-G protein yeast system' (Fig. 1). The whole process can be divided into two parts: mutants construction and characterization. There are many concepts and sources for selecting mutants, such as from modeling prediction (**Chapter 3**), and sequence motifs or specific areas known to be important in other receptors (**Chapters 4** and **5**). For the characterization of mutants in this thesis we focused on three differences between the mutant and the wild-type receptor: agonist efficacy, antagonist binding and expression level. Our overall aim was to find important residues involved in or critical for G protein coupling and receptor activation. Not only did we study different wild-type receptors and mutants, but also in the context of a "library" of yeast MMY strains containing one G protein subtype. The yeast strains used in this thesis were thus classified into five families: $G_{\alpha WT}$ (MMY12), $G_{\alpha s}$ (MMY28), $G_{\alpha i}$ (MMY23, MMY24 and MMY25), $G_{\alpha 12}$ (MMY19 and MMY20), and $G_{\alpha q}$ (MMY14, MMY16 and MMY21) corresponding to the last five C-terminal residues of the mammalian G_{α} subunit exchanged for the corresponding sequence stretch in the yeast G protein. A tyrosine residue (Y) at the C-terminus of the G_{α} subunit proved vital for controlling the activation of GPCRs, which was discussed in **Chapter 3**. In this way we determined G protein coupling profiles of one single GPCR (whether wild-type or mutant). This

approach allowed us to compare the G protein coupling of different receptors (within or outside subfamilies) and to identify key residues or motifs critical for specific G protein coupling or control switching between different G protein pathways.

The wild-type hA_{2B} receptor (**Chapter 3**) was promiscuous in its G protein coupling preference and activated all yeast strains, although to a different extent. In the presence of nicotinic acid the wild-type $hHCA_2$ receptor activated almost all G protein pathways except $G_{\alpha q}$ (MMY14) and $G_{\alpha s}$ (MMY28), which we did not use further as the empty plasmid (i.e. without receptor present) showed a high constitutive activity. The $hHCA_2$ receptor was more promiscuous in its G protein coupling preference than the $hHCA_3$ receptor, which only activated $G_{\alpha i1}$ (MMY23) and $G_{\alpha i3}$ (MMY24) pathways (**Chapter 5**).

The importance of residues in motifs: DRY and NPxxY(x)$_{5,6}$F; Helix 8 and C terminus

At first, we made a small number of mutants to establish and develop the entire assay. Computer predictions derived from crystal structures or homology models proved an efficient way to select mutants for deciphering their role in receptor-G protein coupling or in receptor activation. In **Chapter 3**, we used a hA_{2B} Receptor/G_s protein homology model, which was generated from the crystal structure of the β_2 adrenergic receptor in contact with the $G_{\alpha s}$ protein (PDB: 3SN6) to predict amino acids of the A_{2B} receptor interacting with the $G_{\alpha s}$ subunit. $R103^{3.50}$, $I107^{3.54}$, $L213^{IL3}$, $S235^{6.36}$ and $L236^{6.37}$ were selected for mutation into alanine as representatives of 16 residues that were shown to interact with the $G_{\alpha s}$ subunit from the homology model prediction. We learned that mutation of a single residue can lead to receptor silence and thus be critical for G protein coupling and receptor activation. $R103^{3.50}$ and $I107^{3.54}$ were shown to be important in G protein coupling and the activation of the hA_{2B} receptor, because the mutant $R103^{3.50}$A failed to couple to all G protein pathways and $I107^{3.54}$A failed to couple to almost all G protein pathways, whereas $L213^{IL3}$ turned out to be more important in G protein inactivation. $S235^{6.36}$A showed the most divergent

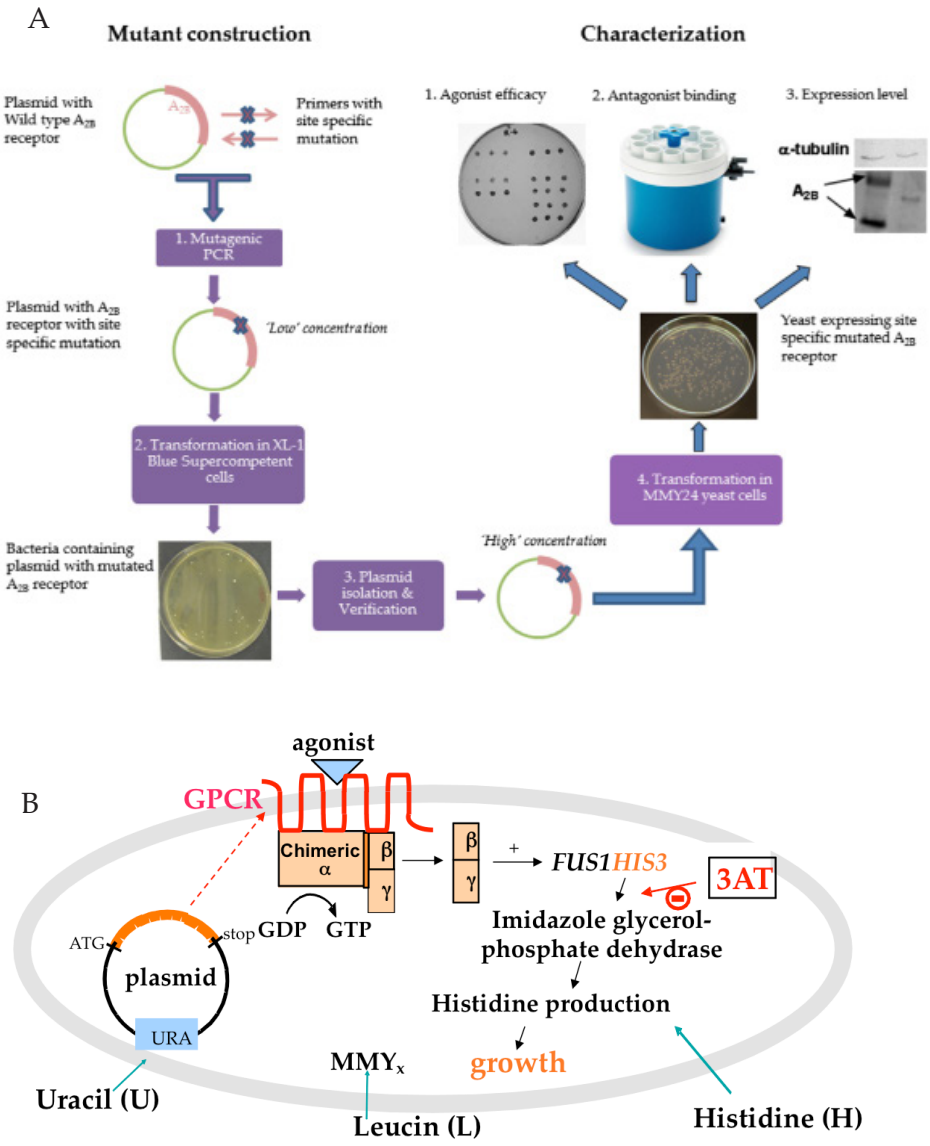

Fig. 1. (A) A schematic overview of "a single-GPCR-one-G protein yeast system" with the experimental set-up used during the research described in **Chapter 3** of this thesis. (B) Schematic drawing of GPCR activation in genetically modified yeast strains[1]. When heterologously expressed mammalian receptors are activated by agonists, β and γ subunits of the yeast G protein disassemble from the α subunit and activate the *FUS1* promoter which in turn activates the transcription of reporter genes *HIS3* which enables yeast cells to synthesize histidine allowing them to grow in histidine-deficient medium. Deficient selection markers medium: MMY strains: YNB-L; one MMY strain with the plasmid: YNB-UL; and functional assay of the GPCR activation (e.g. agonist efficacy): YNB-ULH.

G protein coupling profile, whereas L236$^{6.37}$A decreased receptor activation in all G protein pathways, although to a different extent.

In **Chapter 4**, we continued with a bigger sequence domain to discover the function of the so-called NPxxY motif and helix 8 in adenosine A_{2B} receptor activation. We characterized the functions of each residue in agonist efficacy, antagonist binding and expression level (Fig. 2). For example, amino acid residues P287$^{7.50}$, Y290$^{7.53}$, R293$^{7.56}$ and I304$^{8.57}$ were found to be critical, because their mutants (substitution with alanine) showed a complete loss of function with respect to agonist binding. The same four mutants lost antagonist binding, except for Y290$^{7.53}$A with some remaining binding. In terms of expression levels, R293$^{7.56}$A showed no expression, whereas the other three mutant proteins had expression levels comparable to the wild-type receptor. There were 8 amino acid residues that are also very important in receptor activation, but not as critical as the four residues: N286$^{7.49}$, V289$^{7.52}$, Y292$^{7.55}$, N294$^{8.47}$, F297$^{8.50}$, R298$^{8.51}$, H302$^{8.55}$ and R307$^{8.60}$, because their alanine mutants showed a partial loss of function in both NECA efficacy and potency. N286$^{7.49}$A and Y292$^{7.55}$A showed a slightly higher antagonist binding than wild-type, while other mutants showed a decrease in antagonist binding compared to wild-type receptor. N286$^{7.49}$A was only slightly expressed (15% of wild-type) and Y292$^{7.55}$A showed a significantly decreased expression level (approx. 50% of control). Many mutants were expressed similarly as the wild-type receptor (N294$^{8.47}$A, F297$^{8.50}$A, R298$^{8.51}$A, H302$^{8.55}$A, R307$^{8.60}$A). V289$^{7.52}$A had a significantly higher expression level than the wild-type receptor.

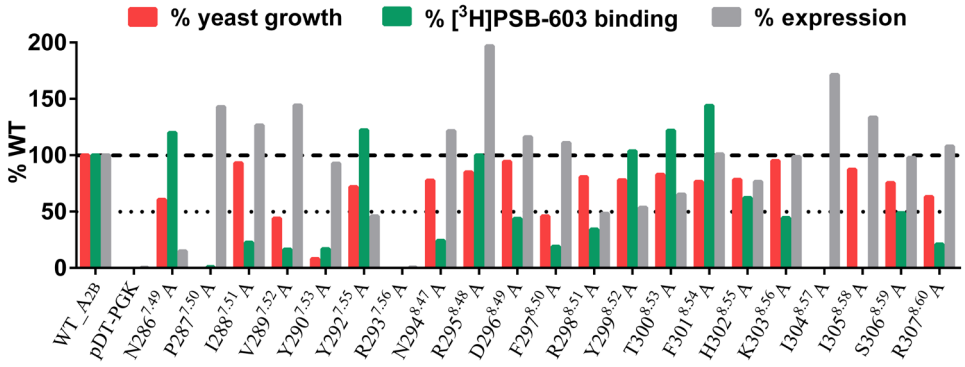

Fig. 2. Characterization of the NPxxY motif and helix 8 mutants of the adenosine hA_{2B} receptor in the strain MMY24 ($G_{\alpha i3}$): agonist efficacy (■), antagonist binding (■), and expression level (■).

Aiming to understand the role of one single residue better we mutated such a residue into amino acids different from alanine. For example, in **Chapter 2,** the following mutants were characterized, $N286^{7.49}Q$, $N286^{7.49}R$ and $N294^{8.47}I$ to better grasp the function and role of the specific side chain of each amino acid. When we aimed to focus on the interaction between two residues, we decided to 'swap' amino acids. For example in **Chapter 2,** $Y290^{7.53}F$ and $F297^{8.50}Y$ as single mutants and the double mutant $Y290^{7.53}F/F297^{8.50}Y$ were characterized on the assumption that there exists an aromatic interaction or pi/pi stacking between the $Y290^{7.53}$ and $F297^{8.50}$ residues stabilizing the receptor in an inactive state. From our experimental data the tyrosine's hydroxyl group in $Y290^{7.53}$ appeared very important in hA_{2B} receptor activation. However, the double mutant $Y290^{7.53}F/F297^{8.50}Y$ showed a greater combined loss of function than both single mutants, and did not act like the wild-type receptor. We thus conclude that the interaction between $Y290^{7.53}$ and $F297^{8.50}$ residues is more complicated than maintaining the aromatic interaction between the phenyl rings of the two side chains.

In **Chapter 5** we particularly focused on the function of the GPCR C terminus by investigating the different behaviors of the two closely related receptors $hHCA_2$ and $hHCA_3$ in G protein coupling. We found that the $hHCA_2$ receptor was promiscuous in its G protein coupling preference, much more than the $hHCA_3$ receptor. We then reasoned that, although the HCA_2 and HCA_3

receptors share high sequence identity, they differ considerably in C-terminus length with HCA_3 having the longest tail. Hence we constructed two mutant receptors by 'swapping' the short (HCA_2) and long (HCA_3) C-terminus. The differences in HCA_2 and HCA_3 receptor activation and G protein selectivity were not controlled, however, by their C-terminal tails, as we observed only minor differences between mutant and corresponding wild-type receptor.

SAR and SKR studies of the HCA_2 receptor

Intrigued by the HCA_2 receptor we embarked on a medicinal chemistry project to design and study a series of agonists for this receptor subtype. It is noteworthy that in **Chapter 6** the results were not obtained from *S. cerevisiae* strains, but from human embryonic kidney (HEK293T) cells, which were transfected with the N-Flag-tagged HCA_2 receptor in pcDNA3.1, as this cellular background is more suitable for performing radioligand binding studies. Structure-affinity relationship (SAR) and structure-kinetics relationship (SKR) studies were combined to investigate a series of biphenyl anthranilic acid agonists (27 compounds in total) for the HCA_2 receptor. Twelve of them showed higher affinity than the reference agonist nicotinic acid. We discovered two compounds, the 4-OH derivative **6g** (IC_{50} = 75 nM) and tetrahydro-anthranilic acid **6z** (IC_{50} = 108 nM) having a long residence time profile on the receptor compared to nicotinic acid, which was exemplified by their kinetic rate index (KRI) values of 1.31 (**6g**) and 1.23 (**6z**) vs nicotinic acid (0.8).

Perspectives

G protein coupling profiles of GPCRs

Our findings on the DRY, $NPxxY(x)_{5,6}F$ and Helix 8 motifs of the hA_{2B} receptor and on the C-terminus of the HCA receptors shed light on receptor-G protein coupling and G protein selectivity, which may help in further understanding the signaling of other GPCRs. With the yeast system at hand we can further focus

on key residues that abolish coupling to a certain G protein pathway and the ones that play important roles in the mechanisms of GPCR/G protein coupling. We can further extend our observations by performing saturation mutagenesis studies and see whether we can confirm if the same mechanisms apply to other receptors. In the future it would be very important to confirm our main findings in human cells or higher order model systems such as rodents or zebrafish.

Our yeast system with the extended G proteins library is very suitable to characterize G protein coupling profiles of other wild-type receptors, which can be very different between different receptors[2-4]. Previous research has also shown that G protein coupling of a receptor is consistent between yeast cells and mammalian cells[4]. Following the studies in this thesis it would be ideal to systematically mutate the whole receptor, yielding a complete map of an individual amino acid's function in GPCR/G protein coupling. However, this is an enormous and laborious project of low efficacy. A more effective way would be to systematically mutate only those amino acids that emerge from previous research, bioinformatics analyses, or predictions from crystal structures or homology models[5]. The activation mechanism of each receptor is most likely unique, however, there are many universal mechanisms as well. For example, Hofmann et al. reported that in rhodopsin interaction networks are formed by conserved residues, $NP^{7.50}xxY(x)_{5,6}F$, $E(D)R^{3.50}$, $Y^{5.58}(X)_7K(R)^{5.66}$, $CWxP^{6.50}$, and also functional microdomains, such as TM3-TM5 and TM5-TM6 interactions formed by $R135^{3.50}$, $E247^{6.30}$, $Y223^{5.58}$ and $K231^{5.66}$[6]. More recently, Flock et al. reported a mechanism of GPCRs and G_α activation in which H5 of $G_{\alpha s}$ is the critical interface element that makes residues in TM3, IL2, TM5, IL3, TM6 of β_2–adrenergic receptor interact[7]. We need to verify all these universal mechanisms and decipher the common mechanism of activation/G protein coupling between different receptors.

Another application for the yeast system with an extended G proteins library is the screening or characterization of functionally selective agonists. Different agonists may show different agonist affinity and efficacy in one G protein pathway, while they may have yet another profile of affinity and efficacy in a second G protein pathway[8, 9]. Since we have a library with agonists

of the $hHCA_2$ receptor we tested each agonist in different MMY strains with one (different) G_α protein. We could then analyze which part of the chemical structures of the agonists is important for activation in one specific G protein pathway (preliminary data not shown).

In conclusion, in addition to G protein coupling profiles of receptors activated by the same agonist, we can also obtain G protein coupling profiles of different agonists for the same receptor.

Activation mechanism of Class B

The yeast system has been used frequently in the Class A receptor subfamily, such as Serotonin (5-HT, 5-hydroxytryptmine)[10], thyroid-stimulating hormone receptor (TSHR)[11, 12], CXC chemokine receptor 1 (CXCR1)[13], also reviewed in **Chapter 2** of this thesis. However, the activation mechanism of members of the Class B family, such as adhesion receptors, has been less investigated. A single-GPCR-one-G protein yeast system is equally suitable to be applied to these receptors to decipher their activation and G protein coupling profiles. Class A and Class B subfamilies share some similar sequence motifs but are mostly completely different (Table 1[14]). There are many orphan receptors in the Class B subfamily, and hence there is no endogenous ligand known to activate the receptors. However, some of the wild-type receptors in this class show high levels of constitutive activity, and thus mutations that decrease or increase constitutive activity are telling for the importance of the original residue in receptor activation. Thus, learning how the motifs function in receptor activation/G protein coupling is very useful to discover and understand general mechanisms of activation in the Class B subfamily.

Table 1. Class A motifs and their class B counterparts[14].

Region	Class	Motif	Function
IL1	A	$K^{1.61}$KLHxxxN	structure
	B	$R^{1.61}$KLHxxxN	
TM2,3	A	$DRY^{3.51}$	activation
	B	$R^{2.39}H^{2.43}$; $E^{3.46}$	
TM3	A	$C^{3.25}$	structure
	B	$C^{3.25}$	
TM4	A	$W^{4.50}$	structure
	B	$W^{4.50}$	
TM5	A	$IxxL^{5.65}$	G protein interaction
	B	$LXXL^{5.65}$	
TM6	A	$CWxP^{6.50}$	activation
	B	P...$TY^{6.48}$	
TM6	A	$KxxK^{6.35}$	G protein interaction
	B	$KxxK^{6.35}$	
TM7	A	$NPXXY^{7.53}$	activation
	B	$VAVLY^{7.53}$	
H8	A	$EFxxxL^{8.54}$	structure/restraint
	B	$EVxxxL^{8.54}$	
TM2,3; TM7	A	$R^{3.50}$ – $E^{6.30}$	ionic/polar lock
	B	$R^{2.39}$ – $T^{6.37}$	

Challenges for the HCA_2 receptor

In **Chapter 6** we identified two compounds, **6g** and **6z**, showing slower dissociation from the receptor than nicotinic acid. Residence time as a parameter might be a better predictor for *in vivo* efficacy and should be considered during lead optimization to potentially make the drug discovery process more efficient. Predictions from a homology model of HCA_2 receptor suggest important structural requirements, such as the carboxylic group forming hydrogen bonds with $R111^{3.36}$ and $R251^{6.55}$; the hydroxyl group forming a hydrogen bond with $D92^{EL1}$; and the benzene ring forming a π-π interaction with $W93^{EL1}$ (Fig. 3). However, we failed to obtain accurate residence time values due to practical issues with the radioligand nicotinic acid. One idea would be to radiolabel other high affinity ligands of the HCA_2 receptor, to obtain a more precise kinetic profile of long or short residence time compounds.

The importance of the HCA_2 receptor has been growing, however, it is somewhat unfortunate that no antagonists have been identified yet for the HCA_2 receptor, which would allow a more detailed pharmacological analysis. We could use our fast and cheap yeast system to screen large compounds libraries to screen for antagonists.

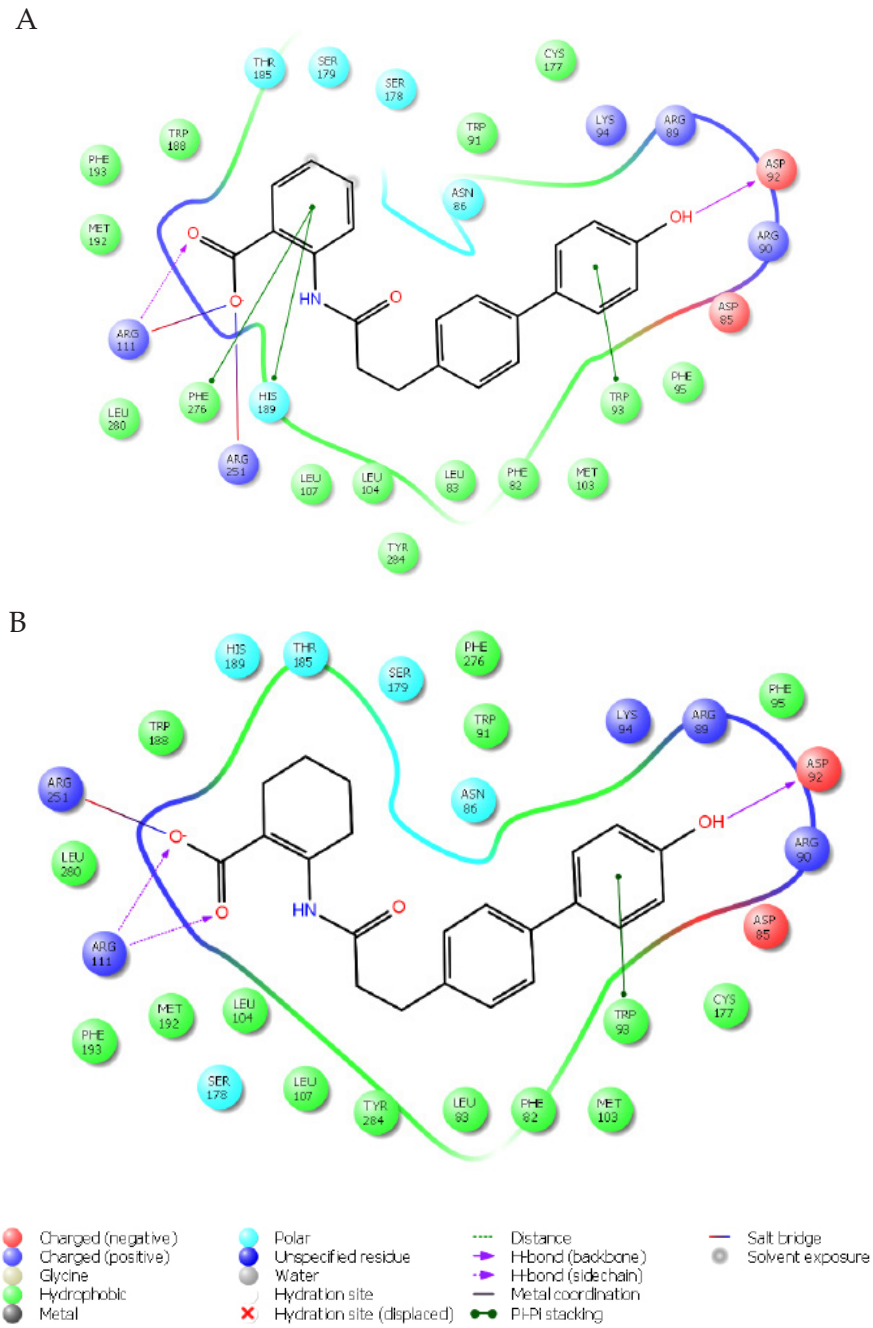

Fig. 3. Interaction map of **6g** (A) and **6z** (B) with surrounding residues in a composite homology model of HCA_2 receptor was constructed based on the structure of both the Serotonin 2b receptor co-crystalized with ergotamine (Protein Data Bank: 4IB4) and the crystal structure of the Free Fatty Acid receptor 1 bound to TAK-875 (Protein Data Bank: 4PHU)[15, 16].

Final notes

We confirmed that a yeast system with an extended library of G proteins is very well suited for the study of GPCR activation, G protein coupling profiles, receptor-G protein binding and G protein selectivity. For example, we used a scanning mutagenesis approach of the NPxxY$(x)_{5,6}$F motif and of helix 8 of the adenosine A_{2B} receptor (A_{2B}R), and learned among others that amino acid residues in these motifs are crucial for receptor function, since alanine mutants of these amino acid residues led to a complete loss of function. Hopefully, such findings can contribute to further drug development.

We also focused on structure-kinetics relationship (SKR) studies next to the more traditional Structure-affinity relationship (SAR) studies. We found two compounds showing longer residence times than nicotinic acid, which may provide clues for further drug discovery efforts on this receptor. All in all, the variety of methods described in this thesis provided us a detailed understanding of receptor function, suggesting that novel avenues for further drug discovery on these established targets is entirely feasible.

References

[1] Beukers, M.W. and IJzerman, A.P. *Techniques: how to boost GPCR mutagenesis studies using yeast.* Trends Pharmacol. Sci. (2005) 26: 533-539.

[2] Buck, L. and Liberles, S.D., *Methods and G proteins for screening and identifying ligands of G protein-coupled receptors*. 2012, Google Patents. 731.

[3] Brown, A.J., et al. *Functional coupling of mammalian receptors to the yeast mating pathway using novel yeast/mammalian G protein α-subunit chimeras.* Yeast (2000) 16: 11-22.

[4] Minic, J., et al. *Yeast system as a screening tool for pharmacological assessment of G protein coupled receptors.* Curr. Med. Chem. (2005) 12: 961-969.

[5] Bertheleme, N., et al. *Arginine 199 and leucine 208 have key roles in the control of adenosine A_{2A} receptor signalling function.* PloS one (2014) 9: e89613.

[6] Hofmann, K.P., et al. *AG protein-coupled receptor at work: the rhodopsin model.* Trends Biochem. Sci. (2009) 34: 540-552.

[7] Flock, T., et al. *Universal allosteric mechanism for G_{α} activation by GPCRs.* Nature (2015) 524: 173-179.

[8] Busnelli, M., et al. *Functional selective oxytocin-derived agonists discriminate between individual G protein family subtypes.* J. Biol. Chem. (2012) 287: 3617-3629.

[9] Stewart, G.D., et al. *Determination of adenosine A_1 receptor agonist and antagonist pharmacology using Saccharomyces cerevisiae: implications for ligand screening and functional selectivity.* J. Pharmacol. Exp. Ther. (2009) 331: 277-286.

[10] Raymond, J.R., et al. *The recombinant 5-HT1A receptor: G protein coupling and signalling pathways.* Br. J. Pharmacol. (1999) 127: 1751-1764.

[11] Neumann, S., et al. *Structural determinants for G protein activation and selectivity in the second intracellular loop of the thyrotropin receptor.* Endocrinology (2005) 146: 477-485.

[12] Kleinau, G., et al. *Principles and determinants of G-protein coupling by the rhodopsin-like thyrotropin receptor.* PloS one (2010) 5: e9745.

[13] Han, X., et al. *Leu128 (3.43)(l128) and Val247 (6.40)(V247) of CXCR1 are critical amino acid residues for g protein coupling and receptor activation.* PloS one (2012) 7: e42765.

[14] Vohra, S., et al. *Similarity between class A and class B G-protein-coupled receptors exemplified through calcitonin gene-related peptide receptor modelling and mutagenesis studies.* J. R. Soc. Interface (2013) 10: 20120846.

[15] Wang, C., et al. *Structural Basis for Molecular Recognition at Serotonin Receptors.* Science (New York, N.Y.) (2013) 1-9.

[16] Srivastava, A., et al. *High-resolution structure of the human GPR40 receptor bound to allosteric agonist TAK-875.* Nature (2014) 513: 124-127.

Summary

G protein-coupled receptors (GPCRs) are one of the largest families of membrane proteins, with approximately 800 different GPCRs in the human genome. Signalling via GPCRs regulates many biological processes, such as cell proliferation, differentiation, and development. Moreover, many hormones and neurotransmitters are ligands for these receptors, and hence it is not surprising that many drugs, either mimicking or blocking the action of the bodily substances, have been developed. It is estimated that 30-40% of current drugs on the market target GPCRs. Further identifying and elucidating the functions of GPCRs will provide opportunities for novel drug discovery. The budding yeast *Saccharomyces cerevisiae (S. cerevisiae)* is a very important and useful platform in this respect. There are many advantages of using a yeast assay system, as it is cheap, safe and stable; it is also convenient for rapid feasibility and optimization studies. Moreover, it offers "null" background when studying human GPCRs. New developments regarding human GPCRs expressed in a yeast platform are providing insights into GPCR activation and signalling, and facilitate agonist and antagonist identification.

In **Chapter 1**, a general description of GPCRs, GPCR activation, G protein and G protein selectivity is presented. In this thesis, we focused our attention on the human adenosine A_{2B} receptor ($hA_{2B}R$) and the family of hydroxycarboxylic acid HCA_2 and HCA_3 receptors. Applications of the *S. cerevisiae* system in GPCR research are introduced as well.

In **Chapter 2**, we summarized the latest findings regarding human GPCRs in studies using *S. cerevisiae*, ever since the year 2005 when we last published a review on this topic. We described 11 families of GPCRs in detail, while including the principles and developments of each yeast system applied to these different GPCRs and highlight and generalize the experimental findings of GPCR function in these systems.

The expression of human GPCRs in *S. cerevisiae* containing chimeric yeast/mammalian G_{α} subunits provides a useful tool for the study of GPCR

activation. In **Chapter** 3, we used a one-GPCR-one-G protein yeast screening method in combination with molecular modeling and mutagenesis studies to decipher the interaction between GPCRs and the C-terminus of different α-subunits of G proteins. We chose the $hA_{2B}R$ as a paradigm, a typical class A GPCR that shows promiscuous behavior in G protein coupling in this yeast system. The wild-type $hA_{2B}R$ and five mutant receptors were expressed in 8 yeast strains with different humanized G proteins, covering the four major classes: $G_{\alpha i}$, $G_{\alpha s}$, $G_{\alpha q}$ and $G_{\alpha 12}$. Our experiments showed that a tyrosine residue (Y) at the C-terminus of the G_{α} subunit plays an important role in controlling the activation of GPCRs. Receptor residues $R103^{3.50}$ and $I107^{3.54}$ are vital too in G protein coupling and the activation of the $hA_{2B}R$, whereas $L213^{IL3}$ is more important in G protein inactivation. Substitution of $S235^{6.36}$ to alanine provided the most divergent G protein coupling profile. Finally, $L236^{6.37}$ substitution decreased receptor activation in all G protein pathways, although to a different extent. In conclusion, our findings shed light on the selectivity of receptor-G protein coupling, which may help in further understanding GPCR signaling.

In **Chapter 4**, we continued to investigate the $hA_{2B}R$. We used a single-GPCR-one-G protein yeast screening method in combination with mutagenesis studies, molecular modeling and bio-informatics to investigate the importance of the different amino acid residues of the $NPxxY(x)_6F$ motif and helix 8 in $hA_{2B}R$ activation. A scanning mutagenesis protocol was employed, yielding 11 single mutations and one double mutation of the $NPxxY(x)_6F$ motif and 16 single mutations of helix 8. The amino acid residues $P287^{7.50}$, $Y290^{7.53}$, $R293^{7.56}$ and $I304^{8.57}$ were found to be essential, since mutation of these amino acid residues to alanine led to a complete loss of function. Western blot analysis showed that mutant receptor $R293^{7.56}A$ was not expressed, whereas the other proteins were. Amino acid residues that are also important in receptor activation are: $N286^{7.49}$, $V289^{7.52}$, $Y292^{7.55}$, $N294^{8.47}$, $F297^{8.50}$, $R298^{8.51}$, $H302^{8.55}$ and $R307^{8.60}$. The mutation $Y290^{7.53}F$ lost 50% of efficacy, while $F297^{8.50}A$ behaved similar to the wild-type receptor. The double mutation, $Y290^{7.53}F/F297^{8.50}Y$, lost around 70% of efficacy and displayed a lower potency for the reference agonist 5'-(*N*-ethylcarboxamido) adenosine (NECA). This study provides new insight into the molecular interplay

and impact of TM7 and helix 8 for hA_{2B} receptor activation, which may be extrapolated to other adenosine receptors and possibly to other GPCRs.

In **Chapter 5**, we focused our attention on the family of HCA receptors, a GPCR family of three members, of which the HCA_2 and HCA_3 receptors share 95% sequence identity but differ considerably in C-terminus length with HCA_3 having the longest tail. The two receptors were expressed and analysed for their activation profile in *S. cerevisiae* MMY yeast strains that have different G protein G_α subunits. The $hHCA_2$ receptor was promiscuous in its G protein coupling preference. In the presence of nicotinic acid the $hHCA_2$ receptor activated almost all G protein pathways except $G_{\alpha q}$ (MMY14). However, the G_α protein coupling profile of the $hHCA_3$ receptor was less promiscuous, as the receptor only activated $G_{\alpha i1}$ (MMY23) and $G_{\alpha i3}$ (MMY24) pathways.

We then constructed two mutant receptors by 'swapping' the short (HCA_2) and long (HCA_3) C-terminus. The differences in HCA_2 and HCA_3 receptor activation and G protein selectivity were not controlled, however, by their C-terminal tails, as we observed only minor differences between mutant and corresponding wild-type receptor. This study provides new insights into the G protein coupling profiles of the HCA receptors and the function of the receptor's C terminus, which may be extended to other GPCRs.

In **Chapter 6**, we focused on the design and synthesis of HCA_2 agonists with the additional quality of having a long residence time on the receptor, as the latter parameter may be linked to *in vivo* efficacy. Structure-affinity relationship (SAR) and structure-kinetics relationship (SKR) studies were combined to investigate a series of biphenyl anthranilic acid agonists for the HCA_2 receptor. In total, 27 compounds were synthesized and twelve of them showed higher affinity than nicotinic acid. Two compounds, **6g (**IC_{50} **=** 75 nM) and **6z** (IC_{50} = 108 nM) showed a longer residence time profile compared to nicotinic acid, exemplified by their kinetic rate index (KRI) values of 1.31 and 1.23, respectively. The SAR study resulted in the novel 2-F, 4-OH derivative (**6x**) with an IC_{50} value of 23 nM as the highest affinity HCA_2 agonist of the biphenyl series, although it showed a similar residence time as nicotinic acid. The SAR and SKR data suggest that an early compound selection based on binding kinetics is a promising addition to

the lead optimization process.

In **Chapter 7**, we summarized our findings in the present thesis and described the advantages of the *S. cerevisiae* system and the importance of residues in conserved sequence motifs, such as DRY and NPxxY. Future perspectives for drug discovery based on our findings with respect to receptor activation and G protein coupling are discussed. All in all, the variety of methods described in this thesis provided us a detailed understanding of receptor function, suggesting that novel avenues for further drug discovery on these established targets is entirely feasible.

Samenvatting

Receptoren die aan een G-eiwit gekoppeld zijn ('G protein-coupled receptors', of afgekort GPCRs) vormen één van de grootste families van membraaneiwitten, met ongeveer 800 verschillende GPCRs in het menselijk genoom. De signalen die door GPCRs worden doorgegeven regelen veel verschillende biologische processen, zoals cel-proliferatie, -differentiatie, en embryonale ontwikkeling. Bovendien werken veel hormonen en neurotransmitters op deze receptoren, en het is dan ook geen verrassing dat er veel medicijnen ontwikkeld zijn die de werking van deze lichaamseigen stoffen blokkeren of nabootsen. Geschat wordt dat 30 tot 40% van de huidige medicijnen die op de markt zijn via GPCRs werken. Het vinden van nieuwe medicijnen is dus gebaat bij verder onderzoek naar de werking van GPCRs.

Een belangrijk hulpmiddel voor dit onderzoek is de gist *Saccharomyces cerevisiae (S. cerevisiae).* Het gebruik van een gist-assay-systeem voor het onderzoek naar de werking van receptoreiwitten heeft veel voordelen: het is goedkoop, veilig, en robuust. Het is goed te gebruiken voor snelle haalbaarheids- en optimalisatie-studies. Bovendien is er geen storend achtergrondsignaal bij de bestudering van menselijke GPCRs, omdat deze niet in de oorspronkelijke gist aanwezig zijn. Nieuwe ontwikkelingen maken het mogelijk om, met in het gist-assay-systeem tot expressie gebrachte menselijke GPCRs, onderzoek te doen naar GPCR activatie en signaaltransductie, en om nieuwe agonisten en antagonisten te identificeren.

Hoofdstuk 1 geeft een algemene introductie van GPCRs, de activatie van GPCRs, het G-eiwit, en G-eiwit selectiviteit. Het proefschrift richt zich verder op de menselijke adenosine A_{2B} receptor ($hA_{2B}R$) en de hydroxycarboxylzuur 2 en 3 (HCA_2 en HCA_3) receptoren. Daarnaast worden verschillende toepassingen van het *S. cerevisiae*-systeem voor GPCR onderzoek geïntroduceerd.

Hoofdstuk 2 geeft een overzicht van de huidige stand van zaken van humaan GPCR onderzoek met *S. cerevisiae,* aansluitend op ons laatste overzicht van dit onderwerp dat in 2005 werd gepubliceerd. Dit hoofdstuk beschrijft in

detail elf GPCR families, samen met de principes en de ontwikkeling van elk gist-assay-systeem dat is toegepast op deze GPCRs, en geeft een samenvatting van de gevonden resultaten over de werking van GPCRs.

S. cerevisiae-stammen die gist-zoogdier chimeren van het G_{α}-eiwit (één van de drie deeleiwitten die samen het G-eiwit vormen) tot expressie brengen zijn uitermate geschikt voor de bestudering van de activatie van GPCRs. **Hoofdstuk 3** beschrijft een "één-GPCR-één-G-eiwit" gist onderzoeksmethode, gecombineerd met moleculair modelleren en eiwitmutaties, om de wisselwerking tussen GPCRs en de C-terminus van verschillende G_{α}-deeleiwitten te ontcijferen. Hiervoor werd de $hA_{2B}R$ als voorbeeldreceptor gebruikt, een representatieve klasse A GPCR die zich uitstekend gedraagt wat betreft G-eiwitkoppeling in dit gist-systeem. De wild-type en vijf gemuteerde $hA_{2B}Rs$ werden tot expressie gebracht in acht verschillende giststammen met verschillende humane G-eiwittypes, daarmee de vier G-eiwit-hoofdklassen dekkend: $G_{\alpha i}$, $G_{\alpha s}$, $G_{\alpha q}$, en $G_{\alpha 12}$. De resultaten lieten zien dat een tyrosine-aminozuur (Y) op de C-terminus van het G_{α}-deeleiwit belangrijk is voor de regulering van de activatie van GPCRs. Er werd ook gevonden dat aminozuren op de receptor zelf, namelijk $R103^{3.50}$ en $I107^{3.54}$ essentieel zijn voor G-eiwitkoppeling en receptor-activatie, terwijl aminozuur $L213^{IL3}$ weer belangrijk is voor de uitschakeling van de receptor. Vervanging van aminozuur $S235^{6.36}$ door een alanine gaf de grootste verschillen in G-eiwitkoppeling tussen de G-deeleiwittypes. Als laatste gaf de alaninevervanging van $L236^{6.37}$ verschillende gradaties van lagere receptor-activatie door alle G-eiwittypes. Deze resultaten verduidelijken de selectiviteit van G-eiwitten voor koppeling aan receptoren, en dragen bij aan het begrip van GPCR signaaltransductie.

Hoofdstuk 4 richt zich op het belang van het $NPxxY(x)_6F$ motief en van helix 8 voor de activatie van de $hA_{2B}R$, met dezelfde methoden als in Hoofdstuk 3 aangevuld met bio-informatica. Aminozuren in het $NPxxY(x)_6F$ motief en helix 8 werden vervangen door een alanine, resulterend in 11 enkelpunts- en één dubbele mutatie van het $NPxxY(x)_6F$ motief en 16 enkelpuntsmutaties van helix 8. Het effect van deze mutaties op de receptoractivatie werd vervolgens onderzocht met het "één-GPCR-één-G-eiwit" gist-systeem. De aminozuren $P287^{7.50}$, $Y290^{7.53}$,

R293$^{7.56}$, en I304$^{8.57}$ bleken essentieel te zijn voor receptoractivatie omdat mutaties tot alanine van deze posities tot compleet verlies van receptoractiviteit leidden. Uit analyse met western blots bleek dat behalve de gemuteerde R293$^{7.56}$A receptor alle andere gemuteerde receptoren tot expressie kwamen in de gist. Andere aminozuren die belangrijk bleken voor receptoractivatie waren N286$^{7.49}$, V289$^{7.52}$, Y292$^{7.55}$, N294$^{8.47}$, F297$^{8.50}$, R298$^{8.51}$, H302$^{8.55}$, en R307$^{8.60}$. Mutatie Y290$^{7.53}$F deed de receptor 50% van zijn maximale activatie verliezen, terwijl F297$^{8.50}$A geen effect had ten opzichte van de wild-type receptor. De dubbel gemuteerde Y290$^{7.53}$F/F297$^{8.50}$Y receptor verloor 70% van zijn maximale activatie en bovendien was referentie-agonist 5'-(*N*-ethylcarboxamido)adenosine (NECA) minder potent op deze receptor. Deze resultaten geven nieuwe inzichten in de moleculaire wisselwerking tussen de transmembraan regio 7 (TM7) en helix 8 en het belang hiervan voor het activatiemechanisme van de hA_{2B} receptor. Het is goed mogelijk dat deze resultaten ook betrekking hebben op de andere adenosinereceptoren en op andere GPCRs.

Hoofdstuk 5 richt zich op de familie van HCA receptoren. Deze familie wordt gevormd door 3 GPCRs, waarvan de HCA_2 en HCA_3 receptoren veel op elkaar lijken met 95% overeenkomst in aminozuursequentie, maar waarvan de HCA_3 een langere C-terminus heeft. Beide receptoren werden tot expressie gebracht in de *S. cerevisiae* MMY stammen met verschillende G_α-deeleiwitten. De HCA_2 receptor kon alle G-eiwitten met verschillende deeleiwitten activeren, behalve de $G_{\alpha q}$ (stam MMY14). De HCA_3 daarentegen kon alleen $G_{\alpha i1}$ (MMY23) en $G_{\alpha i3}$ (MMY24) activeren.

Vervolgens werden twee gemuteerde receptoren samengesteld door de korte (van de HCA_2R) en de lange (HCA_3R) C-temini om te ruilen. Het bleek dat deze gemuteerde receptoren zich hetzelfde gedroegen als de wild-type receptoren wat hun selectiviteit voor de verschillende G-eiwittypes betreft. Hieruit kan worden geconcludeerd dat de verschillen tussen de C-termini van deze receptoren niet voor de selectiviteit voor de verschillende G_α-deeleiwitten zorgen. Deze resultaten geven nieuwe inzichten in de G-eiwit-koppelingsprofielen van de HCA receptoren en de functie van de C-terminus, welke mogelijk ook betrekking hebben op andere GPCRs.

Hoofdstuk 6 richt zich op het ontwerp en de synthese van agonisten voor de HCA_2 receptor met een lange verblijfstijd op de receptor. Een langere verblijfstijd op de receptor leidt waarschijnlijk tot een betere *in vivo* effectiviteit van de agonist. Met behulp van structuur-affiniteitsrelatie- (SAR) en structuur-kinetiekrelatie-studies (SKR) werd een serie van biphenyl-anthranylzuur agonisten voor de HCA_2 receptor onderzocht. Een collectie van 27 liganden werd gesynthetiseerd en 12 hiervan hadden een hogere affiniteit dan referentie-ligand nicotinezuur. De twee liganden **6g** (IC_{50} = 75 nM) en **6z** (IC_{50} = 108 nM) hadden een langere verblijfstijd op de receptor dan nicotinezuur, met respectievelijke *kinetic rate index (KRI)* waarden van 1.31 en 1.23. Van de biphenylserie was de nieuwe 2-F, 4-OH variant **6x** de agonist met de hoogste affiniteit voor de HCA_2R met een IC_{50} waarde van 23 nM, ook al was de verblijfstijd op de receptor gelijk aan die van referentie-ligand nicotinezuur. Deze SAR en SKR resultaten geven aan dat een vroege selectie van liganden gebaseerd op bindingskinetiek een veelbelovende toevoeging is voor *lead*-optimalisatie.

Hoofdstuk 7 vat de resultaten van dit proefschrift samen. De voordelen van het *S. cerevisiae*-systeem en het belang van de aminozuren in geconserveerde receptormotieven zoals DRY en NPxxY worden beschreven. De vooruitzichten die de gepresenteerde receptoractivatie- en G-eiwitkoppelings-resultaten bieden op medicijnonderzoek worden behandeld. Kort samengevat heeft de verscheidenheid van de gebruikte methodes in dit proefschrift geleid tot een gedetailleerd begrip van receptorwerking. Dit geeft aan dat ondanks dat de besproken receptoren al ruim onderzocht zijn, er nog altijd nieuwe kansen liggen voor verder geneesmiddelonderzoek.

Curriculum Vitae

Rongfang Liu was born in Tacheng, Xingjiang, China on September 5th, 1986. She finished secondary education in Tacheng High School in 2004. Thereafter she studied biology at Lanzhou University (Gansu, China) from 2004 to 2011, where she obtained her bachelor and master degree. Her master research focused on the interaction between brassinosteroid and NO signaling pathways, and she also explored the pathogenesis of mental diseases (at Kunming Institute of Botany). Then she decided to further her training in biomedical science with an emphasis on drug discovery. She went abroad to do her PhD with support from the China Scholarship Council. She started as a PhD student at the department of Medicinal Chemistry at the Leiden Academic Centre for Drug Research (Leiden University, The Netherlands) under the supervision of Prof. Ad IJzerman from 2011 to 2016. Her PhD project focuses on activation and biased signaling of G protein-coupled receptors, in particular of the hydroxy-carboxylic acid 2 and 3 receptor ($HCA_{2/3}$) and the adenosine A_{2B} receptor. The results of her research are described in this thesis.

List of publications

Liu, R., Wong, W., IJzerman, A. P. *Human G protein-coupled receptor studies in Saccharomyces cerevisiae.* Biochem. Pharmacol. (2016) 114: 103-115.

Liu, R., van Veldhoven, J. P., IJzerman, A. P. *The role of the C-terminus of the human hydroxycarboxylic acid receptors 2 and 3 in G protein activation using G_{α}-engineered yeast cells.* Eur. J. Pharmacol. (2016) 770: 70-77.

Guo, D., Pan, A. C., Dror, R. O., Mocking, T., **Liu, R.,** Heitman, L. H., Shaw, D. E., IJzerman, A. P. *Molecular basis of ligand dissociation from the adenosine A_{2A} receptor.* Mol. Pharmacol. (2016) 89: 485-491.

Liu, R., Nahon, D., le Roy, B., Lenselink, E. B., IJzerman, A. P. *Scanning mutagenesis in a yeast system delineates the role of the NPxxY(x)$_{5,6}$F motif and helix 8 of the adenosine A_{2B} receptor in G protein coupling*. Biochem. Pharmacol. (2015) 95: 290-300.

van Veldhoven, J. P*., **Liu, R*.,** Thee, S. A., Wouters, Y., Verhoork, S. J., Mooiman, C., Louvel, J., IJzerman, A. P. *Affinity and kinetics study of anthranilic acids as HCA_2 receptor agonists.* Bioorg. Med. Chem. (2015) 23: 4013-4025.

Liu, R., Groenewoud, N. J., Peeters, M. C., Lenselink, E. B., IJzerman, A. P. *A yeast screening method to decipher the interaction between the adenosine A_{2B} receptor and the C-terminus of different G protein α-subunits.* Purinergic Signal. (2014) 10: 441-453.

Qu, T., **Liu, R.,** Wang, W., An, L., Chen, T., Liu, G., Zhao, Z. *Brassinosteroids regulate pectin methylesterase activity and AtPME41 expression in Arabidopsis under chilling stress.* Cryobiology (2011) 63:111-117.